DEVELOPMENT OF A SOLID ROCKET PROPELLANT NONLINEAR VISCOELASTIC CONSTITUTIVE THEORY. VOLUME I. TEXT

Richard J. Farris, et al

Aerojet Solid Propulsion Company

Prepared for:

Air Force Rocket Propulsion Laboratory

June 1973

Unclassified
Security Classification

AD-769264

DOCUMENT CONTROL DATA - R & D

(Security classification of title, body of abstract and indexing annotation must be entered when the overall report is classified)

1. ORIGINATING ACTIVITY *(Corporate author)*

Aerojet Solid Propulsion Company
Sacramento, California

2a. REPORT SECURITY CLASSIFICATION

Unclassified

2b. GROUP

None

3. REPORT TITLE

Development of a Solid Rocket Propellant Nonlinear Viscoelastic Constitutive Theory

4. DESCRIPTIVE NOTES *(Type of report and inclusive dates)*

Final Report (May 1971 - June 1973)

5. AUTHOR(S) *(First name, middle initial, last name)*

Richard J. Farris and Richard A. Schapery

6. REPORT DATE	7a. TOTAL NO. OF PAGES	7b. NO. OF REFS
June 1973	~~566~~ 246	156

8a. CONTRACT OR GRANT NO.	9a. ORIGINATOR'S REPORT NUMBER(S)
F04611-71-C-0046	
b. PROJECT NO.	Final Report
c.	9b. OTHER REPORT NO(S) *(Any other numbers that may be assigned this report)*
d.	AFRPL-TR-73-50

10. DISTRIBUTION STATEMENT

Approved for Public Release
Distribution Unlimited

11. SUPPLEMENTARY NOTES	12. SPONSORING MILITARY ACTIVITY
Report is in two volumes, Volume I - Text and Volume II - Appendices	Air Force Rocket Propulsion Laboratory Edwards, California

13. ABSTRACT

This program was designed to develop three dimensional nonlinear viscoelastic equations that could describe the stress-strain response of solid propellant materials for complex loading conditions. The approach used was to identify and mathematically model the underlying mechanisms contributing to the constitutive nonlinearity and to then include these effects within the framework of a continuum constitutive theory.

The program was successful in meeting its objectives and some of the program developments and conclusions are as follows. The dominant mechanisms leading to the nonlinear stress-strain response is microstructural damage in the form of the Mullins' stress-softening effect and vacuole dilatation. Reversible nonlinearities were found to be of secondary importance. These effects have been modeled and combined into a constitutive theory that works very well for fitting the distortional stress-strain behavior under complex loading conditions. This theory is a permanent memory constitutive theory and contains irreversible effects of the past history on the current response. Time effects are included through time-dependent structural damage as well as the ordinary viscous energy dissipation. The experimental work consisted of determining the three dimensional strain response due to complex stress histories at temperatures from -65°F to +150°F and superimposed hydrostatic stress-states from 0 to 1000 psi. To handle the large masses of data generated on this contract computerized characterization techniques were developed wherein the equations could be fit to large masses of data.

DD FORM 1 NOV 65 1473

Unclassified
Security Classification

14. KEY WORDS	LINK A		LINK B		LINK C	
	ROLE	WT	ROLE	WT	ROLE	WT
1. Nonlinear Viscoelasticity						
2. Constitutive Theory						
3. Thermoviscoelasticity						
4. Solid Propellant						
5. Mechanical Behavior						
6. Stress-Strain Behavior						
7. Composite Materials						
8. Finite Deformations						
9. Material Characterization						
10. Computerized Characterization						

A

When U. S. Government drawings, specifications, or other data are used for any purpose other than a definitely related Government procurement operation, the Government thereby incurs no responsibility nor any obligation whatsoever, and the fact that the Government may have formulated, furnished, or in any way supplied the said drawings, specifications, or other data, is not to be regarded by implication or otherwise, or in any manner licensing the holder or any other person or corporation, or conveying any rights or permission to manufacture, use or sell any patented invention that may in any way be related thereto.

AFRPL-TR-73-50

DEVELOPMENT OF A SOLID ROCKET PROPELLANT NONLINEAR VISCOELASTIC CONSTITUTIVE THEORY

Volume I - Final Report

Prepared by:

Aerojet Solid Propulsion Company
Sacramento, California

Authors

R. J. Farris, ASPC and R. A. Schapery, Texas A&M

June 1973

AFRPL-TR-73-50

Air Force Rocket Propulsion Laboratory
Director of Science and Technology
Air Force Systems Command
Edwards, California

IV

FOREWORD

This program was sponsored by the

Air Force Rocket Propulsion Laboratory
Director of Science and Technology
Air Force Systems Command
Edwards, California, 93523

The technical effort reported herein was accomplished under Contract F04611-71-C-0046 and covered the period from May 1971 through June 1973. Mr. Norman Walker was the Air Force project engineer at the start of this contract until he left AFRPL. Dr. Randy L. Peeters was the Air Force materials engineer for the remainder of this contract.

The program was completely successful in meeting its objectives. The success of the program was due to the combined efforts of key personnel at two facilities, the Aerojet Solid Propulsion Company and the Texas A&M Research Foundation. The Aerojet team performed an extensive experimental effort, developed computerized characterization techniques, and performed theoretical work in developing constitutive equations which accurately model the multi-axial behavior of composite propellants. The team at the Texas A&M Research Foundation supported the effort by performing theoretical and experimental work to develop mathematical models for characterizing solid propellants under realistic states of strain. The emphasis of their work was to develop simple constitutive equations based on thermodynamic principles for visco-elastic materials having microstructural damage.

The key technical personnel on this program were: Dr. Richard J. Farris who directed the Aerojet effort and coordinated the overall effort as the Program Technical Manager, and Dr. Richard A. Schapery who directed the Texas A&M effort. Mr. Frederick H. Davidson performed all of the experimental work at Aerojet and Mr. Dennis F. Vronay was primarily responsible for the computerized characterization work. Mr. L. E. Lewis and Mr. R. T. Shankle performed the Texas A&M experimental effort which was under the guidance of Mr. Scott Beckwith.

This technical report has been reviewed and is approved.

Dr. Randy L. Peeters (MKPB)
Materials Engineer, AFRPL
Edwards, California

ABSTRACT

This program was designed to develop three dimensional nonlinear viscoelastic equations that could describe the stress-strain response of solid propellant materials for complex loading conditions. The approach used was to identify and mathematically model the underlying mechanisms contributing to the constitutive nonlinearity in these highly filled polymeric materials and to then include these effects within the framework of a continuum constitutive theory. Also considerable theoretical work was done showing how the resulting mathematical representations could be contained within the framework of a thermodynamic theory and viscoelastic fracture mechanics. During the course of this contract considerable experimental as well as theoretical work were performed since the development of the theory was based on modeling observable effects. The experimental work consisted of determining the three dimensional strain response due to complex stress histories at temperatures from -65°F to +150°F and superimposed hydrostatic stress-states from 0 to 1000 psi. In total over 250 experiments were run using uniaxial and biaxial volumetric dilatometers and the stress-strain-strain invariant-time history of each experiment is stored on magnetic tape and can be made available for others to use.

The program was successful in meeting its objectives and some of the program developments and conclusions are as follows. The dominant mechanisms leading to the nonlinear stress-strain response is microstructural damage in the form of the Mullins' stress-softening effect and vacuole dilatation. Reversible nonlinearities such as second order hereditary strain effects were found to be of secondary importance. These effects have been successfully modeled and combined into a relatively simple constitutive theory that works very well for fitting the distortional stress-strain behavior under complex loading conditions. This theory is a permanent memory constitutive theory and contains irreversible effects of the past history on the current response which are not included in the usual fading memory viscoelastic theories. Time effects are included in the permanent memory theory through time-dependent structural damage as well as the ordinary viscous energy dissipation. The bulk effects were also modeled and good agreement could be obtained only when the vacuole gas phase compressibility was included in the constitutive theory which resulted in a mixed stress-invariant-strain invariant representation. To handle the large masses of data generated on this contract computerized characterization techniques were developed wherein the equations could be fit to large masses of data to determine the applicability of the theory. For constant temperature conditions the theory could be fit within a standard deviation of ± 12% of the observed distortional stress data for approximately forty complex experiments using the entire response curve to failure. The overall accuracy dropped when all the temperature data was analyzed together to about ± 15%. The bulk response predictions were poorer and typical deviations were ± 25% nevertheless all of the proper trends were in the predictions and much of these errors were no doubt experimental.

TABLE OF CONTENTS

TABLE OF CONTENTS (CONT.)

TABLE OF CONTENTS (CONT.)

TABLE OF CONTENTS (CONT.)

TABLE OF CONTENTS (CONT.)

LIST OF FIGURES

LIST OF FIGURES (CONT.)

LIST OF FIGURES (CONT.)

LIST OF FIGURES (CONT.)

LIST OF FIGURES (CONT.)

LIST OF FIGURES (CONT.)

LIST OF FIGURES (CONT.)

LIST OF FIGURES (CONT.)

LIST OF SYMBOLS

a_1, A_2	Functions of temperature
a_D, a_f	Functions appearing in Schapery's equations
A_i	Constant coefficients
A_T	Time-temperature shift function
b	Constant
c	Constant
D(t)	Damage measure
E	Modulus or strain energy density
E_1, E_2, E_3	Principle strains
E_{ij}	Lagrangian finite strain measure
E'_{ij}, $E^{(D)}$	Distortional strain
f, f_1, f_2	Functions
F	Helmholtz free energy
G	Shear modulus of elasticity
G(t)	Shear relaxation modulus
$G'(\omega)$	Dynamic viscoelastic moduli, in phase component
$G''(\omega)$	Dynamic viscoelastic moduli, out of phase component
i	Subscript usually referring to directions
I_1, I_2, I_3	Strain invariants
I_d	Dilatational strain invariant
I_γ	Octahedral strain invariant
I_2', I_3'	Deviatoric strain invariants

j	Subscript usually referring to direction
J_1, J_2, J_3	Stress invariants
k	Subscript usually referring to direction, also used as summing indices
K_i	Kernel functionals
L_i	Kernel functionals
M	Constant
n, N	Number constant
$N(\tau)$	Distribution function
p, p_i	Orders of Lebesque norms
P	Pressure
P_i	Polynomials
Q_i	Generalized forces
q_i	Generalized displacements
$\overline{s}$	Standard deviation
S	Entropy or chronological time
t_k	Exposure time
t	Real time
t'	Reduced time
T	Temperature
V	Free energy
u_i	Displacements
v	Volume
V_o	Original volume

ΔV	Change in volume
V_f	Volume function
W	Work
y_i	Spatial coordinates
α_i, β_i	Exponents
ϵ, ϵ_{ij}	Small strain
$\epsilon^{(D)}$, ϵ', ϵ_{ij}'	Distortional small strain
$\bar{\epsilon}$	Mean strain
δ	Initial void content at P = 0
σ_{ij}, σ	Stress
σ_{ij}', $\sigma_{ij}^{(D)}$, σ'	Distortional stress
$\sigma_{kk}/3$	Mean pressure = $(\sigma_{11} + \sigma_{22} + \sigma_{33})/3$
$\sigma_{(Bulk)}$	Bulk component of stress
$\sigma_{(Shear)}$	Shear component of stress
τ	Strain intensity factor
τ_c	Critical strain intensity factor at failure
τ_i	Relaxation times
ξ	Dummy real time
ξ'	Dummy reduced time
ω	Frequency
λ	A bulk modulus
$\lambda(t)$	A time dependent bulk modulus

$\lvert\ \rvert$	Absolute value
$\lvert\lvert f \rvert\rvert_p$	pth order Lebesque norm = $\left\{ \int_0^t \lvert f \rvert^p \, d\xi \right\}^{1/p}$
$\lvert\lvert f \rvert\rvert_\infty$	Infinite norm = $\max_t \lvert f(\xi) \rvert$
δ_{ij}	Kronecker delta = $\begin{cases} 1 & i = j \\ 0 & i \neq j \end{cases}$

SECTION I

INTRODUCTION

This report is the final technical report submitted in fulfillment of the requirements of Contract F04611-71-C-0046 "Development of a Solid Rocket Propellant Nonlinear Viscoelastic Constitutive Theory," which was sponsored by the Air Force Rocket Propulsion Laboratory, Edwards, California. The report covers work performed by both the research team at the Aerojet Solid Propulsion Company and a research effort performed on a subcontract at Texas A&M University over the period from May 1971 through June 1973.

The technical discussion covers essentially two subject areas. The first includes the four tasks of the original work statement in the Air Force's proposal request which were associated with identifying and mathematically modeling the mechanisms causing propellant constitutive nonlinearity. In the response to this proposal request it was indicated that the original objectives had, for all practical purposes, already been accomplished in separate research efforts and that considerable progress beyond the scope of the original objectives could be realized in the same performance period. The report, therefore, is responsive to the original work statement in the proposal request and, in addition, presents the results of a considerable extension of this effort, in the opinion of the research team, forms the basis for a realistic approach to describing the response of composite propellants for general loading conditions. All phases of these constitutive developments are based on attempts to model real propellant behavior within the framework of continuum theory. The wealth of experimental data obtained on this program should make it relatively easy for other researchers to test their theories against real observations.

1. Program Objective

The ultimate objective of this effort is to develop a constitutive theory which will closely model the nonlinear time dependent behavior exhibited by solid propellants. The immediate objective of this particular program, as stated in the proposal request, was to establish the origins of, and elucidate the mechanisms for solid propellant nonlinear response. The program was to include Task I - a Literature Search; Task II - Nonlinear Mechanisms Identification; Task III - Mathematical Modeling of These Nonlinear Mechanisms, and Task IV - the Development of a Simple Constitutive Theory.

The first portion of the technical discussion covers the four tasks in the original work statement which were to satisfy the original objectives of this program. The second part of the technical discussion covers the modified and extended objectives of this program and presents an experimentally based three dimensional constitutive theory for solid propellants.

SECTION II

SUMMARY AND CONCLUSIONS

The immediate and ultimate objectives of this contract have been successfully achieved. This report demonstrates that (1) the dominating causes of propellant nonlinearity have been identified as the Mullins' Effect and vacuole dilatation, (2) these and other features of propellant response have been successfully modeled, (3) these models have been extended to three dimensional constitutive equations, and (4) the equations have been given a thorough test and proven successful.

The three dimensional theory is based on experimental observations and the constitutive mathematics was designed within the framework of continuum mechanics theory to describe the observed response. In addition to developing these equations of state it has been shown how these equations might relate to a thermodynamic energy model using Schapery's theory.

The last part of this report describes perhaps one of the most thorough experimental investigations of propellant behavior ever undertaken. Complex multiaxial experiments were conducted using gas dilatometers to obtain the three dimensional strain information required in the characterization process. These tests were conducted on pressurized uniaxial and pressurized strip biaxial specimens from -65°F to +150°F using superimposed pressures from atmospheric to 1000 psi with complex deformation-time histories involving strain reversals, multiple relaxations and various rates of pull.

The constitutive theory was then fit to large masses of experimental data incorporating the entire response curve to failure, using computerized multiaxial characterization methods developed on this contract. These data clearly demonstrate that the equations not only can contain propellant response, but they indeed do a very good job of describing the multiaxial stress-strain response to general loading conditions.

This report goes into considerable depth in describing what was done, and why it was done, to help others develop an understanding of propellant behavior. Although this program has been extremely successful there is still considerable room for improvement in both the theory and the computerized characterization techniques, mostly to make them easier to use, apply, and understand. Additional verification work and streamlining is being performed on a follow-on AFRPL contract, F04611-73-C-0060, which has just begun. In addition two dimensional finite element structural analysis codes will be developed based on the constitutive representation from this contract. Hopefully, based on the success of this continuing effort nonlinear viscoelastic grain stress analysis will soon be a reality.

SECTION III

TECHNICAL DISCUSSION

This section of the report is divided into two parts which pertain to the immediate and ultimate objectives of the proposal request.

Section 1 provides an evaluation of the four tasks of the original work statement, the requirements of which had already been largely satisfied prior to this contract. It describes and presents models of known effects which strongly influence propellant mechanical response. Included in this section is an approach to rate independent and rate dependent plasticity with no time effects, as well as viscoplasticity, since plasticity type mechanisms can and do influence propellant aging response.

Section 2 of the technical discussion describes a realistic approach to obtaining three dimensional constitutive equations for materials such as solid propellants. It is a theory based on including the effects of the models in Section 1 into a three dimensional equation of state and fitting these nonlinear models to large masses of real three dimensional stress-strain data.

1. Immediate Objective

The immediate objective is described in the RFQ as being, "to establish the origins and the mechanisms by which solid propellants obtain their nonlinear response." To achieve this goal the Air Force recommended the investigator complete the following four tasks.

Task I: A literature search covering the areas of sources of propellant nonlinearity and nonlinear constitutive theory.

Task II: The underlying microstructural mechanisms leading to propellant nonlinearity are to be identified by an experimental and theoretical examination of the information obtained in Task I.

Task III: Having identified these mechanisms, they are to be mathematically modeled with the intent of using these models as the basis for constructing a three-dimensional nonlinear constitutive theory capable of predicting propellant response.

Task IV: Having modeled the sources of propellant nonlinearity, the investigator is to construct a simple nonlinearity viscoelastic constitutive theory and a series of experiments, from which theoretical predictions can be compared with experimental results.

The objectives of Tasks I through IV, and much more have already been achieved by Farris[1,2]. Much of this work was recently accomplished during his studies at the University of Utah, 1967-1969, where the subject of both his Masters Thesis[2] and Doctorial Dissertation[1] was the nonlinear viscoelastic behavior of highly filled polymeric materials such as solid propellants. The remainder of the work was accomplished at Aerojet both before and after his academic leave of absence to the University of Utah from 1967 to 1970. The earlier work consisted of his experimental studies and theoretical models describing the dewetting phenomenon and its influence on the stress-strain-dilatational behavior of composite propellants[5,6,7] and his experimental and theoretical models predicting the influence of filler size blends on the modulus and viscosity of solid propellants.[8] Extensions and applications of the work he performed in Utah were the subject of a one year Navy contract[9] whose purpose was to develop and apply accurate and meaningful nonlinear viscoelastic constitutive equations to the stress analysis of solid propellant system in the range of no vacuole dilatation nonlinearities. Dr. Farris was the principal investigator of this program, which was completed in May 1971.

The discussion below demonstrates that the technical objectives described by the four tasks of the proposal request had already been completed. To simplify this reporting, the technical objectives described in Tasks I through IV of the proposal are reproduced in full at the beginning of each subsection below and are followed by a description of the work which, in our opinion, satisfies these goals.

(1) Task I - Literature Search

Requirement:

The contractor shall conduct a complete literature survey. In this survey he shall look for two categories of information. One, he shall be concerned with literature pertaining to the sources of solid propellant nonlinearity. He will be interested in ideas and information as to what causes the material to be nonlinear and what the mechanisms involved are. These will include such things as dewetting, particle interactions, etc. The second body of information that the contractor shall be concerned with is solid propellant type nonlinear constitutive theory. This will include both

simple and complex solid propellant material response models. In some instances the first and second category will be inseparable. This is fine since the purpose of this dual search is not to separate the material but rather to insure that both categories of information are searched for, whether together or separate. The primary aim of this task is to establish a solid foundation, based on past investigations, from which this program can proceed.

Part of the requirements of any complete masters or doctoral study is a survey of the literature pertaining to the thesis subject. Farris' three year studies on nonlinear viscoelasticity at the University of Utah included such a literature survey. It should be mentioned that besides having one of the finest engineering libraries in the western United States, the University of Utah was the origin of the Solid Rocket Structural Integrity Abstracts, (SRSIA), and during the first year of his study there, Farris was responsible for screening and selecting material to be used in the abstracts. Thus he has had the opportunity to survey practically all obtainable current work in the field of viscoelasticity and material microstructure since the literature searched for the SRSIA was very complete. He was selected for the assignment because of his broad background in propellant mechanical behavior. The results of his literature searches produced the basis for Farris' later work. The purpose of this literature search was nearly identical to that described in the RFQ and, perhaps, a little broader in scope. A systematic search was made covering:

- Theoretical works on viscoelastic constitutive theory, linear and nonlinear, such as the works of Green, Rivlin and Spencer,[10,13] Coleman and Noll,[14,18] Trusdell,[19,20] Wang,[21,22] Volterra,[23] Pipkin,[24,25] Herrmann,[26] Lianis and Coworkers,[27,29] Schapery,[30,32] Huang and Lee,[33] Dong,[34,35] Williams,[36] Tobolsky,[37,38] Alfrey,[39] Ferry,[40] and others.[41-51]

- Applications of nonlinear viscoelastic constitutive theories such as the works of Findley, Lia, and Onaran,[52-57] Gottenberg,[58] Lockett,[59-60] Valanis and Landel,[61] Lee and Huang,[33] Schapery,[31,32] Freudenthal,[62] Ward,[63-65] and others.[66-71]

- Experimental studies on the mechanical behavior of particulate filled elastomers such as the works of Schippel,[72] Payne,[73] Mullins,[74-77] Bueche,[78,79] Smith,[80] Farris,[1,5-8] Oberth,[81] Neilson,[82] Freudenthal,[83] Kelley,[84] Schwarzl,[85] Hess, and Ford,[86] and Dannenberg,[87-88], and others[3-9].

- Empirical and theoretical approaches to filler reinforcement such as the works of Einstein,[89] Brinkman,[90] Roscoe,[91] Sweeny and Geckler,[92] Robinson,[93] Fidleris and Whitmore,[94] Mooney,[95] Vand,[96] Eilers,[97] Chung,[98] Schwarzl and Coworkers,[99] Farris,[8] Oberth,[81] Hess and Ford,[86] Bueche,[78-79] and others.

- Empirical models describing the behavior of filled polymers such as the work of Mullins,[76] Bueche,[78-79] Farris,[5-8] Payne,[73] Blatz and Coworkers,[100] Fishman and Rinde,[101] and others.

(a) Results of the Literature Search

Conclusions drawn from this literature search coupled with considerable analysis are as follows.

- There are two rigorous mathematical rules a material's response must satisfy before it can be classified as linear, these are:

  HOMOGENEITY (Scalar multiplication) - If an input $\varepsilon_1(t)$ results in the output $\sigma_1(t)$, then the output to the input $b\varepsilon_1(t)$ is $b\sigma_1(t)$, where $\varepsilon(t)$ is an arbitrary strain history and b is a constant.

  ADDITIVITY (Boltzmann Superposition) - If an input $\varepsilon_1(t)$ results in the output $\sigma_1(t)$, and the input $\varepsilon_2(t)$ results in the output $\sigma_2(t)$, then the output due to the input $\varepsilon_1(t) + \varepsilon_2(t)$ is $\sigma_1(t) + \sigma_2(t)$ for all arbitrary inputs.

- Nonlinearity is defined only as the failure to satisfy one of these rules.

- It is possible for a material's response to satisfy the mathematical homogeneity condition and not obey the additivity requirement.

- The only requirement for linearity used by the propellant industry is the homogeneity rule[102,103] which in itself cannot guarantee linear response.[1,2] The use of incomplete linearity conditions is the principal reason researchers have been under the impression that propellants are linear viscoelastic materials at small strains. Farris' work clearly shows that experimentally and theoretically propellants can obey the homogeneity rule of linearity (i.e., have relaxation moduli independent of strain magnitude) and still be highly nonlinear materials.[1,2,9]

· At small strains before measurable vacuole dilatation, propellants appear to obey the homogeneity rule and fail the additivity rule.[11] Therefore, in this range of strain they have nonlinear but mathematically homogeneous constitutive equations.

· Nonlinear constitutive equations that were mathematically homogeneous had not been studied or recognized prior to Farris, hence propellants exhibited a type of behavior not studied theoretically.

· The term "viscoelastic" as applied to a certain class of materials has different meanings to different groups.

Experimentalists generally classify as viscoelastic all elastic solid materials displaying time dependent response such as relaxation and creep, no matter what the cause. (The word elastic is used here in the classical sense which means complete recovery of shape when the tractions are removed).

Theorists on the other hand generally restrict viscoelastic materials to elastic solids that possess fluid characteristics. These materials contain viscous dampening and no irreversible changes in microstructure.

· Those that recognize the need for additional classification of viscoelastic materials have come up with two terms, fading memory and nonfading or permanent memory, which are described below.

> Fading memory viscoelastic theories are valid for viscoelastic materials whose time effects are reversible such as those caused by internal viscous dampening.
>
> Permanent or nonfading memory viscoelastic theories are required for viscoelastic materials possessing additional time effects or memory phenomena not caused by internal viscosity and more permanent in nature.

· Time effects and memory phenomena in filled polymers such as propellants are dominantly caused by an essentially irreversible break down of the microstructure, i.e., elastic polymers filled with chemically inert elastic fillers often yield time dependent viscoelastic materials even though neither component exhibits any time or memory effects.

· Time and memory effects in filled polymeric materials not caused by internal viscosity have been termed the Mullins' Effect.

· The Mullins' Effect is caused by localized strain inhomogeneities produced by having near-rigid fillers embedded in a rubbery matrix. These effects were investigated rather thoroughly by Mullins in about 1947.[74-76] Mullins was very critical of the viscoelastic theories of Tobolsky and co-workers and stated these theories were not valid for filled polymers.

· Bueche modeled the Mullins' effect for the time independent case and obtained a one-dimensional constitutive equation that contained a history dependent stress softening but no time effects such as relaxation or creep.

· This stress softening due to microstructural breakdown occurs in the absence of any detectable vacuole dilatation.[1,9]

· The Mullins' effect is the step which preceeds and leads to vacuole dilatation in composite materials.

· Nearly all of the theoretical work done on viscoelastic representations has dealt solely with fading memory materials wherein all the time effects are caused by internal viscosity and no microstructural irreversibilities occur.

· Linear viscoelasticity is the simplest fading memory theory.

· Propellants and other filled polymers fall into the class of permament memory materials because it is the irreversible Mullins' effect at small strains and the irreversible vacuole formation at large strains that is controlling the response, not just internal viscosity.

· Even the most sophisticated fading memory viscoelastic constitutive theory, such as Green, Rivlin, and Spencer's theory for materials with memory, cannot accurately describe propellant response to a general input since these theories do not contain the proper types of mathematical devices needed for permanent memory materials.

· Only one theoretical approach was found that actually treated permanent memory viscoelastic behavior.[34] This approach was an abstract extension of an already abstract theory and was too general to be of direct value, however, it did aid in pointing out the deficiencies of fading memory theories and pointed out some of the problems that must be overcome if a successful theory is to be developed.

(2) Task II - Nonlinear Mechanisms Identification

Requirement:

> Taking the information collected from Task I as a starting point the contractor shall conduct a theoretical and experimental program to determine the basis of solid propellant nonlinearities. He will be looking for sources and mechanisms of the nonlinear material response. The terms sources and mechanisms refer to material activity on a microscopic level

such as polymer chain slippage, bond breaking, binder filler separation, filler cracking, etc. He will be interested in one, two and three dimensional loads as well as reasonable variety of loading histories and thermal conditions. When the contractor uses solid propellant in his investigations, the propellant employed will be the same as is being used in the Air Force sponsored Reaction Rate Failure Criterion program. The primary objective of this task is to identify the major sources of and mechanisms involved in solid propellant nonlinear material response.

Data from the literature search clearly revealed the underlying causes of propellant nonlinearity. These effects were known to occur in propellants. However, like many other things they have been ignored because no one knew how to handle them. The principle causes of propellant nonlinearities are the Mullins' Effect and vacuole formation. Other possible sources of nonlinearity are nonlinear viscosity contributions and plasticity type effects. These effects are described briefly below.

(a) Mullins' Effect

Viscoelastic materials have a "memory": that is, their present state depends upon their entire past history. Nearly all of the integral viscoelastic constitutive theories used to date for polymeric materials such as solid propellants are based on the concept of "fading memory." This means that a material is more sensitive to its immediate past than to their distant past. A physical interpretation of fading memory constitutive laws, both linear and nonlinear, indicates that such materials tend to forget the distant past. This theory implies no permanent change in microstructure, or damage caused by the deformation. A fading memory material can undergo no irreversible changes in structure and can be thought of as attributing the time effects, such as relaxation and creep, to internal viscosity.

There is considerable evidence that all the hysteresis effects observed in propellants and most of the viscoelastic behavior are caused by the time dependent failure of the polymer on a molecular basis and are not due to internal viscosity.[1,2] At near equilibrium rates and small strains, propellants exhibit the same type of hysteresis that many lowly filled, highly crosslinked rubbers demonstrate at large strains.[1] This phenomenon is called the "Mullins' Effect" and has been attributed to micro-

structural failure. Mullins postulated that a breakdown of particle-particle association and possibly also particle-polymer breakdown could account for the effect.[74-77] Later Bueche[78,79] proposed a molecular model for the "Mullins' Effect" based on the assumption that the centers of the filler particles are displaced in an affine manner during deformation of the composite. Such deformations would cause a highly non-uniform strain and stress gradient in the polymer between particles, especially in the direction of stretch. He assumed that polymer chains attached themselves at both ends to neighboring filler particles and that these chains ruptured when the particles were separated enough to extend the chains to near their full elongation. He derived a model from which he could calculate the difference in stress levels at a given elongation for the first and second stretching cycles.[78] It is this type of model that is generally accepted as being representative of the molecular behavior which causes the "Mullins' Effect". Figure 1 illustrates this behavior for repetitive stretching to increasing strain levels. In highly crosslinked rubbers, the effect only depends upon strain and is generally irreversible.[74,77] However, if the prestressed composite is allowed to rest for long times in the relaxed state, a portion of the original stiffness might be regained.[74-77,84] This recovery or rehealing appears to be a complex function of the recovery temperature and time, nevertheless, it can and does greatly influence the materials behavior.

All of the theoretical and nearly all of the experimental work done in studying this phenomenon has been on materials similar to the rubber found in automobile tires. These are highly crosslinked rubbers that are usually filled to about 20 volume percent with very fine carbon black. Propellants, on the other hand, are lowly crosslinked and highly filled with coarse particles. The relative particle spacing is consequently much more severe and the polymer chains are on the average hundreds of times longer in propellants than in tire rubber. The probability of finding a larger portion of the chains connecting particles would be greater in propellants and the effect therefore should be much stronger and occur at smaller strains,[1] but the same basic mechanism proposed by Bueche still applies. This polymeric chain failure is therefore the step which precedes the vacuole formation process which causes the stress and dilatational nonlinearities observed at larger strains.[5-7] Multiple stretch data on propellants at large strains with and without a superimposed pressure environment demonstrate that propellants also exhibit the Mullins' type hysteresis at large strains in the absence of measurable dilatation.[81]

The time independent "Mullins' Effect" can account for the near equilibrium hysteresis observed in propellants at low strains, but cannot account for the nonlinear time effects.[1,2,103] There is considerable evidence, however, that the Mullins' Effect in propellants is a very strong function of time.[1,2,103] Time dependent chain failure can be readily demonstrated by simply examining some of the routine tests run on solid propellants and also examining the influence of filler on the viscosity of a given polymer.

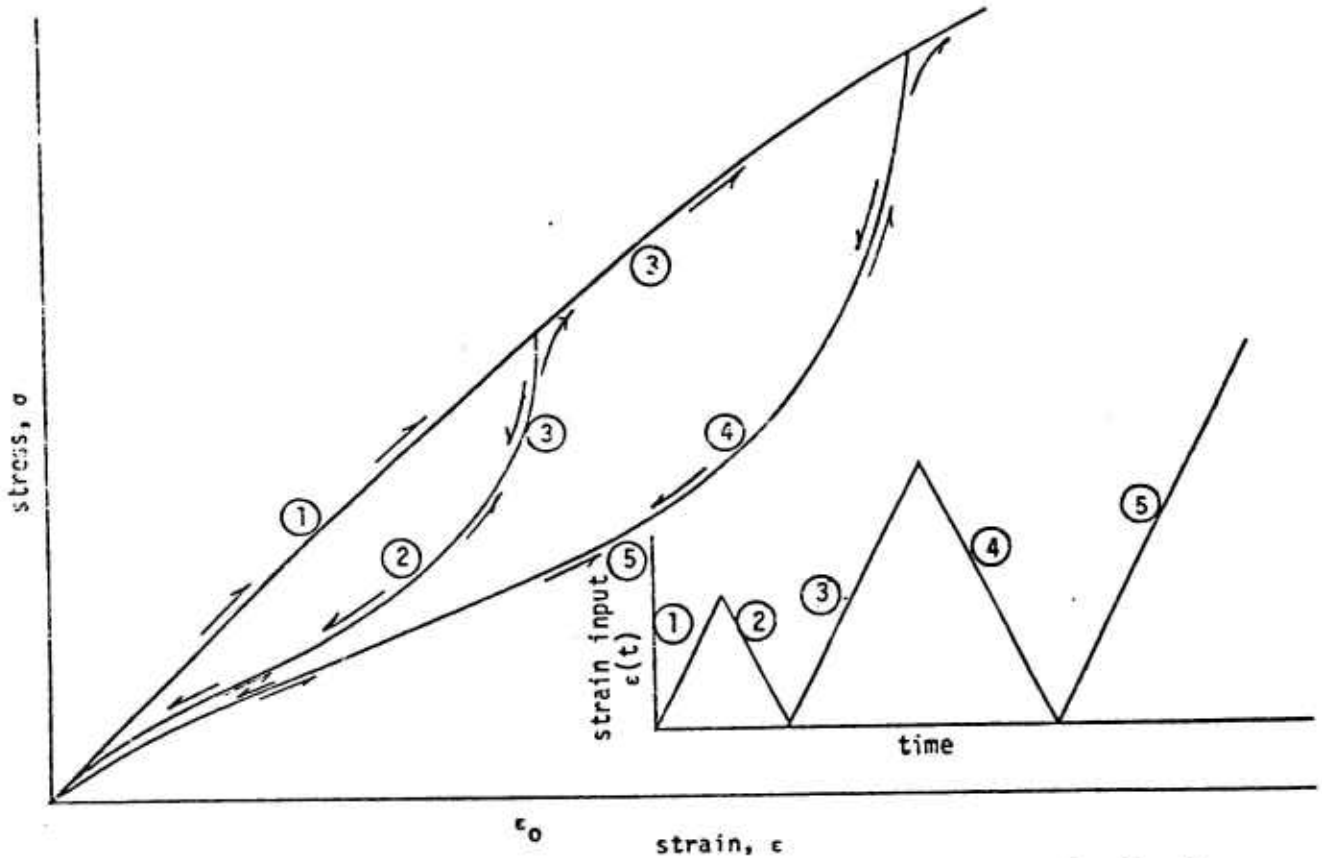

Figure 1

Typical propellant equilibrium stress strain behavior when the direction of strain is reversed.

One of the simplest ways of demonstrating a time dependent Mullins' Effect is through the strain endurance test. In this test, a sample is strained to some level and held there for several days or longer. The only measurement taken is the time to failure, if the sample fails within the test period. The point of interest here is that samples fail while held at conditions of constant strain when the stress is slowly relaxing or at most constant. This type of failure is clear evidence of a time dependent Mullins' Effect and also demonstrates that some portion of the time dependent stress relaxation must be due to chain failure.

Another example of a time dependent Mullins' Effect is that of a lowly crosslinked polymer, with little or no time dependency when unfilled, which becomes significantly time dependent when filled,[83] as shown in Figure 2. The more filler incorporated into the system, the more marked the time effect. Many propellant polymers fall into this category and nearly all propellants show time dependence over such long times that true equilibrium data cannot be obtained. This time dependence in the composite material and no time dependence in the unfilled polymer cannot be explained by the argument that the polymeric strain rates are higher in the composite than in the pure polymer since the time effects continue for such long times, and many propellant binders show no time dependence even at very short times.

Tests such as those described above indicate that the constitutive equations and degree of microstructural damage must be highly coupled effects. One of the existing concepts now being used to predict failure in propellants calculates the state of stress using fading memory constitutive theory and then uses these calculated stresses in cumulative damage relations to predict failure.[104] The assumption that the degree of damage and the constitutive equation are uncoupled can only lead to erroneous results for materials exhibiting the Mullins' Effect.

The Mullins' Effect occurs in propellants at very small strains and experimental evidence[83] indicates that a majority of the time dependency in propellant-like materials can be attributed to this phenomenon. Mullins himself criticized Tobolsky's spring-dashpot viscoelastic theory saying it was unjustifiably applied to filled polymers and would provide misleading results. All of the recent work going on in the propellant business demonstrating the inadequacies of linear and nonlinear viscoelastic predictions are doing nothing more than reverifying Mullins' conclusions which were made in 1947. Clearly anyone familiar with the mechanical behavior of composite propellants who reads Mullins' papers will immediately recognize that propellants exhibit the same type of mechanical behavior and the same memory mechanisms as the materials Mullins examined. The only real difference between propellants and the lowly filled materials Mullins examined is filler content and the crosslink density of the polymer, however each of these factors should and do cause the Mullins effect to occur at much lower strains and be more dominant in propellant like materials.

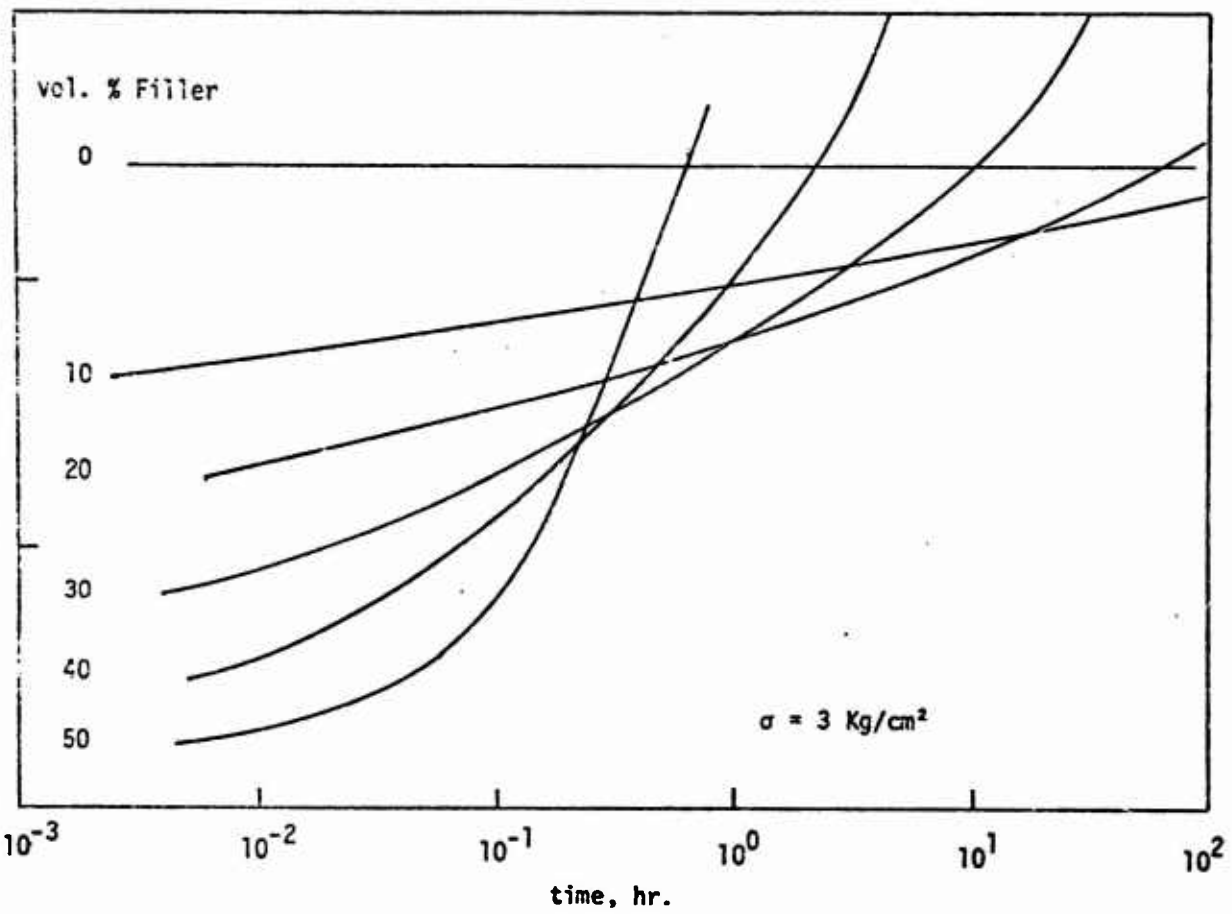

Figure 2

CREEP OF SODIUM CHLORIDE FILLED POLYURETHANE RUBBER.

(b) Vacuole Dilatation

As mentioned above, the Mullins' Effect contributes strongly to the nonlinear and time dependent behavior of composite propellants in the ranges of strain prior to any detectable vacuole dilatation, or at high pressures which suppresses volumetric dilatation in soft propellants. At larger strains, after sufficient microstructural damage has occurred, vacuoles begin to form in the polymer or at the polymer-filler interfaces causing further stress softening. These vacuoles naturally must form in the zones of maximum damage which would depend upon the local polymeric composition, bond strengths, local packing characteristics, local distribution of chain lengths and many other unknown factors.

The strong influence of vacuole formation on the stress-strain behavior of composite propellants can best be appreciated when one understands that the process by which these materials fail is initiated early in the stress-strain history by the formation and growth of vacuoles which cause a dilatation of the composite material, a loss in filler reinforcement and, hence, a nonlinear response and in general a physically unstable material. Efforts have been made to understand this phenomenon since it was first discovered by Schippel[72] in 1919 while he was studying the behavior of filled vulcanizates. Since then other investigators have verified Schippel's findings on solid propellants and other polymeric systems containing fillers of various kinds.[5-7,73,80,81,105]

The influence of these vacuoles on the stress-strain behavior was not directly assessed until Farris developed the gas dilatometers which permitted the stress, strain, and volumetric behavior to be measured simultaneously over a broad range of test conditions including wide ranges of strain rate, pressure, and temperature.[5] Since then Farris[5-7] and others[101,105] have demonstrated that the yielding nature in the stress-strain behavior is coincidental with vacuole formation. Farris later developed models to interpret the dilatation-strain behavior in terms of the frequency of vacuole formation. He also derived simple stress-strain-dilatation functions which assumed the instantaneous modulus was linearly related to the volume fraction of solids particles entering into the vacuole process. These models agree very well with experimental data and have been widely accepted[7] and expanded upon,[106] and form the basis for some of the cumulative damage work going on in the industry today. Like the Mullins' effect, which eventually leads to the vacuole formation stage, the vacuole formation process has never been considered in propellant grain stress analysis because no one knew how to handle the problem, although the influence of volumetric dilatation on the stress-strain behavior is well known. Figures 3 through 6 are included to demonstrate the strong influence dilatation has on propellant behavior. The stress-strain-dilatation behavior of three typical Aerojet propellants (Figure 3) demonstrates that the yielding nature of the stress-strain curves is coincidental with the volumetric increase. The influence of temperature on the stress-strain-dilatation behavior of one

STRESS-STRAIN-DILATIONAL BEHAVIOR OF THREE HIGHLY FILLED POLYURETHANE PROPELLANTS

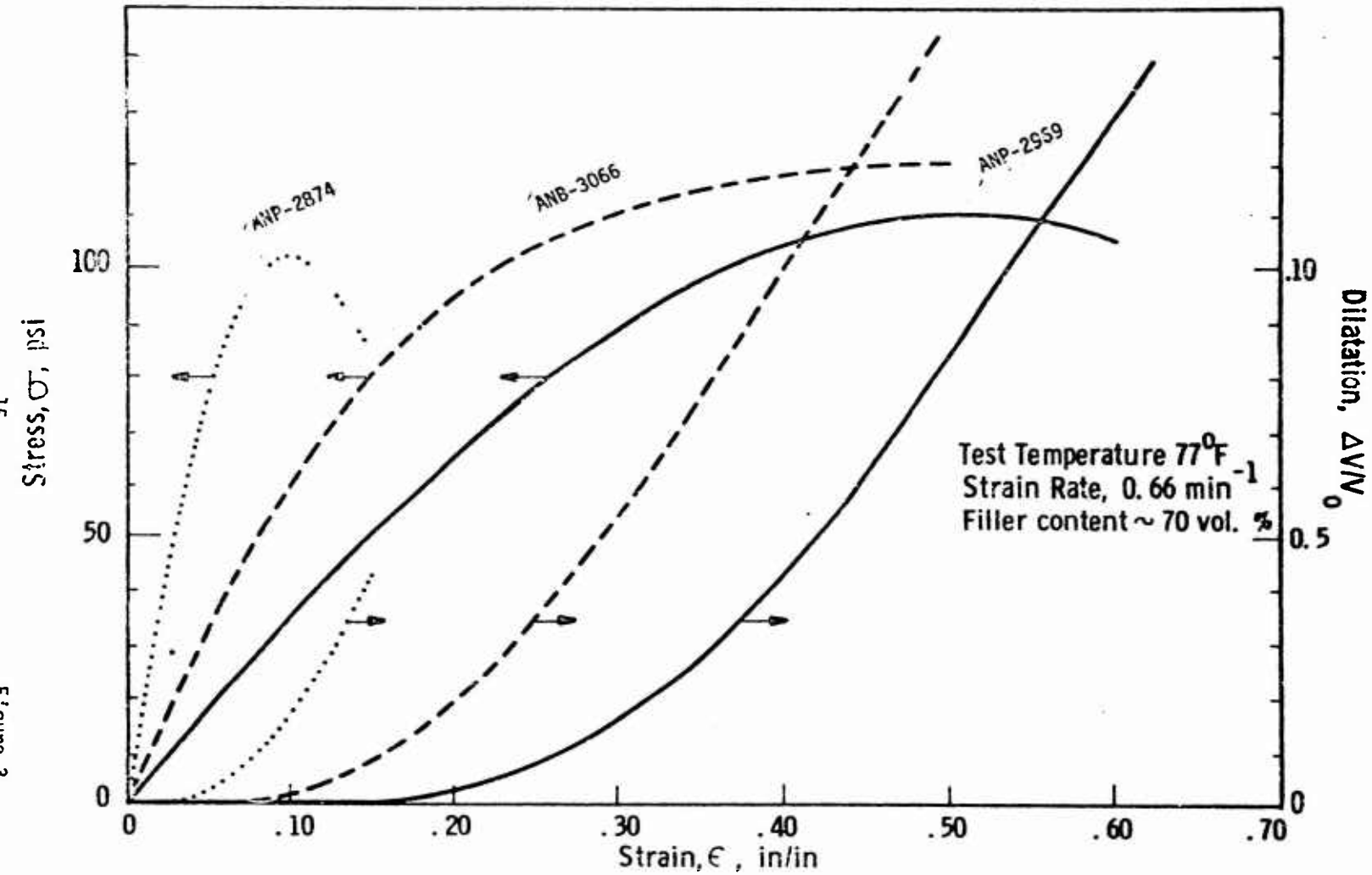

Figure 3

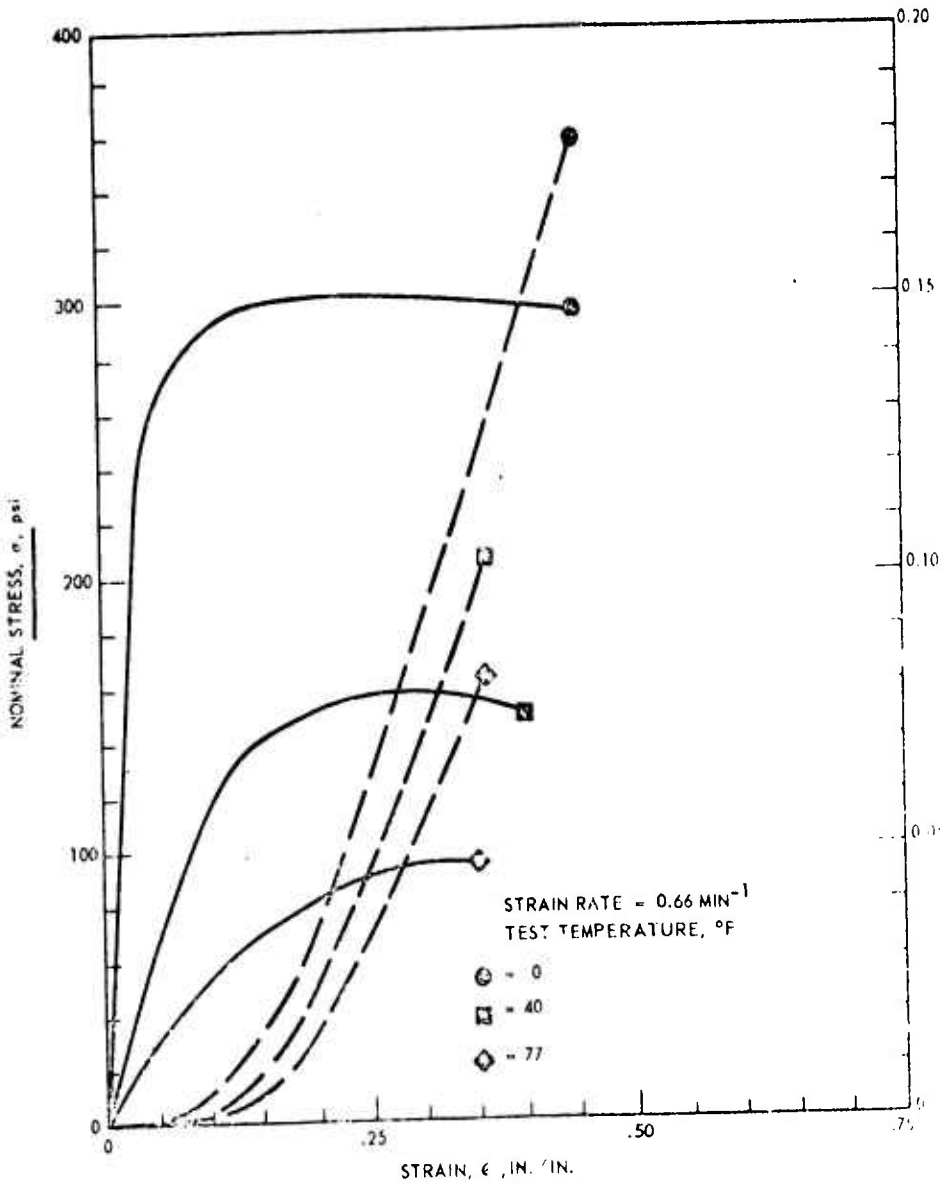

EFFECT OF TEMPERATURE ON THE STRESS-STRAIN-DILATATION BEHAVIOR OF ANP 2862 PROPELLANT

Figure 4

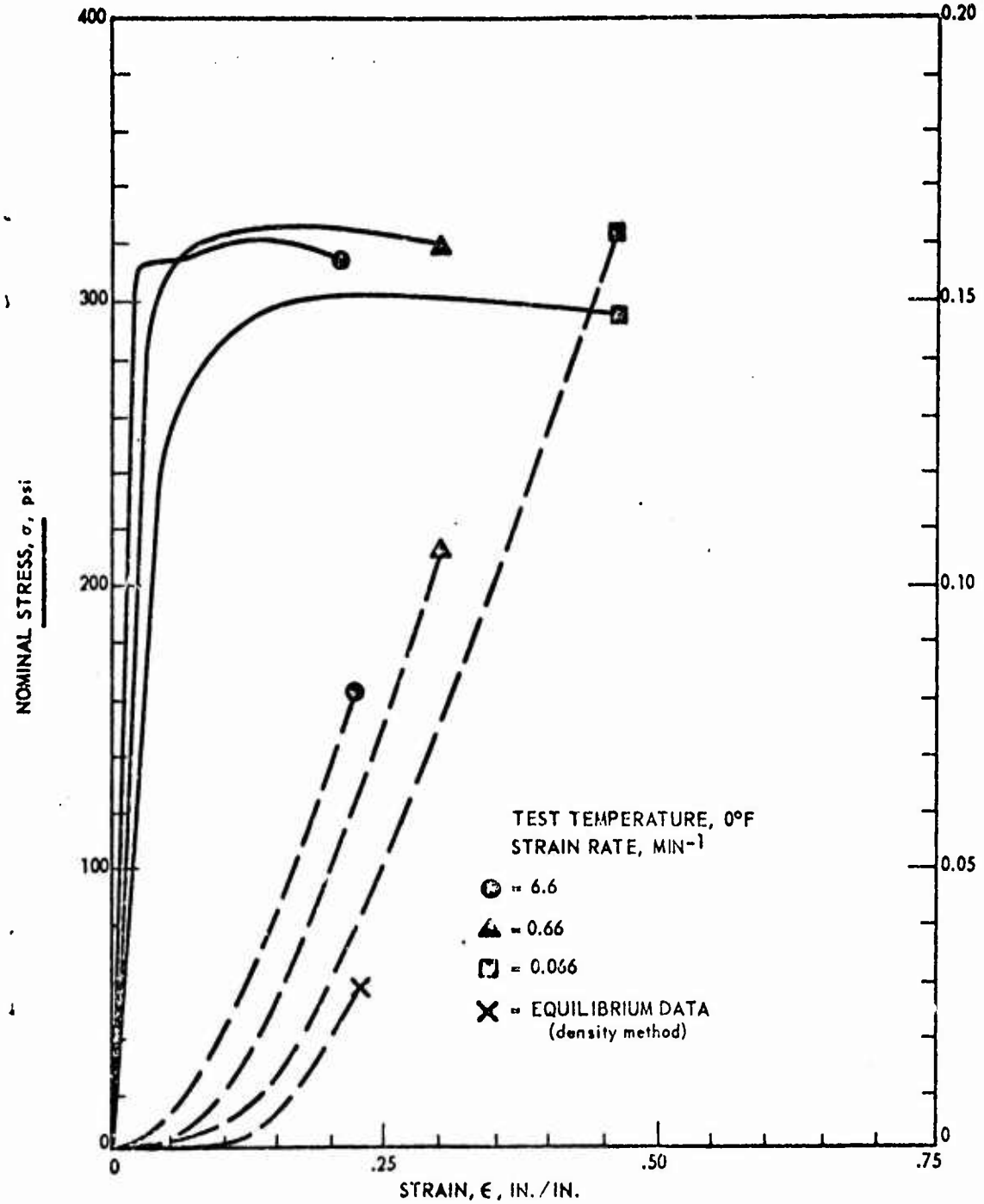

EFFECT OF STRAIN RATE ON THE STRESS-STRAIN-DILATATION BEHAVIOR OF ANP 2862 PROPELLANT

Figure 5

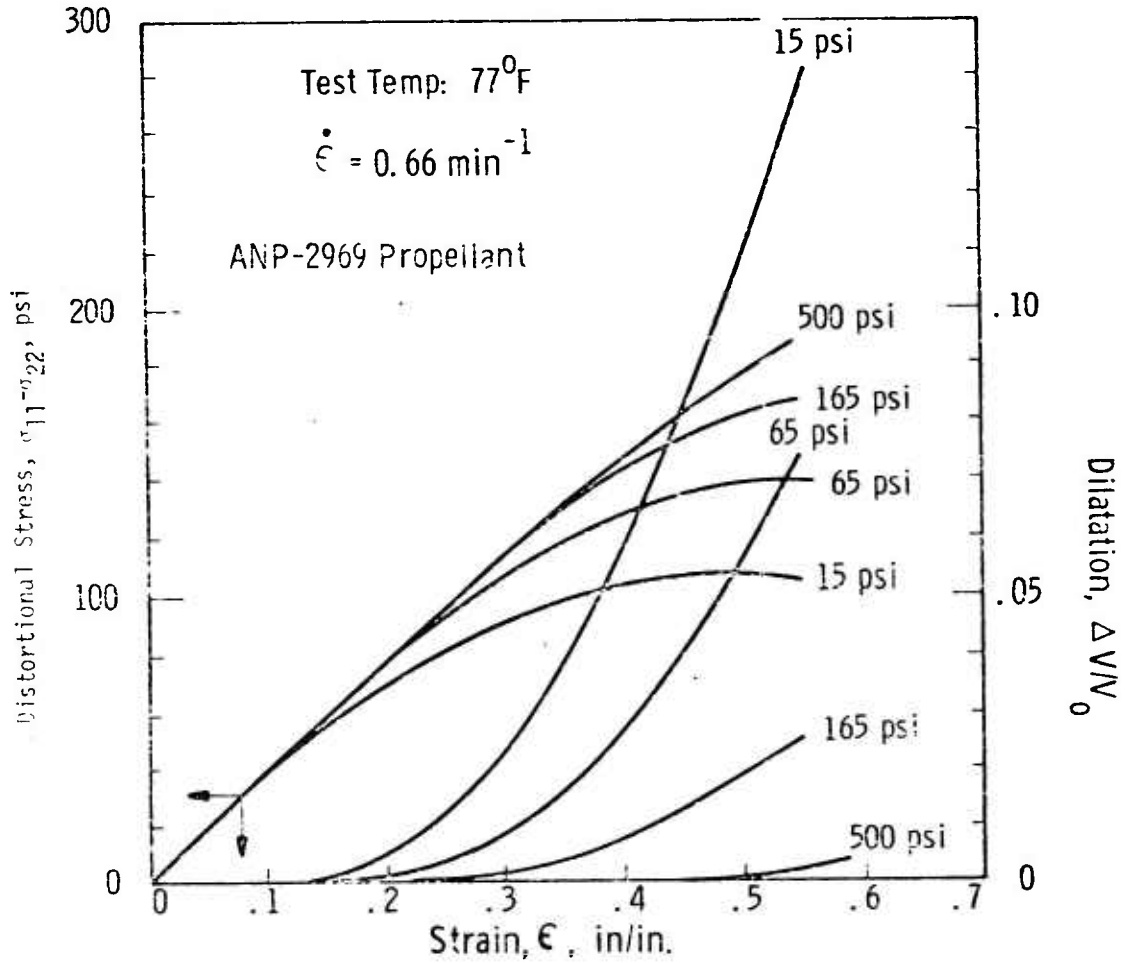

Figure 6

MEASURED STRESS-STRAIN AND DILATATION-STRAIN BEHAVIOR OF A HIGHLY FILLED ELASTOMER (63.5 VOL. %) AT A SERIES OF HYDROSTATIC PRESSURES

propellant, ANP-2862, tested at constant strain rate is illustrated in Figure 4. Strain rate also is a significant factor as shown in Figure 5. Figure 6 illustrates the influence of a superimposed hydrostatic pressure on the distortional stress-strain-dilatation behavior of ANP-2969 propellant. In all of these materials yielding, and hence additional nonlinear response, is coincidental with the volumetric increase. Further the degree of yielding depends on the amount and rates of volumetric increase in a simple way.(7)

Again it should be emphasized that prior to measurable dilatation propellants are still highly nonlinear materials. This earlier nonlinearity is caused by the earlier stages of the Mullins' effect whereas the vacuole dilatation can be looked upon as being the final stages of the Mullins' effect. Altogether, microstructural degradation at small strains in the absence of volume change and vacuole dilatation at larger strains, the Mullins' Effect, dominates the mechanical and failure behavior of composite solid propellants. Without a doubt the Mullins' effect and subsequent side effects are the chief sources of nonlinearity in all highly filled polymeric materials.

(c) Reversible Nonlinearities

As described in previous sections, a large portion of propellant nonlinearities can and must be attributed to the Mullins' Effect and vacuole formation. There is, however, evidence of some nonlinearity due to reversible, time-dependent mechanisms of the type existing in unfilled amorphous polymers. This time-dependence is usually due to internal viscosity; i.e., the resistance of the long chain-like molecules to relative internal motion. Another reversible source of time-dependence is known to exist in polysulfide rubber wherein chemical bonds break and reform at equal rates; stress relaxation under constant strain, for example, occurs because stressed bonds break and then reform in such a way that the reformed bonds do not support any stress.(37) These mechanisms give rise to nonlinear viscoelastic stress-strain behavior when the polymer is under large strains.

Although the applied strains on a propellant specimen may be small, internal strain concentrations due to the filler particles can produce, of course, high matrix strains and consequent overall nonlinear response due, in part, to reversible mechanisms.

Some of the propellant data to be discussed later shows that (1) under increasing or constant strains the reversible effects are relatively small; (2) they may be significant during recovery or decreasing strain histories; and (3) they are significant under small amplitude vibrational straining, with or without a superposed static strain.

(d) Plasticity Effects

Plasticity effects cannot be excluded from propellant response, in fact there is considerable evidence indicating it should be included as a part of aging. As an example of plasticity effects in cross-linked amorphous-polymers the reader is referred to the fine work of Tobolsky et al[37] on chemical stress relaxation and permanent set. In their studies it was found that suffering 100% permanent set was not uncommon for otherwise elastic polymers when they were strained and exposed to elevated temperatures for short times or modest temperatures for long times. Even though these materials suffered large permanent set they did not necessarily have different response properties after exposure which to some would indicate "no aging." Similar data is easy to obtain on propellants and just as shown by Tobolsky nearly 100% permanent set is observed on high temperature exposures such as 180°F for a few weeks or exposure at 275°F for two days.

According to Tobolsky these effects are caused by continuous changes occurring in the polymer in the form of chain scission and reformation. Equal rates of breaking and forming bonds results in no change in response properties (i.e. no apparent aging) yet results in large degrees of permanent set. Polysulfide rubbers have natural chemical exchange reactions, according to Tobolsky, leading to this effect. If the rate of scission is higher than the rate of reformation a softening type aging phenomenon is observed. Naturally if the rate of scission is slower than the rate of formation of chains then a hardening type aging is observed. These effects are important in rocket grain stress analysis since large changes in stress-free temperature can occur if plastic rather than elastic behavior is characteristic of the propellant. Post cure and other effects occurring in the strained state will definitely lead to plastic type behavior in propellants which can negate all types of elastic analyses.

(3) Task III - Mathematical Modeling

Requirement:

> With the establishment of the major contributive sources of nonlinearity in solid propellants, and the mechanisms by which they contribute, the contractor shall attempt to mathematically model these mechanisms. In his mathematical modeling the contractor shall strive for simplicity and accuracy. In deriving his models the contractor shall test these mathematical models with further experimentation, if necessary, to insure their validity.

The material provided below demonstrates that mathematical models already exist for the Mullins' Effect, vacuole formation, nonlinear viscosity effects, and plasticity effects. These models are well established and all have been used in nonlinear constitutive theories that have shown excellent agreement with the behavior of real propellants. The discussion below goes into a fair amount of detail describing these models and the types of behavior they contain, however, considerably more detailed derivations and descriptions exist in the original works.

(a) Mullins' Effect

There have been various models and mechanisms proposed for the "Mullins' Effect". Bueche proposed a model based on chains failing due to physically non-homogeneous local deformations.[78,79] His model was not sufficiently general and included no time effects, only strain history effects. In this section a general one-dimensional model will be developed for the time dependent "Mullins' Effect"which clearly demonstrates the coupling between the constitutive equation and the degree of damage. The model provides insight into the mechanism of behavior and indicates key variables or measures that should be used in the general multidimensional constitutive equation. Before proceeding, it would be wise to clarify the main differences between filled and unfilled polymers. The equilibrium constitutive equation for crosslinked amorphous polymers has been developed from the statistical theory of rubber elasticity assuming ideal rubber behavior.[107] There are six basic assumptions made in the development of the statistical theory of ideal rubber behavior. They are:

- There is no change in internal energy with isothermal deformations.
- The end-end displacement of a polymer chain is small compared to its actual length.
- The relative end-end displacements (λ_x, λ_y, λ_z) of all polymer chains in the system are equal for homogeneous motions.
- The relative chain deformations occurring microscopically are the same as the deformation of the body for homogeneous motions.
- There is no interaction between polymer chains
- A polymer chain never fails.

These assumptions dictate that the configurational entropy associated with a polymer chain be given by a Gaussian distribution and enable simple addition of the contributions of each chain. The Gaussian distribution is only valid for end-end chain displacements that are small compared to the actual chain length since they actually allow for end-end displacements from zero to infinity.[107] Corrected configurational statistics for large deformations provide what is called the Langevin Function.[107] The Langevin Function provides the correct configurational entropy since it limits the end-end separation of a chain to the chains actual length.[107] The Gaussian distribution appears as the first term in the Langevin Function which is essentially a virial expansion. The main difference between these two distributions is the force-deformation relation they give for a polymer chain[107] which is illustrated in Figure 7. The great stiffening experienced when a chain is near full extension can be simply observed by stretching a rubber band to failure.

The main difference between filled and unfilled systems is that even under equilibrium conditions the relative end-end displacement of all polymer chains in the system are not equal. Instead one finds, by any form of analysis, that the local strains in a filled system subjected to a physically homogeneous deformation are a very strong function of filler content, position, particle shape, and the distribution of chain lengths. The prime reason for the physically nonhomogeneous local deformations of the polymer is that the centers of the filler particles must undergo near affine or similar deformations since they are rigid and cannot occupy similar positions at the same time. The polymer being highly extensible and mobile is forced to undergo large variations in local strain. It is therefore not valid to assume the force contribution of each chain is similar, nor is it valid to assume the end-end displacements are small since very large strains can occur locally. Even small macroscopic strains can cause some fraction of the material to undergo very large local strains. For such conditions it is valid to assume that a chain will fail if some critical condition is exceeded. It is this type of localized failure that causes the Mullins' Effect in filled polymers. Such failure must preceed vacuole formation which is common in filled polymers. This behavior can be modeled for one dimensional behavior in a fairly general way by making the following assumptions:[1]

- The relative axial deformation of any given polymer chain is proportional to the axial applied strain, the proportionality constant differing from chain to chain.
- Each polymer chain has the same elastic, but not necessarily linear, stress-strain law.
- Each polymer chain fails and remains failed if at any time in its history some failure criterion is exceeded.

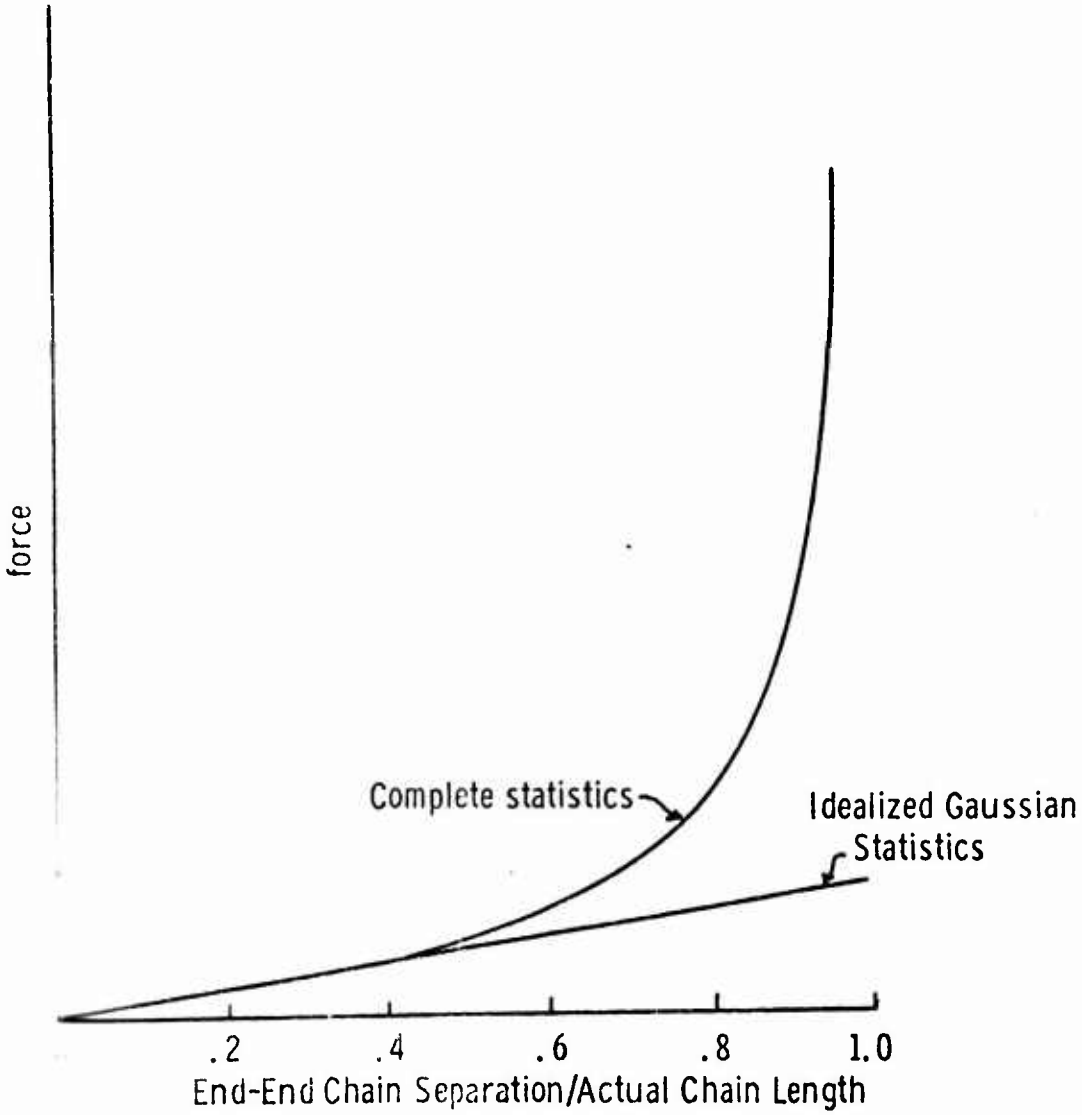

COMPARISON BETWEEN FORCE DEFORMATION BEHAVIOR OF A POLYMER CHAIN USING GAUSSIAN STATISTICS AND LANGEVIN STATISTICS.

Figure 7

In these assumptions physically non-homogeneous local deformations, a non-linear stress-strain law for each element, and the possibility of having some of the elements fail have all been taken into account. Since the desired end result of this work is accurate constitutive relations for materials exhibiting permanent memory phenomenon that can be used in engineering analysis, emphasis will be placed on the behavior of elements, not necessarily on polymer chains. The resulting equations appear to be of value for describing many materials, not only filled amorphous polymers.

(b) Life Fraction Cumulative Damage Models

Life fraction cumulative damage models have been used to describe time dependent failure, and other processes, for materials subjected to variable histories when the failure behavior for a constant nonvarying history is time dependent. These theories are based on what some term Miner's Law[108] or Robinson's life fraction hypothesis[109]. The logic behind the approach is very simple and is simply a way of accumulating what some have defined as damage or a damage factor. If the time to failure for a sample subjected to a constant strain of ε_1 is t_{f1}, then the damage factor for an identical sample subjected to the same strain ε_1 for a time t is defined as (t/t_{f1}). When the damage factor accumulates to unity one naturally expects the sample to fail. This method really adds nothing to predictions at constant history, but what is important is that it provides a reasonable means of predicting failure when one sample is subjected to a variable history. This can be accomplished by simply accumulating the damage for each strain increment as

$$D(t) = \sum_{k=1}^{n} (t_k/t_{fk}) \qquad (1)$$

Here the t_k is the time the sample spent at strain level ε_k and t_{fk} is the time to failure for the constant history of strain level ε_k. This line of reasoning can be simply generalized to include temperature, humidity, and other factors by simply expressing t_{fk} as a function of these variables. This method of failure prediction has been quite successful in a number of applications including solid propellants. Naturally the technique is not restricted to strain, but can be expressed in terms of stress, or in the case of multiaxial states principle values or invariant forms can be used. For the purposes here, however, a strain formulation will be used. This greatly simplifies the problem since the desired end result is to express stress-state in terms of some functional of the strain history, thus stress will appear only on one side of the resulting equations. If the intent was to express strain in terms of stress history then a stress cumulative damage formulation would be simplest. Again however it should be emphasized that since the elements in the formulation were assumed elastic and have no time effects, knowing the strain provides the stress in the element, hence the two formulations are exactly equivalent. Also it should be pointed out that the simplest way to express the damage relation is by an integral representation rather than a summation. The two forms are equivalent but the integral representation is much easier to use and is given by

$$D(t) = \int_0^t d\xi / g(\epsilon(\xi)) \tag{2}$$

where $t_{f_k} = g(\epsilon_k)$ and ξ is dummy time

(1) Determination of Chain Failure

The first assumption, that the internal local strains $\epsilon_i(x_j,t)$ are proportional to the applied strain $\epsilon(t)$ by the proportionality factor $\tau_i(x_j)$ which differs from element to element can be expressed mathematically as

$$\epsilon_i(x_j, t) = \epsilon(t)\tau_i(x_j), \tag{3}$$

where ϵ_i = axial strain in the i^{th} element

ϵ = applied axial strain

τ_i = strain intensity factor for the i^{th} element

x_j = spatial coordinates, j = 1,2,3

Assuming for the moment a power law strain-time to failure relation when the strain history in the k^{th} element is constant gives

$$t_{fk} = c|\epsilon_k|^{-p} \tag{4}$$

where $|\ |$ denotes absolute value or magnitude, and p and c are constant values which are material properties.

The damage equation for the k^{th} element now becomes

$$D_k(t) = \sum_{k=1}^{n} \frac{t_k}{t_{fk}} = \frac{1}{c} \sum_{k=1}^{n} t_k|\epsilon_k|^p \tag{5}$$

or equivalently in our integral representation as

$$D_k(t) = \frac{1}{c} \int_0^t |\epsilon_k(\xi)|^p d\xi \tag{6}$$

where ξ = dummy time

Recalling that $\varepsilon_k(t)$ is the local strain in the k^{th} element and is related to the applied strain $\varepsilon(t)$ by $\tau_k(x_j)\varepsilon(t)$, Equation (6) can be rewritten as

$$D_k(t) = \frac{|\tau_k|^p}{c} \int_0^t |\varepsilon(\xi)|^p \, \xi d \qquad (7)$$

Since failure occurs when $D_k(t) = 1$, this equation can be solved to determine what value the intensity factor, $\tau_k(x_j)$, must take on so that failure of that element occurs at the current time t. Doing so finds the critical value of τ_k at the current time t. Naturally any elements having intensity factors greater than τ_k will have already failed and those having lesser intensity factors have not yet failed. This critical value of τ_k which for convenience will be called τ_c and becomes

$$|\tau_c| = C^{1/p} / \{ \int_0^t |\varepsilon(\xi)|^p \, d\xi \}^{1/p} = C'/||\varepsilon||_p \qquad (8)$$

where $C' = C^{1/p}$

and $||\varepsilon||_p = \{ \int_0^t |\varepsilon(\xi)|^p \, d\xi \}^{1/p} = p^{th}$ order Lebesque Norm.

At this point perhaps it is best to recall physically just what has been accomplished in our model. Mathematically our model allows for an arbitrary local strain gradient between filler particles caused by the near rigid filler particles embedded in a soft polymer matrix. A simple physical picture of our model would be nearly identical to that proposed by Bueche and is illustrated in the sketch below.

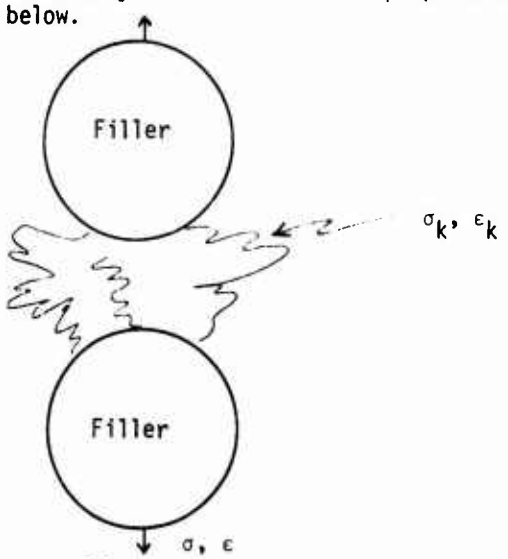

In this sketch $\sigma_k(t)$ is the stress in the k^{th} chain element and $\varepsilon_k(t)$ is the strain in the k^{th} element. The strains differ from element to element but are proportional to the overall sample strain $\varepsilon(t)$, the proportionality factor τ_k differing from chain to chain. A simple power law cumulative damage failure hypothesis was assumed valid for these elements and has determined that all chains having intensity factors greater than τ_c have failed and those with lesser intensity factors are still contributing to the state of stress, hence if

$$\tau_k \geq \tau_c \text{ element has failed} \qquad (9)$$

$$\tau_k < \tau_c \text{ element still exists}$$

where $|\tau_c| = C'/||\varepsilon||_p$

Note that nothing has been stated about the stress-strain behavior of the composite material, only applied critical conditions on the annihilation of elements. This upper bound of the intensity factor is a functional of the strain history of the element. It allows the element's failure to be functionally dependent on time and strain magnitude at constant temperature which is very similar to an absolute reaction rate mechanism.

(2) Influence on Stress-Strain Behavior

The stress-strain behavior of the sample is determined by adding the stress contributions of each chain in the appropriate manner to satisfy one dimensional equilibrium. Thus the total sample force, which is the stress times the area, must be equal to the sum of the microscopic forces. This equilibrium relation can be expressed mathematically as

$$\sigma(t) = \frac{1}{A} \sum_{i=1}^{n} \sigma_i(t)\, A_i \qquad (10)$$

where $\sigma(t)$ = observed stress on sample

A = sample area

$\sigma_i(t)$ = stress in i^{th} chain

A_i = area of i^{th} chain

Nothing has been said yet about the local stress-local strain function other than it was assumed to be elastic. Assume this local stress-strain function is the arbitrary but monotonic function $f(\epsilon_i)$, given in the sketch below.

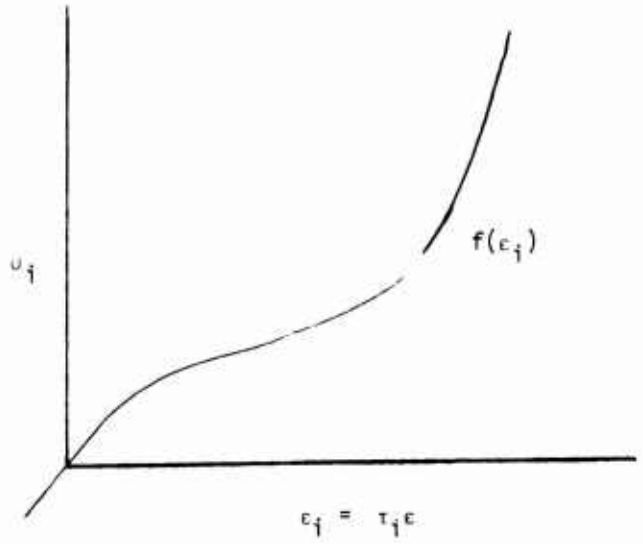

Now at any instant in time the applied strain on the sample is constant, however, since each element can have a different intensity factor, each element is at a different point on its stress-strain curve, and naturally some have failed according to the damage hypothesis. This behavior is precisely what happens in solid propellants. Substituting $f(\epsilon_i)$ for the local stress σ_i and $\tau_i\epsilon$ for ϵ_i in $f(\epsilon_i)$ Equation 10 becomes

$$\sigma(t) = \frac{1}{A} \sum_{i=1}^{n} f(\tau_i \epsilon)\, A_i \qquad (11)$$

where the summation only extends over the surviving elements.

Just as before Equation (11) can be more conveniently expressed in an integral form using distribution theory as

$$\sigma(t) = \int_{b}^{\tau_c(t)} N(\tau) f(\tau\epsilon) d\tau \qquad (12)$$

where $N(\tau)d\tau$ is the fraction of elements in a unit cross-section having intensity factor between τ and $\tau + d\tau$, and b is some arbitrary lower limit of τ and our upper limit is naturally τ_c.

Substituting the previously found relation for $\tau_c(t)$ the simple stress-strain relation becomes

$$\sigma(t) = \int_b^{C'/||\varepsilon||_p} N(\tau)\, f(\tau\varepsilon)\, d\tau \qquad (13)$$

Equation (13) is valid for any local stress-strain function and any distribution of strain intensity factors providing the failure criteria is by a power law cumulative damage rule. The equation can easily be generalized however to even account for more complex behavior. For example, the microstructure might be composed of m different species with local properties b_ℓ, C'_ℓ, P_ℓ, $f_\ell(\tau\varepsilon)$, and $N_\ell(\tau)$ and the total behavior would simply be

$$\sigma(t) = \sum_{\ell=1}^{m} \int_{b_\ell}^{C'_\ell/||\varepsilon||_{p_\ell}} N_\ell(\tau)\, f_\ell(\tau\varepsilon)\, d\tau \qquad (14)$$

Another possibility is that perhaps the simple power law representation was not general enough to define failure. Again this poses no great problem since p^{th} order Lebesque norms can be used to approximate any monotonic function, thus one might find by some other means of analyses that

$$\tau_c(\tau) = C_1/||\varepsilon||_{p_1} + C_2/||\varepsilon||_{p_2} + C_3/||\varepsilon||_{p_3} + \ldots \qquad (15)$$

This relation, just like Equation (8) can be used in Equation (12) to provide another stress-strain functional. Therefore, it is seen that models of the sort described above are quite general. Models however are only useful in providing key measures that should be used in more general relations. In this case one finds L_p norms are pertinent parameters. Models can be complicated greatly to attempt to account for three dimensional and other effects, however, they nearly always become so cumbersome they lose all their value. For example, even to approximately determine $N(\tau)$ analytically for our simple one-dimensional model would require having to know the distribution of chain lengths, the filler content, the particle

shapes, the local packing characteristics and then use these parameters combined with some very sophisticated statistical assumptions in an approximate analyses. Now even the simplest of these questions is impossible to answer using our most sophisticated technology. To go to three dimensional models requires concern with orientation of the chains and numerous other factors that have filled texts on polymer chain configurational statistics that few if any analysts understand. To be effective, models must be simple. When simple models predict correctly one can be reasonably sure the assumptions going into the model are correct. For constitutive theories models generally tell you what measures to use in more general equations. For example the one-dimensional, generalized Kelvin or Maxwell spring dashpot models indicate the relaxation modulus is a key parameter. Imagine solving exactly by models a three dimensional assembly of springs and dashpots oriented arbitrarily. Besides being a near impossible task even for the most sophisticated of mathematicians, the model does not have much physical appeal either. What one does however is to include the essential features of the simple model in a more general approach and thus from models one can arrive at three dimensional linear viscoelasticity. The same equations can be arrived at by other means but these are usually after the fact and require more sophisticated explanations that took years to develop. Generally they never would have been developed if it were not for the simplified models. Few scientific theories are based on pure abstract thought.

Our simplified model suggests the constitutive equation is dependent upon not only the current value of the strain but also the p^{th} order Lebesque norm of the strain history. The use of p^{th} order Lebesque norms in a constitutive theory are not unique to this model. Coleman and Mizel[45,46] and others have also proposed using these types of measures in viscoelastic constitutive equations. The development herein was not motivated by these earlier works, which were developed from a pure mathematical functional analysis approach. The development here stems from attempting to model the microstructural behavior of highly filled polymers. It so happened that key variables in this model constitutive equation happened to have the same mathematical form as L_p norms. These models may therefore in some way physically justify the use of L_p norms in constitutive theory.

If Equation (13) is used to calculate the state of stress, one finds the equation also includes failure of the material. If, on the other hand, a polynomial approximation is assumed for both $N(\tau)$ and $f(\tau\varepsilon)$, the integrations can be performed yielding the following equation

$$\sigma(t) = A_1\varepsilon P_1(\varepsilon/||\varepsilon||_p) + A_2\varepsilon^2 P_2(\varepsilon/||\varepsilon||_p) + \ldots + A_n\varepsilon^n P_n(\varepsilon/||\varepsilon||_p) + \ldots \tag{16}$$

where A_i = constants

P_i = polynomials in the variable $(\varepsilon/||\varepsilon||_p)$

$P_i(1) = 1$

This equation contains some very interesting behaviors even in very simplified forms. One special case, however, is worth noting. Recall earlier it was stated Bueche derived a similar model for the case when the stress response was independent of time and dependent only on strain history. Bueche used a maximum strain failure criterion for his elements rather than a cumulative damage criterion. The point of interest is that when the L_∞ norm is used in the constitutive equation, Bueche's special case is exactly recovered. This is because the L_∞ norm has the property that it is exactly equal to the largest value of the function being evaluated in its history. Other properties of L_p norms are given below.

$$||f||_p = \left\{\int_0^t |f(\xi)|^p d\xi\right\}^{1/p}$$

a) $||af||_p = |a|\,||f||_p$

b) $||f+g||_p \leq ||f||_p + ||g||_p$

c) $||fg||_1 \leq ||f||_p ||g||_p$

d) $||f-h||_p \leq ||f-g||_p + ||g-h||_p$

e) $||f||_\infty = \lim_{p\to\infty}\left\{\int_0^t |f(\xi)|^p d\xi\right\}^{1/p} = \text{Maximum}\ \ |f(\xi)|_0^t$

In the above equations f, g, and h are time functions, p and a are constant scalars, and ξ is a dummy time.

Another interesting, and encouraging, feature of our constitutive equation is that it is very simple to force it to obey the first rule of linearity while it must always fail the second rule; the same behavior observed in propellants.

A simple example of such a relation is

$$\sigma(t) = 100\ \varepsilon(t)\ [1 + (\varepsilon(t)/||\varepsilon||_p)^n], \text{ where } n \text{ is an even integer.} \quad (17)$$

Equation (17) gives a relaxation modulus that is independent of the applied strain magnitude, and will obey the homogeneity requirement of linearity for all scalars, with any arbitrary strain input. Equation (17) is not linear, however, as norms are not superposable except in the most trivial examples. The material represented by Equation (17) is therefore non-linear, but for many types of tests used for material characterization it could not be distinguished from a linear viscoelastic material. In fact, the parameters n and p appearing in this constitutive equation can be adjusted so that the derivative of the constant strain rate test is proportional to the relaxation modulus; a commonly cited property of a linear viscoelastic material.[36] Careful examination of the stress output to various strain inputs confirms the non-linear nature of this equation and indicate it is within the range of this simple equation to describe the one-dimensional response of solid propellants at small strains. To demonstrate this ability, the stress outputs for a variety of strain inputs have been determined for different values of n and p.

These data are illustrated in Figures 8 through 13. In these calculations the ratio n/p has been kept constant; therefore, all of the materials would exhibit the same relaxation modulus. However, as clearly indicated by these figures, the behavior to other inputs is different for the different values of n and p. This feature of giving the same output for one test, yet a different output for other tests, is characteristic of non-linear systems. If the material were linear, this feature would be impossible since one test dictates the results of all other tests for linear systems. Characterization of non-linear materials is therefore a difficult task as many tests must be used. Individuals familiar with the behavior of linear viscoelastic materials and the non-linear behavior of composite solid propellants will observe great similarity between the data illustrated in Figures 8 through 13 and the behavior of these materials.

(c) Other Models

The models of polymer chain failure based on a life fraction cumulative damage model leads to fairly simple mathematical representations for both chain failure[1] and a simple one dimensional constitutive equation,[1] no matter how complex the loading history. These life fraction models were by no means the only models studied during Farris' three year study at the University of Utah. Absolute reaction rate models were evaluated using the theory of Eyring,[110,115] and the possibility of chain slippage

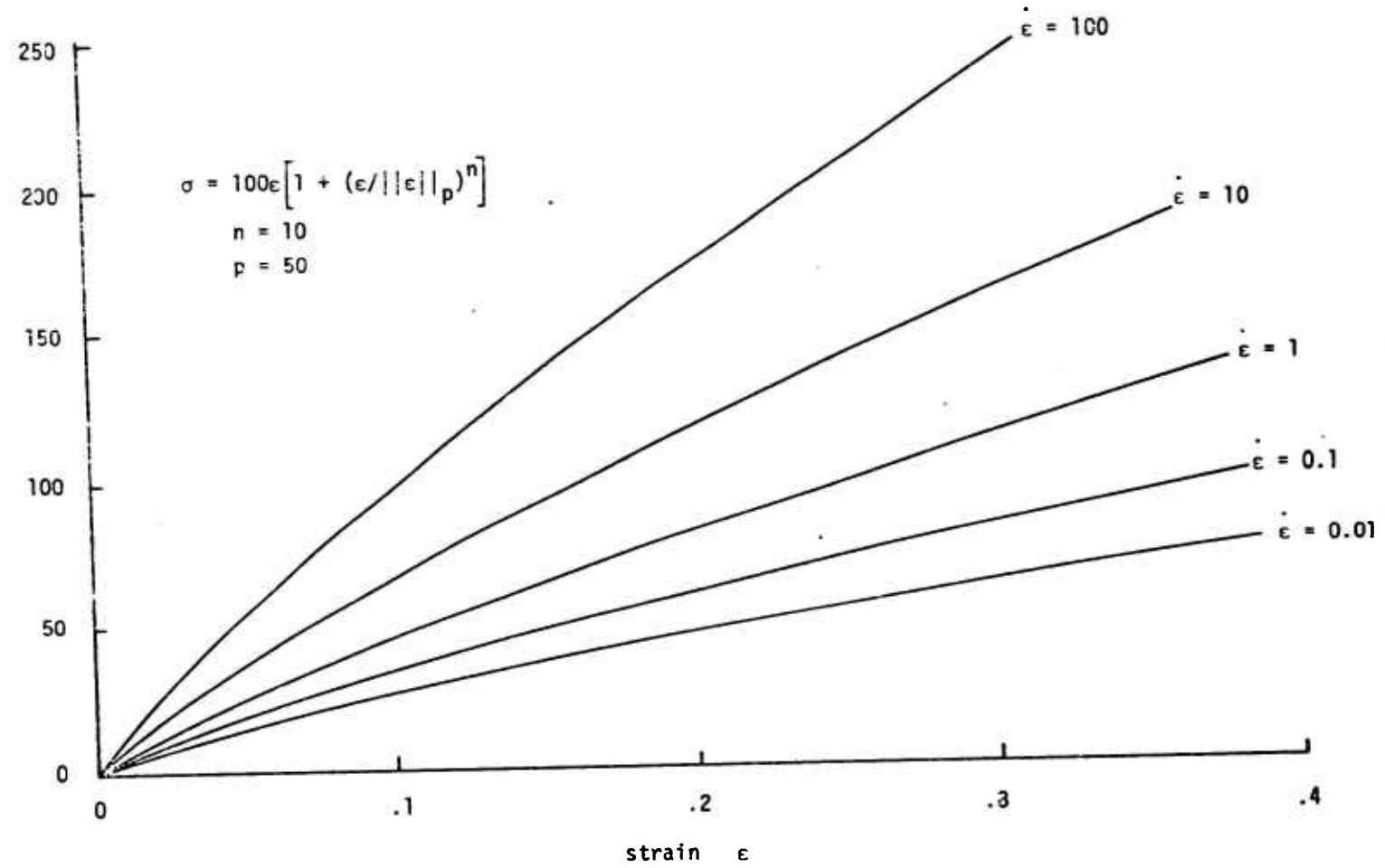

Figure 8

CALCULATED CONSTANT RATE STRESS-STRAIN BEHAVIOR OF A PERMANENT MEMORY MATERIAL

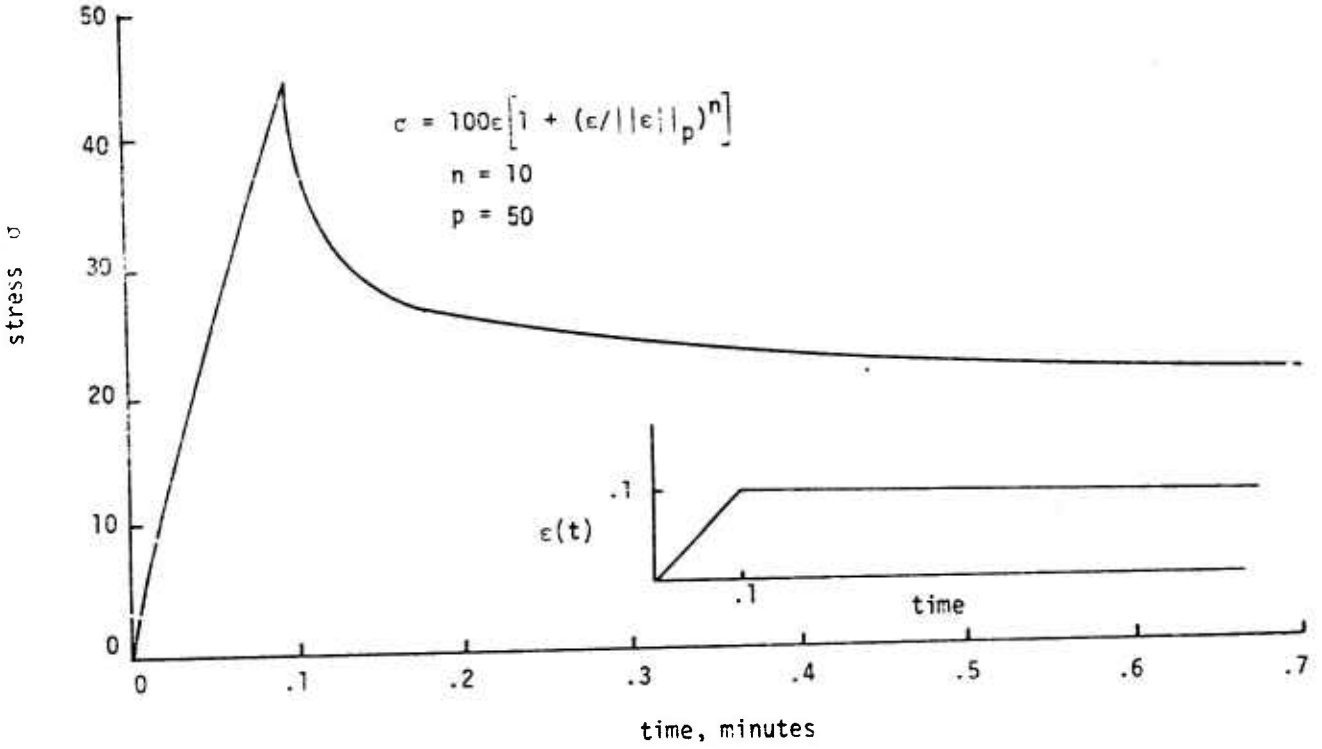

Figure 6

CALCULATED RAMP STRAIN STRESS RELAXATION BEHAVIOR OF A PERMANENT MEMORY MATERIAL

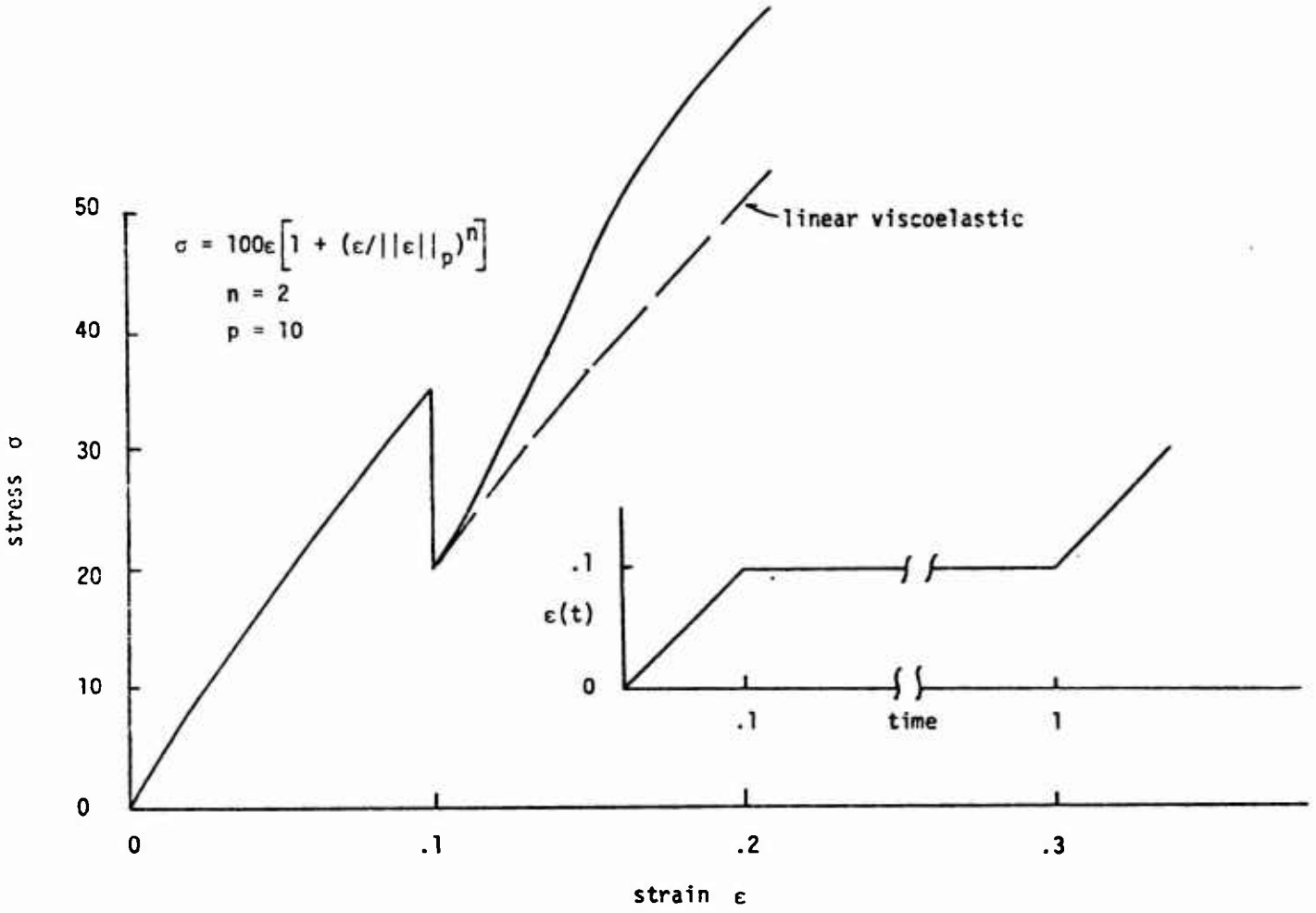

Figure 10

CALCULATED PERMANENT MEMORY STRESS-STRAIN RESPONSE TO AN INTERRUPTED RAMP INPUT

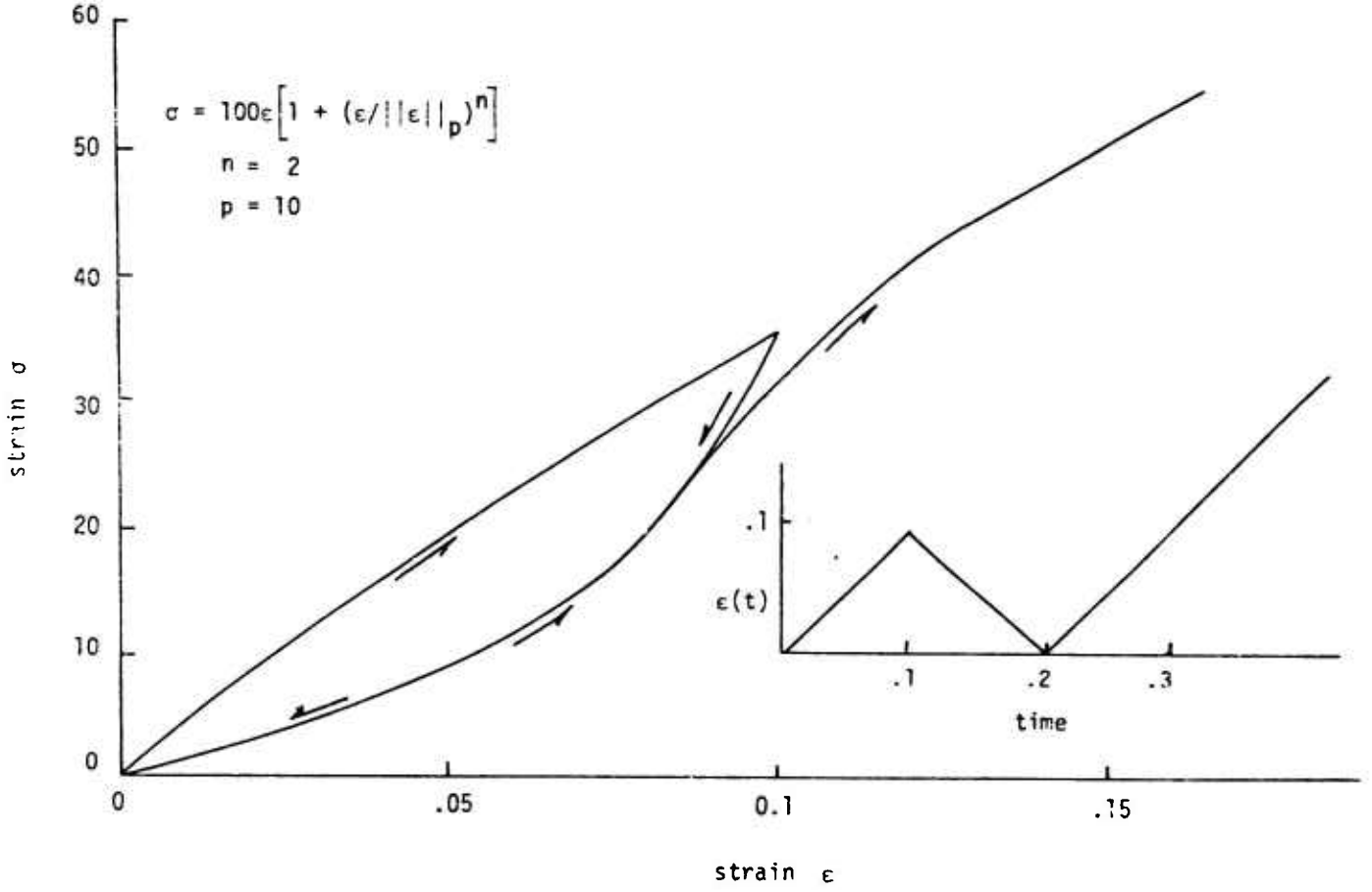

Figure 11

CALCULATED PERMANENT MEMORY HYSTEPESIS RESPONSE TO A REVERSED RAMP-STRAIN INPUT

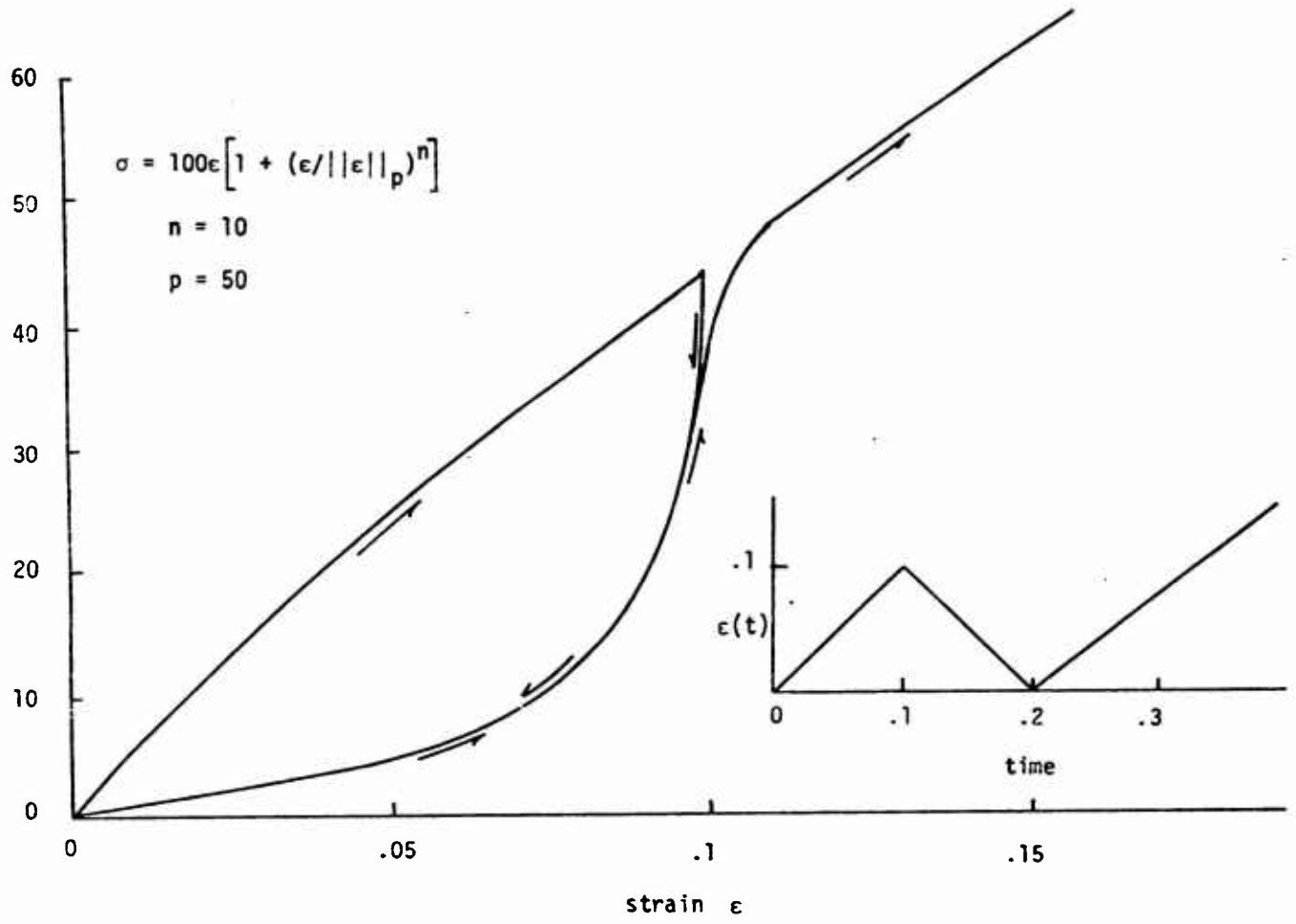

Figure 12

CALCULATED PERMANENT MEMORY HYSTERESIS RESPONSE TO A REVERSED RAMP STRAIN INPUT

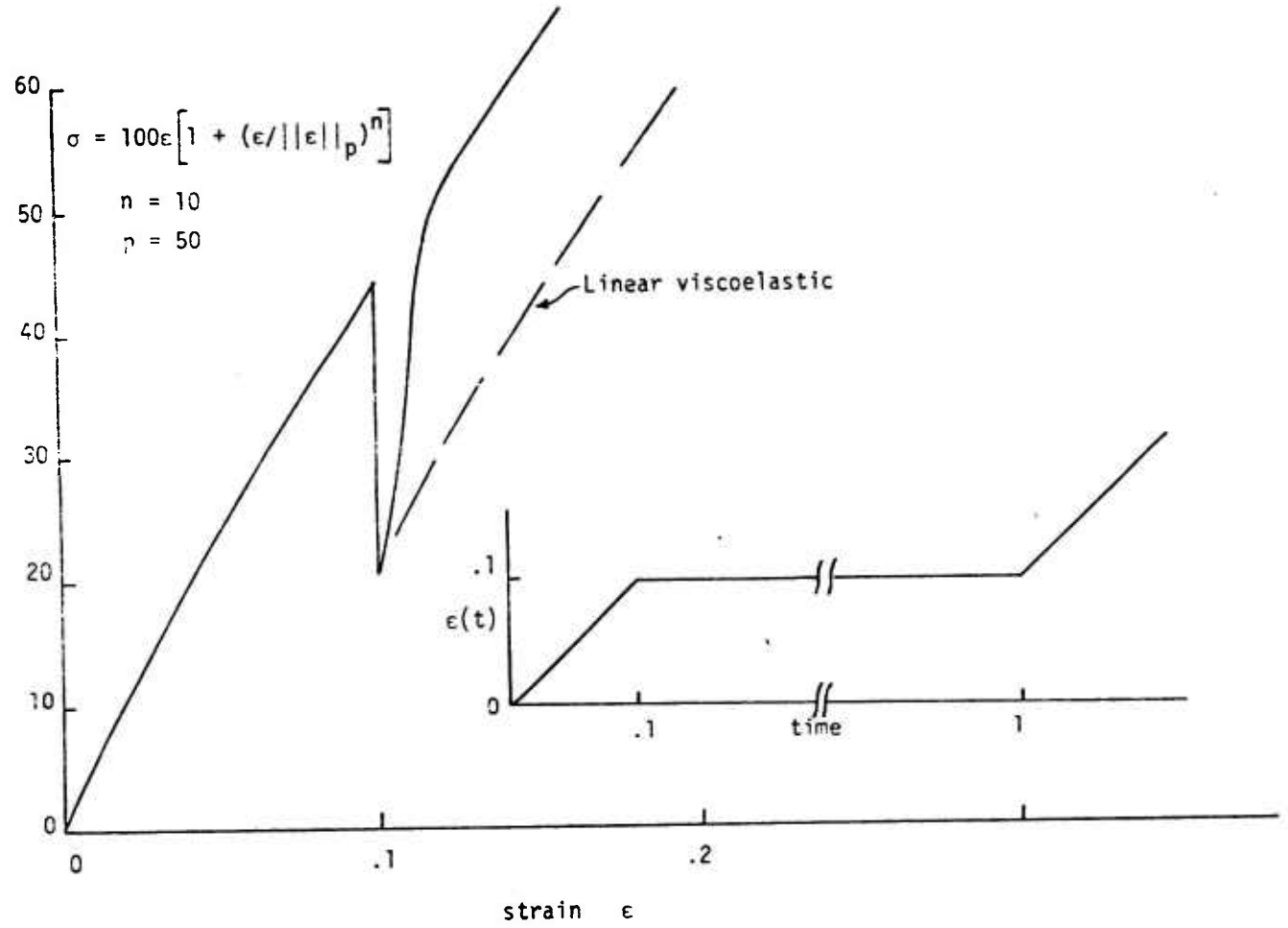

CALCULATED PERMANENT MEMORY STRESS-STRAIN RESPONSE TO AN INTERRUPTED RAMP INPUT

Figure 13

was investigated and modeled by combining so called Jenkin's elements,[116,117] i.e. ideal elastic-plastic spring elements in series with a Coulomb slip damper, with the linear viscoelastic Maxwell elements. This latter case did not appear to contain the proper overall type of behavior propellants are known to display, however, it did contain some of the necessary features. The absolute reaction rate models based on Eyring's works were the first models studied because of the work of Robinson and Graham[115], and all the polymer failure studies going on throughout the world using this approach.[110-115] The equation of interest for this approach is

$$\frac{dn}{dt} = f(N,T,\sigma)e^{-E(T,\sigma)/RT} \tag{18}$$

where N = number of chains

t = time

T = absolute temperature

E = activation energy

R = gas constant

Nearly all the attempts to use this equation, both in theoretical analysis and experiments have been for conditions of constant stress. In solid propellant there exists strong local stress gradients between particles even though the material as a whole is subjected to constant load conditions. Even after making gross simplifications, equations of the reaction rate form become extremely complex and difficult to handle when these stress or strain gradients are substituted into the equation, whereas, on the other hand, the life fraction equations were still, by comparison, quite simple to handle even for variable loading histories. It should not be forgotten that what one is trying to derive is some method of predicting chain failure that is sensitive to both stress magnitude and time. Both the life fraction equations and the absolute reaction rate equations allow for dependence in each of these variables. Hence, selection of one form over the other should be based on experimental evidence that one form is preferable to another or the fact that one method is simpler and easier to apply than the other. The absolute reaction rate equation, as it stands, has two unspecified functions, $f(N,T,\sigma)$ and $E(T,\sigma)$, hence an infinity of functional forms of this type are possible. Thus anyone using the absolute reaction rate method will have to make gross simplifications, however, after doing so the resulting equations are still unbearably complex and thus of little or no benefit. It has been demonstrated by Grownes[118,119] that the life

fraction method and the reaction rate method are identical when certain restrictions are placed on the functions $f(T,\sigma,N)$ and $E(\sigma,T)$, which naturally should be expected, since the same variables enter into each equation. Since the life fraction method was easily incorporated into models and a constitutive theory, it was selected for use over the reaction rate models. The reasons for this were many, however, the major ones are listed below.

- Life fraction models are much simpler to manipulate and allow complex histories to be included.
- As a limit case, life fraction models allow for history dependence with no time dependence by using L_∞ norms in the equations. This case is impossible using reaction rate equations. Also this case of history dependency and no time dependency occurs in the materials of interest. (74-79)
- Since models tend to average effects, it is more important to include each effect simply in the model rather than get too involved in details over any one effect, thereby, complicating the model.
- Thermal effects can be included easily in the life fraction models by using a reduced time to produce similar effects as the temperature dependence in the reaction rate models.
- Considerable evidence exists that Farris' models and equations contain the identical types of memory mechanisms propellants display. These memory mechanisms are registered in L_p norms which fall out of the life fraction models and are properties of these norms.
- Since L_p norms are used in the life fraction models, the great knowledge of the nonlinear functionals developed in the field of functional analysis can be brought to bear on the subject. For example, using a functional analysis between theorem on L_p norms, namely

$$||f + g||_p \geq ||f||_p + ||g||_p,$$

it can be simply proven that the creep due to a constant load f combined with a cyclic load g will be greater than the sum of the motions due to each load acting separately. Using the power of this branch of science greatly aids in the theoretical developments and applications of these theories.

(1) Vacuole Formation

The strong influence of vacuole formation on the stress-strain behavior of a highly filled elastomer can best be appreciated when one understands that the process by which these materials fail is initiated very early in the stress-strain history by the Mullins' Effect. After sufficient microstructural damage has occurred, vacuoles form and grow with continued straining in these localized high damage regions, causing a dilatation of the composite material, a loss in filler reinforcement, and in general, a physically unstable material. Efforts have been made to understand this phenomenon since it was first discovered by Schippel[72] in 1919, when he was studying the behavior of filled vulcanizates. Many other investigators[5-7,80] have verified Schippel's findings on solid propellants and other filled polymeric systems. The influence of these vacuoles on the mechanical behavior of highly filled elastomers received little direct attention for nearly fifty years, mainly because of the difficulty in assessing the frequency of their occurrence and the lack of reliable equipment to obtain simultaneous measurements of stress, strain, and dilatation. In 1964 Farris developed the gas dilatometer[5] which overcame the measurement problem. His dilatometeric devices enabled him to obtain simultaneous and continuous measurements of stress, strain, and dilatation on uniaxial tensile samples over broad ranges of temperatures, strain rates, and conditions of hydrostatic pressure. Later Farris developed mathematical models for (a) assessing the frequency of vacuole formation in terms of the dilatation-strain behavior[7] and (b) describing the apparent first stretch stress-strain nonlinearities in terms of the microstructural damage.[7] These early models have been well accepted throughout the industry and have provided the bases for some similar studies[106], and also for some cumulative damage models.[120] These models are extremely simple in nature and yet work very well which verifies the validity of the assumptions going into the models. The discussion below provides a short description of the means by which these stress-strain and dilatation-strain models were developed.

After studying the behavior of many systems it became apparent that it was not the magnitude of the volume change that was important but instead the fraction of the total solids about which vacuoles existed. Since the only significant contribution to strain-induced volume dilatation in filled elastomers comes from the vacuoles, a logical manner in which to study the frequency of the microstructural failures was to develop a suitable model expressing dilatation in terms of strain and the frequency of their occurrence.

(a) Development of a Dilatational Model

In developing such a model attention should be focused on a single filler particle contained in the elastomer matrix while the material is being strained. The elastomer and particle remain bonded until at some arbitrary strain, associated with some critical

stress required to cause internal failure, a vacuole is formed about the filler particle because of rupture of either the filler-elastomer bond or failure in the elastomer itself[7,81]. It is difficult to know the precise shape of each vacuole and its instantaneous behavior under continued straining but direct microscopic examination indicates that for rigid, nearly spherical filler the following assumptions hold:

- Vacuoles form arbitrarily at any magnitude of strain.
- Each vacuole is an ellipsoid of revolution with the two equal minor axes fixed by the diameter of the particle.
- After formation, the major axis of a vacuole increases linearly with strain at a rate proportional to the size of the contained particle.

Since the elastomer that comprises the filler-containing matrix is nearly incompressible and the filler is for all practical purposes rigid and, therefore, undergoes no real straining, the total volume change at any point in strain may be simply expressed as the sum of all the vacuole volumes existing at that strain. Hence

$$\Delta V = \sum_{i=o}^{N} V_i \tag{19}$$

where ΔV = total change in specimen volume

V_i = volume of the ith vacuole

N = number of filler particles in specimen = constant

The volume of a spherical particle is:

$$V_{pi} = (4/3)\pi a_i^3 \tag{20}$$

where V_{pi} = volume of ith particle, a_i = radius of ith particle.

The volume of the ellipsoid of revolution is:

$$V_{eli} = (4/3)\pi a_i^2 b_i \qquad (21)$$

where V_{eli} = volume of the ith ellipsoid; b_i = major axis of ellipsoid $\geq a_i$

The vacuole volume is the difference between the volumes of the ellipsoid and the particle.

$$V_i = (4/3)\pi a_i^2 (b_i - a_i) = V_{pi}(b_i - a_i)/a_i \qquad (22)$$

where V_i = volume of ith vacuole.

Thus, if $b_i - a_i > 0$ the ith vacuole exists, (23a)

if $b_i - a_i = 0$ the ith vacuole does not exist. (23b)

The assumption that after a vacuole has formed ($b_i - a_i > 0$) the major axis of each vacuole increases in length with strain at a rate proportional to the particle contained within may be expressed as

$$db_i/d\varepsilon = Ca_i \qquad (24)$$

where ε = macroscopic material strain; C = constant of proportionality. And since a_i is constant for each vacuole we have

$$\frac{d[b_i - a_i)/a_i]}{d\varepsilon} = C \text{ if } b_i - a_i > 0 \qquad (25)$$

and naturally if the vacuole has not formed we have

$$\frac{d[(b_i - a_i)/a_i]}{d\varepsilon} = 0 \text{ if } b_i - a_i = 0 \qquad (26)$$

From eqs. (25) and (26) it follows that

$$dV_i/d\epsilon = CV_{pi} \quad \text{if } b_i - a_i > 0 \tag{27}$$

and

$$dV_i/d\epsilon = 0 \quad \text{if } b_i - a_i = 0 \tag{28}$$

differentiating both sides of eq. (19) with respect to strain yields:

$$d\Delta V/d\epsilon = d/d\epsilon \sum_{i=1}^{N} V_i = \sum_{i=1}^{N} dV_i/d\epsilon \tag{29}$$

The summation of dV_i in eq. (29) can be conveniently divided into two terms since the total number of particles in the material is equal to the sum of the number of vacuoles that exist, n, and the number of vacuoles that do not exist, N - n.

Therefore

$$d\Delta V/d\epsilon = \sum_{i-1}^{N} dV_i/d\epsilon = \sum_{i=1}^{n} dV_i/d\epsilon + \sum_{n+1}^{N} dV_i/d\epsilon \tag{30}$$

From eq. (23) it is apparent that for all n vacuoles in the first summation $b_i - a_i > 0$, and that for all those in the second summation $n + 1 \longrightarrow N$, $b_i - a_i = 0$. Applying eqs. (27) and (28) to eq. (30) yields

$$d\Delta V/d\epsilon = \sum_{i=1}^{n} CV_{pi} + \sum_{n+1}^{N} 0 = C\sum_{i=1}^{n} V_{pi} \tag{31}$$

Dividing both sides of Equation (31) by the total material volume V_o we have

$$(1/V_o)(d\Delta V/d\epsilon) = C/V_o \sum_{i=1}^{n} V_{pi} = CV_f \tag{32}$$

where V_f = volume fraction of solids about which vacuoles exist.

The second derivative of dilatation with respect to strain is then proportional to the rate at which new vacuoles are forming about the volume of unaffected particles.

$$(1/V_o)(d^2\Delta V/d\varepsilon^2) = CdV_f/d\varepsilon \tag{33}$$

In the special case where all the particles are the same size Equations (32) and (33) become

$$(1/V_o(d\Delta V/d\varepsilon) = C'n \tag{34}$$

and

$$(1/V_o)(d^2\Delta V/d\varepsilon^2) = C'dn/d\varepsilon \tag{35}$$

(where $C' = 4c\pi\alpha_i^3/3V_o$) in which case it is apparent that the first derivative of dilatation with respect to strain at any strain, ε, is proportional to the number of vacuoles formed up to that strain, and the second derivative of dilatation with respect to strain is proportional to the rate at which new vacuoles are forming. Statistically these two derivatives describe the cumulative and instantaneous frequencies of vacuole formation, respectively. In the general case these frequency distributions are in terms of the volume fraction of solids affected rather than the number as indicated by Equations (32 and 33). Figure 14 illustrates the general shape of the dilatation-strain behavior and its first and second derivatives, and as predicted by the model the first and second derivates take on the shape of cumulative and instantaneous frequency distributions.

To evaluate the constant, C, experimental data were obtained on systems containing fillers of unimodal sizes at various concentrations, since these systems tend to form vacuoles about all the filler particles. Plotting the maximum slopes of the dilatation-strain curves against the volume fraction of filler contained in the material (Figure 15) yielded a value of C = 1. This is to be expected since the constant C as defined by Equation (25) can be interpreted as the average ratio of the microscopic to macroscopic strain rates after the vacuole has formed. If the number of particles affected per unit volume is sensibly constant everywhere in the material, then on the average these microscopic and macroscopic strain rates must be equal.

When blends of different sizes of filler are used, microscopic examination indicates that vacuoles form only about the coarse particles when the sizes differ greatly. Dilatation data on such systems agrees with these findings and for such cases the maximum rate of dilatation with respect to strain was found to equal the volume fraction of coarse filler.

SCHEMATIC REPRESENTATION OF DILATATION-STRAIN RELATIONSHIP AND ITS FIRST AND SECOND DERIVATIVES

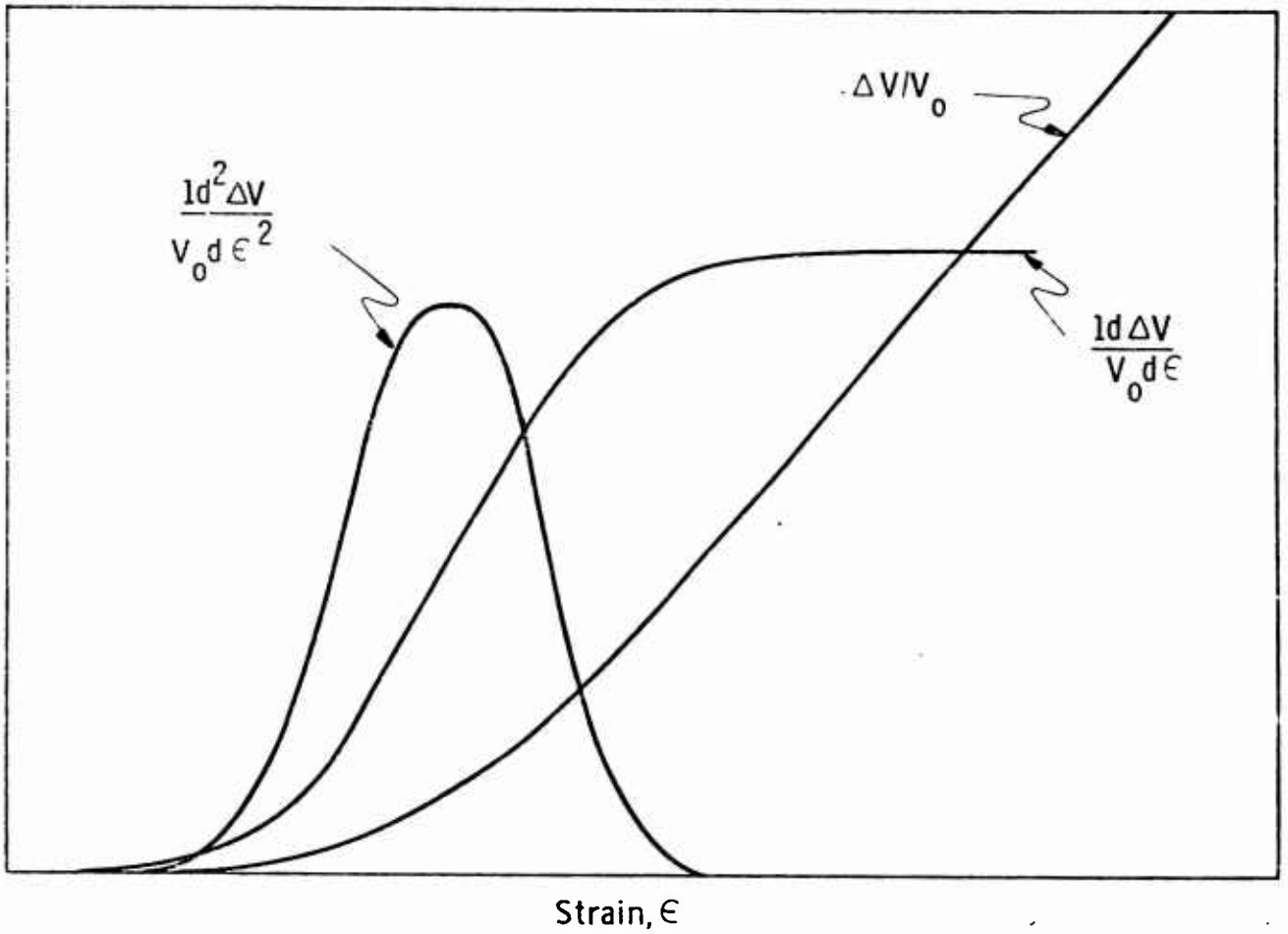

Figure 14

EFFECT OF FILLER CONTENT ON MAXIMUM RATE OF DILATATION

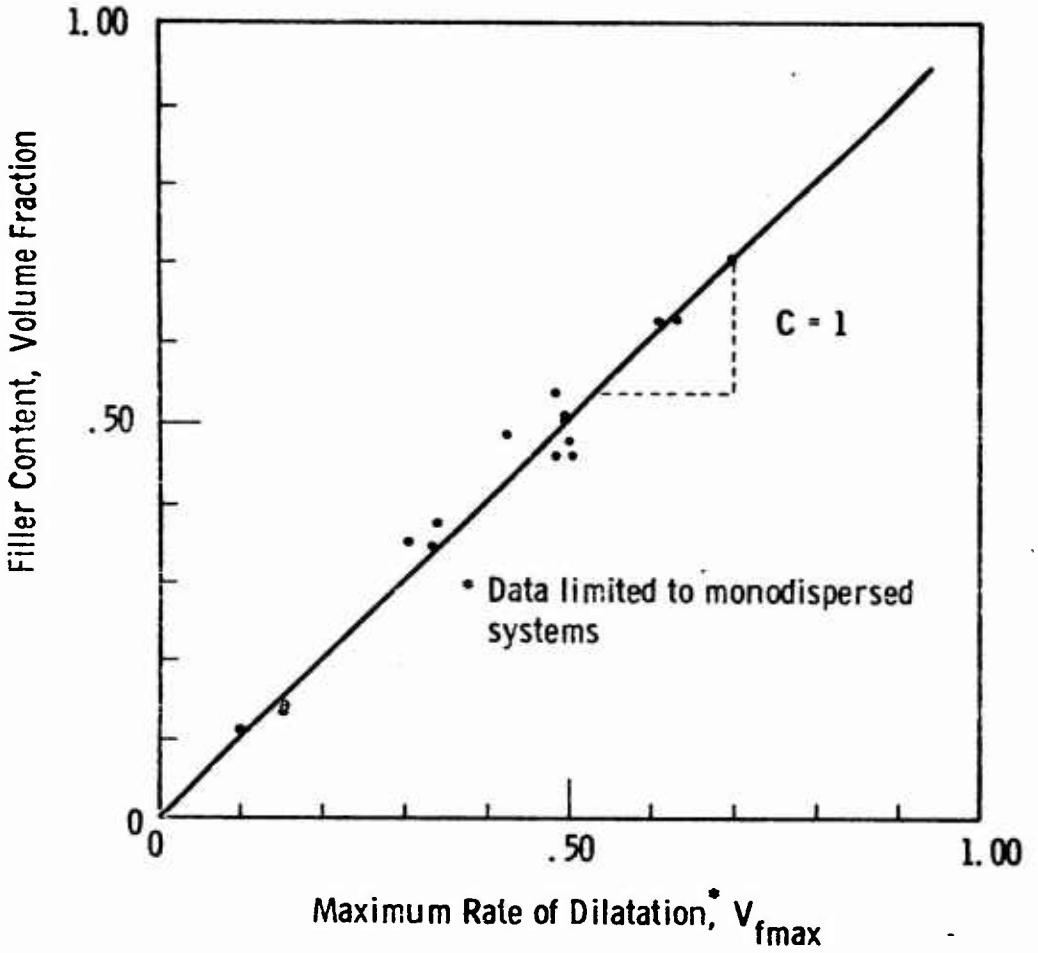

Figure 15

The frequency distributions derived from this method of analysis are for all practical purposes normal or Gaussian, as are nearly all random processes dealing with large numbers. They can therefore be characterized by normal statistical parameters requiring only a mean, standard deviation, and the total probability density. The mean $\bar{\varepsilon}$, is the value of strain about which the distribution of these microscopic failures is centered; the standard deviation, s, is a measure of the broadness of the distribution; and the total probability density V_{fmax}, describes the total volume fraction of solids about which vacuoles are going to form. Because of the symmetry of the Gaussian function one may obtain these statistical parameters, $\bar{\varepsilon}$, s, and V_{fmax}, directly from the dilatation-strain curve as long as the process has gone to completion (i.e., $d(\Delta V/V_o)/d\varepsilon$ becomes constant).[7]

The excellent agreement between the calculated and measured values of dilatation using this simple means of data analysis is illustrated in Figure 16. The corresponding frequency distributions for the corresponding dilatational behavior are given in Figure 17.

(b) Vacuole Formation and the Stress-Strain Response

The statistical interpretation of the dilatation-strain behavior clearly illustrates that the number of vacuoles does not depend upon the magnitude of the dilatation, but instead upon its rate of change with respect to strain. Therefore it is possible to have relatively large volume changes with low vacuole densities or small volume changes with very large vacuole densities. Since the modulus of elasticity of highly filled elastomers is largely due to the reinforcing action of the bonded filler particles, and the first derivative of dilatation with respect to strain is a measure of the amount of solids about which vacuoles exist, strong correlations between the change in modulus and the degree of vacuole formation can be made. These correlations will yield, for materials of this type, simple stress-strain functions, the form of which naturally depends upon the model selected. Many such models were investigated, and of these the very simple phenomenological model described below appears to fit the behavior of all highly filled elastomers and, therefore, appears to be a correlation of general applicability.

This stress-strain model comes from the fact that there is great similarity between the first and second derivatives of stress and dilatation with respect to strain as shown in Figure 18. An excellent first-order approximation of this similarity would state that the second derivatives of stress and dilatation with respect to strain differ only in sign and magnitude. Interpreting this in the light of the statistical model of dilatation would state that the instantaneous modulus, $d\sigma/d\varepsilon$, is linearly related to the vacuole density. This approach results in a simple stress-strain-dilatation relation.

COMPARISON OF DILATATIONAL MODEL AND EXPERIMENTAL DATA ON FOUR PROPELLANTS

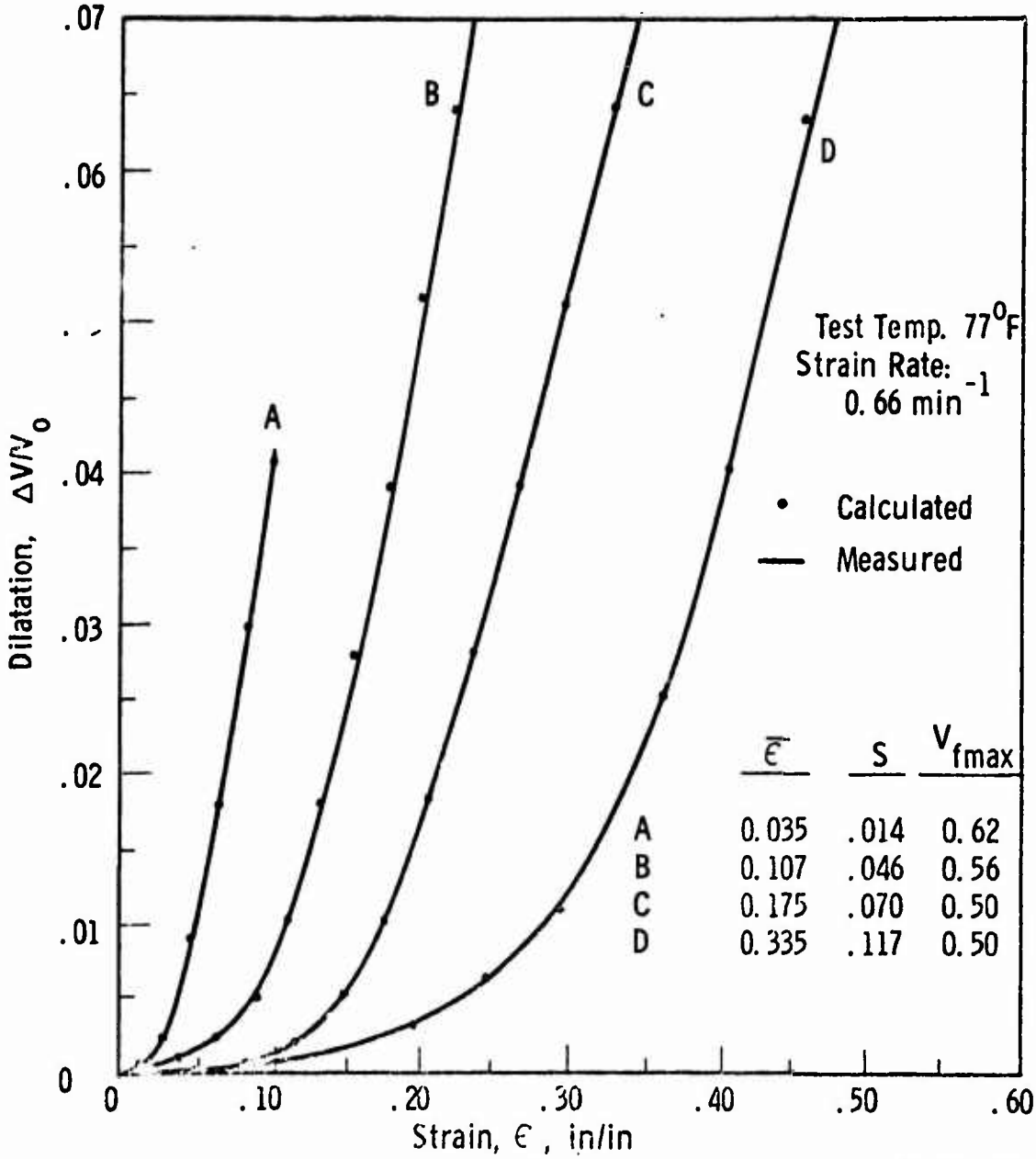

Figure 16

COMPARISON OF DISTRIBUTIONS OF VACUOLE FORMATION FOR DATA IN FIGURE 3.16

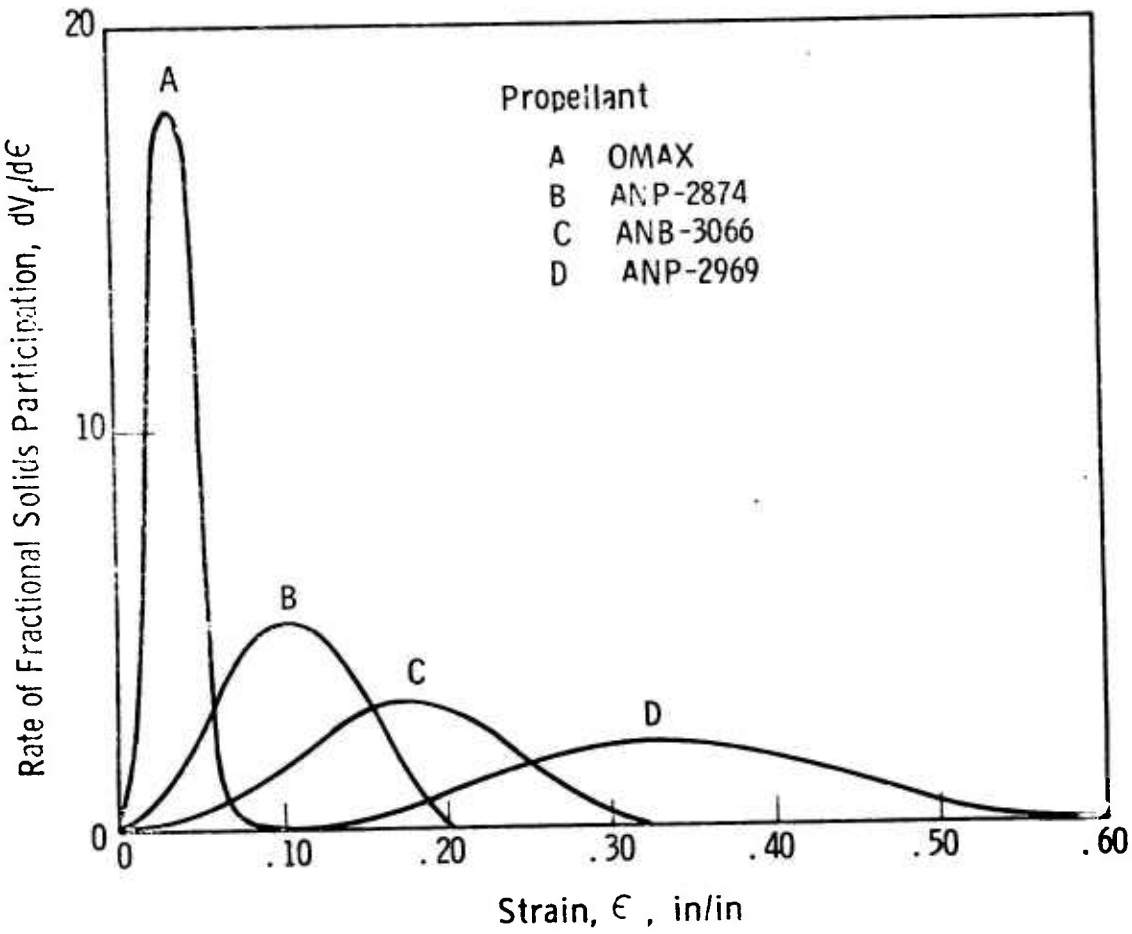

Figure 17

SCHEMATIC REPRESENTATION OF DERIVATIVES OF STRESS AND DILATATION WITH RESPECT TO STRAIN

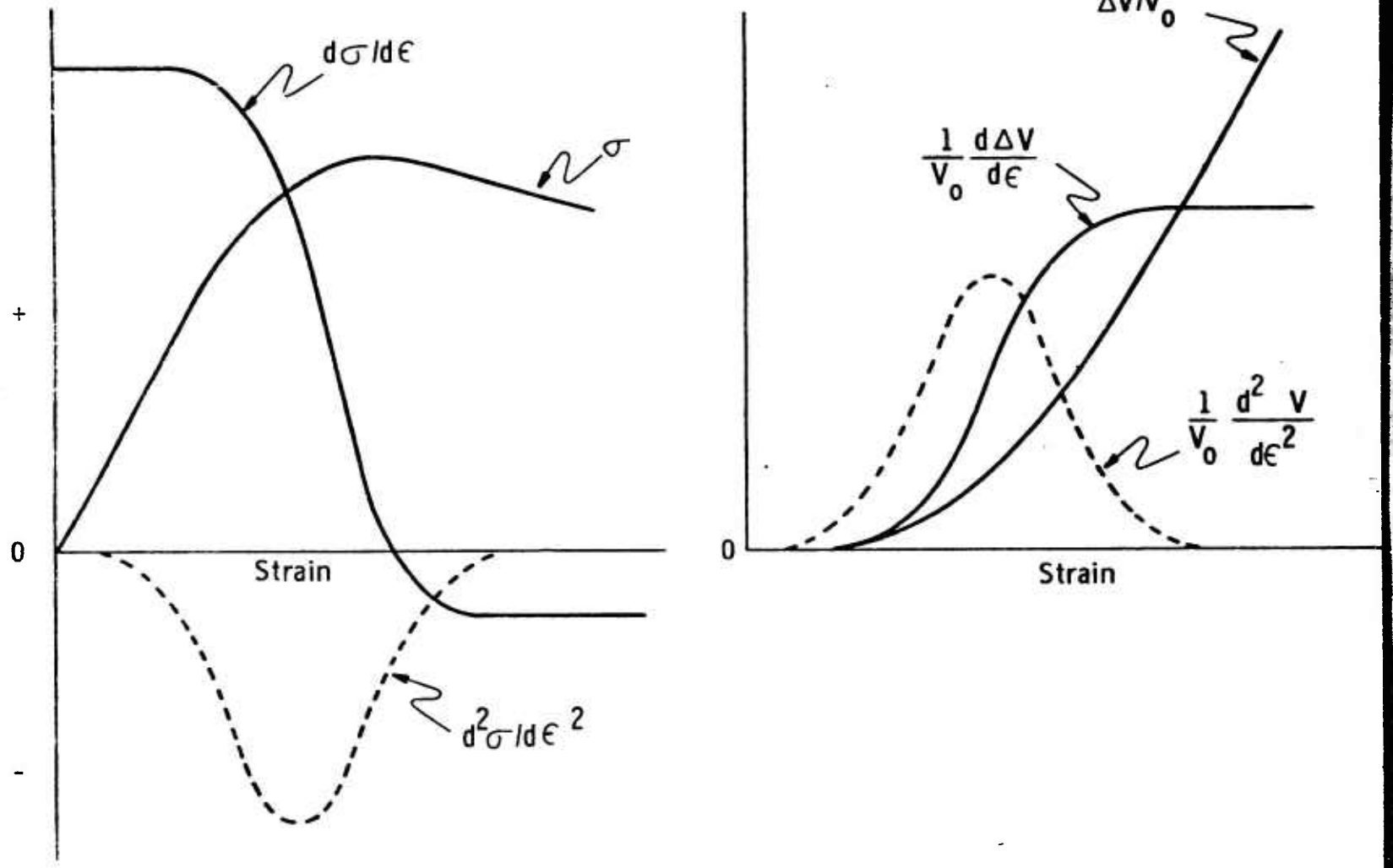

Figure 18

$$\sigma = E_1\varepsilon - E_2(\Delta V/V_o) = E_1\,[\varepsilon - \beta(\Delta V/V_o)] \qquad (36)$$

where σ = stress; E_1 and E_2 = constant moduli; $\beta = E_2/E_1$.

This stress-strain relation has shown excellent agreement with experimental results except at very large volume changes. This should be expected, since giving each vacuole equal weight in its effect on the modulus is, perhaps, an oversimplification. Nevertheless this approach confirms the fact that the shape of the stress-strain curve is related to the distribution of vacuole formation and confirms the intuitive approach taken by many researchers who judge the quality or structural integrity of these materials by the shape of their stress-strain curves. A slight modification of this simple model which gives a decreasing weight to new vacuoles and reduces to the above model at small volume changes is:

$$\sigma = E\varepsilon e^{-\beta(\Delta V/V_o)/\varepsilon} \qquad (37)$$

This equation fits excellently data obtained over a broad range of test conditions as illustrated in Figures 19, 20, and 21. As might be expected the constant β does not appear to depend strongly upon rate or temperature, indicating that this vacuole process modifies the material behavior in the same way over a broad range of test conditions. In this simple model the material, which is normally viscoelastic, is assumed to have a constant modulus. There are no doubt some nonlinearities due to a time-dependent modulus but, since for most cases these are negligible compared to those caused by vacuole formation, they can be ignored. Exactly how much of the nonlinearity is due to time dependency and how much is due to vacuole formation is easily shown by conducting tests under similar time and temperature conditions with the material subjected to a superimposed hydrostatic pressure, as will be shown later.

(c) The Effect of Pressure

The effect of hydrostatic pressure on the stress-strain behavior of highly filled elastomers is quite marked since pressure influences the microscopic failure mechanism giving rise to the formation of vacuoles. When the composite material is deformed, highly focused triaxial stresses develop in the binder near the surface of each filler particle. Vacuole formation is initiated when these stresses exceed some critical value.[81,121] Since the effect of pressure is to cause each component of these stresses to originate from a negative boundary, the failure process will be influenced accordingly. The effect of pressure is beneficial because it retards vacuole formation and thereby extends the range of the stress-strain response of highly filled elastomeric materials before yielding begins.

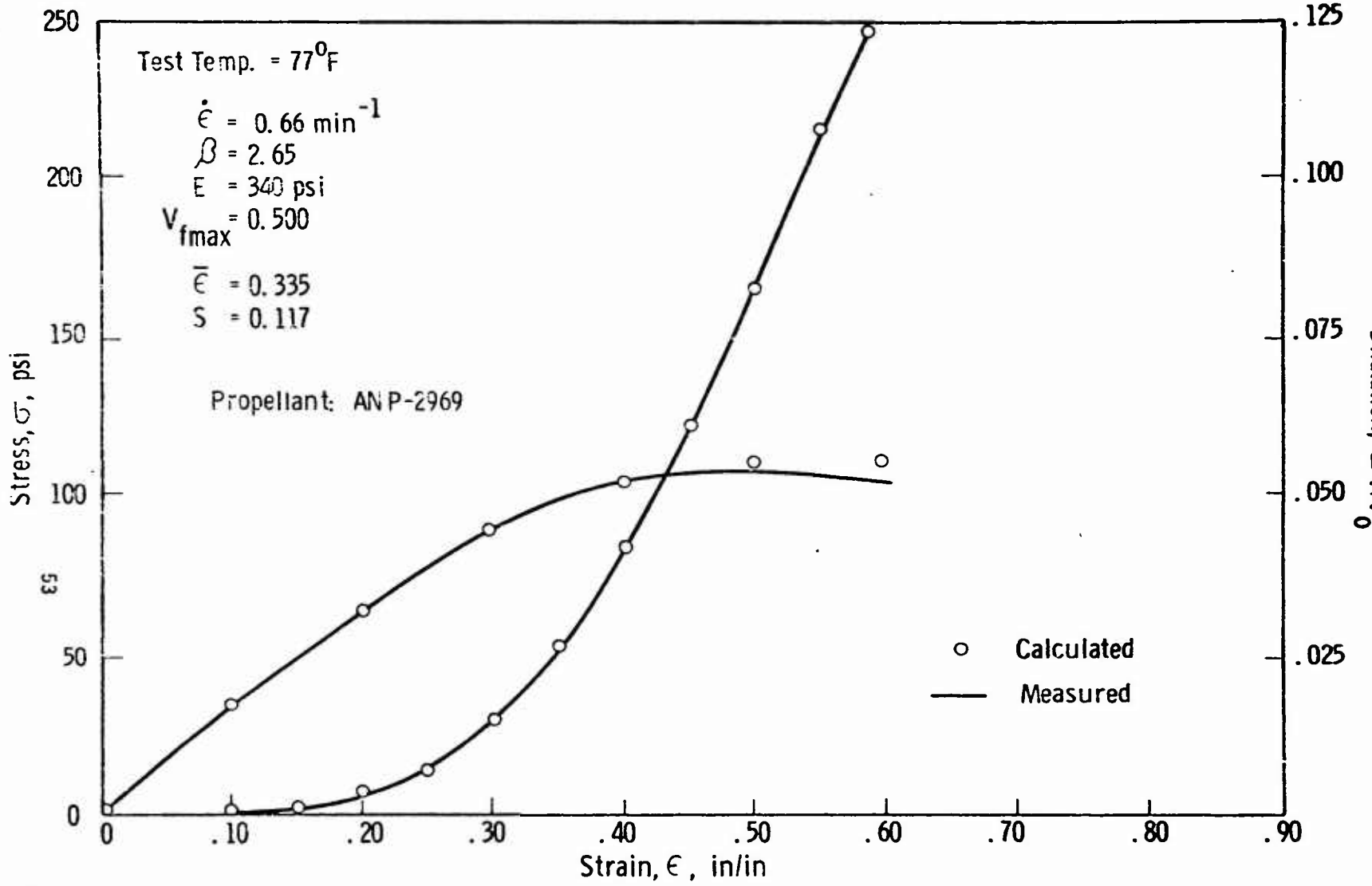

Figure 19

COMPARISON BETWEEN CALCULATED AND MEASURED STRESS-STRAIN AND DILATATION-STRAIN BEHAVIOR FOR A 63.5 VOL. % FILLED POLYURETHANE PROPELLANT

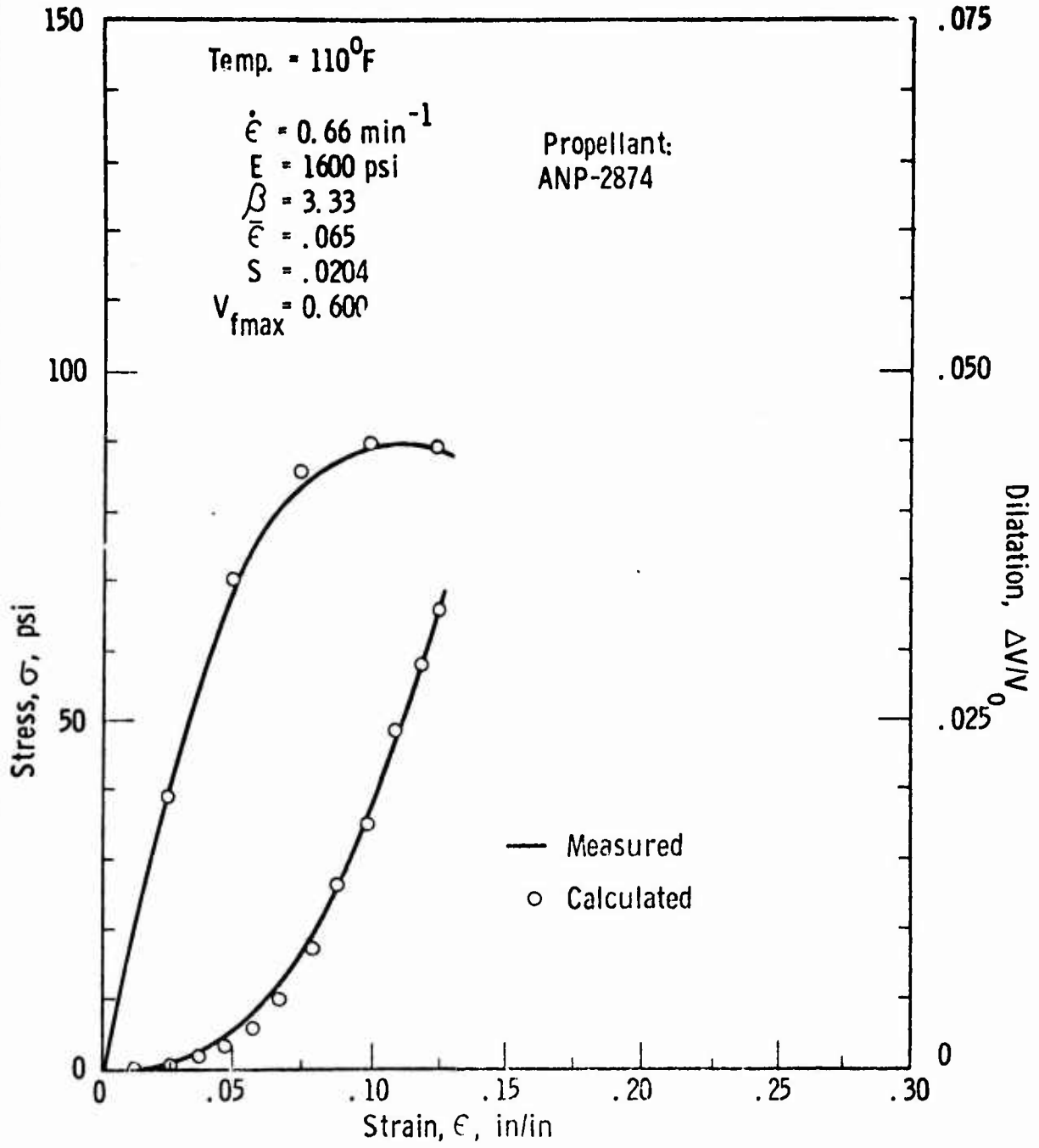

COMPARISON BETWEEN CALCULATED AND MEASURED STRESS-STRAIN AND DILATATION-STRAIN BEHAVIOR FOR A 73.5 VOL % FILLED POLYURETHANE PROPELLANT

Figure 20

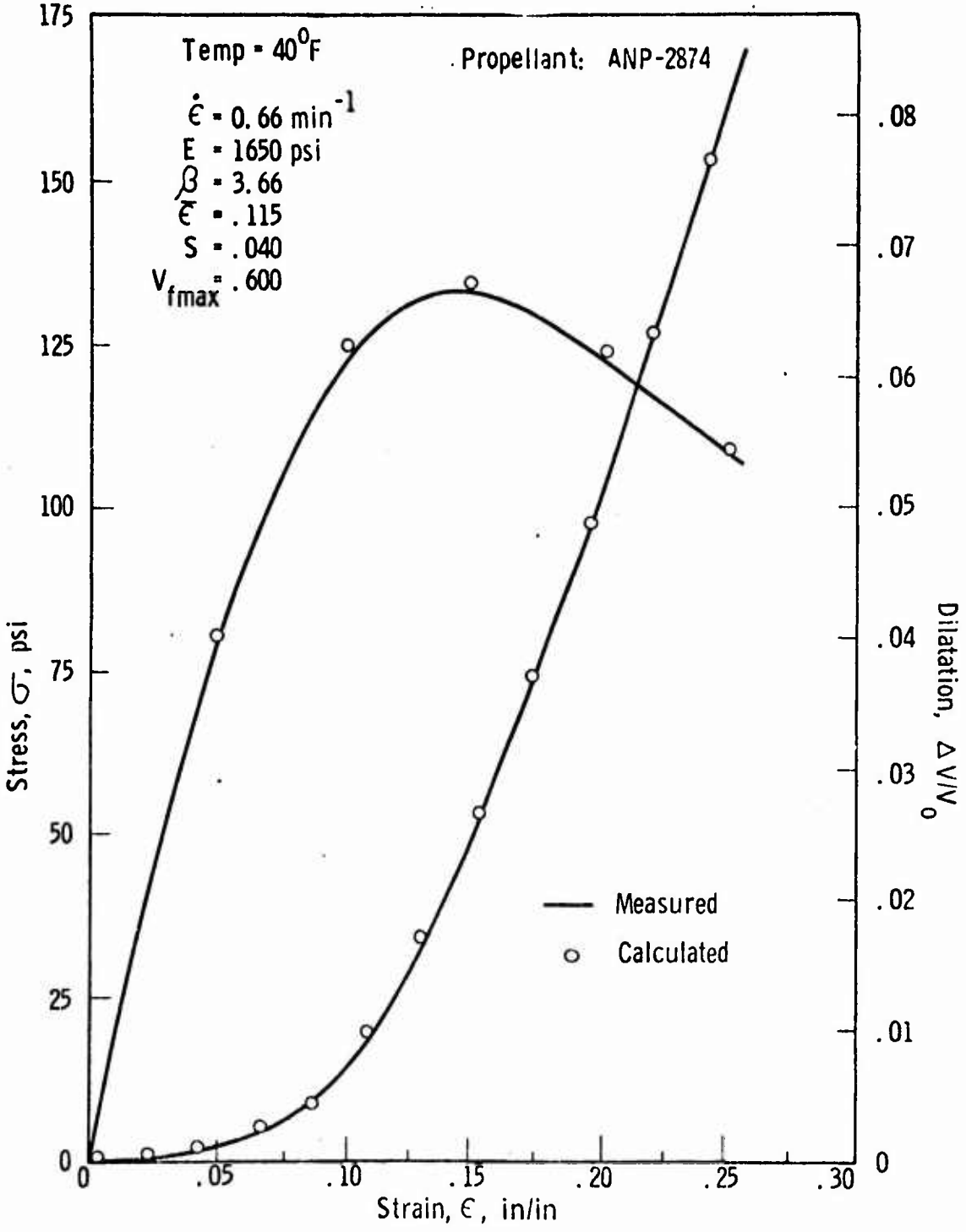

COMPARISON BETWEEN CALCULATED AND MEASURED VALUES OF STRESS-STRAIN AND DILATATION-STRAIN BEHAVIOR FOR A 70.5 VOL. % FILLED POLYURETHANE PROPELLANTS

Figure 21

Figure 6 illustrates the stress-strain and dilatation-strain response at different pressures for a slow strain rate. Also since the material becomes increasingly compressible as the number of vacuoles increase, it becomes more and more difficult for the vacuoles to grow in size with increasing strain under a high pressure environment. The rate of dilatation with respect to strain no longer becomes a direct measure of the number or amount of vacuoles since it also becomes a function of pressure and the material resistance to pressure, i.e., its modulus.

The effect of pressure and modulus on vacuole growth can be determined assuming the same degree of vacuole formation was reached in each case. This latter assumption is partially justified since for all test conditions it appears as if the final rate of volume change became constant, indicating, according to the statistical model, a fixed amount of flaws. Figure 22 illustrates the excellent exponential relation between the final rate of volume change and pressure. The lower the material modulus, the stronger the dependency. Partial proof that the same degree of damage is reached is that the product of the slope of the line and the modulus appears to be constant, about -3. The relation would therefore become

$$\left(\frac{d\Delta V/V_o}{d\varepsilon} \right)_{max} = \left(\frac{d(\Delta V/V_o}{d\varepsilon} \right)_{max \text{ at } P = 0} e^{-2.9p/E} \tag{38}$$

which is very similar to the standard compressibility equation for an elastic substance which may be expressed as

$$V = V_o e^{-[3P(1-2\nu)]/E} \tag{39}$$

(where ν = Poisson's ratio) and Poisson's ratio would be very low for such a material.

In the statistical treatment of the dilatation process one can probably correctly conclude that the observed maximum rate of dilatation is only a measure of the amount of solids about which vacuoles exist at atmospheric pressure and that as a function of pressure it may be expressed approximately as

$$V_f \tilde{=} (d\Delta V/V_o/d\varepsilon)e^{KP/E} \tag{40}$$

where $K \gtrsim -3$.

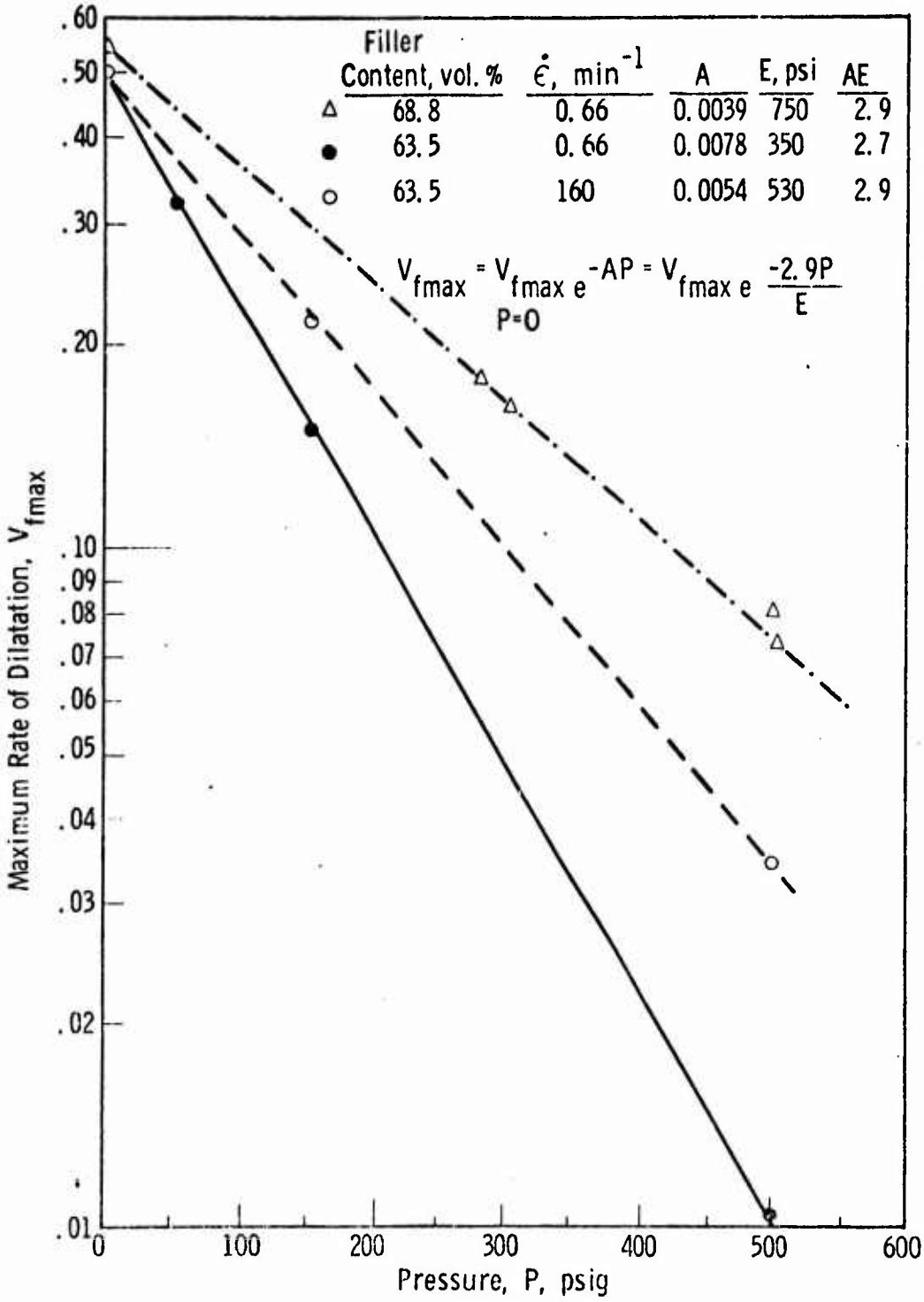

THE EFFECT OF SUPERIMPOSED HYDROSTATIC PRESSURE AND MODULUS ON THE MAXIMUM RATE OF DILATATION

Figure 22

In testing the simple stress-strain and dilatation models for these data one finds that they fit quite well, the only difficulty being that the constant β in the stress-strain function and the parameter V_{fmax} in the dilatation function are strongly dependent on modulus and pressure. However, since β was derived assuming that dilatation and its derivative were a measure of vacuole density and it has already been shown that this is only true at atmospheric pressure, one would expect the apparent β to increase by the same amount V_{fmax} decreased with increasing pressure. Figure 23 illustrates the excellent fit of these models to the experimental data and the data in Table 1 indicates that the product of β and V_{fmax} is apparently constant for all conditions of temperature, rate, and pressure for a given material, thereby giving substance to the validity of these models.

Others have also attempted to model the influence of vacuole formation on the stress-strain behavior of propellants. Blatz, McQuarrie and Shen[100] proposed one theoretical model assuming nonadherent particles. Fishman[101] and Rinde proposed a strain energy model and recently Lindsey and Murch[122] have proposed a model based on an extension to Drucker's yield hypothesis for plastic materials.[123] Also Freudenthal[83] derived a simple stress-strain model based on some of the work done by Schwarzl, Bree, and Strick.[99] As one can clearly see there is an abundance of models for interpreting the influence of vacuole formation, or dewetting as some prefer to call it, on the stress-strain behavior of composite propellants. Some of these models were theoretical while others were stochastic phenomenological models. All of these models associate strong nonlinearities with vacuole dilatation. It appears Schippel showed excellent foresight when he said of the vacuoles in 1919, "Their cumulative effect in a substance which has the ability to withstand comparatively enormous elastic strains is worthy of serious consideration from a physical standpoint."

(c) Reversible Nonlinearities

There are certain strain histories for which reversible time-dependent behavior cannot be neglected, as discussed in Section III.1.(2)(c) In the linear range of mechanical behavior, the mathematical model normally used to describe this type of time-dependence is the so-called Boltzmann superposition integral.

For example, the isothermal, uniaxial stress-strain equation is written

$$\sigma = \int_{-\infty}^{t} E(t-\xi) \frac{d\varepsilon}{d\xi} \, d\xi \qquad (41)$$

where σ is the time-dependent stress response to a strain history

ε and $E(t)$ is the so-called relaxation modulus (i.e., the ratio of stress-to-strain in a constant strain test.

COMPARISON OF MEASURED AND CALCULATED STRESS-STRAIN AND DILATATION-STRAIN BEHAVIOR OF A HIGHLY FILLED PROPELLANT AT A SERIES OF PRESSURES

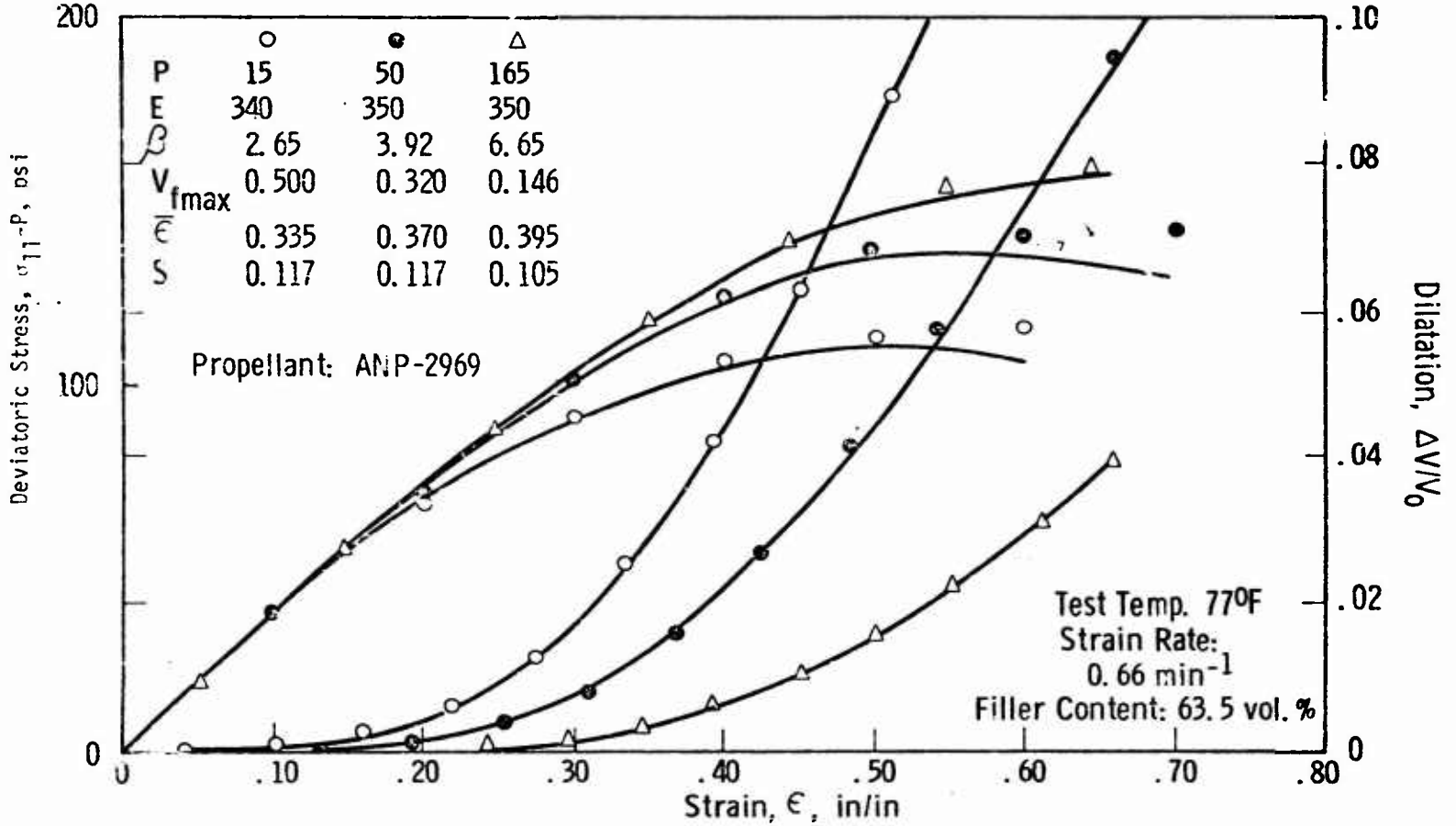

Figure 23

TABLE 1

COMPARISON OF βV_{fmax} FOR VARIOUS TEST CONDITIONS

Temperature, ^{o}F	ε, min^{-1}	Pressure P, psia	V_{fmax}	β	βV_{fmax}
		63.5 vol. % Filled Polyurethane Rubber			
77	0.66	15	0.50	2.65	1.32
77	6.6	15	0.50	2.52	1.26
77	160	15	0.50	2.54	1.27
77	0.66	50	0.32	3.92	1.26
77	0.66	165	0.146	6.65	0.97
77	0.66	500	0.01	100	1.00
77	160	165	0.20	4.46	.89
77	160	500	0.034	37.8	1.29
		70.5 vol. % Filled Polyurethane Rubber			
110	66	15	0.60	3.33	2.00
77	66	15	0.55	3.74	2.06
40	66	15	0.60	3.66	2.19
0	66	15	0.70	2.86	2.00

Equation (41) is the most general linear uniaxial stress-strain equation which can be written for a non-aging material. With a general multiaxial state of stress, the same type of integrals connect the stress and strain tensors.

When a material is represented by the familiar generalized Maxwell model, Equation (41) still applies, but the relaxation modulus takes on the special form of a sum of exponentials.

$$E(t) = E_e + \sum_{i=1}^{M} E_i \, e^{-t/\tau_i} \qquad (42)$$

where E_e = long-time (equilibrium modulus)

E_i = modulus of i^{th} spring

$\tau_i \equiv \eta_i/E_i$ = relaxation time of i^{th} Maxwell element

Several models have been proposed to extend this so-called "hereditary" or "fading memory" representation to nonlinear, reversible behavior. The multiple integral expansion proposed by Green, Rivlin, and Spencer (see Equations (67) and (68)) is one such generalization; but it is very difficult to use in the presence of strong nonlinearities and fading memory, and it does not readily lend itself to the incorporation of physical simplifications.

On the other hand, Schapery[30] has used a physical approach to the problem of characterizing nonlinear fading memory effects by utilizing nonequilibrium thermodynamic principles. By bringing together experimental observations on a wide variety of materials (metals and polymers) continium mechanics, and thermodynamic theory, he has developed a relatively simple three-dimensional constitutive theory which has been successfully used to characterize various materials,[31] including anisotropic, fiber-reinforced plastic.[126] While this theory is capable of describing non-fading memory,[32] primary application has been to fading memory materials, and only the latter type will be discussed in this section.

Finally, it should be pointed out that molecular models of the nonlinear reversible behavior of amorphous polymers have received some attention in the literature.[127] However, even for only uniaxial loading, the existing theories are far too complex for engineering use.[31]

(1) Thermodynamic Model

The thermodynamic theory used by Schapery will be reviewed here, and then used to derive a one-dimensional stress-strain equation (detailed development of the theory can be found in References 30 and 128).

It should be emphasized, however, that the thermodynamic development itself will not be restricted to one-dimensional behavior, but will actually provide the basis for a three-dimensional constitutive theory; the 3-D stress-strain equations will be reviewed briefly later.

Another point to be emphasized is that the thermodynamic theory provides isothermal and nonisothermal constitutive equations. It also provides the basic equations for calculation of temperature change due to straining, such as occurs in a vibrating propellant grain. Nonequilibrium thermodynamics introduces time effects in a constitutive theory, and shows how they must be represented analytically to be physically correct.

The theory is based on application of the first and second laws to systems which are not required to be in equilibrium, and therefore provides much more information than does classical (equilibrium) thermodynamic theory. In continium mechanics, it is convenient to use the following forms of the laws.(129)

First Law: There exists an internal energy U with the property that, for all processes,

$$\frac{dH}{dt} + \frac{dW}{dt} = \frac{dU}{dt} \tag{43}$$

where dH/dt and dW/dt are the rate of heat addition and rate of mechanical work done on the system, respectively.

Second Law: There exists an absolute temperature, T, and entropy S with the property that

$$\frac{dS}{dt} = \frac{dH}{dt}\,\frac{1}{T} + \frac{dS'}{dt} \tag{44}$$

where

$$\frac{dS'}{dt} \geq 0 \tag{45}$$

is the so-called entropy production which is never negative. (When $dS'/dt = 0$, the equations of elasticity result, and when $dS'/dt > 0$, the equations of viscoelasticity result.)

The thermodynamic system is now defined. It is considered to be a material element of fixed mass (i.e., a specimen) under a uniform state of strain specified by the six quantities $q_1, q_2 \ldots q_6$. For a linear viscoelastic material, these six quantities are identically equal to the sixth component of the strain tensor, while for a nonlinear body they may either equal the finite strains or be algebraic functions of the strains. Without loss in generality, the mathematics are simplified by assuming the body has unit volume in a chosen reference state.

The rate of mechanical work can always be written in the form

$$\frac{dW}{dt} = \sum_{M=1}^{6} Q_i \frac{dq_i}{dt} \tag{46}$$

where Q_i is the so-called generalized force. When the six q_i are equal to the strains, Q_i must be equal to the six stresses in order to satisfy Equation (46). On the other hand, if q_i are functions of strain, one must use Equation (46) to find the relation between stresses and generalized forces. These measures of strain are often called observed variables.

The measures of strain, q_i ($i = 1, \ldots 6$), and temperature, T, are not sufficient to define the thermodynamic state of a time-dependent polymeric material, while they are sufficient for an elastic material. Additional "hidden variables", q_i ($i = 7, \ldots N$), must be introduced to define the internal molecular or atomic configuration of the material.* Although these N-7 variables must be included in the development of the theory, they do not appear in the final constitutive equations and therefore, for our purposes, do not have to be identified with any specific physical mechanism.

Nevertheless, in order to emphasize the generality and validity of this approach, the hidden variables' physical significance will be reviewed. Their purpose is to completely characterize the materials' free energy (see Equation 47), and therefore they may be thought of as defining such things as (1) lattice distortions and location of interstitial atoms in a metal; (2) configurations of the chainlike molecules in amorphous polymers, as well as changes in chemical energy due to bond breakage and reformation; and (3) molecular configurations and degree of crystallinity in semi-crystalline polymers. In creep of a polycrystalline metal, for example, the external distortion reflects the combined action of grain boundary sliding, internal slipping of grains, twinning, etc. Even with large amounts of plastic flow the lattice is not greatly distorted; indeed, it is sufficient to use only second-order terms in q_i ($i = 7, \ldots N$) in the free energy representation which turns out to greatly simplify the development of stress-strain equations for metals. This example for metals was given to show how physically based simplifications can be introduced into the theory when one has some knowledge of a material's microstructure.

Development of a constitutive equation begins with the introducton of the so-called Helmholtz free energy (per unit initial volume) defined as,

$$F = U - TS \tag{47}$$

---

* More generally, hidden variables are defined as all of those entering in the free energy for which the generalized force is always zero. (i.e., $Q_i = 0$; $i = 7, \ldots N$).

(For the special case of pure elastic behavior, this function is the strain energy). Let us now combine the First and Second Laws with Equation (47) and obtain a very important inequality:

$$\sum_{i=1}^{N} \left(Q_i - \frac{\partial F}{\partial q_i}\right) \frac{dq_i}{dt} \geq 0 \qquad (48)$$

in which, by definition, $Q_7 . . . .Q_N = 0$, and $F = F(q_1, . . .q_N, T)$. Also, the left-hand side is TdS'/dt.

Equation (48) forms the basis for the development of a three-dimensional constitutive theory. The fact that the left-hand side must be non-negative for all physical processes is very important, as it can be shown to imply that,

$$Q_i - \frac{\partial F}{\partial q_i} = \sum_{j=1}^{N} b'_{ij} \frac{dq_i}{dt} \qquad (49)$$

Further, when strain rates are sufficiently small, the matrix b_{ij} is, at most, a function of q_i and T; it is also symmetric ($b'_{ij} = b'_{ji}$), according to Onsagers principle.(129)

Consider the significance of the set of N equations in Equation (50). We have the six equations for i = 1, ...6,

$$Q_i = \frac{\partial F}{\partial q_i} + \sum_{j=1}^{N} b'_{ij} \frac{dq_i}{dt} \qquad (50)$$

plus the additional N-6 equations.

$$0 = \frac{\partial F}{\partial q_i} + \sum_{j=7}^{N} b'_{ij} \frac{dq_i}{dt} \qquad (51)$$

Free energy F is a material function in that it reflects the physical makeup of the material. The matrix element, b_{ij}, can be interpreted as a nonlinear viscosity coefficient, and also represents a material function. If, by some means, these material functions F and b_{ij}, are known then Equation (49) can be solved, in principle, to obtain a three-dimensional set of stress-strain equations. This solution is accomplished

as follows: Equation (51) is a set of N-6 equations which can be solved for the N-6 hidden variables q_i (i = 7. . . . N) in terms of the measures of strain, q_j (i = 1 . . . 6), and temperature. When these hidden variables are substituted with Equation (50), what results can be put in the form of an integral equation relating the stress and strain tensors and temperature; by this process of eliminating hidden variables from Equation (50), the original set of first-order differential equations is converted to an expression which yields the stress tensor as a functional of strain and temperature. (Although consideration has not been given to the problem of calculation temperature, an energy equation has been derived which could be used in the calculation of temperature.[30])

The solution outlined above can be obtained explicitly only if (1) the material is linearly viscoelastic; in this case, coefficients b_{ij} are functions of only temperature and F contains only linear and quadradic terms in q_i; or, if, (2) the material is nonlinear but the free energy and viscosity coefficients depend in a simple way on q_i.

Fortunately, the above condition (2) appears to be satisfied by many materials, including many metals and polymers,[32] in their nonlinear range of behavior.

Specifically, for polymers,

$$b'_{ij} = a_D \, b_{ij} \tag{52}$$

where $b_{ij} = b_{ji}$ is a constant matrix; all nonlinear viscosity effects enter in the scalar coefficient, a_D. In the linear range $a_D = 1$, and for all cases the Second Law requires that $a_D > 0$. The free energy can be taken as a quadratic function of the hidden variables,

$$F = F_e + \frac{1}{2} \sum_{i=7}^{N} \sum_{j=7}^{N} a'_{ij} \, q_i \, q_j \tag{53}$$

where $F_e = F_e (q_1, \cdots q_6)$ = long-time strain energy

$a'_{ij} = a'_{ji} (q_1, \cdots q_6)$ = matrix defining nonlinear elastic behavior of the polymer network during time-dependent deformations.

(For simplicity, temperature dependence of F is omitted in the present discussion). Furthermore, our studies have shown that an assumption analogous to Equation (52) can be used; viz.

$$a_{ij} = a_F \, a_{ij} \quad (i, j = 7 \cdots N) \tag{54}$$

where a_{ij} are constants and the scalar $a_F = a_F(q_1, \ldots q_6)$ reflects nonlinear, finite strain behavior of the polymer network, excluding its long time response. In the linear range of behavior $a_F = 1$; otherwise $a_F > 0$ as long as the material is mechanically stable.(30)

Finally, in concluding the thermodynamic development, it is important to emphasize the following features:

In the thermodynamic model, the strength of the nonlinearities is not at all restricted because a_D, a_F and q_i ($i = 1, \ldots 6$) may have as strong dependence on strain as the experimental data requires.

The primary assumptions are that all elements of the matrices b_{ij} and a_{ij} vary with respect to strain through common scalar factors, a_D and a_F, respectively.

The factors a_D and a_F reflect third and higher order dependence of the entropy production and free energy, respectively, on the measures of strain.

The motivation for introducing the factors a_D and a_F is based on the uniaxial and biaxial stress-strain behavior observed for many materials.

Through the use of scalar energy functions F and dS' /dt, implications of experimental information obtained from simple stress states are immediately and naturally extended to a three-dimensional theory.

Microstructural damage (Mullins' effect and flaw propagation) can be interpreted thermodynamically as processes for which there are large changes in free energy (primary bond rupture) and entropy production (large relative motions between molecules following local rupture). Thus a_D, a_F, and F_e can be expected to depend on the amount of damage as described by Farris' theory.

(2) A simple Stress-Strain Equation

Just how a specific stress-stress equation is obtained from the thermodynamic theory will be illustrated here for a one-dimensional stress-state. Further, it will be shown that this equation is equivalent to a model consisting of nonlinear springs and dashpots.

The thermodynamic system is a bar under uniaxial loading. There is only one observed variable, q_1, say, and one generalized force Q_1. The lateral strain is included in the set of hidden variables as, by assumption, no force acts on the sides of the bar. The constitutive equation is derived by introducing special forms (52) and (54), into Equation (51), and then eliminating the hidden variables from (50). After much work the result can be written in terms of engineering stress and strain as follows:

$$\sigma = \frac{dF_e}{d\varepsilon} + a_F \frac{dq_1}{d\varepsilon} \int_{-\infty}^{t} \Delta E(\chi-\chi') \frac{dq_1}{d\rho}\, d\rho \qquad (55)$$

where

$$\chi \equiv \int_0^t \frac{a_F}{a_D}\, dt' = \text{reduced time}$$

$$\chi(\rho) = \int_0^{\rho} \frac{a_F}{a_D}\, dt'$$

$$\Delta E(\chi) = \sum_{i=1}^{M} E_i\, e^{-\chi/\tau_i} = \text{time-dependent part of the } \underline{\text{linear}} \text{ viscoelastic relaxation modulus (see Equation (42).}$$

$$q_1 = q_1(\varepsilon) = \text{measure of strain}$$

There are four nonlinear material properties in this equation to be found from experiment: F_e, q_1, a_F, and a_D; there is also one time-dependent function, $\Delta E(\chi)$, which is the transient component of the linear viscoelastic relaxation modulus.

Equation (55) reduces to Equation (41) for isothermal behavior of a linear viscoelastic material when

$$q_1 = \varepsilon,\ a_D = a_F = 1, \text{ and } F_e = E_e\varepsilon^2/2.$$

Temperature dependence has not been explicitly discussed. However, upon returning to the thermodynamic theory and including temperature dependence in the free energy and entropy production, it is found that

F_e, a_D and a_F may, in general, be temperature-dependent, and that thermal expansion enters Equation (55).(30) Indeed, when $F_e = E_e\varepsilon^2/2$, $a_F = 1$, $a_D = a_T$, the constitutive equation for a thermorheologically simple material results.

Perhaps a better feeling for the physical significance of Equation (55) can be had by recognizing that it is equivalent to the mechanical model in Figure (24) wherein the dashpots' viscosities η_i' have a common non-linearity.

$$\eta_i' = a_D\eta_i \qquad (\eta_i = \text{constants})$$

Similarly, with exception of the far left spring, the spring moduli E_i' are given by

$$E_i' = a_F E_i \qquad (E_i = \text{constants})$$

Recall that the Mullins effect and vacuole formation reflect molecular bond rupture and consequently large changes in the free energy. Thus, one possible mechanical model that combines permanent and fading memory, is the one in Figure(24) in which the free energy-based functions F_e and a_F (and possibly the entropy coefficient a_D) change with molecular damage.

(d) Plasticity Effects

To represent plasticity effects in a materials response requires special consideration to memory phenomenon in the constitutive equation. Plasticity by definition means permanent set in solid materials after all loads are removed. A solid is defined as a material having a non-zero distortional equilibrium modulus whereas a fluid is defined as having a zero distortional equilibrium modulus. Elasticity by definition means complete recovery of some reference shape upon removal of all loads.

Thus the main difference between elastic and plastic materials is the concept of a permanent or changing stress free configuration for each element in the body. Viscous effects in solid materials must fall into the categories of either viscoelasticity or viscoplasticity and implies time dependent elastic or plastic effects.

There has been much confusion as to just what types of constitutive representations are required to describe plasticity type stress-strain behavior. Naturally the phenomenological incremental plasticity theory which decomposes the strain tensor into an elastic, plastic and viscous parts contains the effects of viscoplastic materials. This type of equation is difficult to use and is somehow quite separately treated in continuum theory. It would appear desirable to have a theory of plasticity that could be treated in the usual manner with regard to functional expansions in the classical continuum definition of a simple material. Considerable work has been done showing

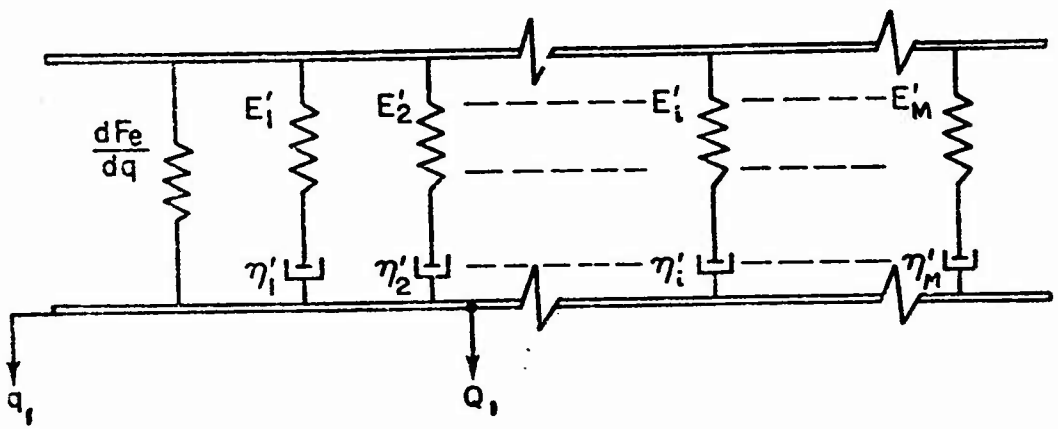

A MECHANICAL MODEL FOR NONLINEAR VISCOELASTICITY

Figure 24

that the so called Frechet multiple integral expansion used by Rivlin and coworkers in their treatments of materials with memory, Equations (67) and (68), are valid for plasticity. These works are erroneous since the multiple integral representation is a fading memory viscoelastic representation when applied to solid materials and can in no way contain plasticity effects. In fact the multiple integral representations cannot even contain nonlinear elastic or viscoelastic effects which have permanent rather than fading memory. Such effects include the time dependent or time-independent Mullins' effect described earlier.

Plasticity effects can be included in hereditary integral constitutive equations by defining a new measure of time, a reduced or material time which depends upon deformation history. Such methods have been suggested by Dong[34] and Rivlin[13] to obtain rate independent but deformation history dependent constitutive equations. As stated earlier it is this researcher's opinion that it is impossible to contain these effects so long as the hereditary arguments are the real time. The work of Dong and Rivlin overcomes the fading memory restrictions included in these hereditary equations by defining what Dong termed chronological variables which were termed material times. Chronological variables must by definition be monotonic functions. Interestingly chronological variables and L_p norms have this monotonic characteristic, thus one possible form of chronological variables are L_p norms. To demonstrate this effect consider the reduced or material time defined as

$$S = \left\{ \int_0^t |\dot{\varepsilon}(\xi)|^p d\xi \right\}^{1/p} = ||\dot{\varepsilon}||_p \tag{56}$$

When this measure of reduced time is substituted into the ordinary linear hereditary integral representation used for linear viscoelasticity,

$$\sigma(t) = \int_0^t E(S - s)\ \dot{\varepsilon}(\xi) d\xi \tag{57}$$

an equation that is history dependent and strain rate dependent but exhibits no creep or stress relaxation results. As an example consider the case when the kernel function E(S-s) is given as a single term Prony series representation

$$E(S-s) = Ae^{-\beta(S-s)} \tag{58}$$

Substituting this kernel function and the time measure, $||\dot{\varepsilon}||_p$, into the integral equation and differentiating with respect to the real time t is the easiest way of demonstrating what the equation contains.

$$\dot{\sigma} = A\dot{\varepsilon} - \frac{B|\dot{\varepsilon}|^p}{P||\dot{\varepsilon}||_p^{p-1}}\sigma \tag{59}$$

where $\dot{X} = \frac{dx}{dt}$

when $p = 1$ this equation becomes

$$d\sigma = Ad\varepsilon - B|d\varepsilon|\sigma \tag{60}$$

This equation obviously contains no strain rate effects since $d\sigma$ is proportional to $d\varepsilon$ for loading and unloading, the proportionality constant depending upon direction and stress magnitude. Also the equation contains no creep or stress relaxation effects, (no dependence on real time t) since when $d\varepsilon$ is zero, time is frozen and $d\sigma$ becomes zero. Thus the stress changes only when the strain changes and history effects are included. Equation (60) contains repeated yielding, permanent set, and effects like the Bauschinger effect of plasticity.

When the order of the reduced time norm p is not unity then the equation contains additional effects. In particular the equation still does not contain creep or stress relaxation since when the time derivative of strain is zero the stress remains constant. The equation does however include strain rate effects since both the terms $|\dot{\varepsilon}(t)|^p$ and $||\dot{\varepsilon}||_p$ depend upon strain rate. Figures 25 and 26 provides a graph of the stress-strain Equation (59) for the value $p = 1$ for repeated loading and unloading demonstrating that plasticity effects are contained by this equation.

To include time effects as well as rate and history effects the material measure of time need only include direct dependence upon real time. For example when the material time is defined as

$$S = a_1||\dot{\varepsilon}||_p + a_2 t \tag{61}$$

Then Equation (57) contains a form of

- Rate independent plasticity $\quad a_1 \neq 0,\ a_2 = 0,\ p = 1$
- Rate dependent plasticity $\quad a_1 \neq 0,\ a_2 = 0,\ p \neq 1$

FIGURE 25 - DEMONSTRATION OF AN INTEGRAL APPROACH TO PLASTICITY USING AN L_p MEASURE OF TIME

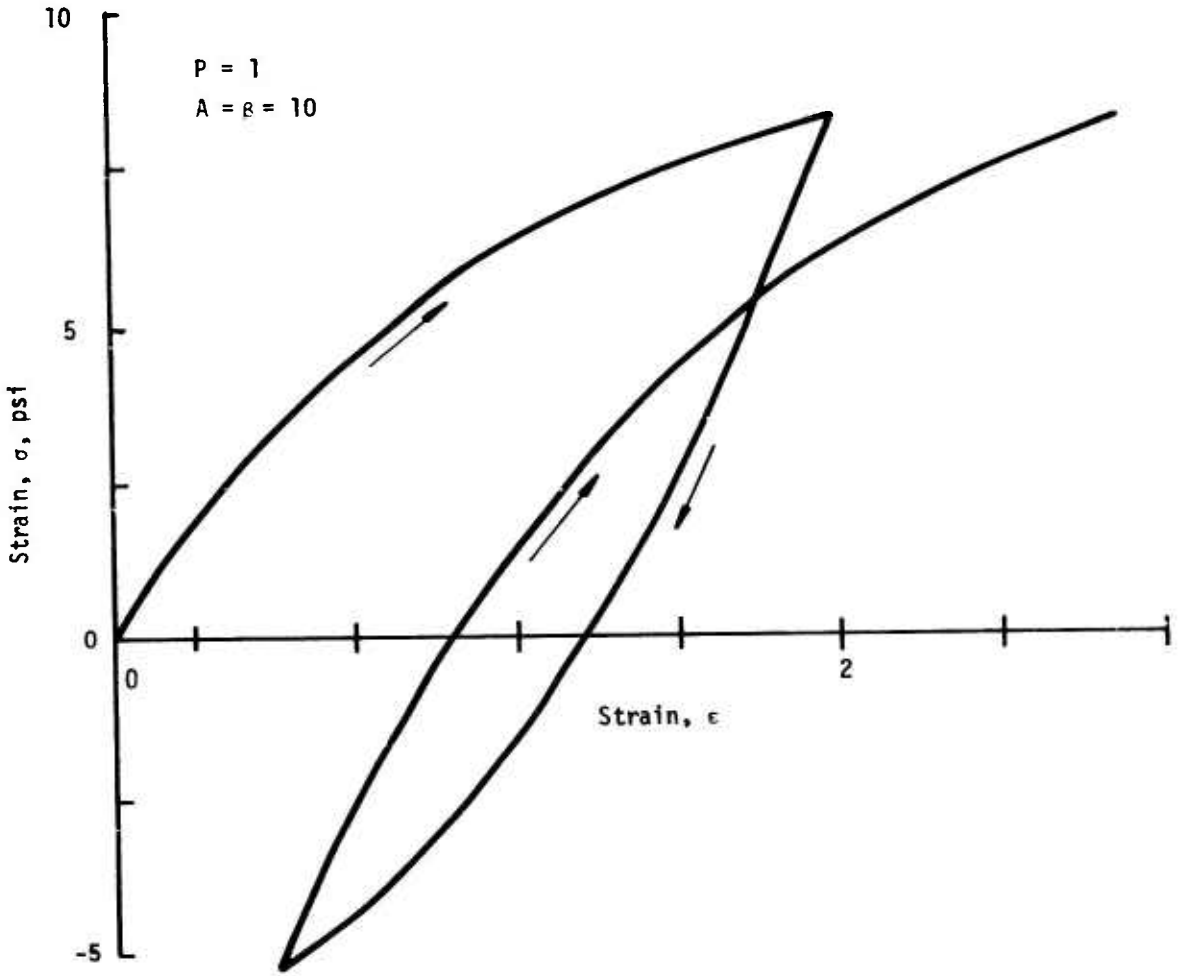

Figure 25

FIGURE 26 - DEMONSTRATION OF AN INTEGRAL APPROACH TO PLASTICITY USING AN L_p MEASURE OF TIME

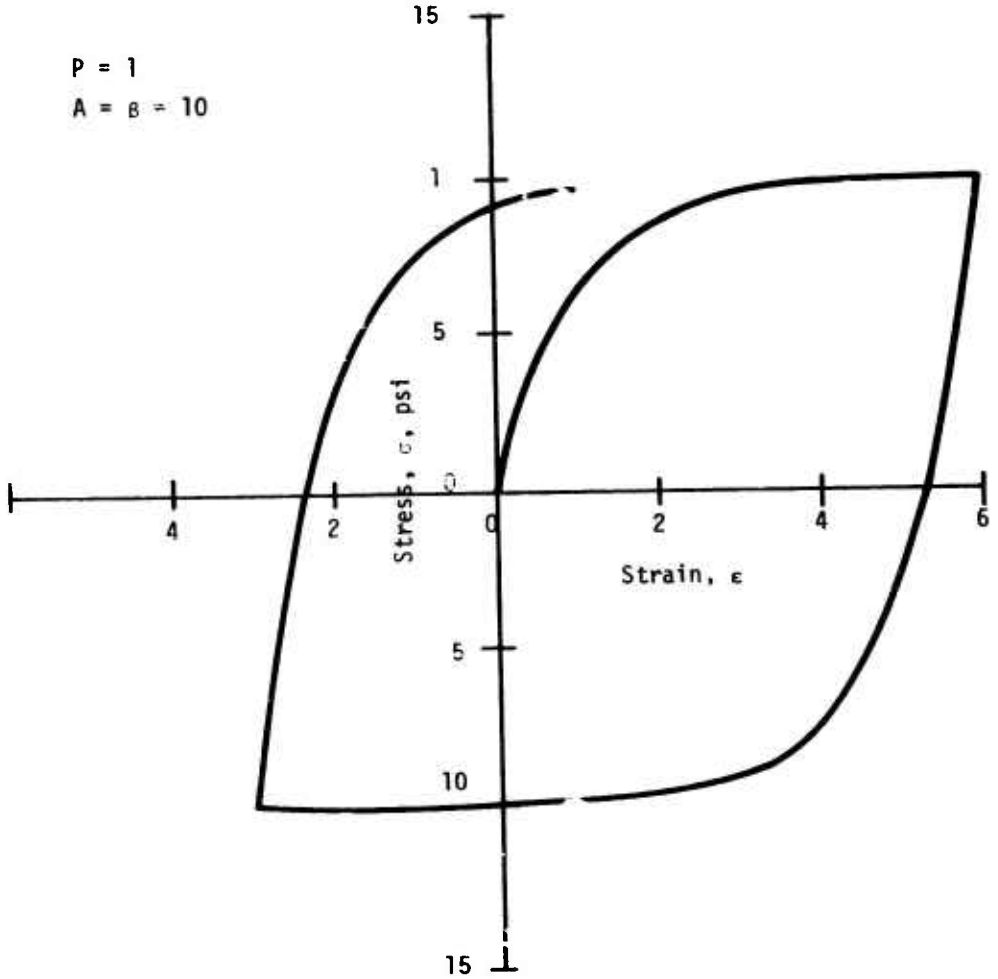

Figure 26

- Linear viscoelasticity $a_1 = 0,\ a_2 \neq 0,$ p arbitrary
- Viscoplasticity $a_1 \neq 0,\ a_2 \neq 0,$ p arbitrary
- Linear elasticity E = constant

Actually the measure $s = a_z t$ is the L_p norm

$$S = ||a_2||_1 \qquad \text{Where } a_2 = \text{constant} > 0 \tag{62}$$

In fact, making a_2 a function of temperature such that $a_2 = 1/A_T$, where A_T is the time-temperature shift function and the reduced time is normally defined as

$$S = \int_0^t d\xi/A_T(\xi) \quad , \tag{63}$$

is nothing more than Equation (62) with a_2 as a function of temperature. In fact the material time defined as

$$S = ||a_1\dot{\varepsilon}||_p + ||a_2||_1 \tag{64}$$

with a_1 and a_2 being temperature dependent functions contains all of the effects discussed earlier with temperature dependence.

To generate three dimensional equations it is necessary only to generalize the above arguments in a manner similar to those of Dong and use an invariant measure of time. For example defining the material time as

$$S = ||a_1 f(\dot{I}_1, \dot{I}_2, \dot{I}_3)||_p + ||a_2||_1 \tag{65}$$

Where I_1, I_2, I_3 = Invariants of the strain tensor yields an invariant measure of time that when substituted into the equation

$$\sigma_{ij}(t) = \int_0^t \left\{ \delta_{ij}\lambda(S-s)\dot{\varepsilon}_{kk}(\xi) + 2G(S-s)\dot{\varepsilon}_{ij}(\xi) \right\} d\xi \tag{66}$$

yields a three dimensional representation for plasticity and viscoplasticity.

Taking $f(\dot{I}_1, \dot{I}_2, \dot{I}_3)$ to be the octahedral strain rate $\dot{\gamma}_{oct}$ and the bulk term $\lambda(S\text{-}s)$ to be constant provides an equation with linear elastic bulk effects and plasticity shear effects with a yield surface dependent on the octahedral shear strain. Obviously these equations can be made more complex by including second order integrals and other effects however it is important to realize that this simple single integral representation can and does contain complex plasticity effects by using a chronological strain measure of time.

Plasticity effects become important in propellants due to aging since chemical rearrangement of the microstructure can and does cause large plasticity effects, especially during high temperature storage.

(4) Task IV - A Simple Constitutive Theory

Requirements:

The contractor shall devise a problem or a series of problems which will adequately test a simple nonlinear constitutive theory. These problems must be of such a nature that results can be obtained experimentally for comparison with calculated solutions. The problems and their relationship to the objectives of this task shall be submitted to the Air Force contracting officer for approval. With these problems in mind the contractor shall construct the necessary constitutive theory to handle them. This constitutive theory shall be based upon what has been learned in Task I through III. The contractor shall then characterize this material and proceed to obtain analytical solutions. The material used in this task must be solid propellant. After he has obtained his calculated solutions he shall proceed to test his answers by conducting a program to obtain experimental solutions. A complete comparison shall be made between calculated and experimental results with an exhaustive discussion presented on the discrepancies, if any. The primary objective of this task is not to develop a final constitutive theory or material characterization procedures but rather to test the validity of the mathematical models of the nonlinear mechanisms. Accordingly, therefore, an extensive amount of effort should not be placed into constitutive theory development but rather the constitutive law should be developed only to such an extent that it can meet the objectives of this task.

(a) Farris' Theory

(1) Equations for Multiaxial States of Stress

In the previous section mathematical models were developed for describing the state of damage due to chain failure and vacuole density. These simple models were then extended to include their effect on the stress-strain behavior and it was demonstrated that each model contained the type of response displayed by composite solid propellants. To extend these models to include three dimensional effects is a most complex problem. Examination of history indicates that attempts to describe the mechanical response of materials has classically taken two paths, (a) the theoretical development of mathematically complete constitutive equations describing the behavior of hypothetical materials and (b) the experimental determination and subsequent empirical mathematical model description of the behavior of real materials to a limited set of loading conditions. Neither approach stands alone and each approach has its merits and difficulties. The complete mathematical description of a hypothetical material is of little value to the engineer if he has no basis upon which to judge whether or not his real materials' responses can be described by the theory, and even if they could be, can the parameters entering into the theory be determined from laboratory tests? On the other hand, the mathematical model description of a real material to one loading condition is generally of little value in predicting the response to some completely different loading condition. This is particularly true for any nonlinear material. In practice, one finds these two approaches must be brought together. This process involves interpreting experimentally based models or empirical relationships in terms of some mathematically complete description of a hypothetical material. This is precisely the approach taken by Farris to extend his one dimensional model relationships to general three dimensional relationships. To accomplish this end, Farris interpreted his model theory in terms of the Green, Rivlin, and Spencer abstract theory for nonlinear materials with memory.[10] Since the Green, Rivlin, and Spencer theory is a fading memory theory[1], and Farris models had permanent memory, some means had to be found to incorporate permanent memory in the Green, Rivlin, and Spencer representations. This obstacle was overcome after careful study of their theory and the resulting constitutive theory described below is applicable to describing propellant response.

The Green, Rivlin and Spencer constitutive equation for isotropic materials can be represented as

$$\underline{\sigma}(t) = K_0(t)\underline{I} + \int_0^t K_1(t,\tau_1)\dot{\underline{e}}(\tau_1)d\tau_1 + \tag{67}$$

$$+\int_0^t\int_0^t K_1(t,\tau_1,\tau_2)\dot{\underline{e}}(\tau_1)\dot{\underline{e}}(\tau_2)d\tau_1 d\tau_2 +$$

$$+ \cdots + \int_0^t\cdots\int_0^t K_n(t,\tau_1,\cdots,\tau_n)\dot{\underline{e}}(\tau_1)\cdots\dot{\underline{e}}(\tau_n)d\tau_1\cdots d\tau_n + \cdots,$$

where $\underline{\sigma}$ = stress tensor

$\underline{\dot{e}}$ = strain rate tensor

$\underline{I}$ = unit tensor

t = current time

τ_i, ξ = generic or dummy times

$$K_n(t,\tau_1,..\tau_n) = K_n[I_1\overset{t}{\underset{0}{(\xi)}}, I_2\overset{t}{\underset{0}{(\xi)}}, I_3\overset{t}{\underset{0}{(\xi)}}, t, \tau_1, .., \tau_n]$$

I_1, I_2, I_3 = strain invariants

At this point in their theory the kernels, K_1, K_2,..K_n, are functionals of the history of the scalar invariants of the Cauchy strain tensor as well as the generic and current values of time. This equation was obtained using the so called Fréchet expansion of a more general functional relationship. Normally the Kernel functionals of equation 67 are again expanded in Frechet expansions to eliminate their dependence on the strain invariants to obtain for nonaging materials.

$$\underline{\sigma}(t) = \int_0^t \{\underline{I}k_1 tr\underline{\dot{e}}(\tau_1) + k_2\underline{\dot{e}}(\tau_1)\}d\tau_1 + \int_0^t\int_0^t \underline{I}k_3 tr\underline{\dot{e}}(\tau_1)tr\underline{\dot{e}}(\tau_2)$$

$$+ \underline{I}k_4 tr[\underline{\dot{e}}(\tau_1)\underline{\dot{e}}(\tau_2)] + k_5\underline{\dot{e}}(\tau_1)tr\underline{\dot{e}}(\tau_2) + k_6\underline{\dot{e}}(\tau_1)\underline{\dot{e}}(\tau_2)\}d\tau_1 d\tau_2$$

$$+ \int_0^t\int_0^t\int_0^t \{\underline{I}k_7 tr\underline{\dot{e}}(\tau_1)tr\underline{\dot{e}}(\tau_2)tr\underline{\dot{e}}(\tau_3) + \underline{I}k_8 tr\underline{\dot{e}}(\tau_1)tr[\underline{\dot{e}}(\tau_2)\underline{\dot{e}}(\tau_3)]$$

$$+ k_9\underline{\dot{e}}(\tau_1)tr\underline{\dot{e}}(\tau_2)tr\underline{\dot{e}}(\tau_3) + k_{10}\underline{\dot{e}}(\tau_1)tr[\underline{\dot{e}}(\tau_2)\underline{\dot{e}}(\tau_3)]$$

$$+ k_{11}\underline{\dot{e}}(\tau_1)\underline{\dot{e}}(\tau_2)tr\underline{\dot{e}}(\tau_3) + k_{12}\underline{\dot{e}}(\tau_1)\underline{\dot{e}}(\tau_2)\underline{\dot{e}}(\tau_3)\}d\tau_1 d\tau_2 d\tau_3 + \int_0^t\int_0^t\int_0^t\int_0^t \cdots \tag{68}$$

In the above equation k_1,k_2 are functions of $(t-\tau_1)$; k_3,k_4,k_5,k_6 are functions of $(t-\tau_1, t-\tau_2)$; and k_7,....,k_{12} are functions of $(t-\tau_1, t-\tau_2, t-\tau_3)$; etc.

In this latter form the equation is restricted to fading memory behavior and is not applicable to composite propellants or other permanent memory materials, however, in the literature one can find numerous examples of misapplying these equations since the restrictions are not well known. It appears the restriction to fading memory is forced on the relations because of the continuity requirements for Frechet functionals[41], although again one can find incomplete proofs stating otherwise. (124) To use this theory for permanent memory behavior one must begin prior to Equation (68) before these restrictions are imposed. If the kernel functionals of Equation (67) were allowed to take on permanent memory measures using L_p norms or other permanent registers, then the equations could contain permanent memory as is easily demonstrated by example[1]. Unlike our model equations which only included permanent memory behavior, these hereitary integral representations also contain internal viscosity time effects. Farris, therefore began with Equation (67) and chose to represent the Kernel functionals invariant dependency using L_p norms of the invariant histories.

It is important to note here that none of the principles of isothermal continuum mechanics are being violated. The only principle that could be violated is that of objectivity which states the constitutive equation should remain invariant to an arbitrary rotation or translation of the reference frame[13]. If the strain measure itself is objective and the stress written as a functional of the objective measure, then the constitutive equation will automatically be objective as shown by Green and Rivlin[10].

In his Ph.D. work, Farris restricted the equations he developed to the class of materials he termed as "homogeneous constitutive equations of degree one." This class of materials always obeys the homogeneity rule of linearity. If the material also obeys the additivity rule of constitutive linearity then the material is linear; if it does not then the material has a nonlinear constitutive equation which is mathematically homogeneous to degree one. Such materials are often confused for linear materials because they have some of the properties of linear materials (i.e. relaxation moduli that are independent of strain magnitude). Farris demonstrated that at small strains prior to volumetric dilatation composite propellants fall into this class of nonlinear materials. He developed a series of correspondence principles from which one could transform a linear elastic solution of an equivalent boundary valued problem into a nonlinear solution, such as Alfery and others have done for linear viscoleasticity. The equations Farris developed need not have such restrictions imposed on them which makes them applicable to larger classes of materials, such as propellants in the highly dewetted state.

The development of constitutive equations which are homogeneous to degree one is quite simple and can be done by simply imposing restrictions or constraints on Equation (67). Recall homogeneity of degree one simply means that scalar multiplication is valid for all scalars. Recall also that the strain invariants are given by

$$I_1 = e_{11} + e_{22} + e_{33}$$

$$I_2 = e_{11}e_{22} + e_{11}e_{33} + e_{22}e_{33} - e_{12}^2 - e_{13}^2 - e_{23}^2$$

$$I_3 = e_{11}e_{22}e_{33} + 2e_{12}e_{13}e_{23} - e_{11}e_{23}^2 - e_{22}e_{13}^2 - e_{33}e_{12}^2 \quad (69)$$

Mathematically the homogeneous constitutive equation of degree one has the property that the equation below holds for all

$$F_{ij}\left[a e_{pq}\left(\overset{t}{\underset{\tau=0}{}}(t,\tau)\right)\right] = a F_{ij}\left[e_{pq}\left(\overset{t}{\underset{\tau=0}{}}(t,\tau)\right)\right] \quad (70)$$

where F_{ij} is an arbitrary functional

real scalars, all strain inputs and all time t. Since the first strain invariant is homogeneous to degree one, the second to degree two, and the third to degree three, non-linear homogeneous constitutive functionals can be constructed within the framework of the Green-Rivlin theory.

From physical reasoning kernel functionals homogeneous to degree less than zero cannot be admitted since they can yield unbounded stresses or singularities which are not real. With this added restriction the most general constitutive equation homogeneous to degree one within the range of applicability of Equation (67) is

$$\sigma_{ij}(t) = \delta_{ij} \int_0^t K_0\left[I_1\left(\overset{t}{\underset{0}{}}(\xi)\right), I_2\left(\overset{t}{\underset{0}{}}(\xi)\right), I_3\left(\overset{t}{\underset{0}{}}(\xi)\right), t, \tau\right] \dot{e}_{kk}(\tau)\, d\tau$$

$$+ \int_0^t K_1\left[I_1\left(\overset{t}{\underset{0}{}}(\xi)\right), I_2\left(\overset{t}{\underset{0}{}}(\xi)\right), I_3\left(\overset{t}{\underset{0}{}}(\xi)\right), t, \tau\right] \dot{e}_{ij}(\tau)\, d\tau \ ,$$

where $K_i\left[a I_1\left(\overset{t}{\underset{0}{}}(\xi)\right), a^2 I_2\left(\overset{t}{\underset{0}{}}(\xi)\right), a^3 I_3\left(\overset{t}{\underset{0}{}}(\xi)\right), t, \tau\right] =$

$$K_i\left[I_1\left(\overset{t}{\underset{0}{}}(\xi)\right), I_2\left(\overset{t}{\underset{0}{}}(\xi)\right), I_3\left(\overset{t}{\underset{0}{}}(\xi)\right), t, \tau\right]. \quad (71)$$

In Equation (71) the kernel functionals are homogeneous to degree zero. If the kernels are independent of the history of the invariants then the equation reduces to that of linear viscoelasticity. If the material is non-aging, equation (70) must reduce to[10]

$$\sigma_{ij}(t) = \delta_{ij} \int_0^t K_0\left[I_1\overset{t}{_0}(\xi), I_2\overset{t}{_0}(\xi), I_3\overset{t}{_0}(\xi), t-\tau\right]\dot{e}_{kk}(\tau)d\tau + \int_0^t K_1\left[I_1\overset{t}{_0}(\xi), I_2\overset{t}{_0}(\xi), I_3\overset{t}{_0}(\xi), t-\tau\right]\dot{e}_{ij}(\tau)d\tau \tag{72}$$

In a similar manner the state of strain can be expressed in terms of the history of the stresses for homogeneous equations of degree one as

$$e_{ij}(t) = \delta_{ij} \int_0^t L_0\left[J_1\overset{t}{_0}(\xi), J_2\overset{t}{_0}(\xi), J_3\overset{t}{_0}(\xi), t-\tau\right]\dot{s}_{kk}(\tau)d\tau + \int_0^t L_1\left[J_1\overset{t}{_0}(\xi), J_2\overset{t}{_0}(\xi), J_3\overset{t}{_0}(\xi), t-\tau\right]\dot{s}_{ij}(\tau)d\tau \ , \tag{73}$$

In Equation (73) the J_i are the principle stress invariants, and the kernels have the property that

$$L_i\left[aJ_1\overset{t}{_0}(\xi), a^2J_2\overset{t}{_0}(\xi), a^3J_3\overset{t}{_0}(\xi), t-\tau\right] = L_i\left[J_1\overset{t}{_0}(\xi), J_2\overset{t}{_0}(\xi), J_3\overset{t}{_0}(\xi), t-\tau\right] . \tag{74}$$

Except for the case when the equations reduce to linear equations, direct inversion from Equation (72) to Equation (73) appears to be virtually impossible. Unlike the linear constitutive equations the power of Laplace transforms cannot be applied since these transforms can be applied only to linear functionals. This difficulty does not mean that the inversion does not exist. In fact the homogeneity condition alone intuitively suggests that the inversion does exist since scalar multiplication must hold for all scalars and this type of one-to-one behavior is characteristic of invertible systems. For the purpose of this report, however, Equation (73) is given as the inverse form of Equation (72) when such an inverse exists.

(2) Experimental Verification for Simple States of Stress

The purpose of this section is to demonstrate that Farris' nonlinear constitutive theory actually works well on propellant data. Doing so we first demonstrate that at small strains propellants obey the first rule of linearity but not the superposition rule. Several different uniaxial tests are then used to characterize the propellants response. These tests include single and multiple step stress relaxation tests, and cyclic strain tests. The propellant tested was an 88 wt% solids CTPB propellant furnished by Hercules, Inc., Bacchus, Utah and an 82 wt% solids polyurethane propellant furnished by Aerojet-General[1]. These tests were performed using a gas dilatometer so that strain levels giving significant volume change could be avoided.

To demonstrate that propellants are nonlinear materials even at small strains, one need only check the superposition principle experimentally. In the range of small strains below detectable dewetting or volumetric dilatation[1,7] most propellants have relaxation modulus independent of strain and in general closely obey the scalar multiplication homogeneity rule. Yet this relaxation modulus cannot be used to accurately predict the response due to other isothermal, low rate, small strain inputs. To demonstrate the inadequacies of linear viscoelastic predictions on solid propellants, laboratory tests where superposition is applicable can be performed. Figure 27 illustrates the stress-strain-dilatational behavior of a typical composite propellant. The dilatation-strain behavior is caused by vacuole formation within the microstructure[5-7] and causes a stress-softening; an obvious type of non-linearity. Below significant dilatation the material appears to have a relaxation modulus that is independent of strain as illustrated in Figure 28. To determine if superposition is applicable, the interrupted ramp-strain stress relaxation test can be employed. Linear viscoelastic theory would predict the stress output for the second loading would be simply the superposition of the initial response with the continuation of the original stress-relaxation response. Figure 29 illustrates the linear viscoleastic prediction and the actual experimental results for this interrupted ramp strain test. From this and other tests it is apparent errors of over plus or minus one hundred percent are typical when linear viscoelastic theory is used to predict the response of propellant materials. To clarify the point, the data in Figure 29 are plotted as stress against strain in Figure 30. Here it is apparent that when the straining is again commenced, the response rapidly rejoins the original constant rate response, whereas the linear theory would indicate it should parallel the original response. Figure 31 illustrates similar test results for the doubly interrupted ramp test plotted stress vs strain. Again the same behavior of rejoining the original constant rate response is shown. Also the errors of linear theory are observed to grow with each cycle. Plotting the relaxation data from each portion of this test in Figure 32 further demonstrates that the relaxation responses for the first and second straining

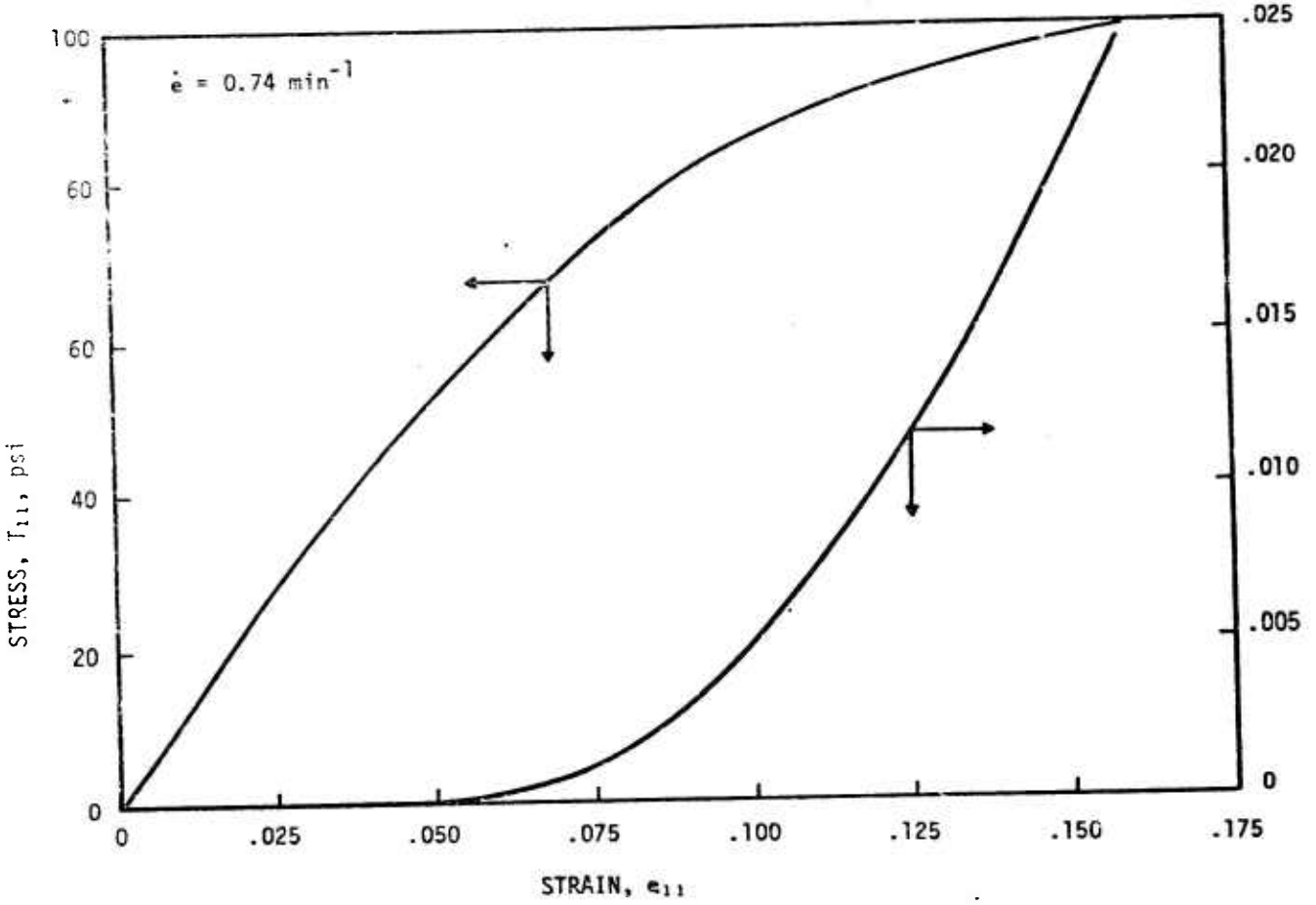

UNIAXIAL STRESS-STRAIN AND DILATATION-STRAIN BEHAVIOR

Figure 27

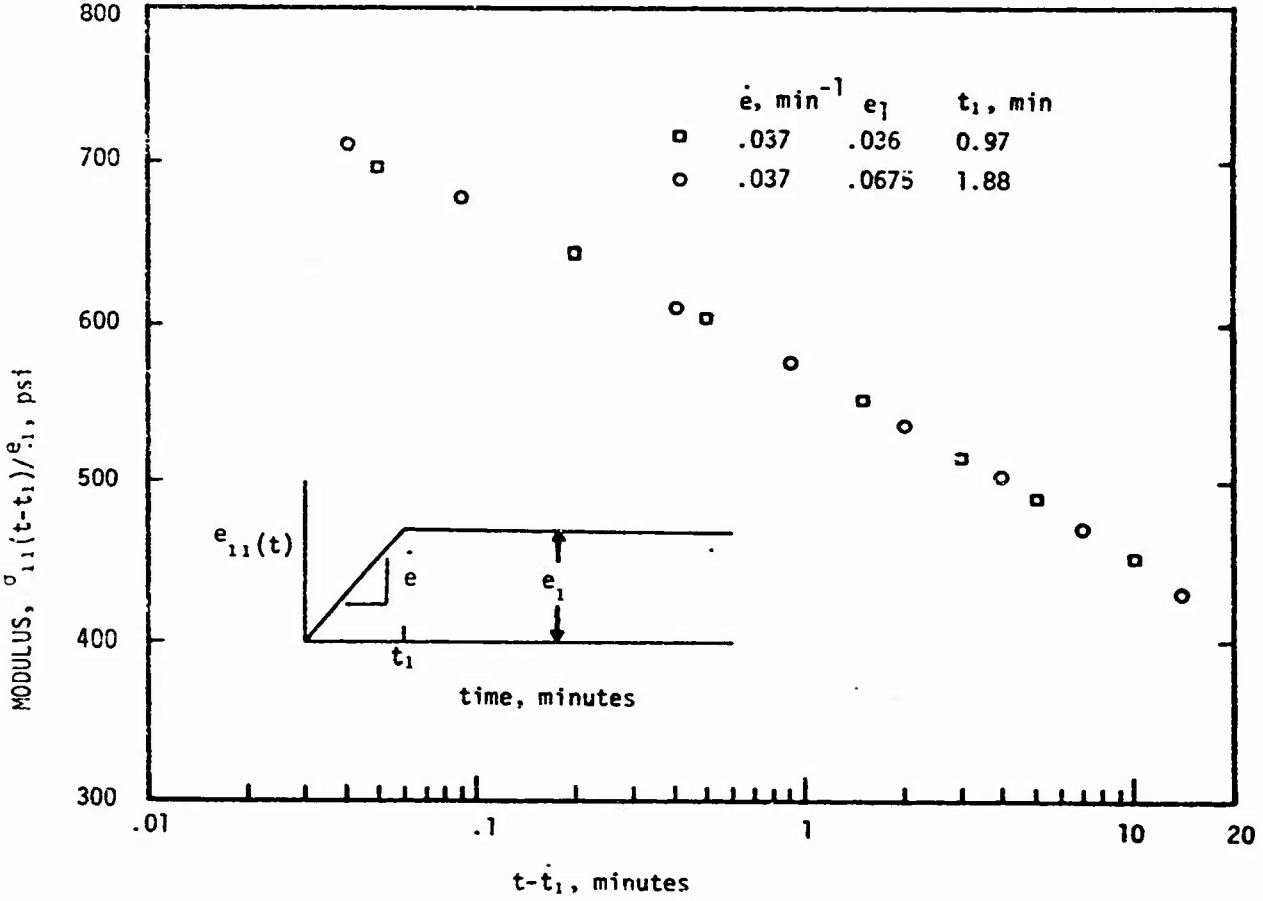

RAMP RELAXATION MODULUS FOR TWO SAMPLES TESTED AT DIFFERENT STRAIN LEVELS

Figure 28

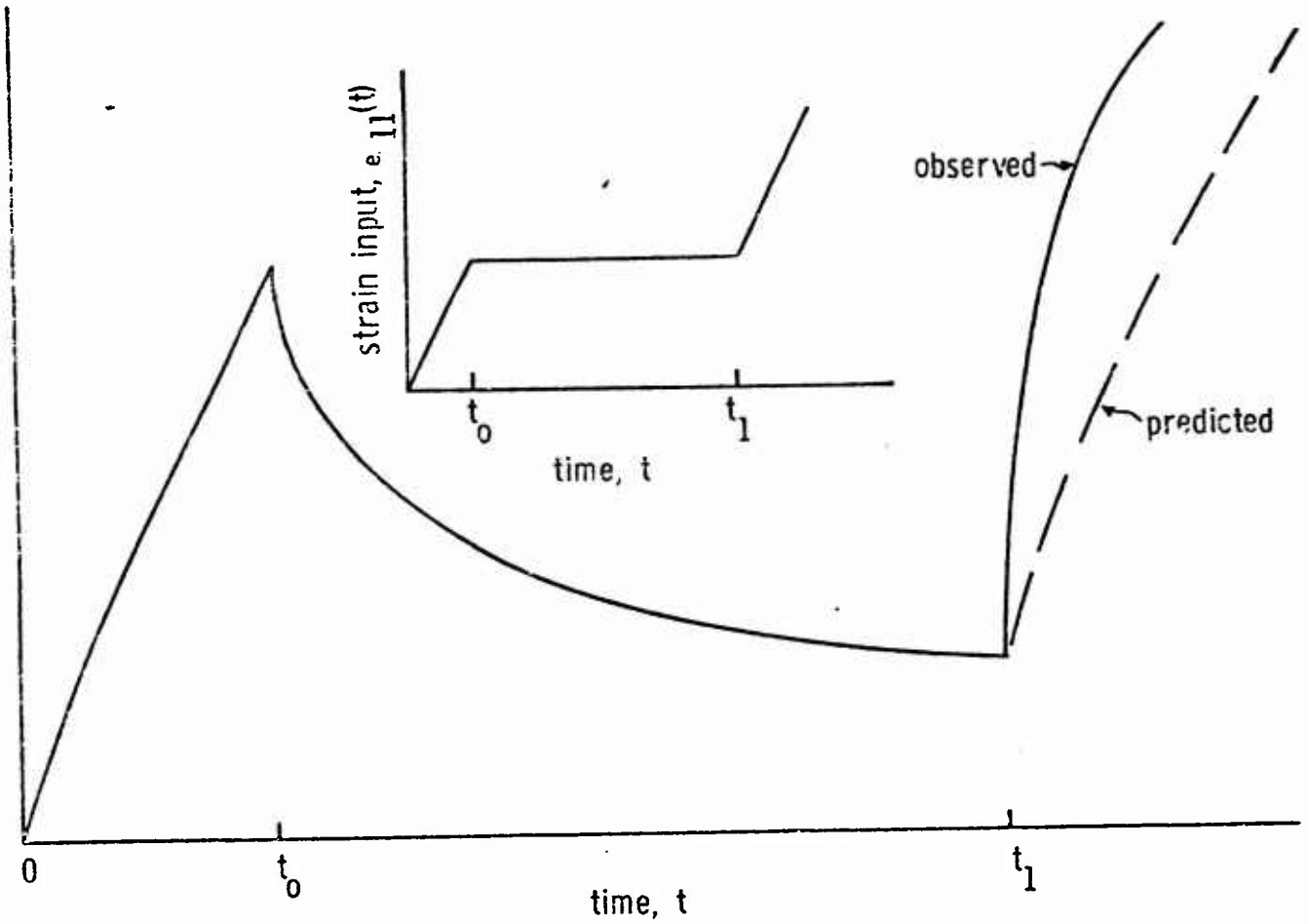

Figure 29

LINEAR VISCOELASTIC STRESS-TIME PREDICTIONS AND EXPERIMENTAL DATA FOR AN INTERRUPTED RAMP STRAIN INPUT ON A TYPICAL COMPOSITE PROPELLANT

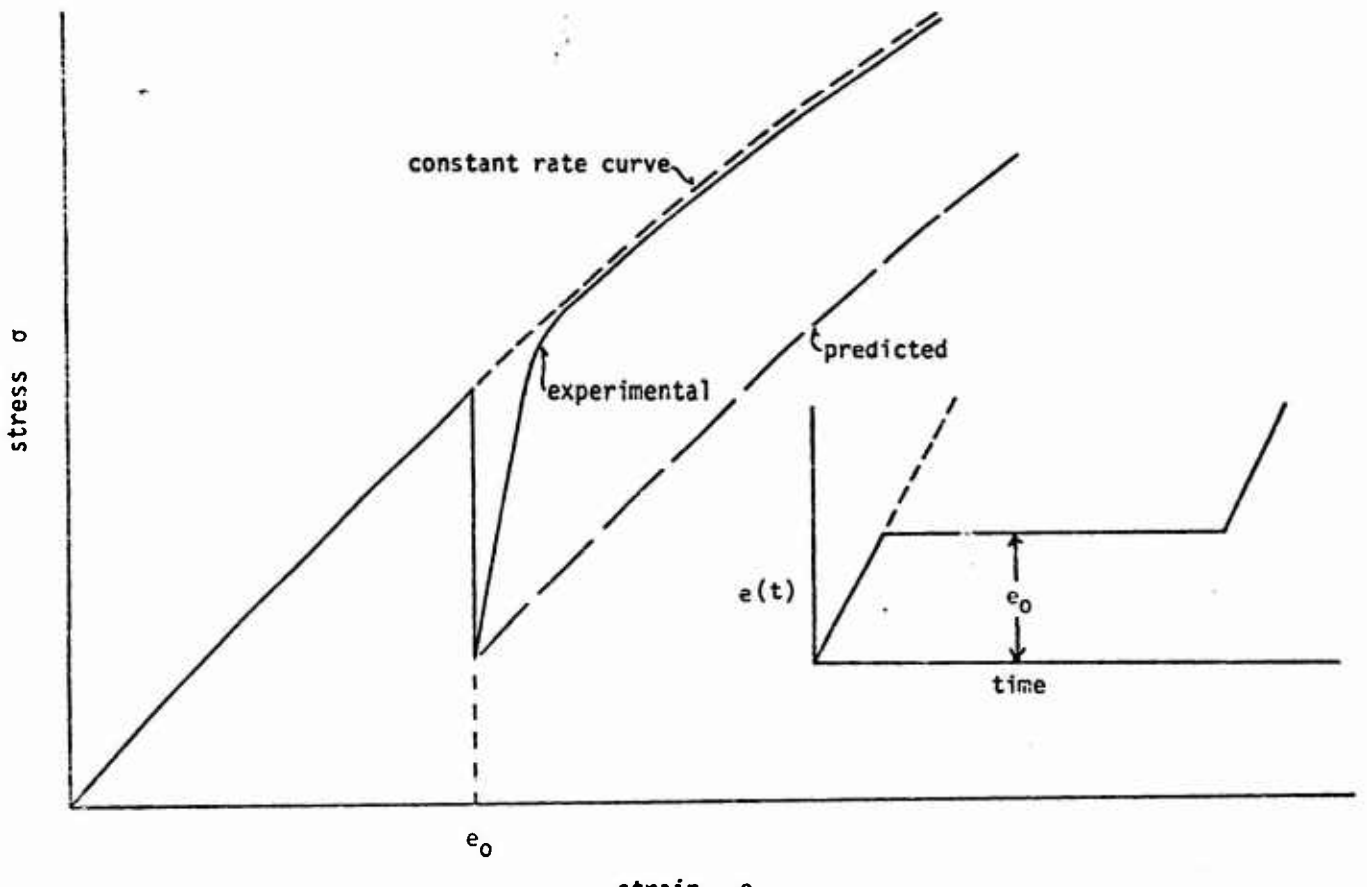

Figure 20

LINEAR VISCOELASTIC STRESS-STRAIN PREDICTION AND EXPERIMENTAL DATA FOR AN INTERRUPTED RAMP STRAIN INPUT ON A TYPICAL COMPOSITE PROPELLANT.

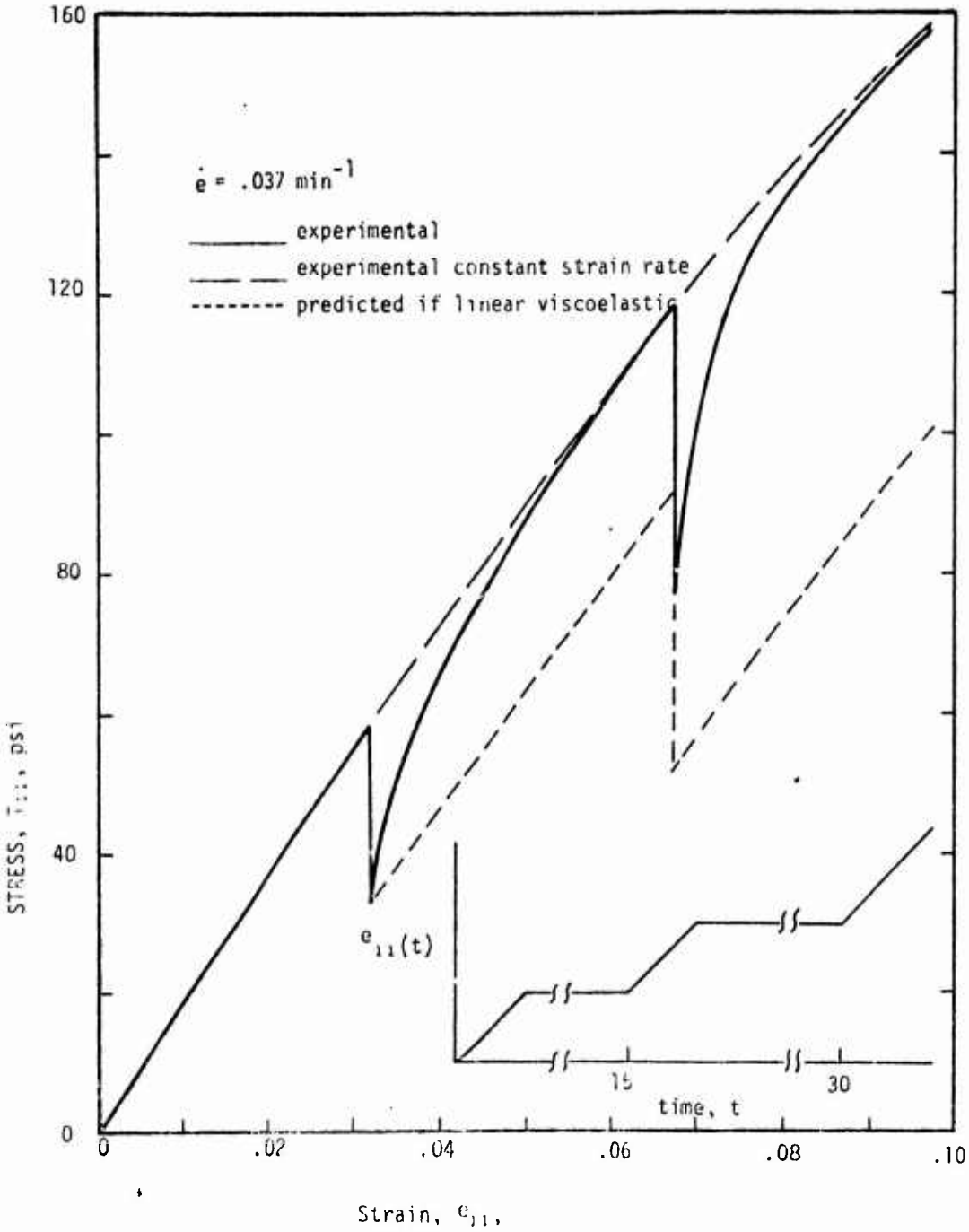

STRESS OUTPUT FOR INTERRUPTED CONSTANT STRAIN RATE TEST

Figure 31

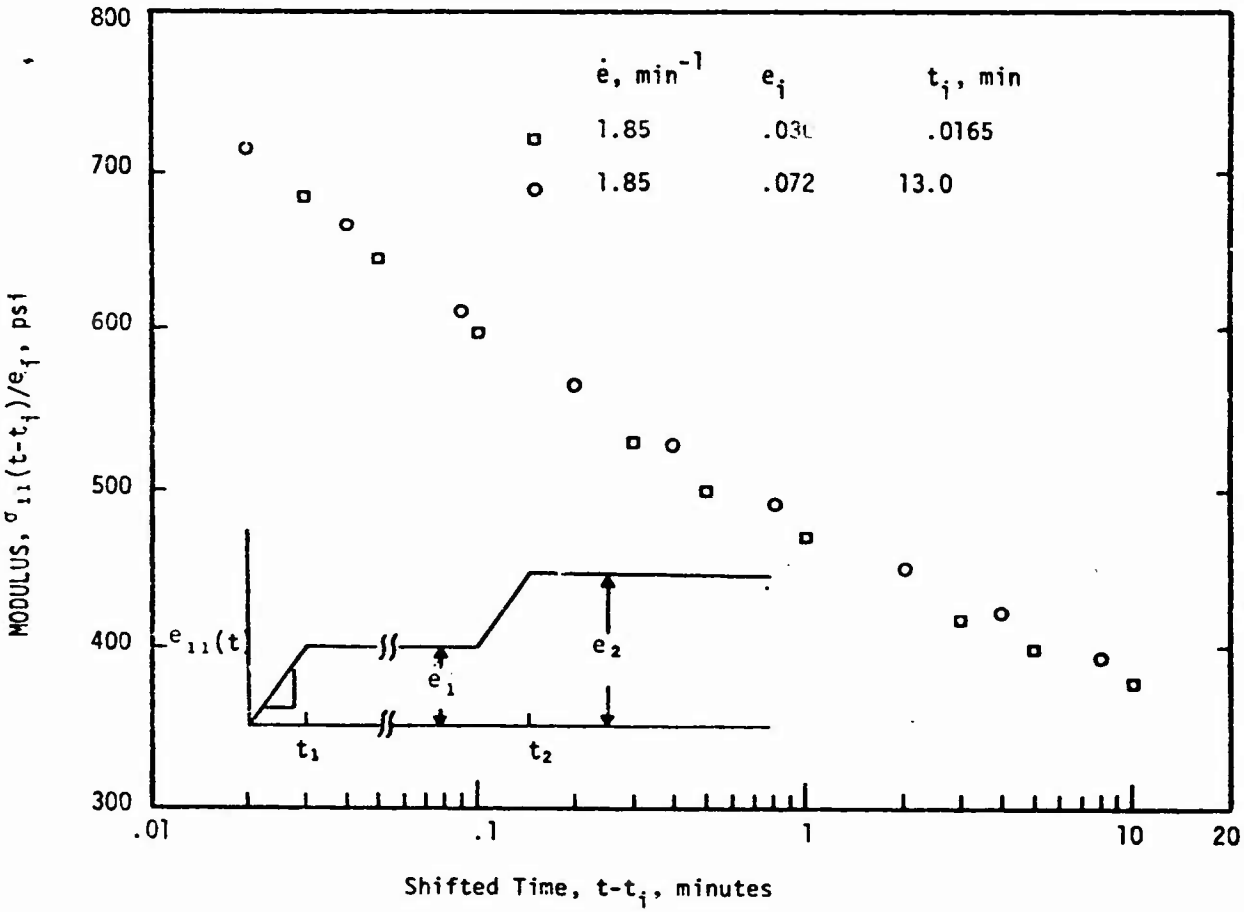

RAMP RELAXATION MODULUS FOR ONE SAMPLE TESTED AT TWO DIFFERENT STRAIN LEVELS

Figure 22

are identical when time is measured from the beginning of each relaxation. Interestingly enough this means that part of the memory of its past has somehow been completely annihilated and that the previous relaxation history has had no influence on the second relaxation. This is not fading memory response since all of the past has not been forgotten. It does however indicate that the fading memory portion of the viscoelastic constitutive equation is for all practical purposes zero as long as the strain is increasing.

Further verification of the homogeneity principle for these materials is presented in Figure 33. In this figure the stress output is compared for two cyclic inputs that differ in amplitude only. As dictated by the homogeneity principle, these data indicate that the ratio of the stress outputs is equal to the ratio of amplitudes of the cyclic strain inputs. The data in Figure 34 compares the linear-viscoelastic prediction for the cyclic data presented in Figure 33. The agreement between the linear predictions and the experimental data are quite good for this test whereas it was found to be poor for the tests discussed earlier in this section. Good agreement between experimental data and linear predictions might be expected for some tests since the material has been shown to satisfy one of the conditions of linearity. Furthermore, the dilatation data on propellants in this range of small strains prior to dewetting indicate near incompressible elastic behavior[1,5]. Incorporating these features into the constitutive equation indicate a valid form(1) would be

$$\sigma_{ij}(x_j,t) = \delta_{ij}P + G\left[\int_0^t f(\xi)\right] e_{ij}(x_j,t)$$

where P = arbitrary pressure

$$e_{ij}(x_j,t) = f(t)e^{o}_{ij}(x_j) \quad \text{for this proportional straining conditions(1)} \qquad (75)$$

$e^{o}_{ij}(x_j)$ = strain at some reference time

The relaxation data for most propellants obeys a simple power law expression as indicated by these data when plotted logarithmically in Figure 35. From the Tarris discussion dealing with material characterization a logical choice for the functional is

$$G\left[\int_0^t f(\xi)\right] = \sum_{i=0}^{N} A_i \left(\frac{||f||_{p_i}}{||f||_{q_i}}\right)^{r_i}, \qquad (76)$$

$$\text{where } r_i\left(\frac{1}{p_i} - \frac{1}{q_i}\right) = -n .$$

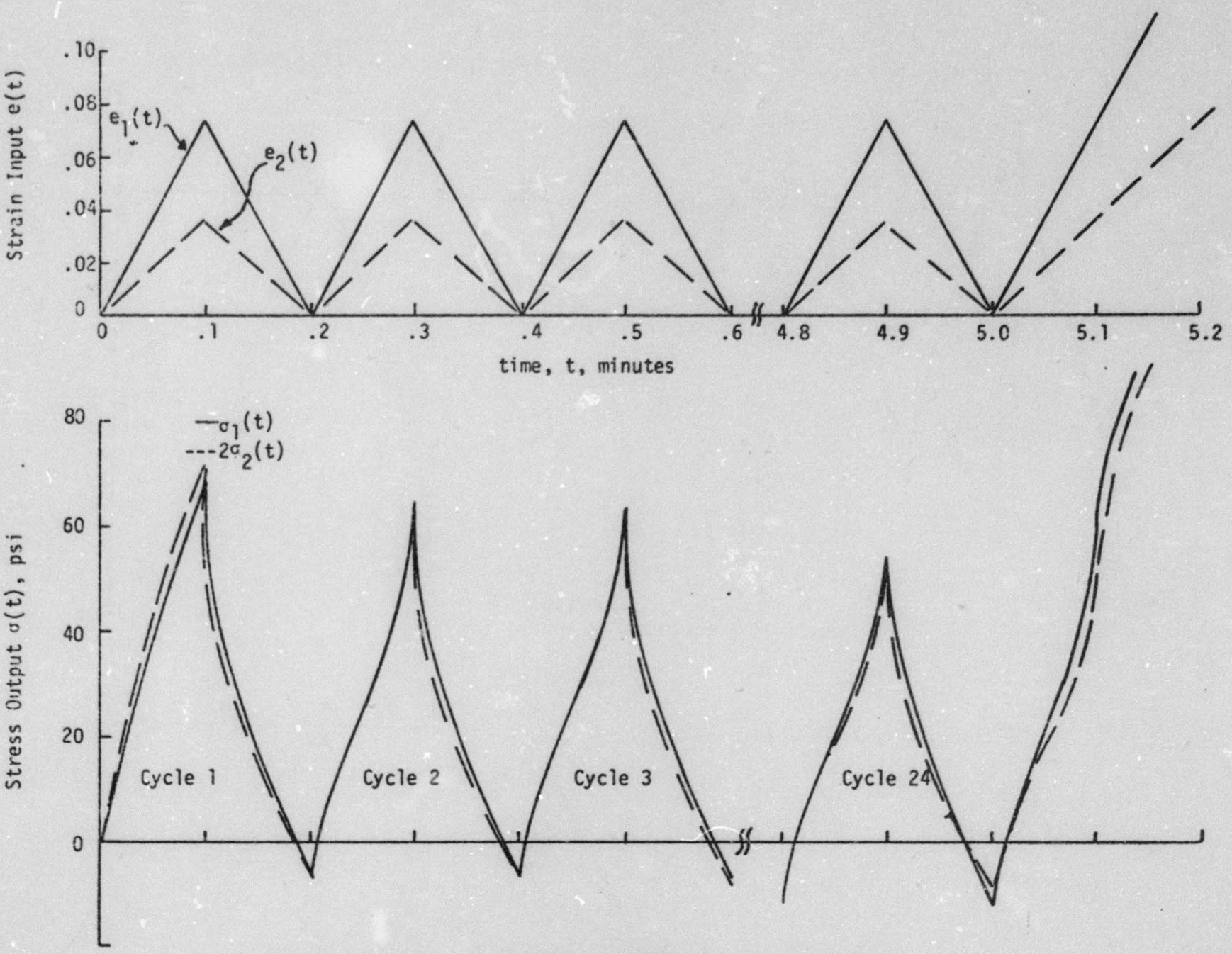

VERIFICATION OF HOMOGENEITY PRINCIPLE FOR A CYCLIC STRESS INPUT

Figure 33

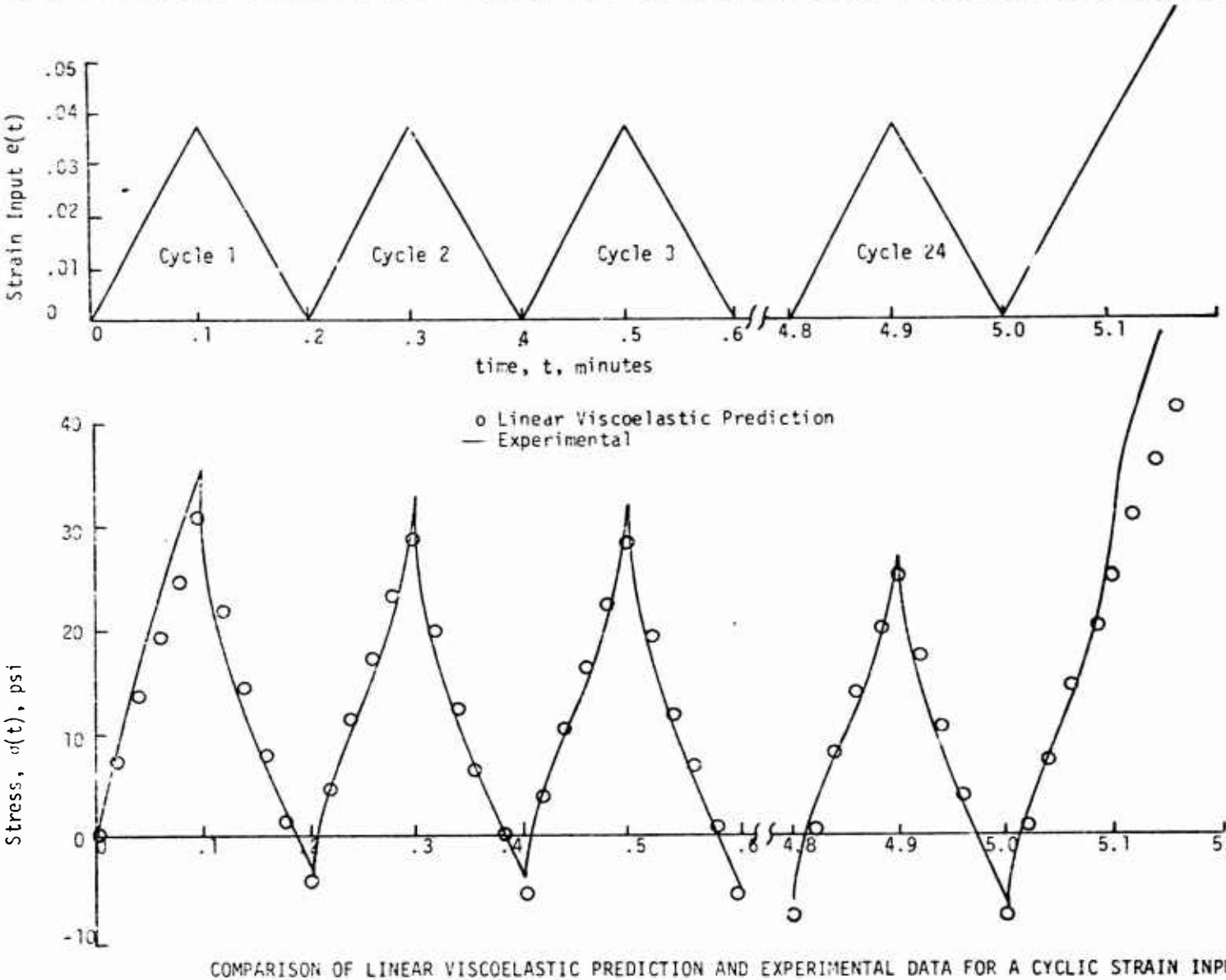

COMPARISON OF LINEAR VISCOELASTIC PREDICTION AND EXPERIMENTAL DATA FOR A CYCLIC STRAIN INPUT

Figure 3

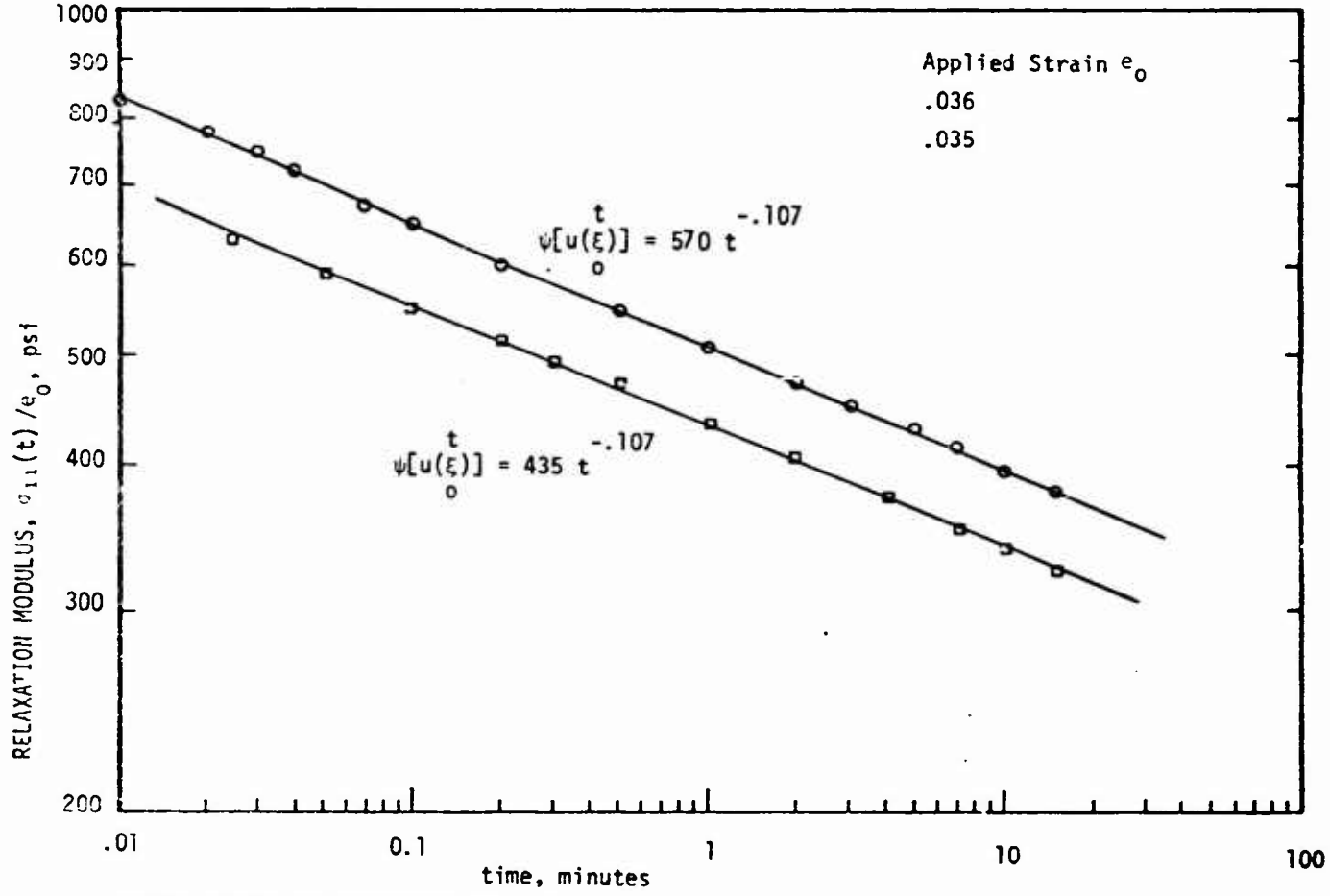

STRESS OUTPUT TO A RAPIDLY APPLIED CONSTANT STRAIN INPUT

Figure 35

For a jump strain Equation (76) then reduces to

$$G\left[u\left(\overset{t}{\underset{0}{\xi}}\right)\right] = E_r(t) = kt^{-n} = t^{-n}\sum_{i=o}^{N} A_i \tag{77}$$

Completion of the characterization process requires only determination of A_i, p_i, q_i and r_i. The complex characterization procedure discussed in the next section was not used for this purpose. Instead only one term was taken choosing $p_1 = \infty$, $A_1 = k$ and graphically determining r_1 and q_1 to fit a few tests. The results of this very simple analysis is demonstrated in Figures 36 through 38 which compare calculated and observed response for several tests plotted as both stress-time and stress-strain. The close agreement between experiment and theory for this single term representation would appear to indicate this is a powerful method of characterization and valid for propellant materials. However, comparing the predictions with the actual data for the cyclic tests, Figures 39 and 40, shows the agreement is not as good as demonstrated in the previous figures. The reasons for this disagreement between prediction and observation lies in the need to have some fading memory viscoelasticity present, since compressive stresses for the state of positive tensile strain cannot come from the permanent memory portion of the constitutive equation. Proper characterization procedures will bring out such defects in the chosen representation.

In an attempt to improve the characterization process a three term expansion was chosen including some fading memory. The constitutive equation chosen has the form

$$\sigma_{ij}(t) = \delta_{ij}P + A_1\left(\frac{|f|}{||f||_{q_1}}\right)^{r_1} e_{ij} + A_2\int_o^t (t-\tau)^{-n_2}\dot{e}_{ij}(\tau)d\tau$$

$$+ A_3\left(\frac{|f|}{||f||_{q_3}}\right)^{r_3}\int_o^t (t-\tau)^{-n_3}\dot{e}_{ij}(\tau)d\tau \ , \tag{78}$$

where P = arbitrary pressure, and

$|\cdot|$ = absolute value.

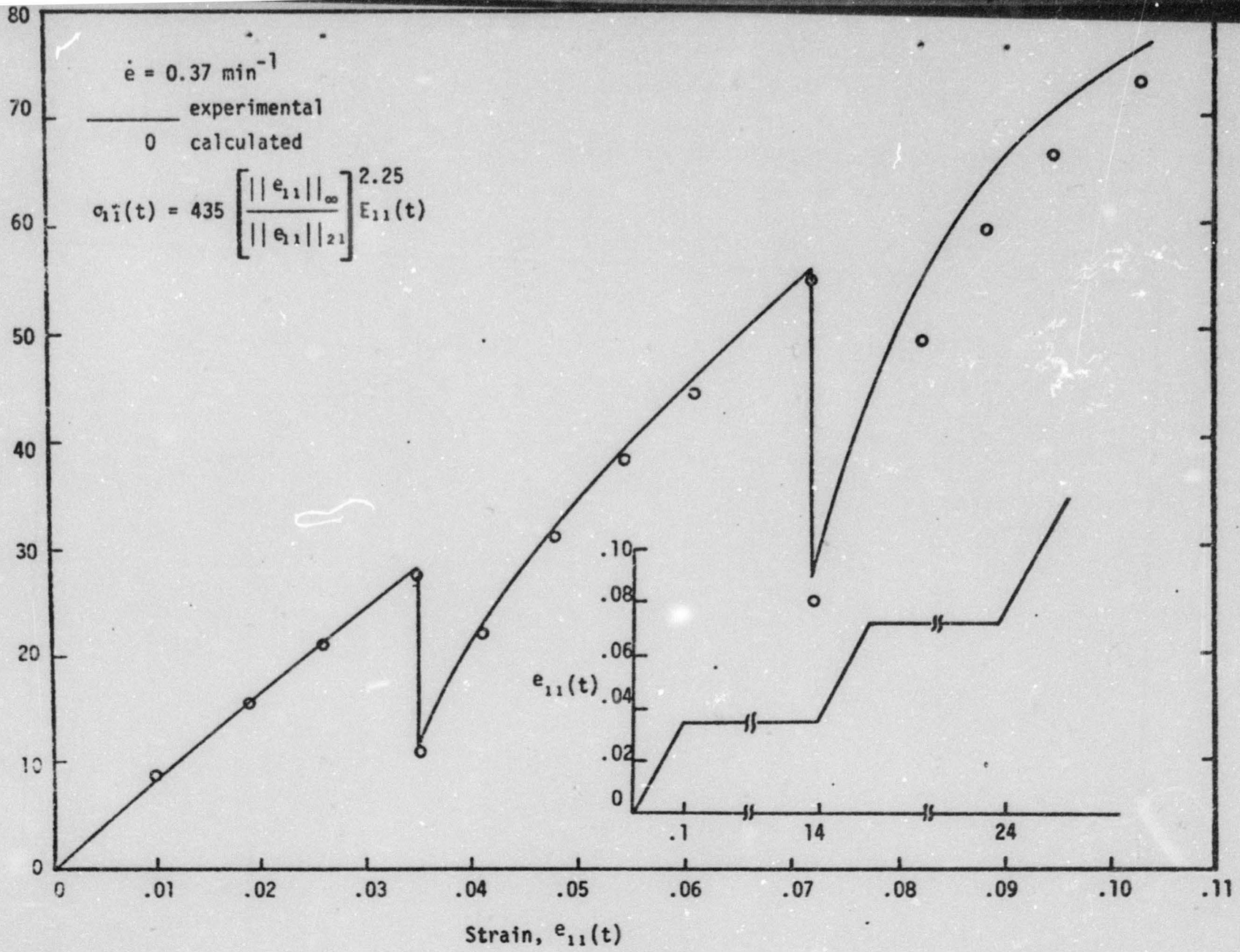

COMPARISON OF CALCULATED AND OBSERVED STRESS-STRAIN OUTPUT FOR AN INTERRUPTED RAMP STRAIN INPUT

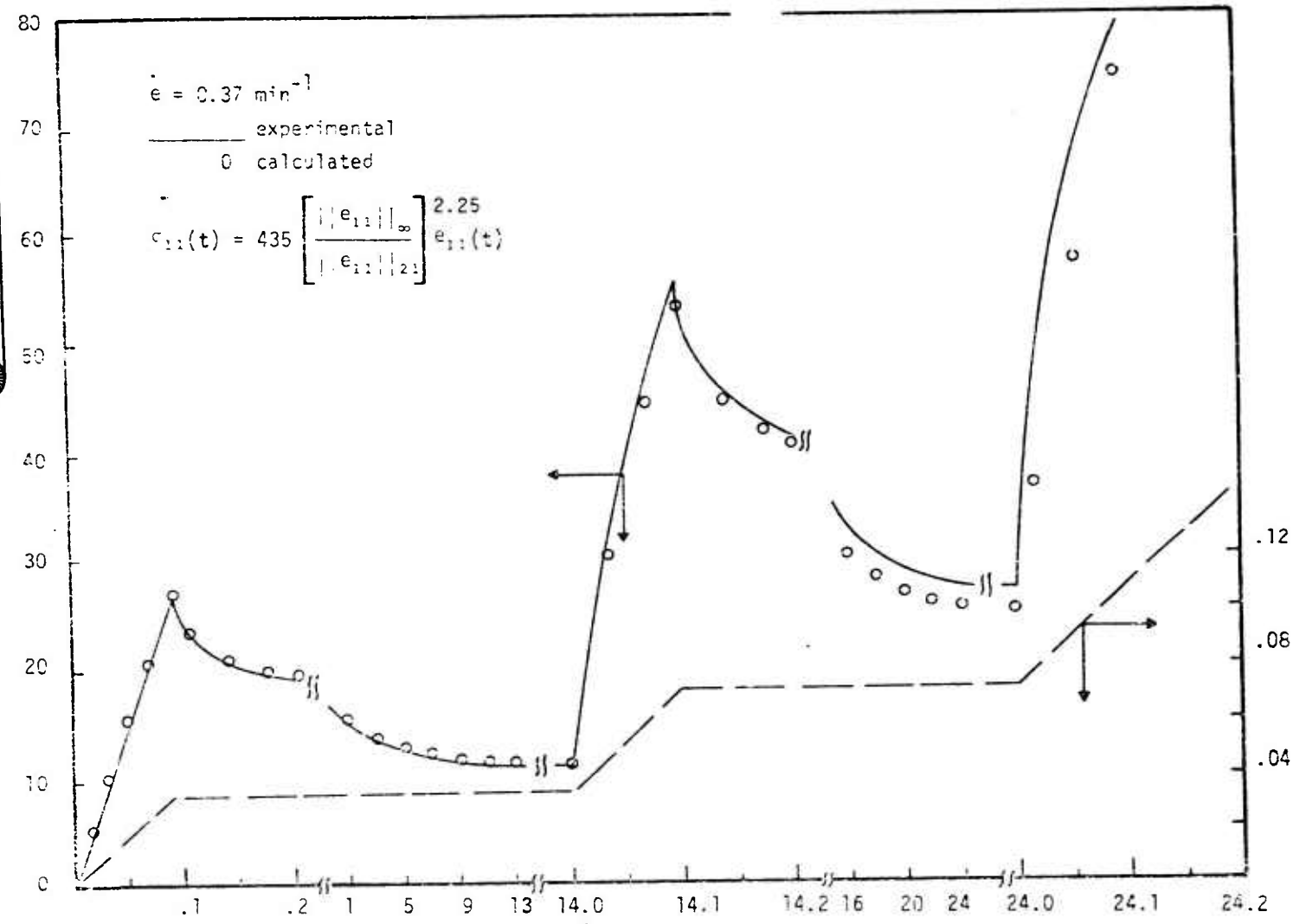

COMPARISON OF CALCULATED AND OBSERVED STRESS-TIME OUTPUT FOR AN INTERRUPTED RAMP STRAIN INPUT

Figure 37

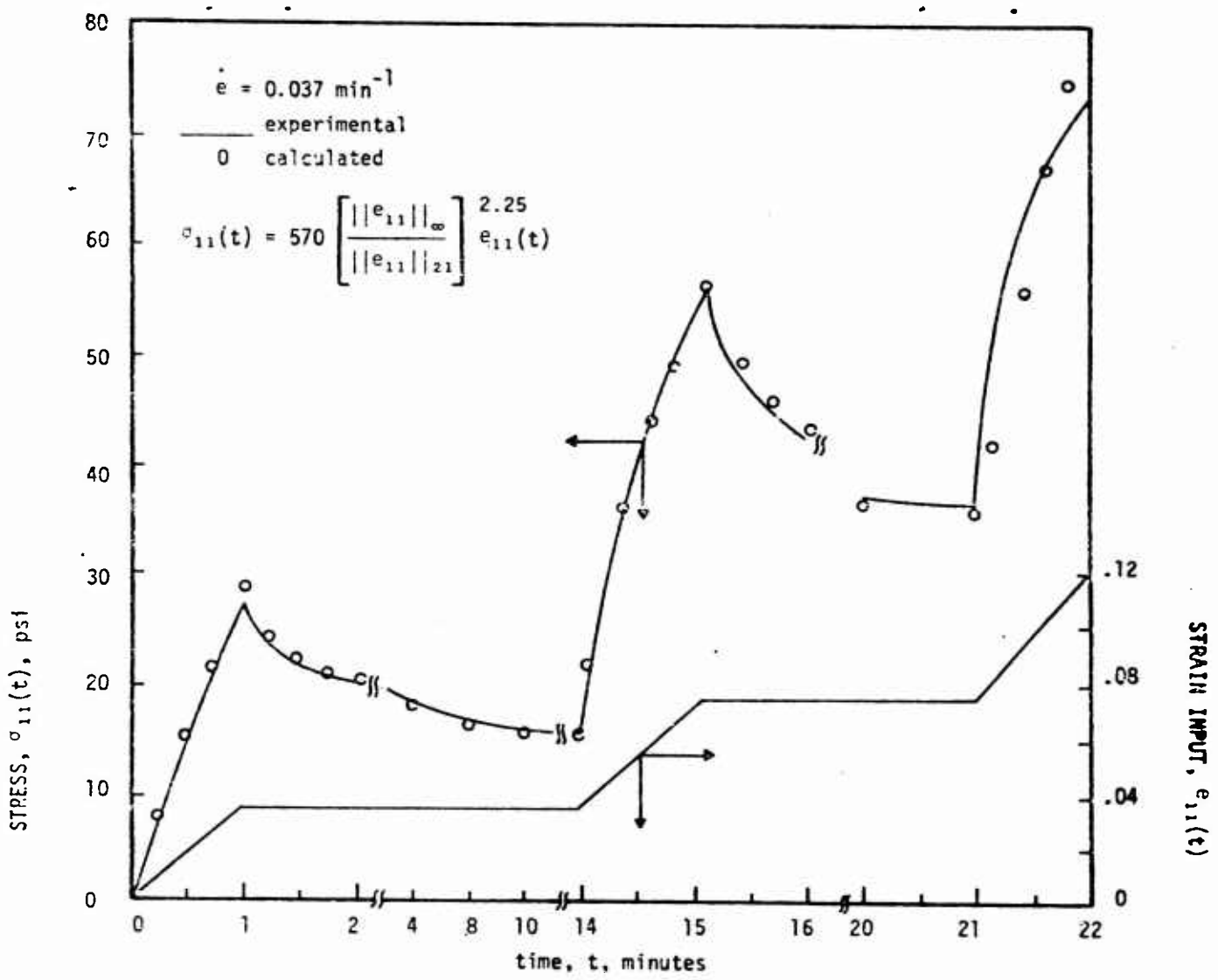

COMPARISON OF CALCULATED AND OBSERVED STRESS-TIME OUTPUT TO AN INTERRUPTED RAMP STRAIN INPUT

Figure 38

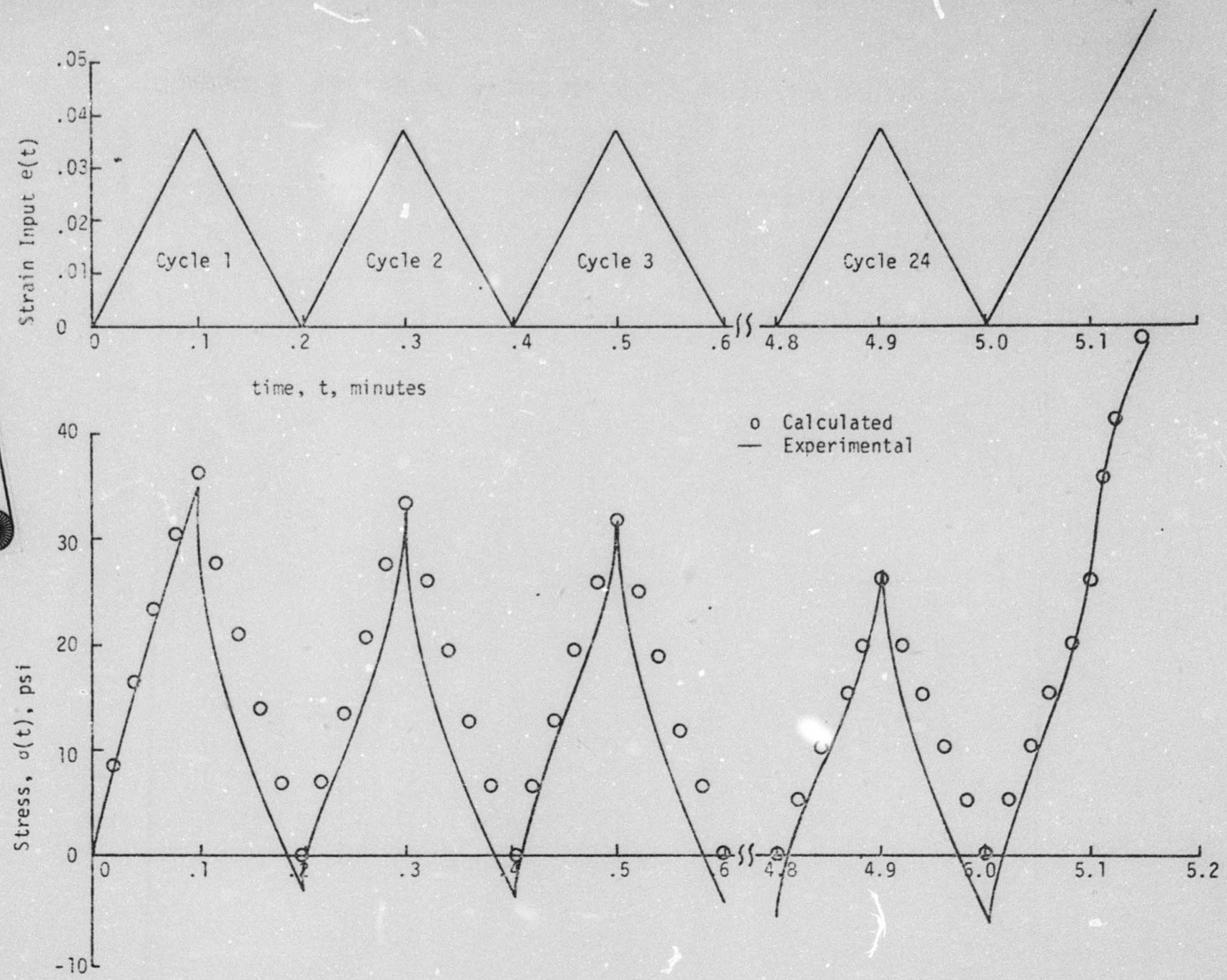

Figure 39

COMPARISON OF EXPERIMENTAL AND CALCULATED STRESS OUTPUT FOR A CYCLIC STRAIN INPUT

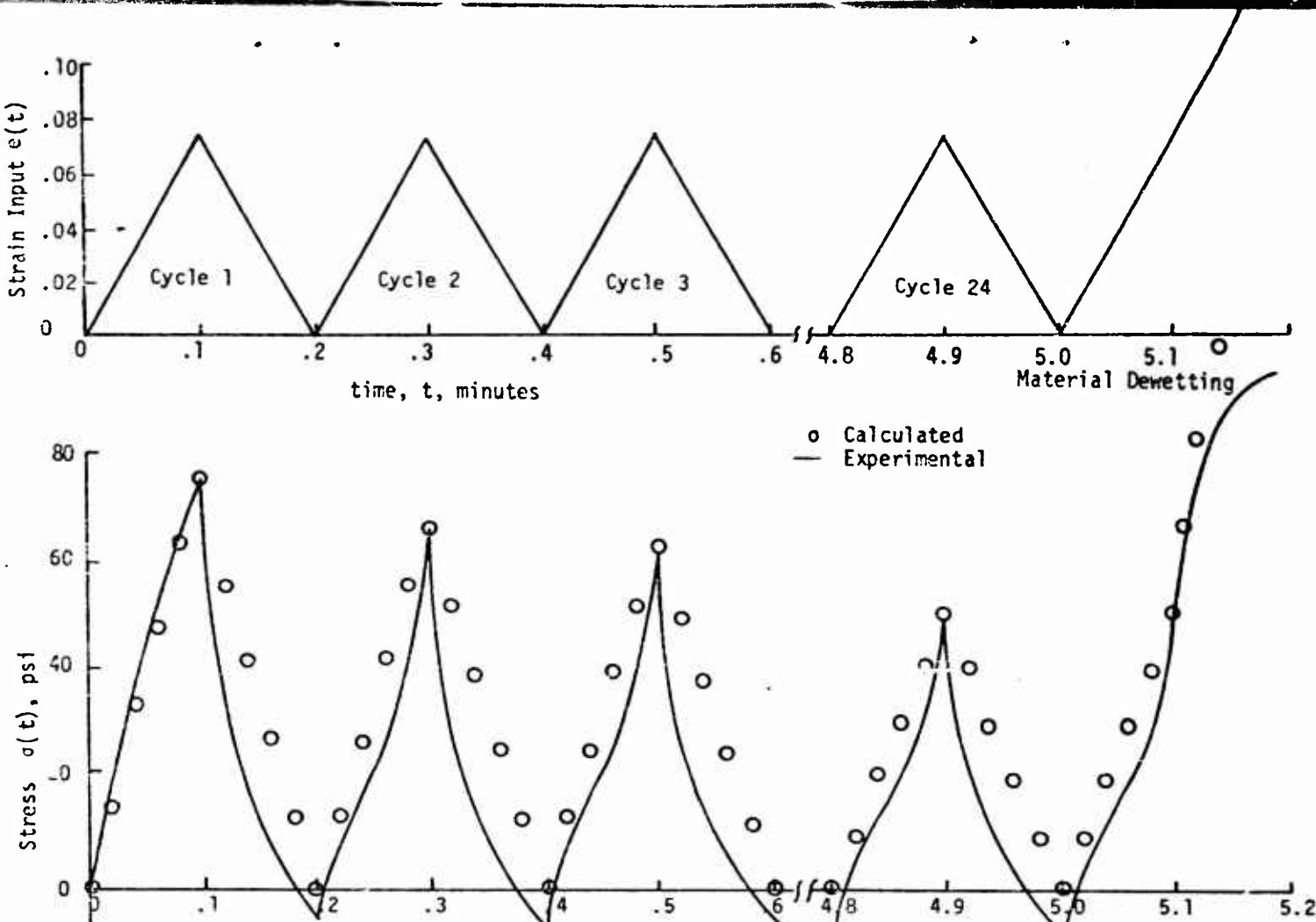

COMPARISON OF EXPERIMENTAL AND CALCULATED STRESS OUTPUT FOR A CYCLIC STRAIN INPUT

A simple analysis of all the test data indicate that the material would be well characterized if the parameters in the equation took on the following values

$$n_2 = n_3 = 0.1$$

$$r_1 = 2.25$$

$$r_3 = 1.0$$

$$q_1 = 21$$

$$q_3 = \infty$$

$$A_1 = A_2 = -A_3 = 570$$

Substituting these values into Equation (78) and rearranging terms yields

$$\sigma_{ij}(t) = \delta_{ij}P + 570\left(\frac{|f|}{||f||_{21}}\right)^{2.25} e_{ij}(t) + \tag{79}$$

$$+ 570\left[1 - \frac{|f|}{||f||_{\infty}}\right]\int_0^t (t-\tau)^{-.1}\, \dot{e}_{ij}(\tau)d\tau \ .$$

For tests where the strain is never decreasing (or never increasing), such as those illustrated in Figures 36 through 38, the last term in Equation (79) contributes nothing since for these tests $|f|$ equals $||f||_\infty$. The data in Figures 36 through 38 calculated by Equation (79) and that calculated by Equation (75) is therefore identical. Comparisons between the calculated and observed data for the cyclic strain inputs is illustrated in Figures 41 and 42. As seen by the data illustrated in these figures, the calculated and experimental data agree quite well. Perhaps other inputs exist, where again the agreement of even this modified constitutive equation will predict poorly. The only way to be assured a nonlinear constitutive equation will predict accurately is to perform all possible tests and compare. Naturally this is impossible, however, the least one should do is use a large number of greatly different tests. Inputs of a similar type to those the material in question will be subjected to in its lifetime, performed at the same temperatures and over the same time scales should be used in realistic characterization procedures.

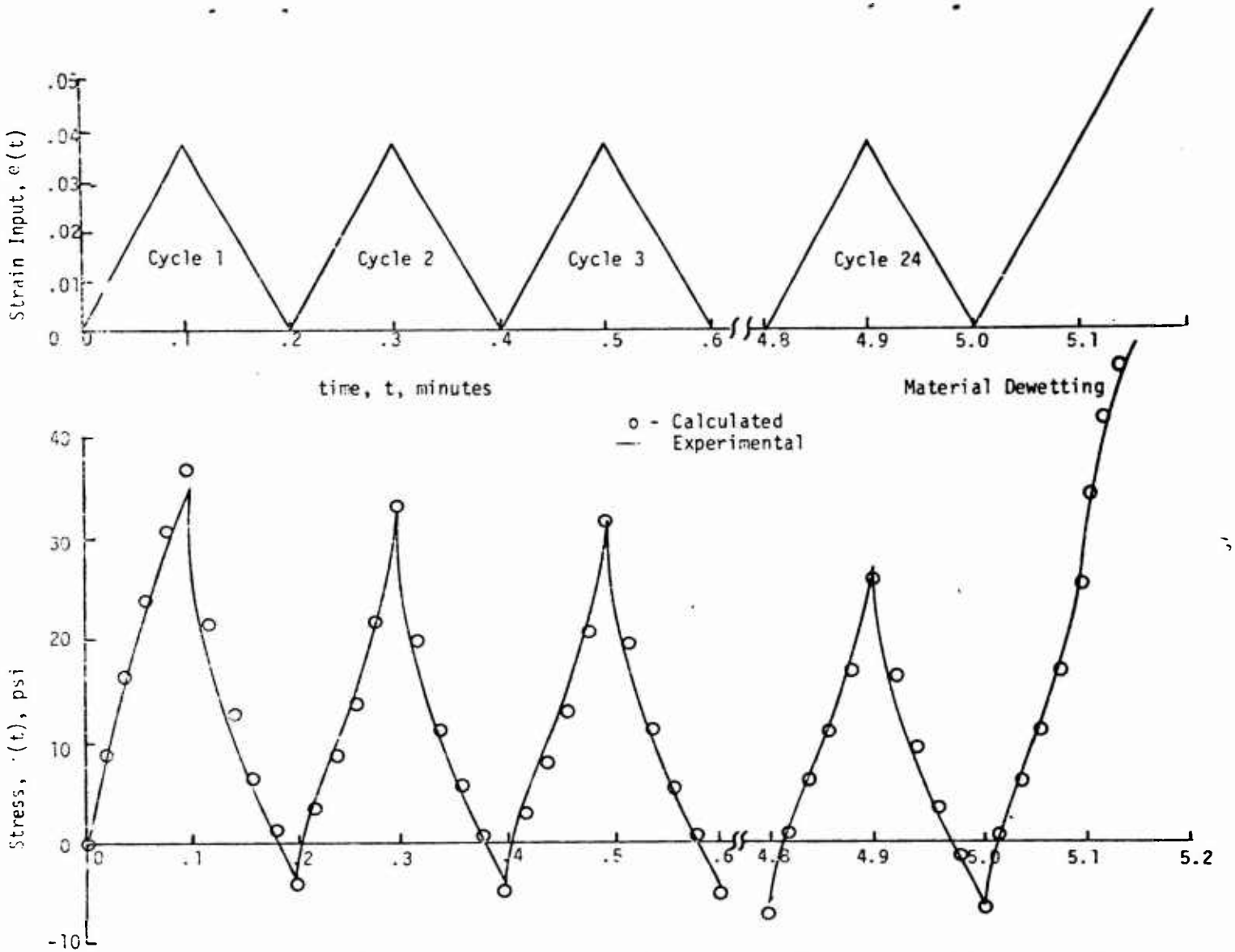

COMPARISON OF EXPERIMENTAL AND CALCULATED STRESS OUTPUT FOR A CYCLIC STRAIN INPUT

Figure 41

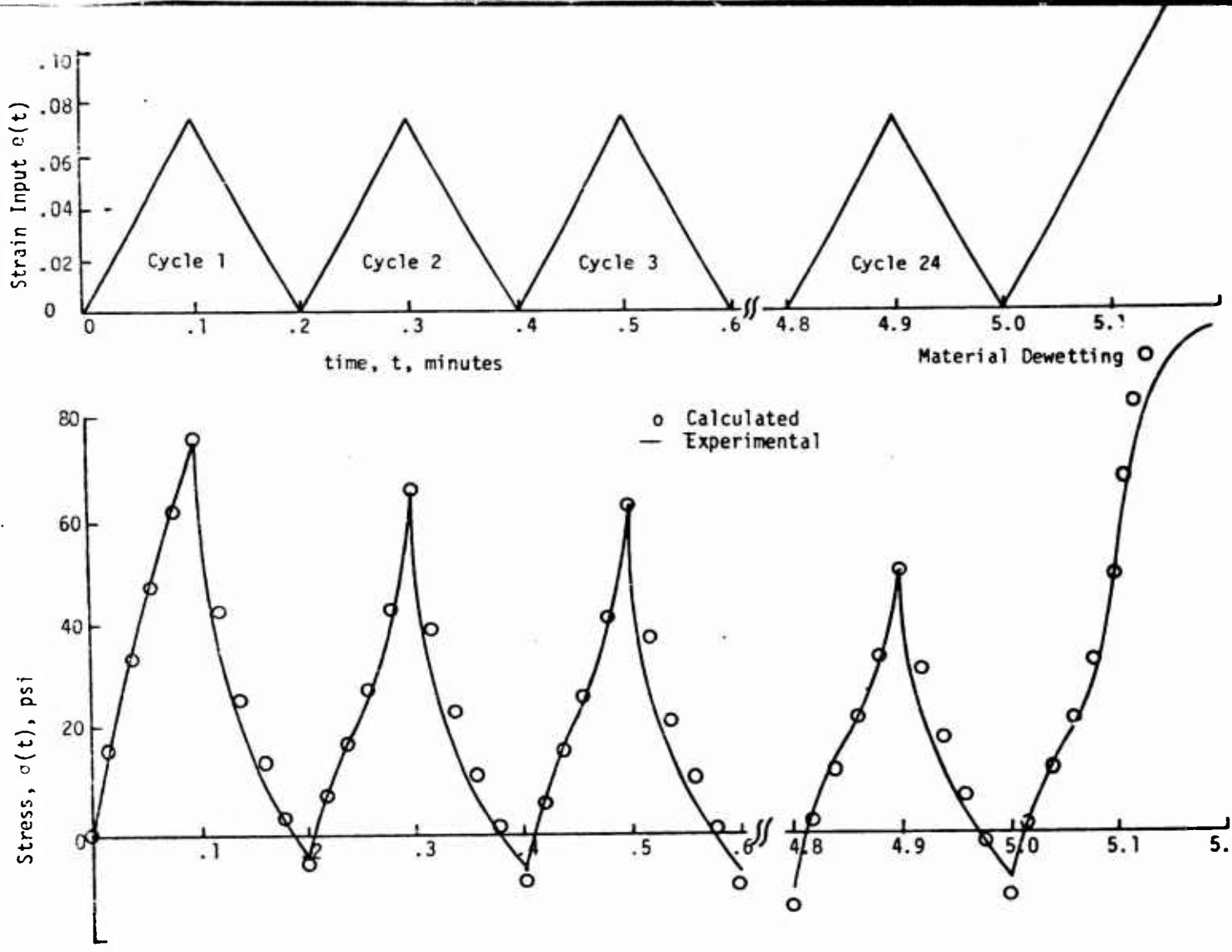

Figure 42

COMPARISON OF EXPERIMENTAL AND CALCULATED STRESS OUTPUT FOR A CYCLIC STRAIN INPUT

In particular, there are two things a rheologist attempting to mathematically describe the behavior of materials should always remember.

- Simply because the chosen representation accurately curve fits the tests used in the characterization procedures does not guarantee accurate predictions for other different tests.
- If a constitutive equation cannot predict the output to a large class of inputs, it is of little value in general stress analysis.

(3) Verification for Nonlinear Thermoviscoelastic Conditions

The equations developed by Farris were given a close and careful study on a Navy contract, "Applications of Nonlinear Viscoelasticity and Cumulative Damage, A Realistic Evaluation of Real Propellant Behavior, NOSC-ORD-0331 No. N00017-70-C-4441."[9] In this study uniaxial, biaxial and shear behavior was studied at several temperatures, 110°F to -75°F, using complex deformation histories involving both tensile and compressive deformations. In addition computerized characterization techniques were developed to fit large masses of experimental data to equations similar to Equation (79) using regression error minimization techniques. Using these methods it was possible to simultaneously fit approximately 100 independent experiments to the equation with deviations between observed and predicted stress data of the order of $\pm$ 12% for 68% of the data, and $\pm$ 24% for 95% of the data. It was also found that the usual concept of a thermorheologically simple material was applicable. Figures 43 through 49 illustrate the excellent agreement between the equation and the experimental data. Hence it appears the equation does contain the necessary mathematics to describe propellant response prior to vacuole formation. In these figures the linear viscoelastic equivalent predictions are based on a material having the identical relaxation moduli and time-temperature shift function. The best linear viscoelastic predictions are based on the best linear viscoelastic fit to all of the data, not just relaxation equivalence. It is apparent from these figures that the nonlinear predictions are far superior to the linear predictions when time and history effects are important.

Figures 50 through 53 illustrate the excellent predictive capability of the equation, based on the isothermal characterization, for to transient thermal experiments where both simultaneous straining and cooling and/or heating experiments were performed using complex histories. It is here that the linear predictions fall far short of reality and stresses twice those of linear theory were observed and predicted by the nonlinear theory.

COMPARISON OF LINEAR AND NONLINEAR VISCOELASTIC PREDICTIONS

WITH CONSTANT TEMPERATURE UNIAXIAL EXPERIMENTAL DATA

Uniaxial

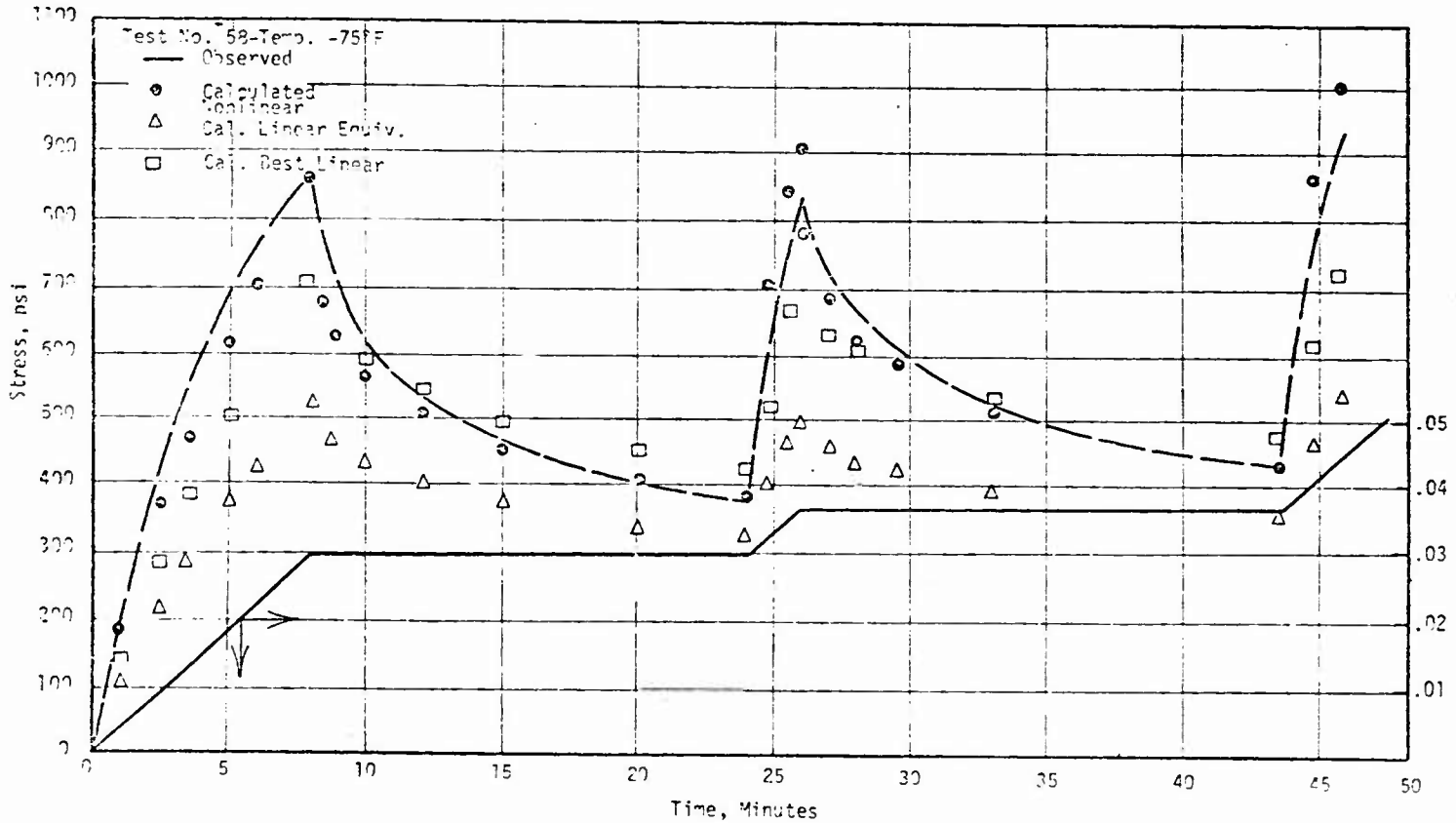

Figure 43

COMPARISONS OF NONLINEAR AND LINEAR

VISCOELASTIC PREDICTIONS WITH EXPERIMENTAL DATA

Uniaxial

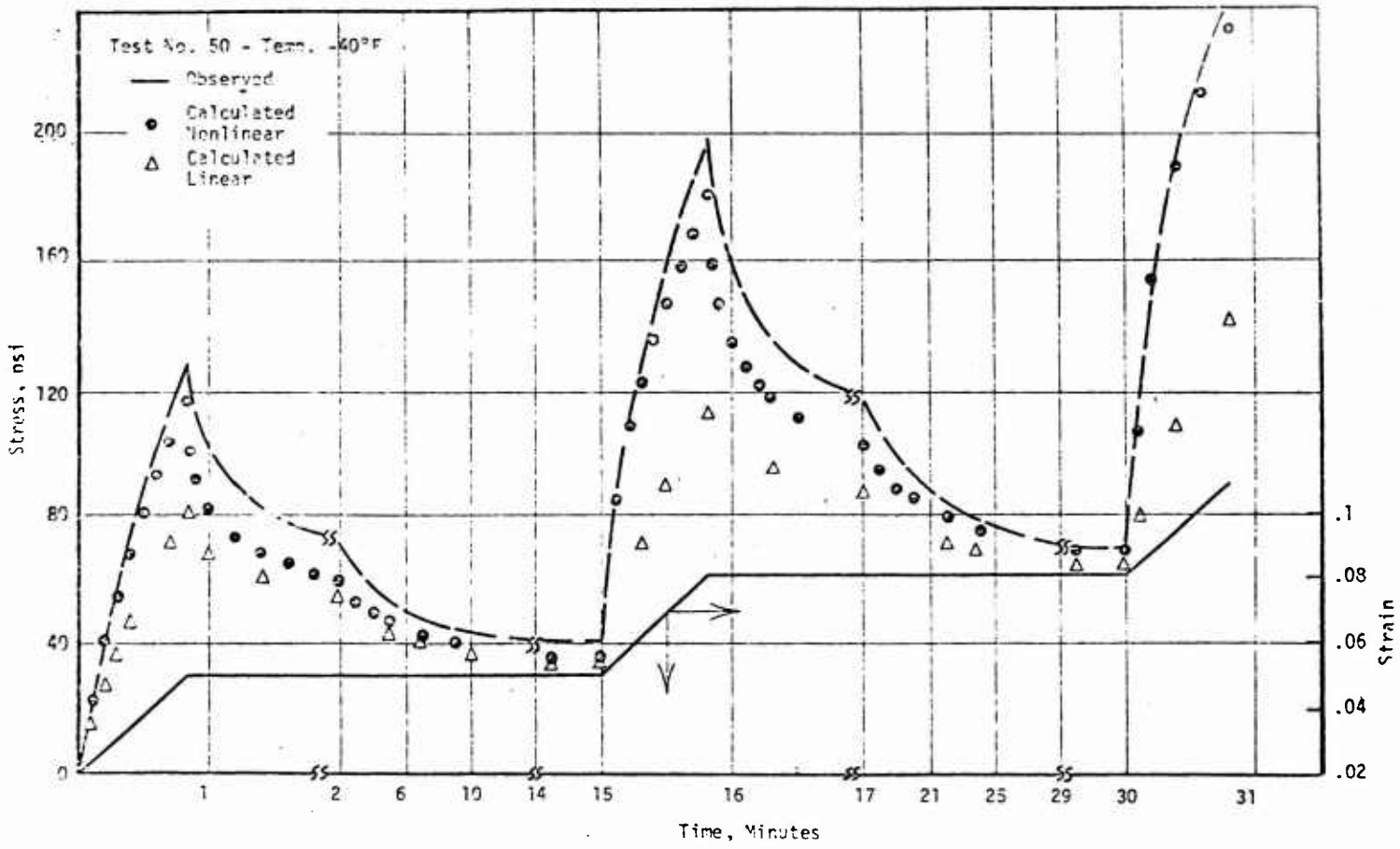

Figure 44

COMPARISONS OF NONLINEAR AND LINEAR

VISCOELASTIC PREDICTIONS WITH EXPERIMENTAL DATA

Uniaxial

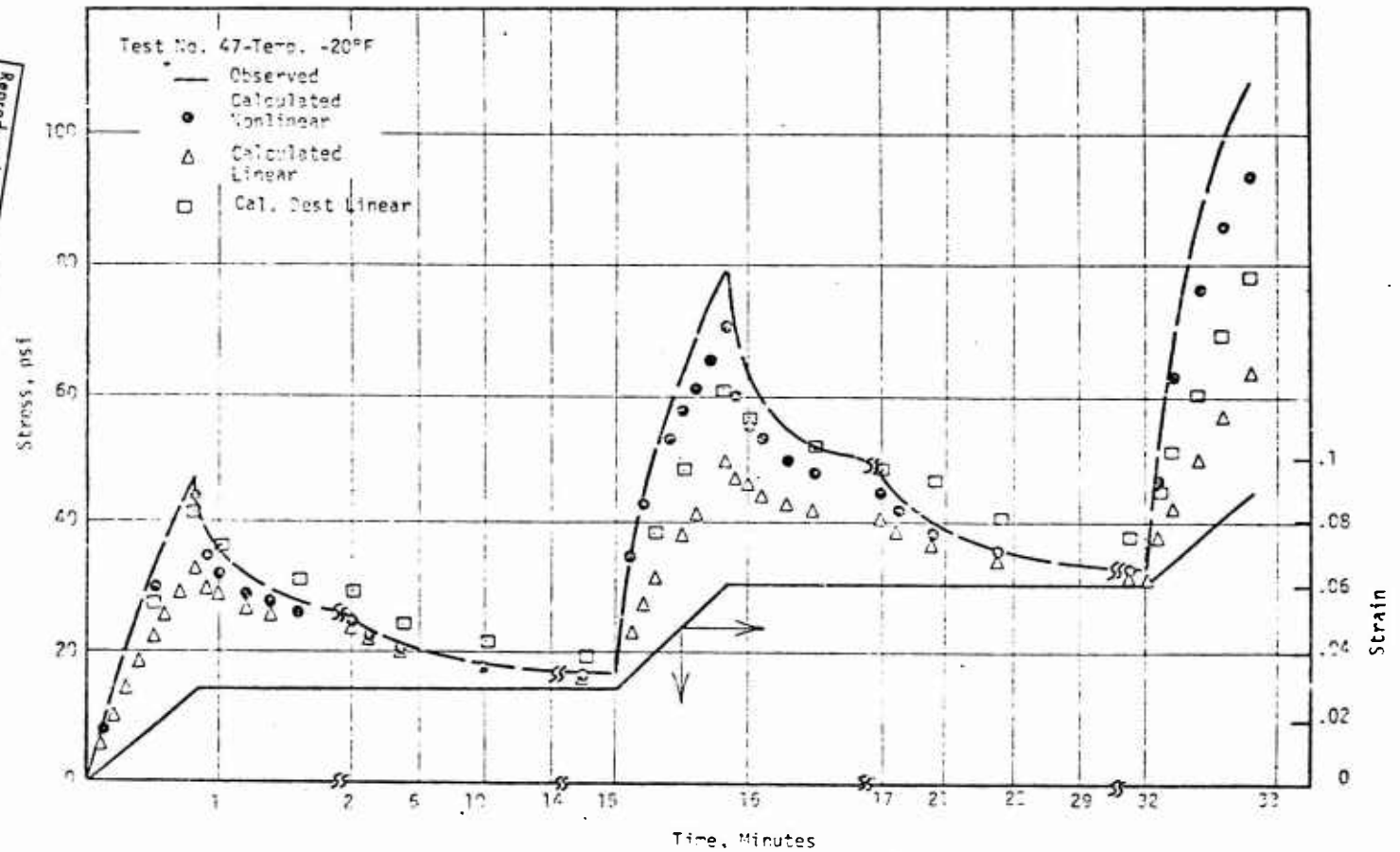

Figure 45

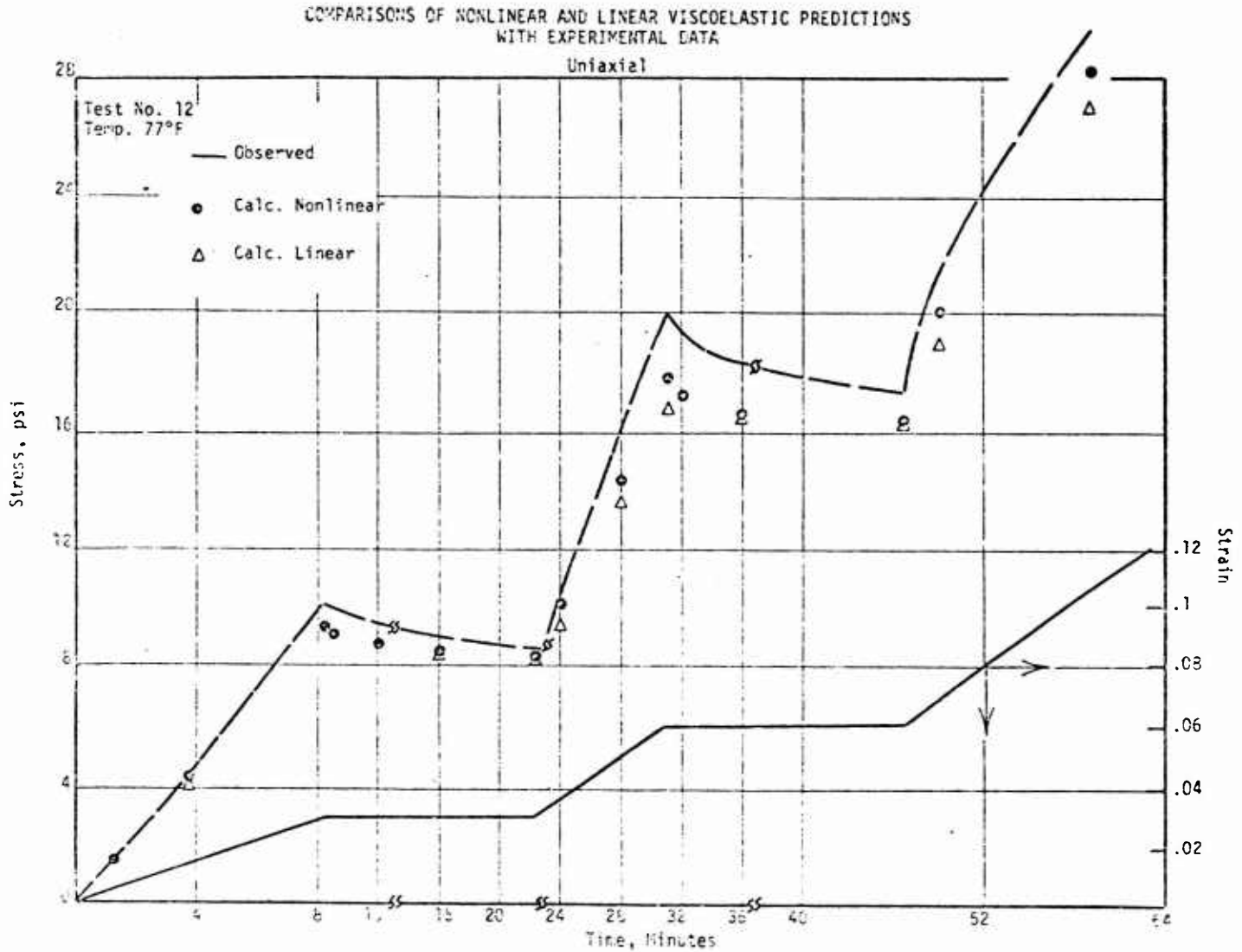
COMPARISONS OF NONLINEAR AND LINEAR VISCOELASTIC PREDICTIONS
WITH EXPERIMENTAL DATA
Uniaxial
Test No. 12
Temp. 77°F
Observed
Calc. Nonlinear
Calc. Linear
Stress, psi
Strain
Time, Minutes
28
24
20
16
12
8
4
.12
.1
.08
.06
.04
.02
4
8
15
20
24
28
32
36
40
52

Figure 46

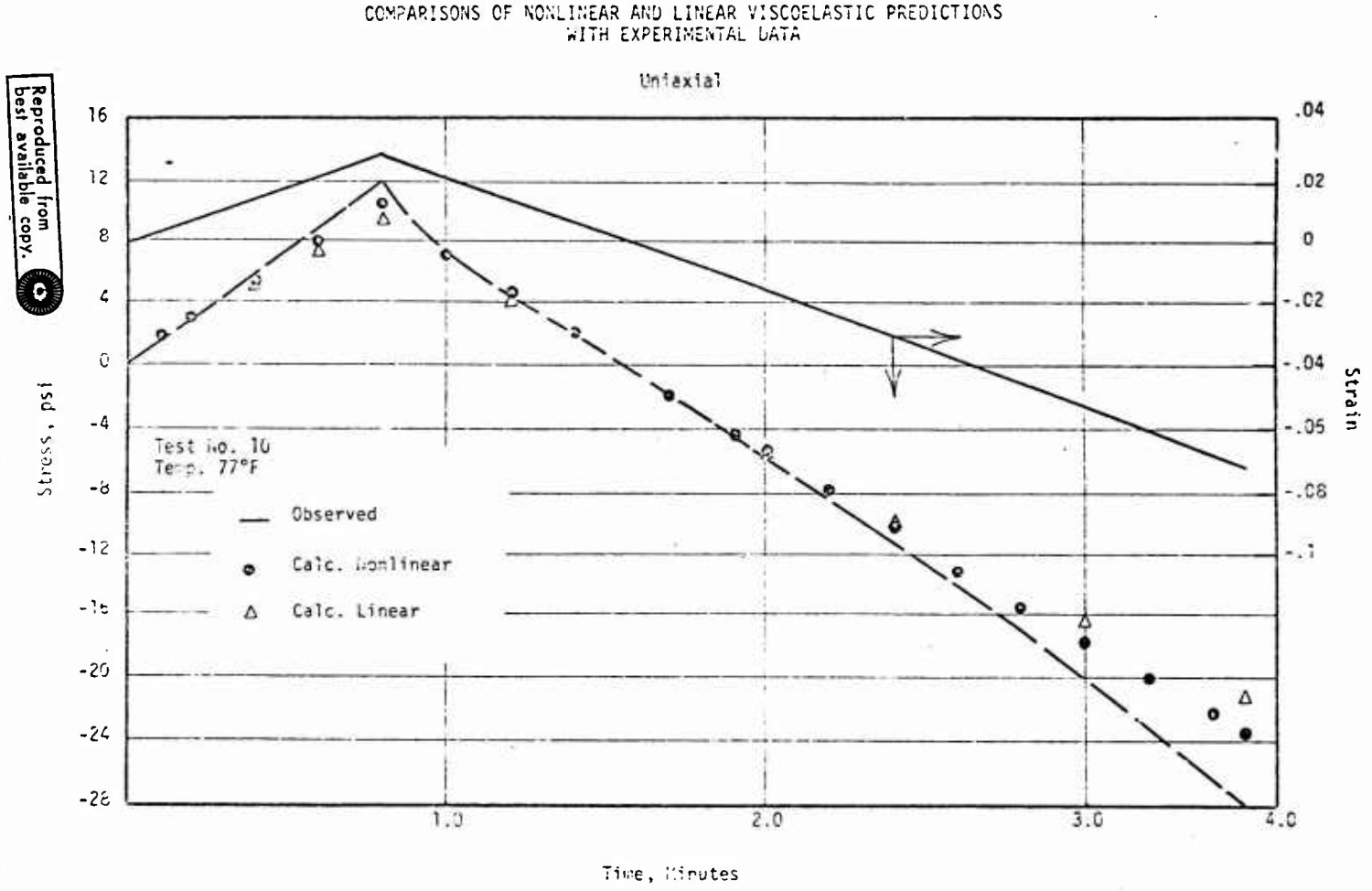

Figure 47

COMPARISONS OF NONLINEAR AND LINEAR VISCOELASTIC PREDICTIONS
WITH EXPERIMENTAL DATA

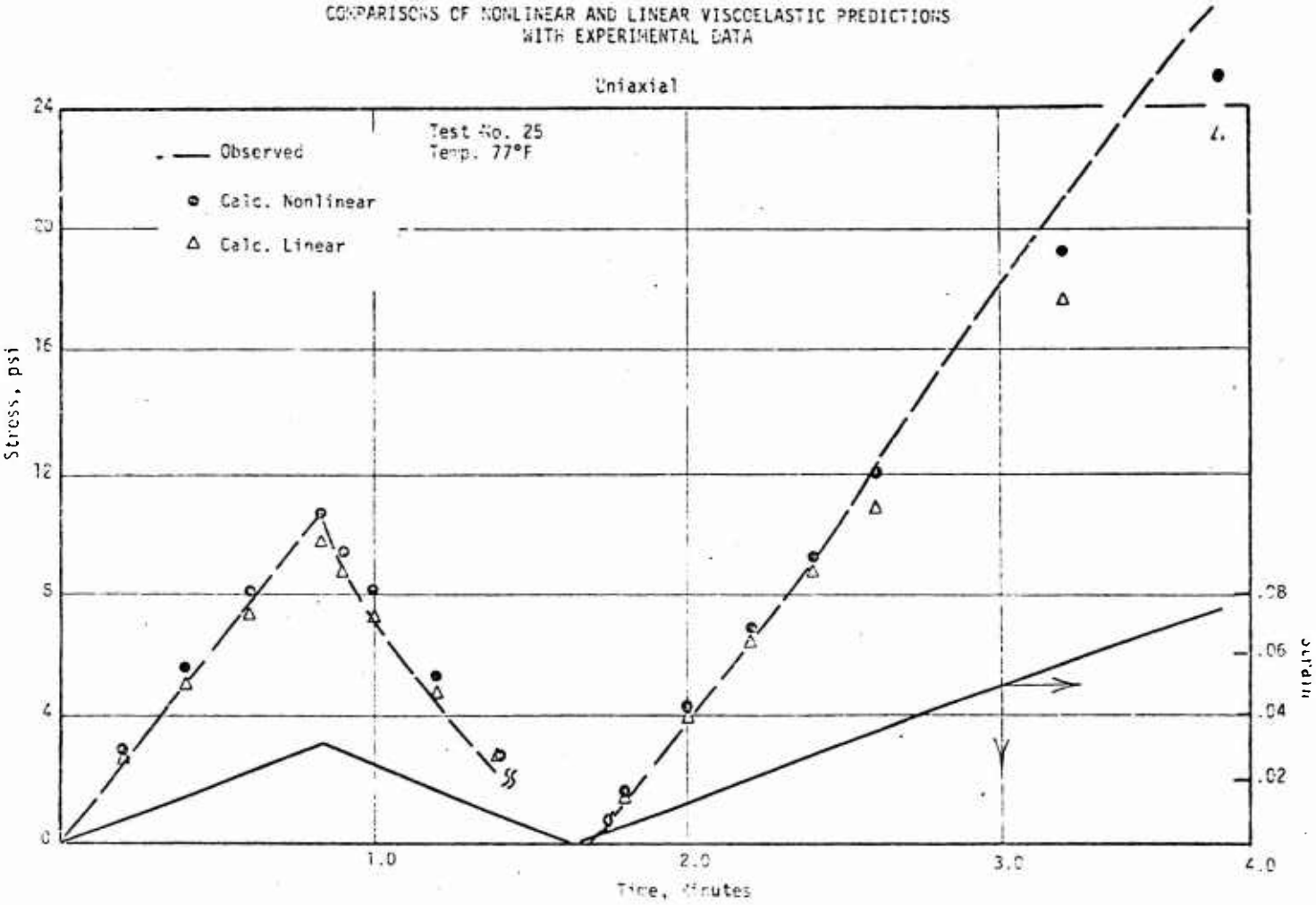

Figure 73

COMPARISON OF EXPERIMENTAL DATA AND NONLINEAR VISCOELASTIC

PREDICTIONS FOR CYCLIC STRAIN TESTS

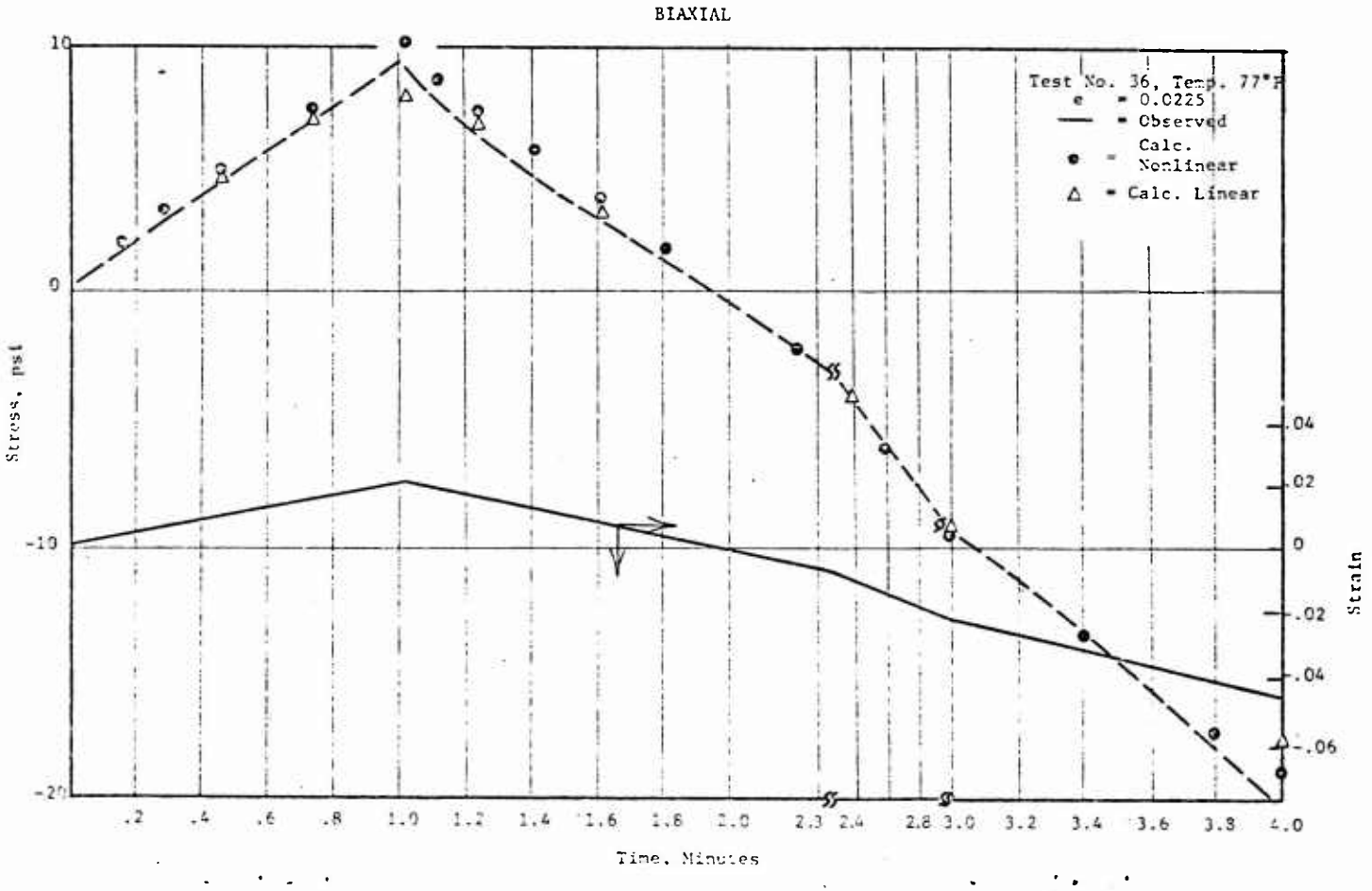

Figure 49

COMPARISON OF LINEAR AND NONLINEAR PREDICTIONS

WITH EXPERIMENTAL DATA FOR UNIAXIAL THERMOVISCOELASTIC EXPERIMENTS

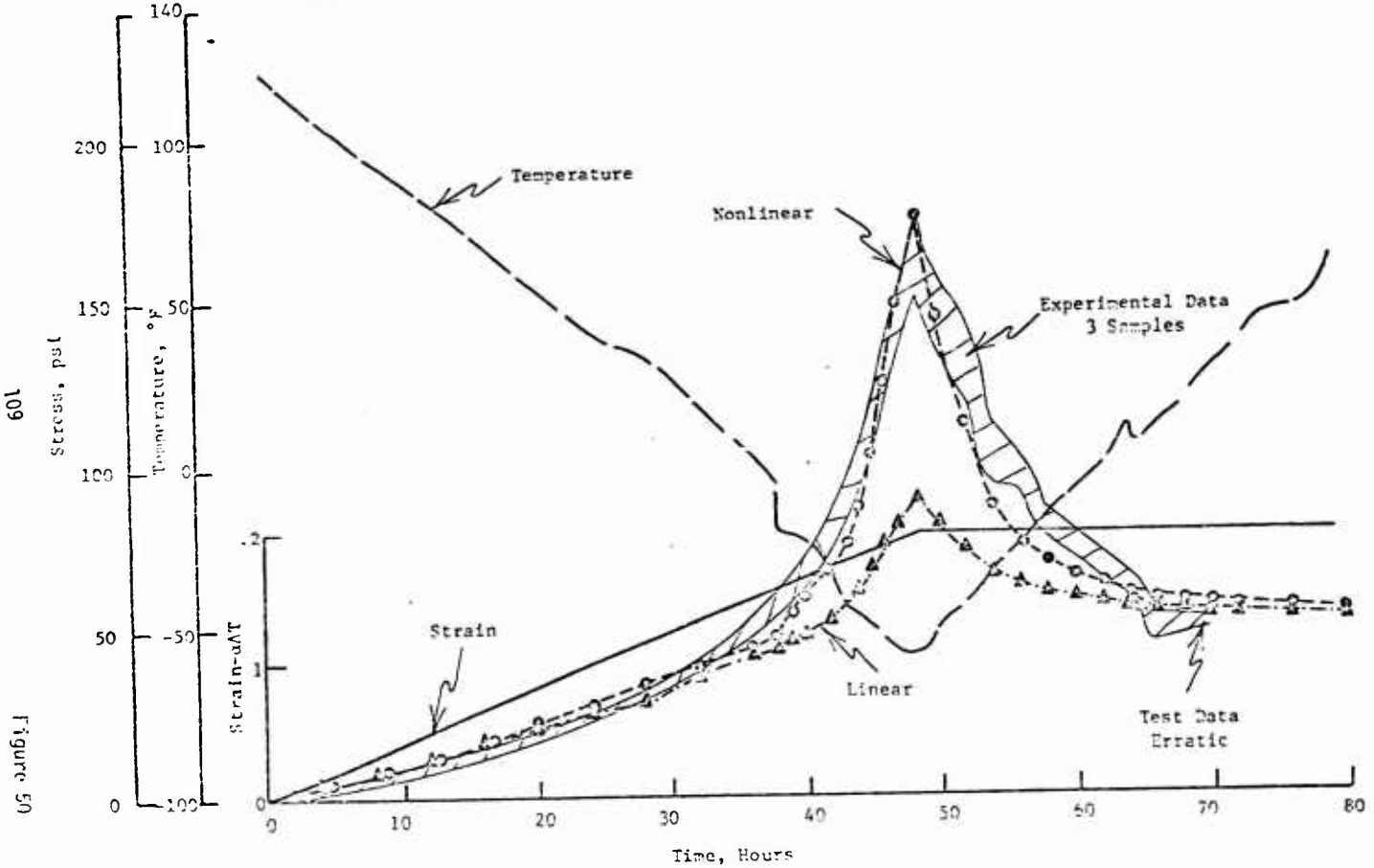

Figure 50

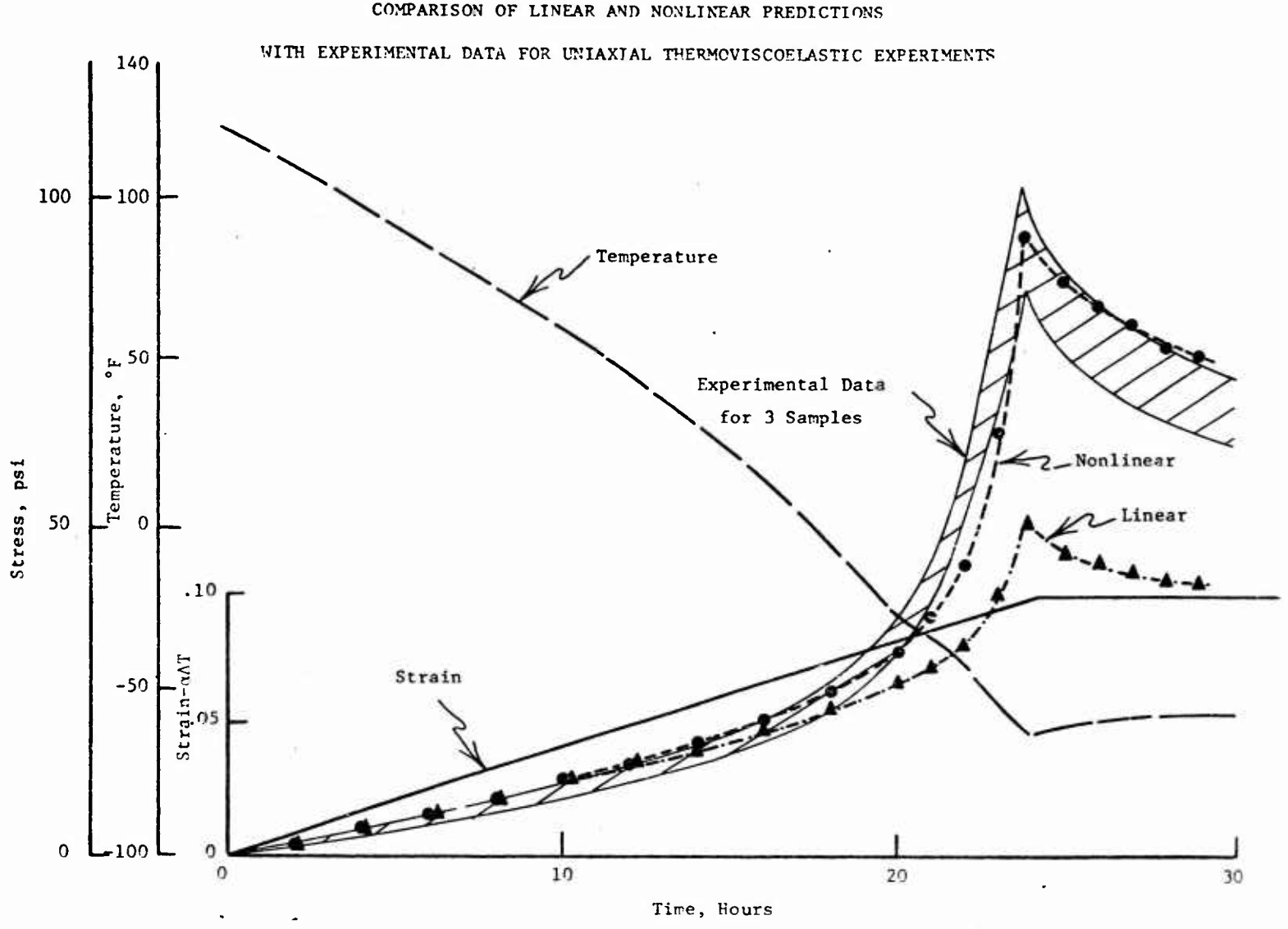
COMPARISON OF LINEAR AND NONLINEAR PREDICTIONS
WITH EXPERIMENTAL DATA FOR UNIAXIAL THERMOVISCOELASTIC EXPERIMENTS
Stress, psi
Temperature, °F
Strain-αΔT
Temperature
Experimental Data
for 3 Samples
Nonlinear
Linear
Strain
Time, Hours
140
100
50
0
-50
-100
.10
.05
0
10
20
30

Figure 51

COMPARISON OF LINEAR AND NONLINEAR PREDICTIONS

WITH EXPERIMENTAL DATA FOR THERMOVISCOELASTIC EXPERIMENTS

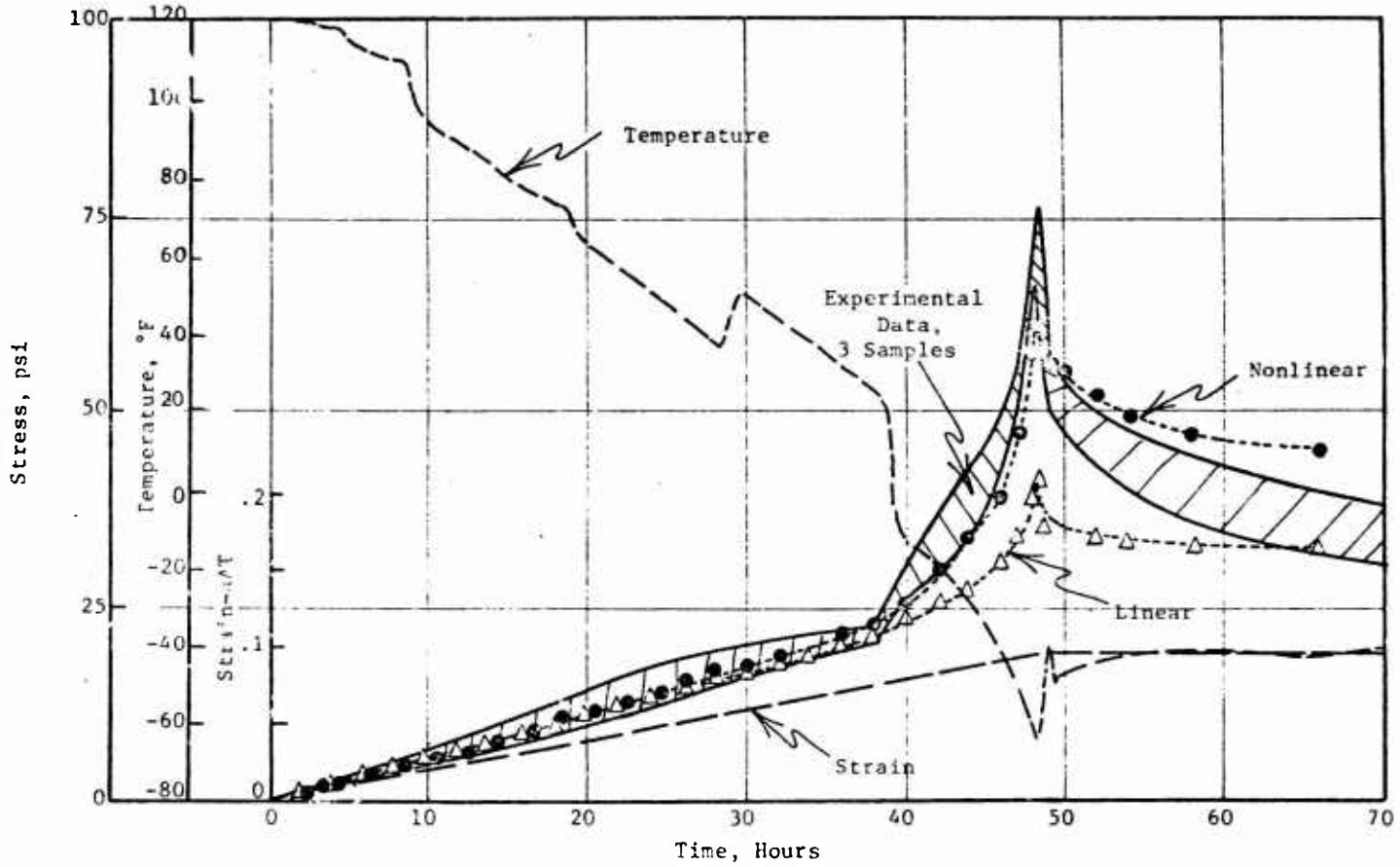

Figure 52

COMPARISON OF LINEAR AND NONLINEAR PREDICTIONS

WITH EXPERIMENTAL DATA FOR UNIAXIAL THERMOVISCOELASTIC EXPERIMENTS

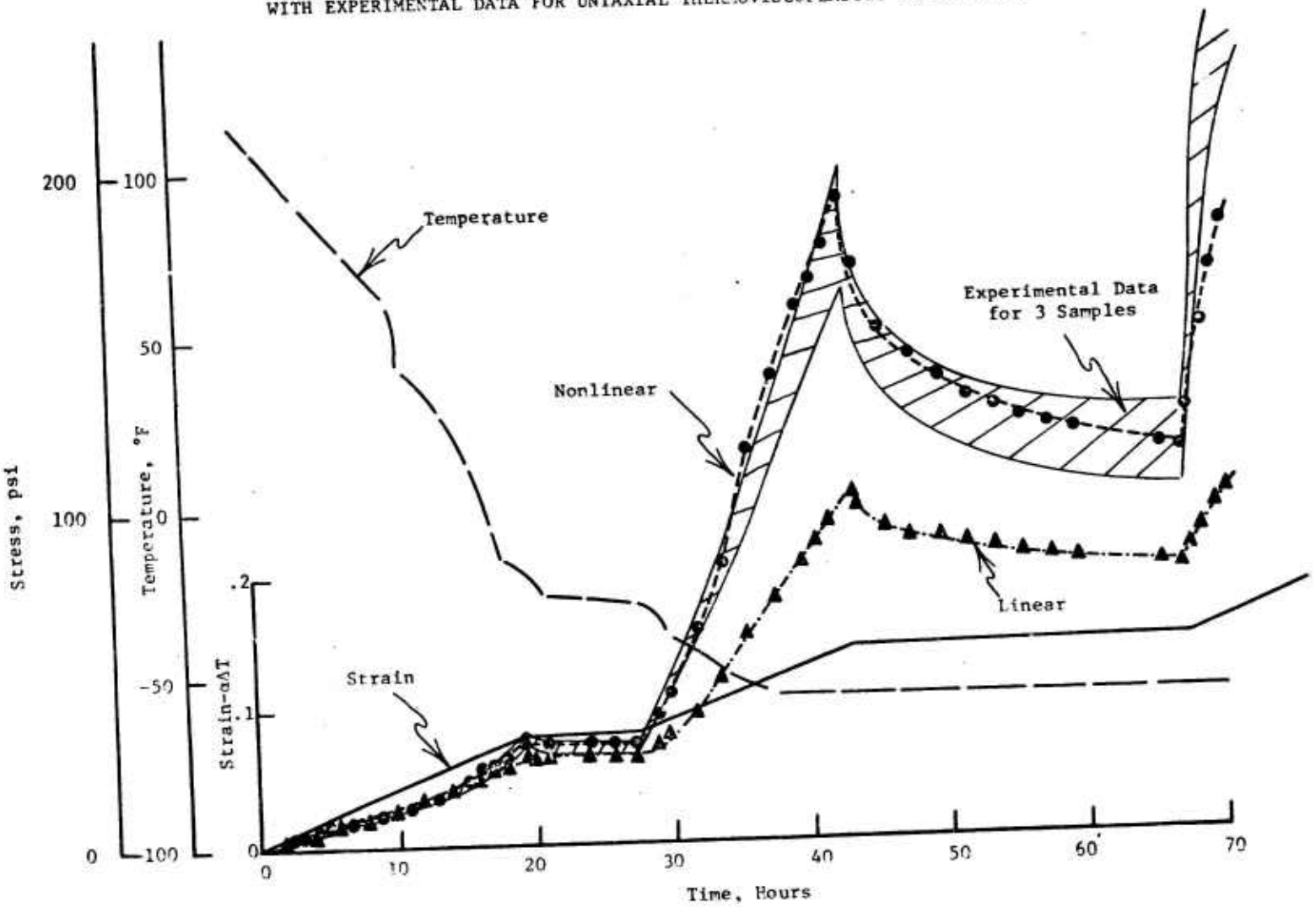

Figure 53

(4) Stress Analysis Methods

These equations were also successfully programmed as a finite element stress code on the Navy contract. This code was for plane strain, case-bonded cylinder solutions where a case, insulation, liner, and propellant system could be analyzed for transient thermoviscoelastic loadings. Aerojet has recently modified its' two dimensional linear viscoelastic codes to accept the nonlinear equation. This new 2-D nonlinear code will handle transient thermal and pressure loads for generalized plane stress or strain conditions for motors with tangentially dependent geometries or finite length grains with longitudinal effects for grains having axisymmetric geometries. This 2-D stress code is not very streamlined for nonlinear applications and is thus limited to 200 elements. The 1-D code is used almost routinely at Aerojet while the 2-D code has seen only limited usage. Both codes will perform linear elastic, linear viscoelastic and nonlinear viscoelastic solutions for transient thermal and pressure problems involving several different materials.

(b) Schapery's Theory

(1) Equations for Multiaxial States of Stress

The thermodynamic equations governing viscoelastic behavior under a general state of stress were given previously. Under the assumption that the free energy and entropy production matrices are given by the factorial forms Equations (52) and (54), the thermodynamic equations can be explicitly solved to find the relations between six generalized forces and six measures of strain.

$$Q_1 = \frac{\partial F_e}{\partial q_1} + \frac{2}{3} a_F \int_{-\infty}^{t} \Delta G\,(\chi - \chi') \frac{d}{d\rho} [2q_1 - q_2 - q_3]\, d\rho \qquad (80)$$

(where χ and χ' have been defined in Equation (55).

plus two similar equations for Q_2 and Q_3; ΔG is the linear viscoelastic relaxation modulus in shear.

Further,

$$Q_4 = \frac{\partial F_e}{\partial q_4} + 2a_F \int_{-\infty}^{t} \Delta G\,(\chi - \chi') \frac{dq_4}{d\rho}\, d\rho \qquad (81)$$

plus two similar equations for Q_5 and Q_6.

These six equations are for a material that is initially isotropic; this implies F_e, a_F, and a_D depend only upon tensor invariants. It has also been assumed, for simplicity, that the linear viscoelastic bulk modulus is essentially constant; this assumption is concerned only with the linear range of behavior, and does not exclude a change in the bulk modulus due to vacuole formation.

In general, the measures of strain, $q_1 \ldots q_6$, are isotropic tensor functions of the strain tensor itself.[30]

If, however, experimental work indicates that the six variables, q_i, can be equated to the six components of the strain tensor itself, ε_{ij} (i, j = 1, 2, 3) term-by-term (e.g., $\varepsilon_{11} = q_1$, $\varepsilon_{22} = q_2$, . . .) then the energy relation implies the six generalized forces equal the six components of the stress tensor (e.g. $\sigma_{11} = Q_1$, $\sigma_{22} = Q_2$ . . .). For example, Equations (80) and (81) become, in the double index notation,

$$\sigma_{11} = \frac{\partial F_e}{\partial \varepsilon_{11}} + \frac{2}{3} a_F \int_{-\infty}^{t} \Delta G\,(\chi - \chi') \frac{d}{d\rho} [2\varepsilon_{11} - \varepsilon_{22} - \varepsilon_{33}]\, d\rho \qquad (82)$$

$$\tau_{12} = \frac{\partial F_e}{\partial \varepsilon_{12}} + 2a_F \int_{-\infty}^{t} \Delta G\,(\chi - \chi') \frac{d\varepsilon_{12}}{d\rho}\, d\rho \qquad (83)$$

These last two equations possess the following interesting property. Suppose a simple shear strain, ε_{12}, is applied to the material, all other strains being zero. Then an elastic component of normal stress, σ_{11}, may result from shear stress, but the viscoelastic component (the integral in Equation (82) is zero. A similar conclusion can be made for a pure normal strain test, in that the viscoelastic component of shear stress is zero. Thus, when the strains ε_{ij} and variables q_i are assumed to be identical, the viscoelastic shear and normal stresses are uncoupled.

On the other hand, if experiments indicate that coupling does exist, it is a simple matter (theoretically) to generalize the equations. Specifically, the six variables are written as isotropic tensor functions of the six strains; implicitly,

$$q_1 = q_1 (\varepsilon_{11}, \cdots, \varepsilon_{23}) \qquad (84)$$

$$q_6 = q_6 (\varepsilon_{11}, \cdots, \varepsilon_{23})$$

Then, using the power condition Equation (46) it is found

$$\sigma_{ij} = \sum_{k=1}^{6} Q_k \frac{\partial q_k}{\partial \varepsilon_{ij}} \tag{85}$$

The desired stress-strain equations are obtained by simply substituting the equations for generalized forces, e.g., Equations (81) and (82) into Equation (85).

It must be emphasized that if Equation (84) has to be used, rather than simply equating q_i and $_{ij}$ term-by-term, generalized forces and stresses cannot be equated; instead, one Equation (85) must be used to obtain equations which are thermodynamically valid.

All of the above three-dimensional equations are valid for either small strains or large strains. For large strains, it is simply a matter of using the tensorially correct quantities; one acceptable set of finite strains is the covariant Lagrangian strain tensor referred to a convected coordinate system, while the stresses are the components of the contravariant stress tensor referred to the same coordinate system.(30)

(2) Experimental Verification

The results of some vibration and monotonic straining tests on solid propellant will be reviewed and compared with Schapery's theory in this subsection.

Vibration Example:

Examined first will be some data obtained by subjecting a thin slab of propellant to a very small sinusoidal shear strain (7×10^{-5} amplitude) over the frequency range of 20-1000 cps; the test apparatus employs a piezoelectric driver, and is described in Reference 132. The data are shown in Figure 54 for various amounts of superposed constant lateral compression.

The constitutive theory Equation (83), yields the following real and imaginary components of the complex shear modulus, $\tau_{12}/2\varepsilon_{12}$.

$$G' = \left[\frac{\partial^2 F_e}{\partial \varepsilon_{12}^2} - a_F G_e\right] + a_F G'(\omega a_\varepsilon) \tag{86a}$$

$$G'' = a_F G''(\omega a_\varepsilon) \tag{86b}$$

where $\partial^2 F_e/\partial \varepsilon^2_{12}$ and a_F are independent of frequency and shear strain but are functions of the amount of lateral compressive strain ε_s.

Furthermore:

$G'(\omega a_\varepsilon)$ and $G''(\omega a_\varepsilon)$ = real and imaginary components of the linear viscoelastic complex modulus, respectively, as functions of reduced frequency, ωa_ε.

$a_\varepsilon = a_\varepsilon(\varepsilon_s) = a_D/a_F$ = strain frequency shift factor.

$G_e \equiv$ long-time (equilibrium) shear modulus.

If Equation (86b) is valid, the G''_ε curves in Figure 54 will form a continuous curve of $G''(\omega a_\varepsilon)$ by translating them vertically an amount log (a_F) and horizontally an amount log a_ε. Figure 55 shows the result of these translations; all five G" curves blend together within graphical accuracy. Similarly, from Equation (86a) it can be seen the quantity $G' - (\partial^2 F_e/\partial\varepsilon^2_{12} - a_F G_e)$ should form a continuous curve of $G'(\omega a_\varepsilon)$ after applying the same vertical and horizontal translations used to obtain $G''(\omega a_\varepsilon)$.

As a check on the theory, note from Figure 55 that superposition of the real part G' onto a single curve is quite good, with the maximum deviation from the $\varepsilon_s = 0$ curve being seven percent. Graphically determined pertinent values are given in Table 2 below. In terms of the previously described spring and dashpot model, they imply: (a) all springs increase in stiffness with lateral compression (columns (2) and (3)); and (b) the relaxation times decrease with lateral compression, column (1).

TABLE 2 - VIBRATION PROPERTIES

Compressive strain ε_s (%)	(1) a_ε	(2) $\frac{\partial^2 F_e}{\partial \varepsilon^2_{12}} - a_F G_e$ (psi)	(3) a_F
0	1	0	1
2.6	0.74	70	1.19
5.2	0.35	228	1.61
7.8	0.18	508	2.19
10.4	0.10	962	2.76

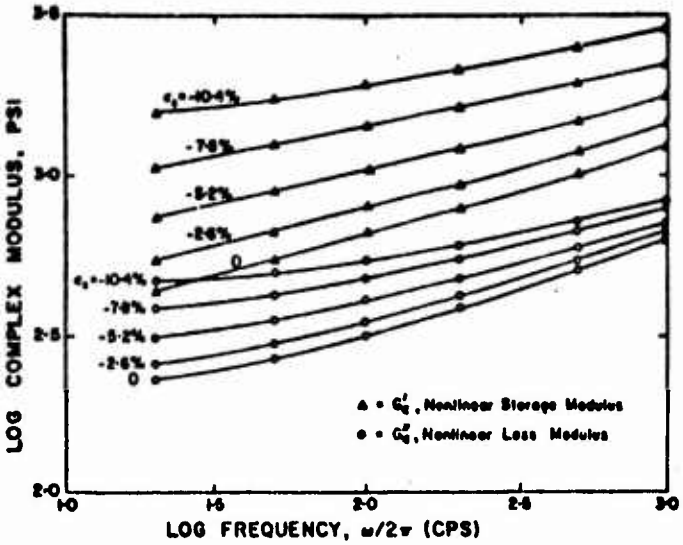

COMPLEX SHEAR MODULUS WITH STATIC LATERAL COMPRESSION, PBAA PROPELLANT, 84 wt. % LOADING

Figure 54

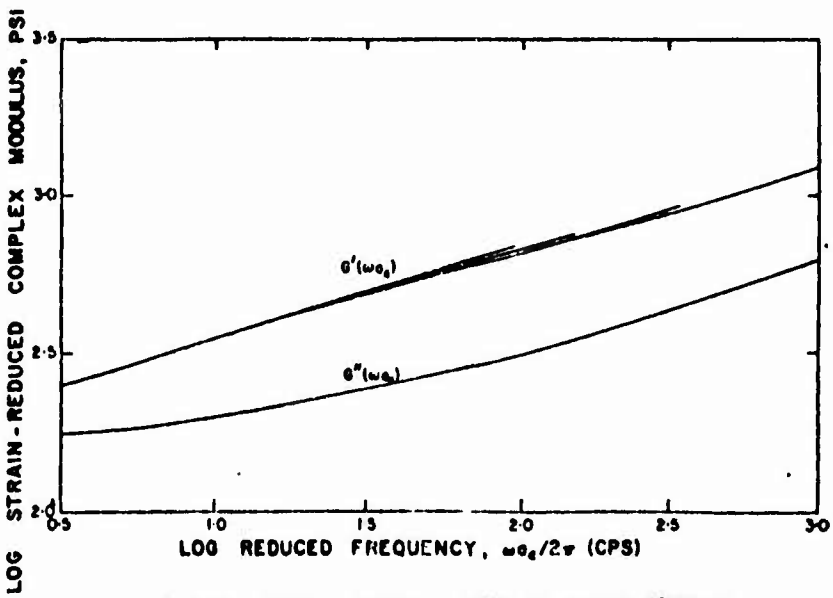

LATERAL STRAIN-REDUCED COMPLEX SHEAR MODULUS, PBA PROPELLANT, 84 wt. % LOADING

Figure 55

The curves shown in Figure 55 are called "Master Curves". They can be interpreted as the real and imaginary components of the linear viscoelastic complex modulus. In principle, these curves, together with the values in Table 2, serve to characterize the material for shear vibrations or other shear strain histories if the assumptions leading to Equation (86) are correct.

One important consequence of these assumptions is that the "Master Curves" in Figure 55 are those for a linear material, and therefore, they must be interrelated according to linear theory. A check on this interrelationship can be made by comparing the measured loss tangent with the linear viscoelastic prediction, which is the well known expression:

$$\left(\frac{G''}{G'}\right)_{thry} = \tan \frac{n\pi}{2}$$

where n = log-log slope of the G' curve.

From Figure 55 $n \simeq 0.28$ and hence

$$\left(\frac{G''}{G'}\right)_{thry} \simeq 0.47$$

In contrast, the low-frequency end of the data in Fig. 55 yields directly from the graph;

$$\left(\frac{G''}{G'}\right) \simeq 0.67 \qquad (\log n a_\varepsilon \simeq 0.5)$$

while at the intermediate and high-frequency end we find

$$\left(\frac{G''}{G'}\right) \simeq 0.50$$

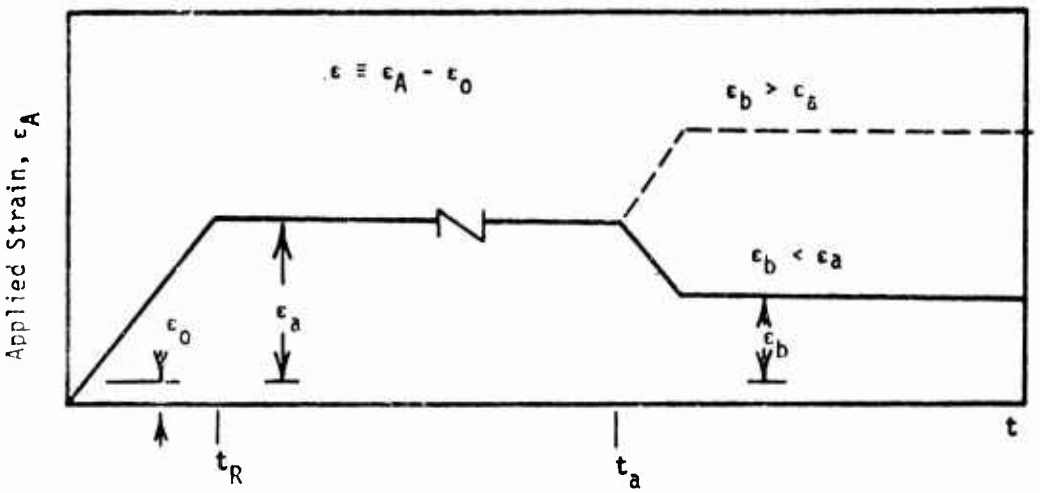

APPLIED STRAIN HISTORY FOR TWO-STEP RELAXATION TEST

Figure 56

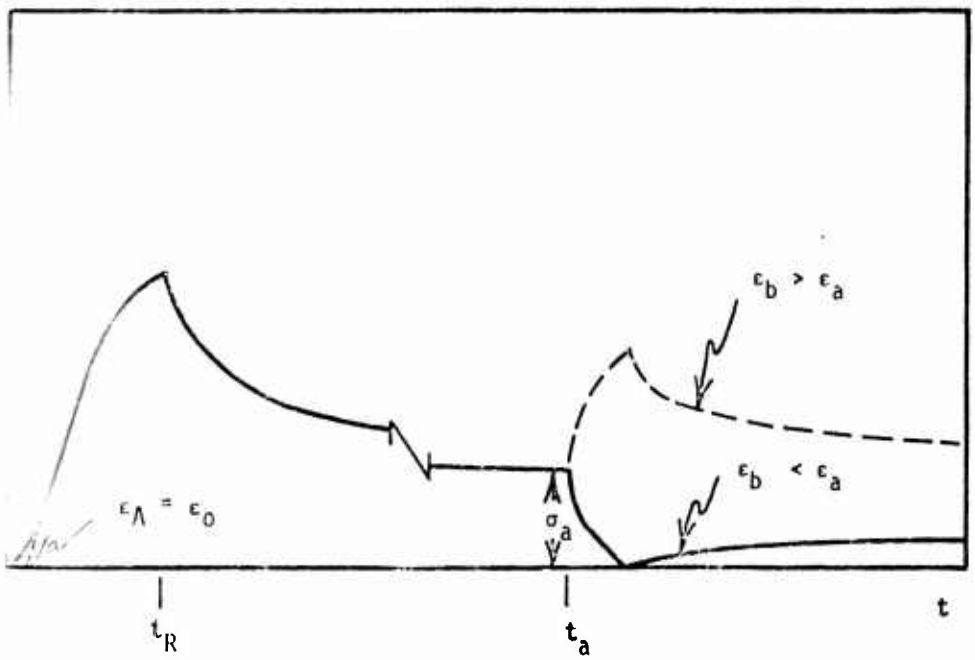

STRESS-TIME TRACE FOR TWO-STEP RELAXATION TEST

Figure 57

Thus, the directly measured loss tangent is higher than predicted (an average error over all frequencies of 10%). This discrepancy is similar to that reported in References 132 and 133 for tensile and shear tests.

Although linear viscoelastic theory seems to account for approximately 90% of the dissipation, there is clearly another mechanism involved. Based on Farris' theory, it is believed that the Mullins' Effect is present even at very small strains (≈ 0.01%) and that a complete characterization requires its inclusion. Further examination reveals that the nonlinear spring and dashpot model in Figure 24 must have dashpots and/or springs whose properties depend on more than just strain.

Two-Step Stress Relaxation: The uniaxial, thermodynamic constitutive equation (55) will be used here, together with some two-step relaxation data on an 82% wt. solids loaded CTPB propellant, to illustrate characterization of the material uniaxial loading and to give another example of reversible nonlinearities. (The data were obtained at the Navy Ordnance Station, Indian Head, Maryland). As a working hypothesis, all nonlinear properties will be assumed functions of only instanteous temperature and strain.

The Equation (55) can be written in a form which is more convenient for data reduction. Specifically,

$$\sigma = h_0 \varepsilon + h_1 \int_0^t \Delta E\,(\chi - \chi') \frac{dh_2}{d\tau}\, d\tau \qquad (88)$$

where the bar is assumed to be unloaded when $t < 0$, and

$$\chi \equiv \int_0^t dt'/a_\varepsilon$$

with a_ε, h_0, h_1, and h_2 material property functions of strain and temperature.

As developed in Reference (31), a single-step relaxation test is not sufficient to evaluate all properties in Equation (88). However, data from the two-step test in Figure 56 and 57 is sufficient if Equation (88) is valid and can be easily used in the characterization process.

During the first step relaxation, Equation (88) yields, upon neglecting the influence of the initial ramp:

$$E_r \equiv \frac{\sigma}{\varepsilon} = h_o + h_1 h_2 \Delta E \left(\frac{t}{a_\varepsilon} \right) \qquad (89)$$

where E_r is the nonlinear relaxation modulus.

On the experimental side, essentially parallel, straight lines were obtained at all times, temperatures ($-85 \leq T \leq 77°F$), and strains, as illustrated for T = -75°F in Figure 58. The toe shown in Figure 57 ($\varepsilon_A < \varepsilon_0$) was subtracted from all data; it was found that the corrected data satisfied the linear viscoelastic relation between constant strain rate and relaxation moduli for $0 \leq \varepsilon \lesssim 2\%$, where $\varepsilon \equiv \varepsilon_A - \varepsilon_0$ is the strain used in the following discussion.

The moduli in Figure 58 imply

$$E_r = E_1 (h_1 h_2 a_\varepsilon^n)\, t^{-n} \quad (E_1 \text{ is independent of strain}) \qquad (90)$$

which shows that only n and the product $h_1 h_2 a_\varepsilon^n$ can be found from relaxation moduli. The strain dependence of $h_1 h_2 a_\varepsilon^n$ is brought out in Figure 59, this dependence (for $\varepsilon \gtrsim 1.5\%$) is due to vacuole formation and growth, based on preliminary dilatometric measurements.

The stress build-up in Figure 57 during the second constant strain $\varepsilon = \varepsilon_b$ region was used to complete the characterization using the theory based on Equation (88) and developed in Reference 31. Specifically, it can be shown that when $(E_r^b \varepsilon_b - \sigma)/\sigma_a$ (where E_r^b = relaxation modulus at strain ε_b, and $\sigma_a = \sigma(t_a)$) is plotted against reduced recovery time, all curves should superpose on the linear visocelastic curve in Figure 60 through horizontal and vertical translations; the amount of translation required provides values of log h_1 and log a_ε.

The nonlinear properties are plotted in Figures 61 and 62 for T = -75°F. Data at other temperatures show similar behavior. Indeed all three properties can be approximated by the piecewise power-law expressions

$$a_\varepsilon = h_1 = h_2 = 1 \text{ for } \varepsilon < \varepsilon_c \qquad (91a)$$

and

$$a_\varepsilon = \left(\frac{\varepsilon}{\varepsilon_c}\right)^{-p} ; \; h_1 = \left(\frac{\varepsilon}{\varepsilon_c}\right)^{q} ; \; h_2 = \left(\frac{\varepsilon}{\varepsilon_c}\right)^{-r} \qquad (91b)$$

for $\varepsilon > \varepsilon_c$, where $\varepsilon_c \approx 3\%$ and $p, q, r > 0$. A slight temperature dependence of p, q, r, and ε_c was observed. The decrease in relaxation times (a_ε) and increase in spring moduli (h_1) with strain is consistent with the above vibration results. These three properties, together with E_1 and n obtained from the small strain range, $\varepsilon \lesssim 1.5\%$, characterize the material under uniaxial loading at any given temperature if the nonlinearities are all reversible.

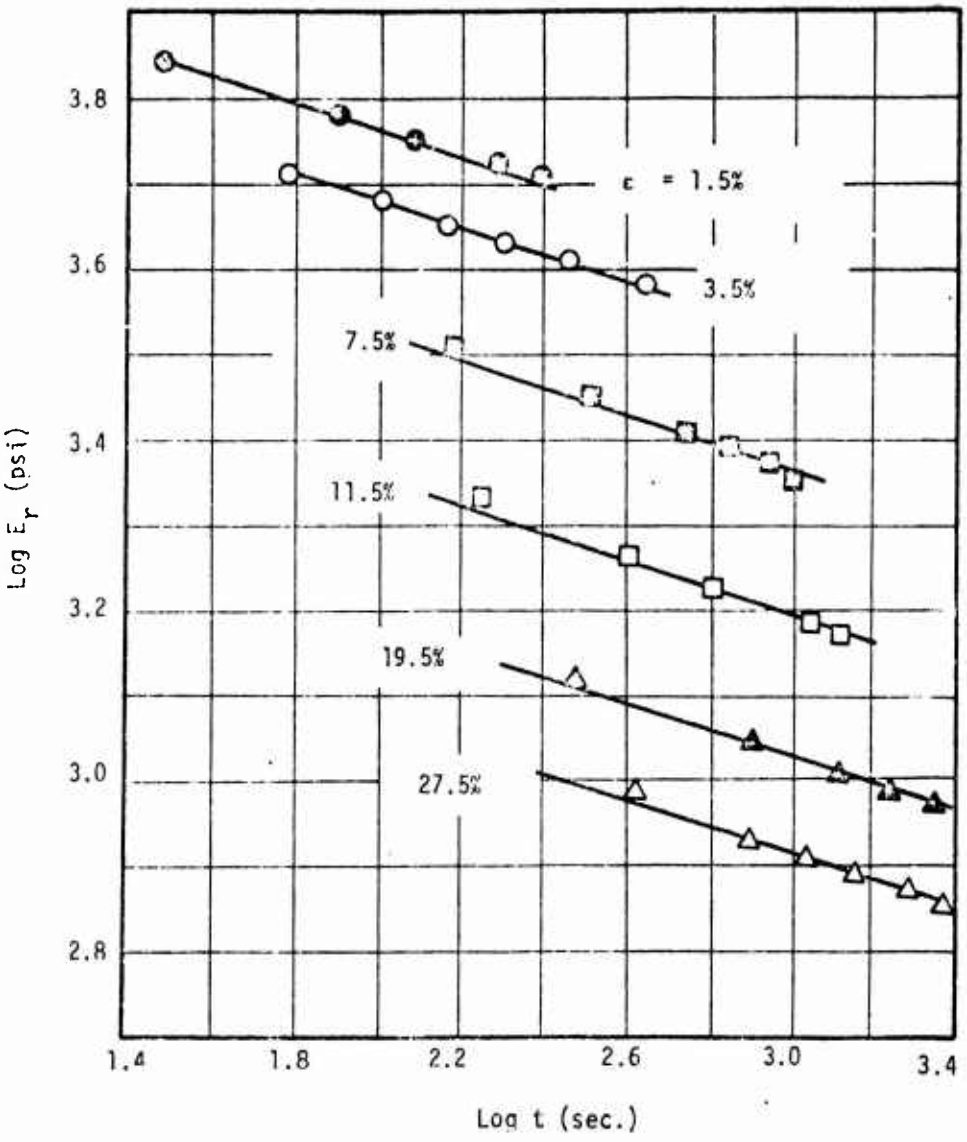

TIME DEPENDENCE OF STRESS RELAXATION MODULUS

T = (-75°F)

Figure 58

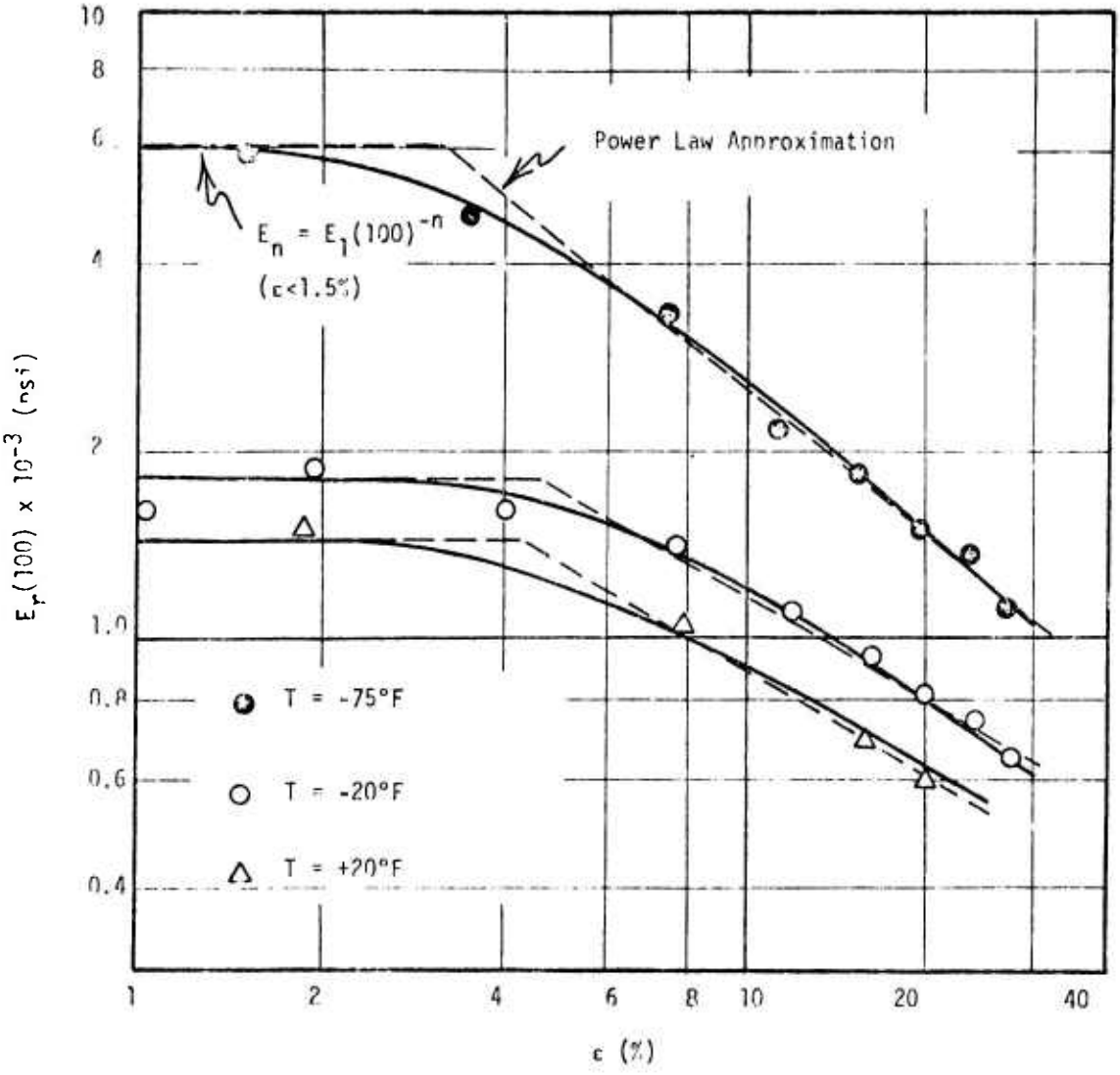

STRAIN DEPENDENCE OF STRESS RELAXATION MODULUS AT

τ = 100 SECONDS

Figure 59

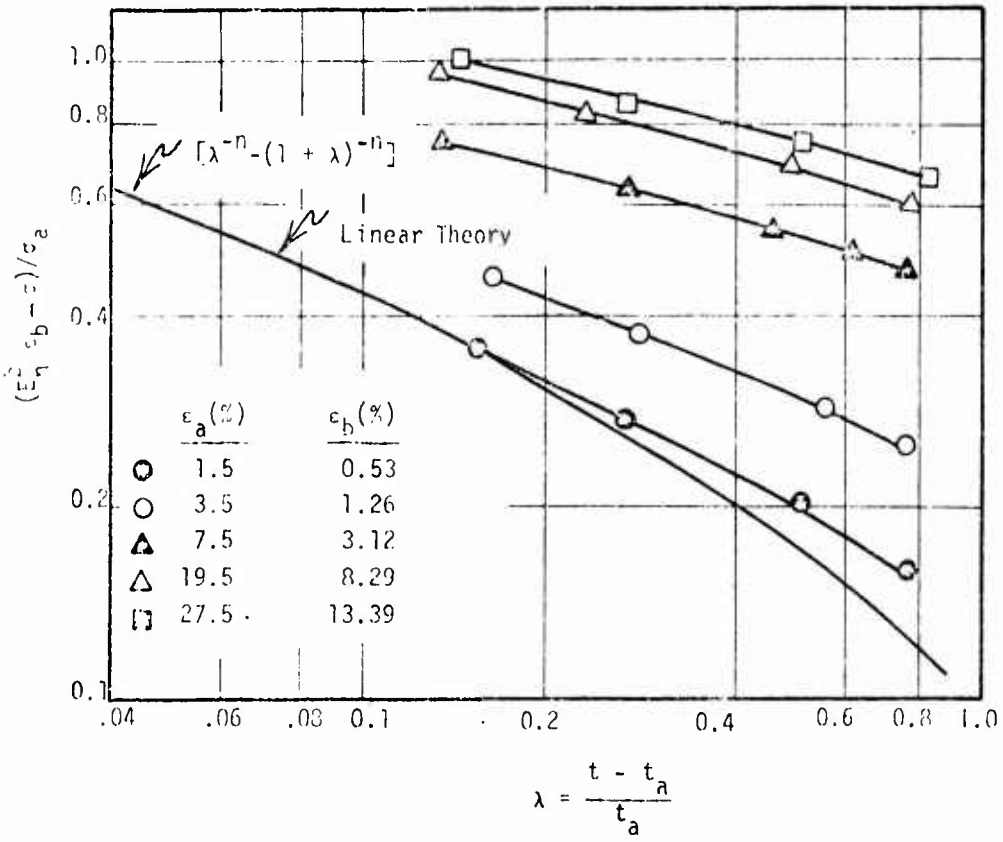

REDUCED DATA FOR SECOND STRAIN STEP (T = -75°F)

Figure 69

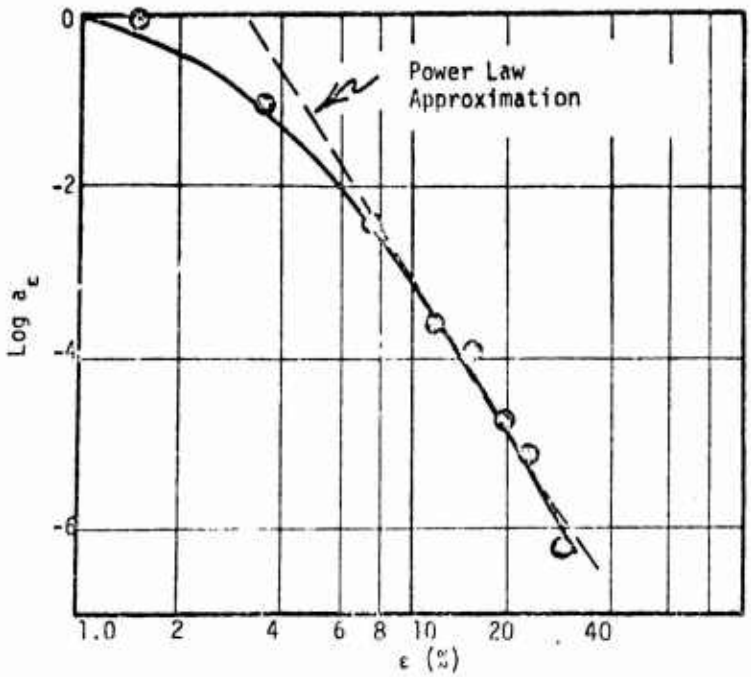

STRAIN DEPENDENCE OF TIME-SCALE FACTOR, a_ε (T = -75°)

Figure 61

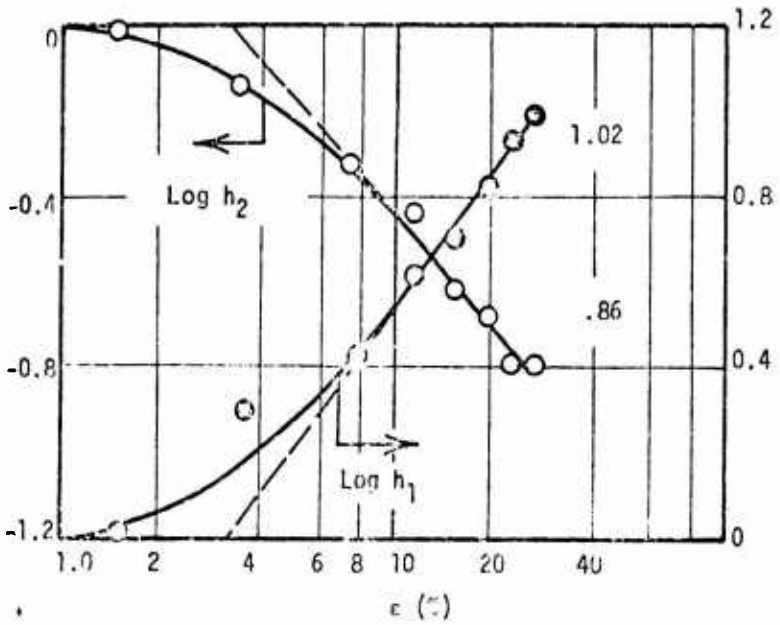

STRAIN DEPENDENCE OF MATERIAL PROPERTIES h_1, and h_2(T = -75°F)

Figure 62

The increase in stress during the second strain step shown in Figure 57 implies that there is at least some reversible nonlinearity present; if all time-dependence were due to internal failure, the material would not show this recovery. On the other hand the small strain data ($\varepsilon < 1.5\%$) in Figure 60 does not fall on the linear theory curve, even though the relaxation modulus is essentially independent of strain in this range; data at other temperatures reveal similar discrepancies. This result again brings out the presence of the Mullins' Effect at small strains. A full characterization requires that Lebesque norms, at least, be included in one or more of the nonlinear properties. A study of stress history in the constant strain rate regions in Figure 57 has further verified this point.

Simultaneous Cooling and Straining

The material properties found in the previous section will be used here to predict the uniaxial stress due to simultaneous application of constant straining and cooling rates. At the outset, it should be noted that constant temperature data are not sufficient to characterize the material for transient temperature applications when the relaxation modulus is a power law in time, as was pointed out earlier in this report. This indeterminacy is true for the linear and nonlinear cases, because, according to Equation (90) the isothermal data does not distinguish between the temperature dependence of the dashpots through (a_ε) and the temperature dependence of the springs through E_1.

Figure 63 shows the stress history in two specimens subjected to identical strain and temperature histories. The nonlinear theory prediction was made using Equation (88) and the assumption that E_1 is constant while a_ε contains all of the temperature dependence in the small strain range. Also shown is the linear-viscoelastic prediction for a thermorheologically simple material. When E_1, rather than a_ε, contains all of the temperature dependence, both linear and nonlinear predictions are so high they can't be plotted on the same graph. However, by incorporating a slight amount of temperature dependence in E_1, the nonlinear prediction can be made to fall on top of the experimental data.

It is very interesting to observe that the linear theory is below the experimental data at low strains and above it at high strains. It is believed the linear theory is low at low strains due to the Mullins' Effect, and high at high strains because of specimen softening due to vacuole growth. The nonlinear theory would be higher if the Mullins' Effect had been taken into account and/or some temperature dependence of E_1 had been used.

Clearly, depending on the strain level, linear theory will either provide conservative or nonconservative predictions. This conclusion has been found true for two other series of tests on the same material with different straining and cooling rates.

Finally, it is noted that the nonlinear theory agrees relatively well with the experimental data, even though explicit dilatational dependence has not been taken into account. This agreement is a consequence of the strain being a monotomically increasing function of time; explicit dependence on dilatation is needed in the characterization if one is to predict response to large cyclic strains.

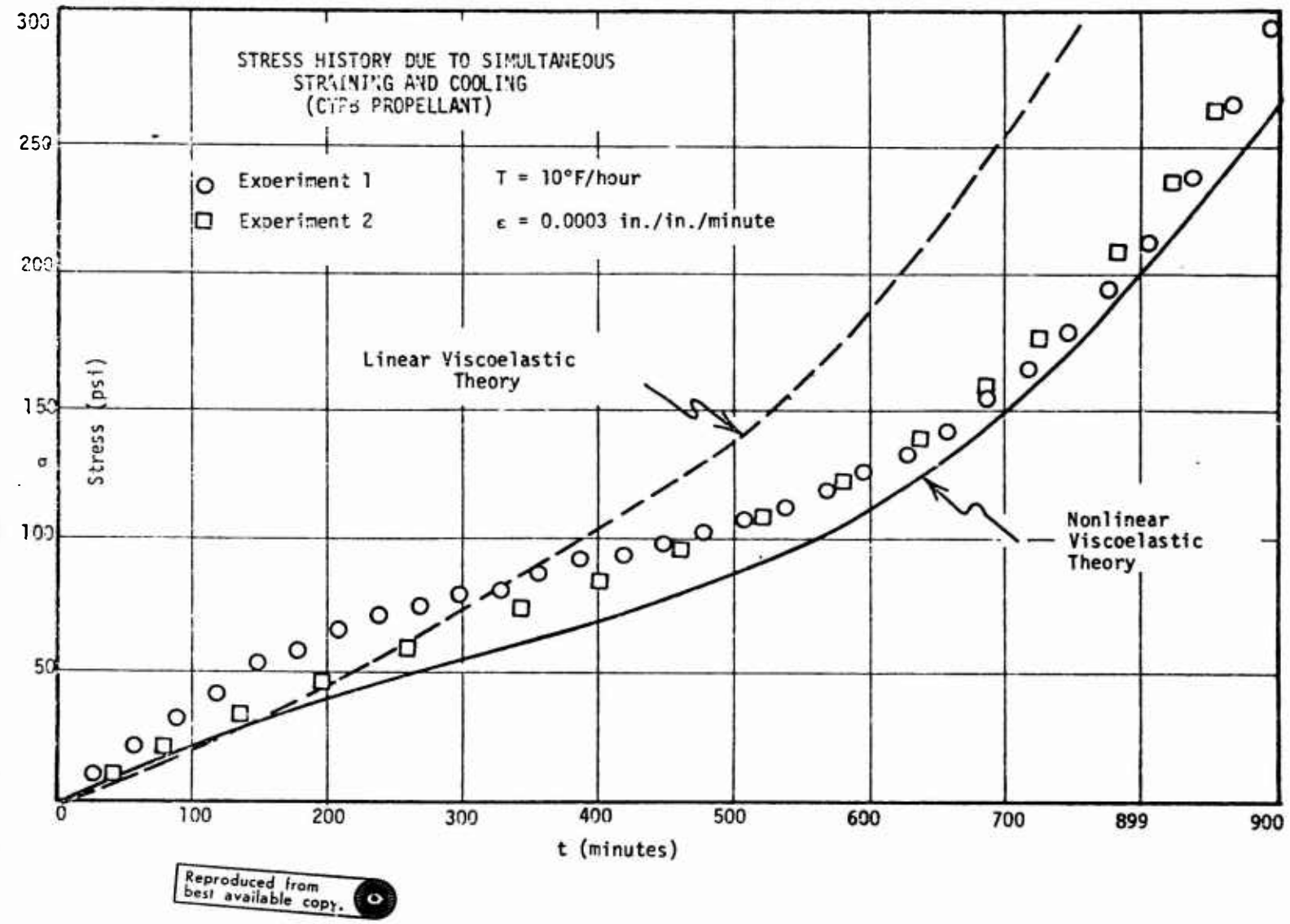

Figure 63

(c) Equivalence of the Theories

The two constitutive theories discussed above are based on somewhat different mathematical and physical arguments. Nevertheless, it has been claimed that both predict propellant behavior correctly. Next will be discussed some conditions under which the two theories become identical.

It is believed that by bringing together the essential features of Farris' physical model and Schapery's thermodynamic model, a simple, but realistic constitutive theory will result.

First consider the relation between the theories when the constitutive equation is homogeneous of order one and the material is mechanically incompressible. The thermodynamic theory (e.g. Equations (80) and (81)) satisfy the conditions if it is assumed:

(1) a_F and a_D are homogeneous of order zero.
(2) The variables q_i and the strains e_{ij} are identical (i.e., $e_{11} = q_1$, $e_{22} = q_2$,...).
(3) $\partial F_e / \partial q_i$ is homogeneous of order one.
(4) $e_{11} + e_{22} + e_{33} = 0$.

The thermodynamic theory can now be written in the compact form:

$$\sigma_{ij} = \delta_{ij} P + G_e e_{ij} + 2a_F \int_0^t \Delta G(\chi - \chi') \frac{de_{ij}}{d\rho} \, d\rho \qquad (92a)$$

For this case, Farris' theory, Equation (4.6), becomes

$$\sigma_{ij} = \delta_{ij} P + \int_0^t K_1 I I_1(\overset{t}{\underset{0}{\xi}}), \; I_2(\overset{t}{\underset{0}{\xi}}), \; I_3(\overset{t}{\underset{0}{\xi}}), \; t - \tau] \; \dot{e}_{ij} d\tau \qquad (92b)$$

These expressions are identical if

$$G_e + 2a_F \Delta G(t) = K_1$$

$$a_D / a_F = 1 \text{ (this implies } \chi - \chi' = t - \tau)$$

in which G_e and a_F are homogeneous functions of $I_i(\overset{t}{\underset{0}{\xi}})$ of order zero.

The interesting point here is that Farris' model implies that the free-energy based terms G_e and a_F depend on quantities that reflect molecular failure; this is exactly what one should expect to find since large free energy changes are associated with primary bond rupture.

Further, Farris found that Equation (79) is one form that nicely fits some propellant data. For this case, equivalence of the theories is obtained by setting

$$G_e = 570 \left(\frac{|f|}{||f||_{21}} \right)^{2.25}$$

$$a_F = \left[1 - \frac{|f|}{||f||_{21}} \right]$$

$$\Delta G = 285\ t^{-0.1}$$

$$a_D = a_F$$

In another interesting study, Farris[6] reported the influence of tensile strain, e_{11}, and a confining pressure, p, on the dilatation, e_{ii}, and uniaxial stress, σ, response of propellant bars subjected to a single constant strain rate. For this loading condition he found that, approximately,

$$\frac{\partial \sigma}{\partial e_{ii}} = - \frac{\partial p}{\partial e_{11}} \tag{93}$$

where e_{ii} = dilatation and e_{11} = tensile strain. It is easily shown that this relationship implies σ and p are derivable from a potential function; i.e.,

$$\sigma = \frac{\partial Fe}{\partial e_{11}} \quad \text{and} \quad p = \frac{\partial Fe}{\partial e_{ii}} \tag{94}$$

But, these equations are identical with Schapery's theory when $a_F = 0$ (i.e. when all time-dependent reversible nonlinearities are neglected). This result is consistent with previous comments in that reversible nonlinearities are not significant under monotonically increasing strain histories.

Although equivalence of the theories has been demonstrated for special cases only, there are many other realistic situations in which equivalence can be established. The important point here is that by combining Farris' structural model theory with a thermodynamic theory, it is possible to (1) easily generalize results from a limited amount of experimental data so as to reduce practical and realistic, three-dimensional constitutive equations and (2) gain insight into the proper and practical way of generalizing either one or both constitutive theories when the data warrants the extension.

2. Ultimate Objective

The discussion above demonstrates that all of the immediate objectives of the contract have been accomplished. This program was designed to use and extend the information obtained by Farris to satisfy the contract's ultimate objective which is "to develop a constitutive theory which will closely model the nonlinear time dependent behavior exhibited by solid propellants." This approach has resulted in the Air Force's obtaining a rather complete constitutive theory at an early date and yet developed by the identical methods they recommended. The discussion below presents the current status of understanding propellant behavior in terms of what is known and what isn't known and discusses various methods of solution that might be employed for the remaining unsolved problems. The problem is then to find the best method to include the three contributing mechanisms of propellant nonlinearity, namely the Mullins' Effect, vacuole dilatation, and reversible nonlinearities, into a general three dimensional constitutive equation that will be applicable to describing propellant response.

(1) Status of Propellant Constitutive Theory at Beginning of Contract

Propellant constitutive theory is in its infancy. Except for work of Schapery[30-32] and the recent work of Farris[1,2] little has been done in the area of nonlinear viscoelasticity that is applicable to propellant response. Nevertheless, there are certain things that are known about propellant behavior and the types of mathematics needed to describe that behavior. Certain other problems remain nearly untouched and, for the most part, have never before been clearly defined.

(a) What Was Known

Many things are known about the nonlinear behavior of composite propellants. These factors must be included in a valid constitutive theory for these materials. The discussion below describes the essential features of what is known about propellant behavior that will greatly influence the constitutive equation.

- Propellants are not fading memory materials. Existing nonlinear constitutive theories such as Green, Rivlin, and Spencer's nonlinear theory for materials with fading memory do not describe propellant response.

- Propellants possess permanent memory characteristics and the only attempts to date to represent the behavior of this type of viscoelastic material is the work of Schapery[30-32], Dong[34], or Farris.[1,9]

- The dominant causes of propellant nonlinearity are known to be, in their order of importance, the Mullins' Effect and vacuole dilatation, which are causes of damage in the material, and also nonlinear reversible fading memory viscoelastic effects. These effects have already been successfully modeled.

- Most of the time effects in propellant materials are due to time dependent damage and have nothing to do with internal viscosity effects.

- For practical engineering purposes, propellants have mathematically homogeneous nonlinear constitutive equations in the range of strain prior to significant vacuole formation.

- Farris' theory for mathematically homogeneous constitutive functionals for isotropic materials is theoretically complete and all existing attempts to use it have shown good agreement between experiment and theory.

- The correspondence principles developed by Farris for his theory permit a linear solution of many boundary valued problems to be transformed into the proper nonlinear solution.

- At strains involving vacuole dilatation, Farris' homogeneous constitutive theory should provide an upper bound estimate of the stresses.

- Experiments performed by Surland[125] and Farris[6,7] demonstrate that the influence of volume change on the stress-state at constant strain is essentially reversible and produces a softening effect that appears to depend only on the dilatation magnitude. Past work suggests this softening effect can be introduced as a modulus multiplier[7].

- Dilatation itself must, at least, be functionally dependent on the deviatoric stress invariants since the influence of pressure is to greatly reduce the dilatation and positive dilatation can occur when all stresses are compressive.[6,7]

- Nearly all propellants are initially isotropic materials.

- At very small vibrational strains propellants appear to be linear viscoelastic materials.

(b) Problems That Remained

There are many unanswered questions about the behavior of composite propellants, and for that matter, many unanswered questions exist about the nonlinear viscoelastic behavior of unfilled amorphous polymers. To date the propellant industry has based most of its analysis on generally unverified assumptions about material behavior that were carry-overs from the polymer industry and all their various rheological theories. It is just in recent years that researchers are becoming aware of the fact that propellants are rather unique materials whose behavior is very complex and not contained in fading memory viscoelastic theory.

Any basis for a constitutive theory should be experimentally verified. Often criteria, which are not totally correct or may be easily misinterpreted are established for categorizing a particular type of behavior. These are essentially traps that many of us often fall into and usually have great difficulty getting out of because the source of the difficulty is not obvious. Examples of such traps are numerous but two are of particular importance to propellant behavior. First and foremost is the so called linearity condition for constitutive functionals, "if doubling the input doubles the output, the material is linear."[102] This behavior is naturally exhibited by all linear materials, however, a large class of nonlinear materials, to which propellants belong, also possess this property[1,2] at small strains. Thus, the criterion is a necessary condition for linearity, but hardly a sufficient condition to guarantee linear response for any material.

The other possible trap is the criterion, "if the data will time-temperature superpose, then the behavior is thermorheologically simple and transient thermal effects can be introduced into the constitutive equation in the form of a reduced time". If a material is thermorheologically simple the data will naturally superpose. Since this is a requirement of thermorheologically simple behavior, however, examples can be constructed wherein thermal effects are not included in a reduced time and the data will still superpose. For such materials transient thermal response computed on the basis of a reduced time will lead to large errors. Again it is observed that the criterion is a necessary condition but not a sufficient condition.

Propellants are nonlinear materials even though they obey the above criterion for linearity and current work at Aerojet lead to questioning the time-temperature superposition concept as totally accounting for all thermal effects. Discussed below are the problems that had to be solved or verified before an accurate three dimensional constitutive theory could be developed for composite propellant materials.

- Although the causes of propellant nonlinearity are known and each effect has been successfully modeled for simple uniaxial behavior, the manner in which these mechanisms interact in a constitutive equation is not completely known. Therefore, determining a proper mathematical form for the constitutive equation that is reasonably simple yet will account for all of these effects is something that must be determined.

- As mentioned above the time-temperature superposition or equivalence assumption postulated by Morland and Lee[134] has not been properly verified experimentally. Simple experiments have been devised to separate effects directly dependent on temperature and those dependent on a reduced time. Experimental data obtained at Aerojet indicate a reduced time does not account for all of the thermal effects.

- Although propellants appear to be initially isotropic, it is well known that some filled materials become highly anisotropic when returned to their original shape after an initial deformation. Such effects, if they exist, can be included in a constitutive equation and should be studied.

- Data obtained by Farris indicate a nonlinear but mathematically homogeneous constitutive equation is valid for propellants in the range of small strains (up to roughly 10%) when the propellant has not dilated significantly. If this type of behavior also held for large strains when the dilatation was suppressed by hydrostatic pressure considerable insight into the large strain behavior of propellants can be obtained. This would not only greatly simplify the general nonlinear constitutive equation but would also provide a means of establishing realistic upper bounds for stress predictions since stress analysis using Farris' nonlinear theory can be accomplished without too much difficulty using the correspondence principles he developed.[1]

- Little is known about tension-torsion coupling in propellants. If coupling does exist then second order tensor dependence must be included in the constitutive equation. It would naturally greatly simplify matters if coupling were not present but only proper experimentation will tell.

- For analysis purposes propellants at long times are always assumed to be elastic materials. Elastic in the sense used here means the material has a fixed reference geometry that does not change with stress or deformation. Thus, elastic materials never undergo changes in reference configuration or exhibit permanent set. Since relaxation phenomena in propellants are dominantly caused by microstructural degradation, which is influenced by stress and temperature, recombination of any of the chains can cause changes in reference configuration such as suggested by Tobolsky's relaxation theory for interchanging networks[37]. This behavior is known to occur in some propellants at very high temperature and is the major obstacle that must be overcome in producing propellants that will survive tegperature sterilization. Propellants cured near 100°F when exposed to say 275°F for several hours often behave as though they were cured at 275°F because of thermally activated chain cleavage and reformation. This phenomenon can occur with no noticeable change in material characteristics other than a change in reference geometry. What happens when a grain is stored for several months at lower temperatures is unknown, however, if such effects occur, they will influence the analysis as strongly as any nonlinearities.

- Little is known about the behavior of propellants under combined multiaxial loading conditions especially of a nonproportional type such as combined tension-torsion when, for example, the material is stretched now and twisted later. Analytically this is a much more complex deformation history than when the tension and torsion are applied together in some proportional manner. Tests such as these will bring out which of the three invariants or what combinations of them must be included in a general representation for propellants.

(c) Realistic Constraints on the Solution

What is known and what is unknown about propellant behavior which will greatly influence the constitutive equation has already been discussed. The problem therefore is to be able to include all that is known and what will be found by additional experimentation into a single mathematical relationship that will accurately represent the behavior of composite propellants. The problems of including these features into a single representation are dominantly mathematical and one finds there is no substitute for experience in this area. As was mentioned earlier, the dominant factors contributing to propellant nonlinearity have already been successfully modeled for one dimensional conditions and show good agreement between experiment and theory. The problem at hand, however, is to develop a three dimensional nonlinear constitutive equation that can contain, for example time and temperature effects, history effects, and strain coupling. To develop detailed three dimensional structural models that contain these effects, as well as the nonlinear mechanisms and their possible interaction is a hopeless task. Instead, what must be done is to incorporate the essential mathematical measures found from our models, such as L_p norms, relaxation times, etc., into some mathematically complete three dimensional theory, thereby retaining the essential features of our models.

General continuum theories have been developed for specific classes of materials and are sufficiently general that many types of behavior can be included. At first it might appear that these theories are just arbitrary polynominal or functional expansions, however, there are many constraints that have been included in these theories from the axioms of continuum mechanics and continuum thermodynamics.[43,44] Many empirical constitutive equations actually violate some of these conditions and are physically meaningless when extended or applied to test conditions different than the conditions for which they were developed. Therefore, it is desirable to mathematically incorporate the features of our models into these general theories since they can not violate any continuum assumptions even for arbitrary loading or thermal histories. In selecting one or more of these mathematical theories consideration will be given to the factors listed below since the equations developed must ultimately be applied to real propellant behavior and in this sense some constitutive theories are highly preferred to others.

- Accuracy - consideration will be given to accuracy. It is essential that the constitutive equation proposed actually contain the types of behavior exhibited by propellants.

- Simplicity - although inherently complex, some theories are much more complex and abstract than others.

- Material characterization - since the parameters in the equations must be interpreted in terms of some specific material, the equations should be such that the material functions appearing in equations can be determined by experiment.

- Numerical analysis - consideration will be given to the types of mathematical operations entering into the constitutive theory since some forms of mathematical operations are more desirable to use on computers than others. If the constitutive equations developed on this program are to be of any benefit they must be used in large scale computer analysis. The ability to perform such analysis will depend on picking an acceptable form of the constitutive theory.

- Physical implications - it would be desirable if terms in the constitutive equation selected could have physical significance such as being measures of damage. Examples of such equations are Schapery's equations wherein certain terms are associated with free energy and others with entropy production.

(2) Experimentation

In order to develop three dimensional constitutive equations for any material three dimensional stress-strain information is required. The standard JANNAF type experimentation only provides one component of strain and stress. This information cannot be used to determine a materials three dimensional equation of state because the experiments do not provide sufficient information to calculate the stress in terms of the deformation history, since all of the invariants of strain are not known. In short, three dimensional stress-strain data is a prerequisite for characterizing a material's response to a known three dimensional equation of state, or determining the types of three dimensional equations governing a materials response. This latter problem is naturally much more difficult since the equations themselves are unknown and viscoelastic and large dilatational effects only serve to further complicate the problem.

This program concentrated on multiaxial experiments that were analyzable and could be used in determining the materials equation of state. The discussion below deals with the experimental methods, the sample geometries, and the types of experiments used in providing the information required for this program.

(a) Experimental Methods

The method used on this program to obtain three dimensional stress-strain data for material characterization was the gas dilatometric method. Aerojet constructed two special gas dilatometers, for use on this contract, one for long slender uniaxial type samples pulled axially, and one for strip biaxial type samples. The gas dilatometer is a relatively simple device used to simultaneously and continuously measure the stress-strain and the volumetric dilatation-strain behavior over a wide range of test conditions.(5) These instruments are complete with load sensors and utilize mechanical test equipment only for their pulling mechanisms and environmental chambers. The volume change is monitored by continuously measuring the change in gas pressure between a constant volume test cavity, which contains the sample, and a pressure reference cavity. Hence an increase in sample volume is reflected as a compression of the gas of the same amount. Direct piston calibration is provided and the Δp versus ΔV relationship is extremely linear for volume changes of over 20% of the sample. Both of these instruments are operational over a very wide range of strain rates, and temperatures from -75°F to +200°F. These uniaxial and biaxial dilatometers can therefore provide stress-strain-dilatation data for the entire deformation history. Since these samples are essentially free from shearing strains and in the uniaxial test $E_{22} = E_{33}$ and in the strip biaxial test $E_{33} = 0$, all of the strains and their invariants can be calculated.

For multiaxial experiments of a more complex nature these instruments are pressurized to perform experiments with multiaxial stress fields. Both the so-called uniaxial and biaxial dilatometers are operational at pressures to 1000 psi. Hydrostatic pressure greatly influences the stress-strain response of propellants and these experiments are essential in valid material characterization. These experiments are easy to perform and are representative of the stress fields in actual rocket motors subjected to gravitational, thermal and pressure loads.

In addition to the three dimensional experimentation, transient thermal experiments were performed wherein the material was subjected to simultaneous straining and temperature changes. No volumetric measurements were possible under these conditions.

(b) Types of Experiments

The types of experiments performed on this contract were many and are described later in this discussion. Only experiments wherein $\sigma_{22} = \sigma_{33}$ = constant with $\sigma_{13} = \sigma_{23} = \sigma_{12} = 0$, σ_{22} = constant with $\sigma_{12} = \sigma_{23} = \sigma_{13} = 0$, and $\sigma_{11} = \sigma_{22} = \sigma_{33} < 0$ with $\sigma_{12} = \sigma_{13} = \sigma_{23} = 0$ were utilized in the experimental program conducted at Aerojet. These multiaxial experiments for lack of better names have been termed "pressurized uniaxial", "pressurized

biaxial" and "bulk compressibility". These experiments are difficult to perform with good precision, however, with the aid of the gas dilatometers these experiments were carried out over a range of temperatures from +150°F to -75°F and pressure levels from 0 to 1000 psi compression using complex deformation histories to bring out the viscoelastic and memory effects. These experiments are also simple to use since the stress and strain fields are always in principle directions and only three equations, the equations of the principle directions, need be used and the redundant shear equations for isotropic materials never enter into the problem.

Why not shear experiments and poker chip experiments? These experiments were considered and rejected for the following reasons. The poker chip experimentation is being performed at Texas A&M under a subcontract for reasons other than actual characterization. The poker chip test is a poor test to use for material response characterization for nonlinear materials since it has rather strong stress and strain gradients and the average values observed or measurable will not reflect the actual conditions. Also it is extremely difficult to make accurate poker chip measurements. Because of the nonhomogeneous deformation and stress fields this test was excluded for actual characterization purposes but was studied at Texas A&M to assess certain constitutive effects. The shear experiment was considered and actually used early in this program with shear stress, shear strain and dilatation being monitored. It was observed, as expected that considerable volume change occurred in shear experiments wherein the shearing faces were free to move normal to the direction of shear. From the types of equations of state being used this type of behavior was expected. Without considerable instrumentation these shear experiments could not be used in material characterization and shear tests were dropped for the reason that the actual deformation field was unknown. A similar situation occurs with simple Mooney-Rivlin rubber elasticity wherein one finds considerably more than shear stresses must be present to yield a simple shear, constant volume deformation for a rubber material.

The great bulk of the testing performed on this contract consisted of pressurized uniaxial and the pressurized biaxial tests using the gas dilatometers. These tests were performed at the following temperatures: 150, 110, 77, 40, 0, -40, -65 °F. Also several strain rates and different deformation histories involving multiple loading and unloading sequences were used to bring out memory effects. In addition tests were conducted over the entire temperature range using the complex deformation histories at an average of five pressure levels at each temperature. These experiments are ideal for characterization since the only unknown value of the stress tensor is the σ_{33} stress in the biaxial strip tests while the strain tensor is completely defined for all experiments. The sample geometry for the uniaxial experiment was a simple rectangular shaped section approximately 0.50"x0.50"x4.00". The sample was end-bonded to aluminum tabs that mate with the jaws in the dilatometer. Nearly all samples failed in the gage section and only a few bond failures were noted. This type of sample provides excellent axial strain information and also the dilatation can be accurately assumed to be uniformly distributed along the sample length. The only exception to this sample shape was at low temperatures where the length was changed to 3.00" to accommodate the higher

strains being observed. The biaxial strip sample again is a simple rectangular piece of propellant 1.00" high by 0.25" thick by 7.00" long. It is also end bonded to aluminum bars that mate with jaws inside the dilatometer test cavity. The great majority of the biaxial tests were good failures in the gage section. Examples of the types of deformation histories used can be seen in the figures used later to compare predicted with observed data.

(3) Improved Nonlinear Viscoelastic Characterization Methods

The methods used to mathematically characterize the propellant response as a nonlinear viscoelastic material on this contract are not the usual methods of measuring the output due to some idealized input, such as constant strain-stress relaxation experiments. Instead complex deformation histories were used on samples of varying degrees of multiaxiality and the data from dozens of independent experiments was simultaneously fit to the constitutive equation using computerized regression methods. In order to successfully achieve this end several computer codes were written to aid and streamline the characterization process. A brief background of computerized constitutive characterization as it applies to this contract and a brief description of the codes developed on this contract are presented below. A users guide and a listing of each code is given in the appendices of this report.

(a) Background

Computerized viscoelastic response and failure characterization was first discussed in Farris' Ph.D. dissertation[1]. This work discussed a simple means of utilizing the vast storage capacity and speed of modern day computers to characterize the response and failure of viscoelastic materials. This idea was then applied on Aerojet's Navy Contract, "Applications of Nonlinear Viscoelasticity and Cumulative Damage, (A Realistic Evaluation of Real Propellant Behavior."[9]. This Navy contract was also the first real application of Farris' nonlinear equations which included time effects due to both viscosity and time dependent structural breakdown. The characterization methods developed on this program were for incompressible materials and as such did not include nonlinearities due to vacuole dilatation. This first computerized characterization code was limited to essentially isothermal conditions for six different deformation histories in uniaxial, biaxial, or shear. The solutions for the integrals for each of these histories were derived analytically and programmed into the code, thereby eliminating the need for numerical integration. This code functioned quite well and was used in characterization processes involving over 2000 data points with little difficulties, and did an excellent job of describing propellant response[9].

The next step in computerized characterization came when AFRPL funded this nonlinear viscoelastic study contract. The purpose of this contract was to develop constitutive equations for propellant materials in the range of vacuole dilatation and high compressibility. To handle the much more complex problems of three dimensional constitutive characterization for nonproportional loading conditions an entirely new code was developed on this AFRPL contract. Like its' predecessor this code could handle uniaxial, biaxial, and shear experiments as well as multiaxial variations of these experiments obtained by the addition of a constant superimposed pressure. Instead of being able to utilize analytical solutions to the integral equations in the code, the integration now had to be performed numerically since the deformation conditions were no longer proportional. Unlike the small strain theory used in the old code, this new code used a finite measure of strain which has an exact measure of dilatation and conserves mass. Since the new codes had to use numerical integration procedures it was not difficult to develop a code which could now handle arbitrary deformation-time histories including those involving changing temperature. As the AFRPL code now stands it is an extremely versatile and useful research tool that is composed of several sub-packages which may be assembled according to the users needs and the types of equations being used in the characterization. In this sense the user must be very familiar with the code construction. Some of the advantages of computerized characterization are listed below.

- All of the data obtained on a material can be used in the characterization process at the same time (e.g. in standard methods the ramp portion of relaxation experiments is ignored).
- Direct comparisons between observed data and constitutive calculations are provided.
- The need for special tests and test equipment are eliminated since characterization can be carried out using data from any experiment.
- The method is much more accurate than usual methods and provides statistical information regarding accuracy and variability.
- Material variability is included in a standard error measure and considered with other errors.
- Complex deformation histories including time varying temperature and multiaxial loading conditions can be used in the characterization process to give a real test to the equation.
- An accurate method of getting at the time-temperature shift function is provided.

. The user need not be an expert in viscoelastic theory or mathematics.

. Having completed the characterization process the multi-axial stress response to any input deformation-time-temperature history can be calculated.

. An inexpensive and practical method for viscoelastic characterization and retention of raw experimental records has been made available.

(b) Representation Used in the AFRPL Computerized Characterization

As mentioned in the previous section the AFRPL characterization code as it exists today is an extremely versatile code made up of several sub-packages. It was designed to permit the user the many constitutive variations required during the research efforts. Obviously an extremely general and practically undefined constitutive equation cannot be used in finite element stress analyses procedures. What must be done in the future is to restrict the code so that it just contains the equations necessary to describe propellant response. Also some of the series approximations used in the characterization code can probably be simply represented as functions of one or two variables such as exponentials. One of the main efforts of our follow-on contract will be to make the constitutive representation as compact as possible to minimize the storage requirements of the finite element stress codes which are to be developed.

The constitutive equation developed on this contract has the form

$$\sigma_{ij}(t) = \delta_{ij}\sigma(t)_{Bulk} + \sigma_{ij}(t)_{Shear} \tag{95}$$

The experimental data suggests that only the shear terms are time dependent and the bulk term is for all practical purposes elastic and can be represented as a polynominal in the strain invariants such as

$$\sigma(t)_{Bulk} = \sum_{k,\ell,=0}^{N_B} A_{k\ell} I_d^{\,k}(t)\, I_\gamma^{\,\ell}(t) \tag{96}$$

The shear term on the other hand is represented as

$$\sigma_{ij}(t)_{Shear} = f(I_d, I_\gamma) \left[\sum_{\ell=1}^{N_S} A_\ell \left(\frac{|I_\gamma|}{||I_\gamma||_{p_\ell}} \right)^{M\ell} E_{ij}(t) \right. \tag{97}$$

$$\left. + \left(1 - \frac{|I_\gamma|}{||I_\gamma||_\infty} \right) \int_0^t G(t'-\xi') \dot{E}_{ij}(\xi) d\xi \right]$$

Where I_d = volume dilatation

I_γ = octahedial shear strain

$$f(I_d, I\gamma) = e^{-kI_d/I_\gamma}$$

ξ, t = chronological and current real time

ξ', t' = chronological and current temperature reduced time

$d\xi' = d\xi/A_T(\xi)$

A_T = time-temperature shift function

$$||I_\gamma||_{P_i} = \left(\int_0^t \frac{|I_\gamma(\xi)|^{P_i} \, d\xi}{A_T(\xi)} \right)^{1/P_i}$$

This equation is fairly simple to use although it appears very complex. It is precisely this type of mathematics that is required to describe propellant response. The details of this equation will be discussed later in this report however it should be pointed out that when the dilatation is zero the equation can simply reduce to that derived and used earlier by Farris. Also when time effects are frozen the equation yields essentially the same types of representations used by Farris in his vacuole dilatation studies. It should also be pointed out that from a numerical point of view the so called L_p norms are much easier to compute than the hereditary convolution integrals appearing in linear viscoelastic relation. Another simplification which is detailed by experimental observations is that the coefficient of the hereditary integral terms is zero for monotonic deformation histories since then $||I_\gamma||_\infty = |I_\gamma|$ which greatly simplifies the constitutive representation for monotonic loading histories.

(c) Characterization Preprogram - NL001

(1) Preprogram Input Requirements

The characterization code, or rather a preprogram to the characterization code, accepts raw experimental data in a very simplified format. This format is very effective and will probably need little modification. This discussion describes the current input format to the characterization preprogram.

The first card for raw data input into the program is a header card and contains the following:

· An alpha-numerical name identifying each separate experiment as a distinct element or block of information that can be retrieved by this name.

· A code to identify the type of experiment

1 = uniaxial

2 = strip biaxial

3 = shear

· The value of the constant superimposed pressure for multiaxial variations of the above experiments

· A code to indicate whether the experiment is a constant or variable temperature experiment.

· An identification element to indicate the propellant type, batch number, etc.

Following this card the preprogram then accepts a description of the response in tabular form as indicated in the format below.

N TEMP(N) $\Delta t(N)$ $\dot{E}(N)$ $\sigma(N)$ $I_d(N)$ Flag

In the above format the terms have the following definitions.

N = Nth data point for this experiment

TEMP(N) = Temperature of sample for this data point. The values are constant except in time varying temperature experiments.

$\Delta t(N)$ = The time interval between data point N and N-1, $\Delta t(N) = t(N)-t(N-1)$. This procedure greatly simplifies data reduction from raw graphical recordings.

$\dot{E}(N)$ = The primary forced strain rate, (shear, uniaxial, or biaxial), between data points N and N-1 based on the small strain measure. This feature also greatly simplifies data reduction since

$$\Delta E(N) = \Delta t(N) \times \dot{E}(N) \text{ and}$$

$$E(N) = \sum_{M=1}^{N} \Delta t(M) \times \dot{E}(M)$$

$\sigma(N)$ = Observed forced stress (uniaxial, biaxial or shear) based on original area at time t(N)

$I_d(N)$ = The measured total volumetric increase, $\Delta V/V_o$, at time t(N)

Flag = 0 if additional data follow

= 1 if this is the last point for the experiment

For future work this format will probably require little or no modification except perhaps an additional flag to indicate the data is acceptable for failure characterization, (i.e., good or premature failure due to end bonding). From the above information, true stress and any strain measure can be computed with ease. The strain measure used above is the normal infinitesimal strain theory

$$E_{ij} = \frac{1}{2}\left(\frac{\partial u_i}{\partial X_j} + \frac{\partial u_j}{\partial X_i}\right) \tag{98}$$

(2) Preprogram Calculations

Following the raw data input to the preprogram an additional card is read in for each propellant. This card contains the following information:

- Bulk modulus
- Volumetric thermal expansion coefficient

The preprogram then corrects the input data for compressibility and thermal contraction at the start of the experiment. These calculations are necessary since (1) samples are prepared and measured at room temperature and change slightly in dimension with temperature, and (2) the gas dilatometer only measures the volume change from initial experimentation conditions and does not measure the small contraction due to pressurization in multiaxial experiments. After correcting the initial conditions the preprogram then calculates for each data point.

- Total time
- The nonzero elements of the strain and strain rate tensors according to some predefined measure. Currently the code uses the Green strain tensor.

$$E_{ij} = \frac{1}{2}\left(\frac{\partial u_i}{\partial X_j} + \frac{\partial u_j}{\partial X_i} + \frac{\partial u_k}{\partial X_i}\frac{\partial u_k}{\partial X_j}\right) \tag{99}$$

- The values of the true stress for the known stresses.
- The invariants of the strain tensor.
- The values of $||I_\gamma||_{10}$, $||I_\gamma||_{20}$, $||I_\gamma||_{30}$, $||I_\gamma||_{40}$, $||I_\gamma||_{50}$, $||I_\gamma||_{60}$ and $||I_\gamma||_\infty$ which are selected values of the pth order Lebesque norms of theoctahedral strain invariant based on real time

$$||I_\gamma||_p = \left(\int_0^t |I_\gamma(\xi)|^p d\xi\right)^{1/p} \tag{100}$$

These latter calculations are only performed for constant temperature experiments since the factor $A_T^{-1/p}$ can be taken out as a constant factor.

(3) Data Storage

As these calculations are made, they, along with the original raw data input are stored on tape by the element name. The value of the preprogram is that it performs calculations that need to be made only once. It transforms the raw data into something useful in constitutive characterization and also corrects the initial conditions. The preprogram tape can then be used as a permanent record of the data and is also used as input to the characterization code. This preprogram has already been of considerable value and has already permitted Aerojet to supply other researchers with tabulations of experimental data on which to test their viscoelastic theories. By maintaining these tapes, updated characterizations can be made as the constitutive relations are updated. Copies of the data obtained on this program can and will be made available to other researchers.

(d) Characterization Code - NL002

(1) Description of Method

The characterization code developed on the AFRPL contract is in principle applicable to any constitutive equation with only minor modifications. The discussion below describes the method for a general nonlinear single integral representation wherein the constitutive nonlinearity is stored in the kernels which are functionals rather than functions. This type of equation contains the representations of Farris and Schapery and a great many other types of viscoelastic relations and can be written as

$$\sigma_{ij}(t) = \delta_{ij}\,\sigma^{(B)}_{(t)} + \sigma_{ij}^{(S)}(t) \tag{101}$$

Where the superscript (B) stands for bulk and the superscript (S) stands for shear. The bulk and shear components of stress are defined as Follows:

$$\sigma^{(B)}(t) = \int_0^t K_1[I_1(\xi'),\ I_2(\xi'),\ I_3(\xi'),\ t'-\tau']\ \dot{I}_1(\tau)\,d\tau \tag{102}$$

$$\xi'=0 \qquad \xi'=0 \qquad \xi'=0$$

and

$$\sigma_{ij}^{(S)}(t) = \int_0^t K_2[I_1(\xi),\ I_2(\xi),\ I_3(\xi'),\ t'-\tau')]\,\dot{E}_{ij}(\tau)\,d\tau \tag{103}$$

$$\xi'=0 \qquad \xi'=0 \qquad \xi'=0$$

In the above representations τ' and ξ' are the generic values of the temperature reduced time, t' is the current value of the temperature reduced time, and t and τ are the current and generic values of the real time I_1, I_2, and I_3 are the three invariants of the strain tensor.

Using the experimental data from the preprogram as input together with the input time-temperature shift function the stresses, $\sigma_{ij}^{(S)}$ and $\sigma^{(B)}$, could be calculated if the kernel functions were defined, since the complete strain tensor and temperature history are known for each experiment. Since the form of the kernels are unknown the problem then is to determine their form by comparing calculated values of stress state with the experimentally observed values stored in the preprogram. This determination can best be accomplished for common experiments, such as uniaxial, biaxial, shear, and multiaxial versions of these experiments, by manipulating the equations to solve for $\sigma_{ij}^{(S)}$ and $\sigma^{(B)}$directly in terms of known stresses. Care must be used in setting up such procedures since there are unknowns such as σ_{33} in biaxial tests. The easiest procedure to use is to calculate distortional stresses, $\sigma_{11} - \sigma_{22}$ for uniaxial and biaxial tests since σ_{22} is at most a known constant pressure for their multiaxial versions. This subtraction process eliminates the common bulk term in each equation. Shear tests are already pure distortion and need no manipulation. The characterization code has therefore been programed to define the following for every experimentally input data point

$$\sigma_{(t)}^{(D)} = \begin{cases} \sigma_{11}(t)-\sigma_{22}(t) & \text{uniaxial or biaxial} \\ \sigma_{12}(t) & \text{shear} \end{cases} \tag{104}$$

$$\dot{E}(t)^{(D)} = \begin{cases} \dot{E}_{11}(t)-\dot{E}_{22}(t) & \text{uniaxial or biaxial} \\ \dot{E}_{12}(t) & \text{shear} \end{cases} \tag{105}$$

and the equation for the distortional stress, $\sigma^{(D)}$, becomes

$$\sigma(t)^{(D)} = \int_0^t K_2[I_1(\xi')\uparrow_{\xi'=0}^{t'}, I_2(\xi')\uparrow_{\xi'=0}^{t'}, I_3(\xi')\uparrow_{\xi'=0}^{t'}, t'-\tau'] \dot{E}^{(D)}(\tau)d\tau \qquad (106)$$

Having resolved the problem of determining two kernel functionals simultaneously the problem is now greatly simplified. The form of the kernel functional, K_2, is determined by expanding it in a representation selected by the characterization code user, thereby making the method quite general. To demonstrate the method consider the not too simple example of linear viscoelasticity using a Prony series expansion which results in

$$K_2[I_1(\xi')_{\xi'=0}^{t'}, I_2(\xi')_{\xi'=0}^{t'}, I_3(\xi')_{\xi'=0}^{t'}, t'-\tau'] = K_2[t'-\tau'] = \sum_{i=1}^{N} A_i e^{-\beta_i(t'-\tau')} \qquad (107)$$

In this type of procedure a family of ten to twenty β_i are selected, usually about one decade apart in time to cover the range of relaxation times, and the coefficients A_i are determined. In almost all currently used techniques these coefficients are determined by a simple collocation technique using a number of points from an already shifted relaxation modulus curve. In the computerized method these coefficients are determined from hundreds to thousands of data points from arbitrary stress-strain histories using an error minimization technique rather than a simple collocation method. For the case described above the constitutive equation for $\sigma^{(D)}$ reduced to

$$\sigma^{(D)}(t) = \sum_{i=1}^{N} A_i \int_0^t e^{-\beta_i(t'-\tau')} \dot{E}^{(D)}(\tau)d\tau = \sum_{i=1}^{N} A_i X_i(t) \qquad (108)$$

In the above equation the $X_i(t)$ can be calculated from every data point in the preprogram using the known deformation-temperature-time histories. Since the values of $\sigma^{(D)}(t)$ are also known for each of these data points the problem then is to determine the best values of A_i by some error minimization technique. Different methods of error minimization are discussed in the following section.

Having determined the values of A_i the computer then calculates the average value of $\sigma^{(B)}(t)$ using the original stress-strain equation since $\sigma_{11}^{(S)}(t)$ and $\sigma_{22}^{(S)}(t)$ can now be calculated.

$$\sigma^{(B)}(t) = \frac{\sigma_{11}(t) + \sigma_{22}(t) - \sigma_{11}^{(S)}(t) - \sigma_{22}^{(S)}(t)}{2} \tag{109}$$

Expanding the bulk kernel function, K_1, in a Prony series results in

$$\sigma^{(B)}(t) = \sum_{i=1}^{N} B_i \int_0^t e^{-\alpha_i(t'-\tau')} \dot{I}_1(\tau) d\tau = \sum_{i=1}^{N} B_i Y_i(t) \tag{110}$$

Here again the computer calculates the values of $Y_i(t)$ for every data point and using the already calculated values of $\sigma^{(B)}(t)$ in another error minimization scheme the values of the coefficients B_i are determined.

The code then calculates and compares stress data with known values such as σ_{11}, σ_{22}, $\sigma_{11} - \sigma_{22}$, and σ_{12}, and presents the data in tabular form with the error for each calculation. Also calculated are values of unknown stress such as σ_{33} for biaxial conditions and the percentage contribution of each term in the series. Terms having negligible contributions can be dropped simplifying the representation.

For nonlinear applications the method is identical except more complex expansions are used for the kernel functionals. For the Farris-Schapery equation discussed earlier the expansion for the distortional kernel would have the following form.

$$K_2 = \left(e^{-BI_d / I_\gamma}\right) \left[\sum_{i=1}^{m} A_i \left(\frac{|I_\gamma|}{||I_\gamma||_{p_i}} \right)^{n_i} + \left(1 - \frac{|I_\gamma|}{||I_\gamma||_{\infty}} \right) \sum_{m+1}^{M} A_i e^{-\beta_i(t'-\tau')} \right] \tag{111}$$

Besides picking a family of Prony series exponents β_i, a family of P_i and n_i as well as a value of B would also have to be pre-selected. Generally, 2 to 5 pairs of $\langle P_i, n_i \rangle$ are sufficient to characterize a propellant and the selection is not very critical so long as a range is bracketed. Terms having small contributions in any of these characterization can be discarded from subsequent runs.

Typical run times for this type of characterization on the Univac 1108 are about 1 minute for 400 data points. One run with over 2000 data points and 200 pages of output was just over 4 minutes. Prime time on the Univac 1108 runs about eight dollars per minute.

(2) Error Minimization

The method used in the AFRPL and Navy characterization codes to determine the linear coefficients appearing in the constitutive equation is a modified "least squares" regression method.[2] Standard regression methods reduce the absolute error between predicted and input data and give much higher weighting to large numbers. When this method is used to describe mechanical response data for viscoelastic materials over broad ranges of test conditions the high stress values are always predicted quite accurately whereas the low stress values are greatly in error. This problem was eliminated by defining a relative error which is simply a normalized weighted absolute error where the weighting factor is the observed stress. This type of error definition forces the least squares method to try and fit every data point to the same percentage accuracy no matter how large or small the observed stress magnitude.

Defining $\bar{\sigma}^{(D)}(N,L)$ as the measured or observed value and $\sigma^{(D)}(N,L)$ as the calculated value of stress for the Nth data point of the Lth experiment the absolute and relative errors for the least squares techniques have the following definitions.

$$\text{Abs Error} = \sum_{N=1}^{N_\ell} \sum_{L=1}^{L'} \left(\bar{\sigma}^{(D)}(N,L) - \sigma^{(D)}(N,L) \right)^2 \qquad (112)$$

$$\text{Rel Error} = \sum_{N=1}^{N_\ell} \sum_{L=1}^{L'} \left(1 - \frac{\sigma^{(D)}(N,L)}{\bar{\sigma}^{(D)}(N,L)} \right)^2$$

In the above equation N_ℓ is the number of data points in the Lth test and L' is the total number of tests.

Recalling that $\sigma^{(D)}$ was expanded in a simple function $\sigma^{(D)} = \sum_{i=1}^{M} A_i X_i$, this expansion can be substituted into the equation for relative error to produce

$$\text{Rel Error} = \sum_{L=1}^{L'} \sum_{N=1}^{N_\ell} \left(1 - \frac{\sum_{i=1}^{M} A_i X_i(N,L)}{\bar{\sigma}^{(D)}(N,L)} \right)^2 \qquad (113)$$

The method of least squares determines the coefficients such that the measure of error is an absolute minimum. It can be simply shown that the error is an absolute minimum when the following condition is met.

$$\frac{\partial \text{Error}}{\partial A_i} = 0 \qquad i = 1, 2, \ldots, M \qquad (114)$$

When the partial differentiation and all of the summations are carried out what remains is a linear system of M equations in which there are M unknowns, $A_1, A_2 \ldots A_M$. This system of equations can be solved using standard methods to determine the values of A_k that best fit the data. This method of relative error minimization is used in the current AFRPL characterization code. It is an excellent method and includes material variability and other types of variability along with constitutive errors in approximating the real behavior. This method is very easy to handle analytically since it results in a linear system of equations to solve.

(3) Refined Coding and Numerical Integration Procedures

The constitutive equation characterization code is an extremely versatile procedure and requires a considerable amount of computer storage. Prior to using the preprogram, it was not difficult to overflow the complete core storage of the Univac 1108 computer with a run that was not excessively large. This overflow was caused by retaining calculated information that was needed later in the procedure so as not to have to recalculate or reread this information again. The preprogram and the use of external storage, fastran drum storage, during the characterization process bypassed this storage requirement and still permitted storage of information needed later in the code. Actually even on a small computer without external storage the code can be developed to handle an unlimited number of data points by retaining only critical information and recalculating quantities as they are needed. This type of code requires an excess of computation and input.

By streamlining the preprogram and the characterization program even further than has been done to date an efficient package can be obtained that would require less storage and considerably less external read and write statements. It is in this area that perhaps the maximum improvements in the users package can be made since much of the computer time is consumed in data manipulations, tape reads and writes, fastran drum storage reads and writes, matrix generation and equation solving, plus computing and comparing stress data. The current method of processing the data is one experiment at a time. It would appear that if the maximum number of data points per experiment and the number of terms in the constitutive equation were limited then blocks of experiments could

be processed simultaneously eliminating many external out of core read and write statements. During the follow-on effort the logic and methods of data manipulation and storage will be critically evaluated and streamlined as much as possible.

One other area where refined coding could be of great value is in the error minimization procedure. Currently a "least squares" method is used because it renders a linear system of equations which are easy to solve. There are other measures of error that are better suited to the needs of constitutive theories, however, they are generally difficult to handle numerically. By way of example the "least squares" method described earlier is giving an averaging type fit to the data trying to minimize the sum of the squares of the deviations from this average value. When these "least squares" constitutive equations are used in structural analyses they will predict "average" stresses. It would seem desirable to have a conservative structural analyses which yielded the highest possible stresses that could be expected. A conservative analyses could be obtained if an error measure reflecting this feature could be used in the characterization code. Also, sometimes it is desirable to have all positive or all negative linear coefficients from an analysis whereas with the least squares method no control over the sign of the coefficients is possible. There exist linear and nonlinear programming approaches to problems of this type and they should be briefly studied and employed if applicable in future codes. These features are more or less the "frosting on the cake" since the existing computerized characterization method is an order of magnitude improvement over existing methods, nevertheless improvements of this type are desirable and would yield a better code.

Also of importance are the numerical integration schemes used for the L_p norms, reduced times, and the hereditary integrals. To some extent the procedures currently being used have been made quite efficient. Computation time for the code is little influenced by types of integration procedures employed since it actually is a small part of the total code. The one area where improved integration procedures could be used is in the cases of transient thermal calculations where higher order quadrature techniques would be valuable. These methods require calculations of the integrand at intermediate points. Since the integrand is only known for the discrete set of input points considerable interpolation is required to use the quadrature methods, however the improved accuracy would possibly justify its' use.

(e) Characterization Code - NL003

This code is identical to characterization code NL002 in all respects up to the calculation of the bulk term, $\sigma^{(B)}(t)$. Then instead of expanding the bulk stress $\sigma^{(B)}(t)$ in terms of the strain invariants, the dilatation is taken as the dependent variable and is expressed in an expansion of the form

$$I_d(t) = \sum_{k,j=1}^{N} \beta_{kl} \left(\sigma^{(B)}\right)^k \left(I_\gamma\right)^j \qquad (115)$$

It is interesting to note that much better fits using fewer terms can be obtained simply by changing the order of dependence. Part of the reason for this is that the dilatation is generally always changing with strain whereas the bulk stress usually starts at one value and approaches some other constant value. Also the bulk stress changes most when the dilatation is very small and difficult to measure causing large amounts of scatter in representations of the form given in NL002. When the dilatation is made the dependent variable the error in this type of regression analyses produces much less scatter. These effects have often times been confusing and hard to explain, nevertheless it has been repeatedly observed that a twenty term expansion for $\sigma^{(B)}(t)$ in NL002 will produce very poor results, yet a four term expansion of the same form with the dilation as the dependent variable produces excellent results. Analytically this is difficult to explain yet these results frequently occur. For this reason much of the data reported later are calculated using NL003.

(f) Post Processor Code

The post processor code is simply a code that provides a listing of the data computed by NL001 which is stored on tape. Selected information from the tape files are printed under properly labeled headings with additional information such as a test description. This code was generated for reporting of experimental data such as those included in the appendix.

(g) Common Subroutine Programs

Most of the characterization codes used on this contract have common subroutines for matrix inversion and printing. These sub-programs are included in the appendices to offer a complete package to those interested in using or improving these codes.

(h) A Characterization Code for Linear Viscoelasticity

Early in this contract a computerized characterization code was developed for linear viscoelastic materials having constant bulk modulus and time dependent shear behavior. This code provided the framework for the nonlinear characterization code. A listing of this code and example fits of propellant data and solithane 113 rubber are included in the appendices. The purpose of including this information on linear viscoelasticity in this report is that it is hoped that researchers will use this code and observe for themselves the deficiencies of linear theory as applied to propellants. Also this code could be greatly useful to those studying the gage-grain interaction problem on instrumented motors since they commonly interpret the gage output in terms of a convolution integral identical in form to that used in linear viscoelasticity. Since this code can provide the kernel function appearing in the integral relationships for arbitrary input histories, it could no doubt increase accuracy and simplify an otherwise complicated problem of gage output interpretation.

(4) A Working Three Dimensional Stress-Strain Law for Composite Propellants

At the start of this program an abundance of experimental and theoretical data existed to help guide the formulation of a three dimensional constitutive equation of state for propellant materials. Many parts of the problem had in effect already been identified and successfully modeled. Each part of the problem had been treated separately and never combined with another part of the apparent solution. For example dilatational effects had been modeled in the absence of time effects[7] and time effects had been modeled in the absence of dilatational effects,[1] etc. The problem then was to put together the pieces of the puzzle that already existed and to fill in the remaining pieces. To accomplish this goal considerable experimental effort was required. A large part of this program effort has been spent on obtaining experimental data of a type never really generated before and developing techniques to handle the data to test the theoretical developments. The experimental objectives and methods have already been discussed as have the computerized methods of data analyses. This portion of the report deals with the theoretical efforts to obtain a good working three dimensional constitutive theory for propellant materials. Much of the theoretical work for this contract was done in the proposal stage. The types of experimental data and required methods of analyses were therefore already defined at the start of the contract and it was not until the data was obtained and the methods of analyses were available that the theoretical assumptions could be really tested. Before proceeding with the actual stress-strain equation development some discussion of constitutive assumptions is in order since any constitutive theory is based on assumptions or facts.

(a) Constitutive Assumptions

(1) Isotropy

Propellants are almost without exception isotropic or at least originally isotropic materials. It is true that due to flow patterns in casting the propellant some particulate orientation is observed causing anisotropic stiffness and burning characteristics. These effects are normally small, 10 to 20%, and are impossible to characterize since these flow patterns are not predictable and no uniform axis of particulate orientation exists. The assumption of treating normal composite propellants as isotropic materials is a good assumption and the only practical one available.

(2) Homogeneity

Composite propellants are homogeneous materials on a coarse scale. Essentially no predictable spatial variation in properties are observable other than in motors requiring several separate batches to fill the chamber and then batch-to-batch properties variation can be important. Generally speaking this type of nonhomogeneity is rarely treated even with elastic analyses and is of no concern to this immediate contract since each batch could be separately characterized and the burden is on the stress analyst to accurately model the structure. About the only exceptions to the homogeneity condition within a batch of propellant would be due to soft-center cures or incomplete cures which would represent a propellant problem, and aging effects such as skin hardening due to loss of volatiles or oxidative crosslinking. These later effects are aging effects and are not a part of this contract.

On a microscopic scale propellants are far from homogeneous materials and would closely resemble soils, masonry materials such as cement-aggregate mixtures, asphalt-aggrate mixtures, and other composite materials. On a scale several times the largest particles in the system a material can be treated as homogeneous so long as no concern is given to local stress oscillations around particles making up what might be termed a repeatable cell of material. In this sense all materials are nonhomogeneous and its just that some materials are more finely subdividable than others. Discussing stress concentrations at crack tips approaching very small radii of curvature is meaningless in materials having a very coarse microstructure since such small curvatures cannot exist. Propellants therefore are homogeneous materials and can be treated using continuuim methods so long as stresses and strains are averaged over elements that are coarse compared to the materials microstructural dimensions. Much of the information regarding propellant stress-strain response has been obtained by analyzing and modeling the behavior within the microstructural nonhomogeneities and averaging them to obtain gross continuum behavior.

(3) Elasticity

The concept of elasticity is a key assumption in material behavior. Propellants are known to suffer from plasticity type effects due to microstructural breakdown and reformation[37] better known as polymer chain cleavage and chain formation, however, these are by and large aging effects. Propellants are for the most part initially elastic materials since they consist of an amorphous crosslinked rubber which comprises the binding matrix for the filler particles. It should be pointed out that of all the assumptions made the elasticity assumption is by far the poorest and the least verified. Large plasticity effects can and do occur in propellant materials with little or no apparent change in response properties. This can occur with equal rates of chain scission and reformation. The chemists formulating propellants are in part directly or indirectly responsible for much of the plasticity effects occurring in propellants since they tend to counteract hardening reactions by incorporating decomposition mechanisms and similarly they counteract chemical breakdown with build-in hardening reactions. In effect they try to balance these effects so that no effective change in polymer crosslink density occurs with storage time. An innocent observer would tend to say that no aging is occurring since the properties tend to remain unchanged with time if the chemist balanced hardening and softening reaction rates. In truth, however, the material is constantly relieving itself of stress by breaking chains which are recombining stress free. At first this might be thought of as a desirable feature, however relieving compressive stresses at high temperatures adds to the tensile stresses during subsequent cooldown and visa-versa. Naturally the chemist is not solely responsible for such actions since there are natural exchange reactions occurring within many polymers such as polysulfides[37]. This is an aging problem and is not dealt with on this contract, however, for many motor systems with limited temperature exposure this effect probably introduces more error in a stress analysis than any nonlinear viscoelastic effects.

(4) Memory Characteristics

Most of the work associated with nonlinear viscoelastic material behavior has dealt solely with fading memory viscoelastic representations. There are various mathematical definitions of fading memory but in essence they all imply no change in response characteristics due to prior deformation after a period of recovery. A physical interpretation of fading memory behavior would imply no permanent changes in microstructure such as those caused by the Mullins' effect or vacuole dilatation. Propellants obviously do not fall into the category of fading memory materials since time and history effects caused by phenomena other than internal viscosities govern much of their behavior. In order to represent the behavior of this type of material mathematical representations having permanent memory registers are required and their development has been the main emphasis of Farris' research over the past 5 years.

(5) Thermorheological Simplicity

A thermorheologically simple material is a material wherein all of the thermal effects can be included in the form of a reduced time which depends upon temperature history. The usual definition of this reduced time is

$$t' = \int_0^t d\xi/A_T(\xi) \tag{116}$$

where A_T is a temperature dependent function, or equivalently

$$dt' = d\xi/A_T(\xi) \tag{117}$$

For linear viscoelastic materials it means that the relaxation moduli which are both time and temperature dependent, $E(T,t)$, can be represented as

$$E(T,t) = E(T_o,t') \tag{118}$$

In other words all of the temperature dependence can be accounted for in a temperature reduced time which is equal to real time at some temperature T_o which can be choosen arbitrarily. This type of behavior has been used on propellants for many years using linear viscoelastic analyses methods and data taken on this program supports these past observations.

(6) Valid Measures of Strain

There are many commonly used measures of strain which satisfy the requirements of continuum analyses. Because of the large strains being seen on this program the measure of strain used in the constitutive representation was the green strain tensor defined as

$$E_{ij} = 1/2\ (u_{i,j} + u_{j,i} + u_{k,i}u_{k,j}) \tag{119}$$

In terms of its' principle values, (E_1, E_2, E_3) the green strain tensor is related to the principle extension ratios used by Rivlin as follows

$$1 + 2E_1 = \lambda_1^2 = (1 + \partial u_1/\partial x_1)^2 \tag{120}$$

$$1 + 2E_2 = \lambda_2^2 = (1 + \partial u_2/\partial x_2)^2$$

$$1 + 2E_3 = \lambda_3^2 = (1 + \partial u_3/\partial x_3)^2$$

Similarly it can be simply shown that

$$(v/v_o) = \lambda_1\lambda_2\lambda_3 = \sqrt{(1 + 2E_1)(1 + 2E_2)(1 + 2E_3)} \tag{121}$$

The main reason this strain tensor was used is that the measure of dilatation is exact and consequently the measure conserves mass, a feature lacking with the usual small strain theory.

The usual definitions of the strain invariants has been used which in terms of principle directions is given as

$$I_1 = E_1 + E_2 + E_3 \tag{122}$$

$$I_2 = E_1E_2 + E_2E_3 + E_3E_1$$

$$I_3 = E_1E_2E_3$$

In addition the deviatoric invariants have been used where the deviatoric strain has been defined as

$$E'_{ij} = E_{ij} - \delta_{ij}I_1/3 \tag{123}$$

Hence the deviatoric invariants in terms of the principle values become

$$I'_1 = 0 \tag{124}$$

$$I'_2 = E'_1E'_2 + E'_2E'_3 + E'_3E'_1$$

$$I'_3 = E'_1E'_2E'_3$$

The octahedral shearing strain defined here as I_γ then becomes

$$I_\gamma = \frac{1}{3}\sqrt{(E_1-E_2)^2 + (E_2-E_3)^2 + (E_3-E_1)^2}^{1/2} \quad (125)$$

or

$$I_\gamma = \frac{1}{3}\left(2I_1^2-6I_2\right)^{1/2} \quad (126)$$

Similarly the deviatoric invariant I_2' can be expressed as

$$I_2' = I_2-I_1^2/3 = -\frac{3}{2}I_\gamma^2 \quad (127)$$

Since the invariant I_1 is not the dilatation as it is in infinitesimal theory, and the volumetric dilatation is a very important parameter in propellant constitutive theory, the dilatation has been defined as I_d and this is an invariant quantity that can be expressed in terms of other invariants as

$$I_d = \Delta V/V_o = (1 + 2I_1 + 4I_2 + 8I_3)^{1/2}-1 \quad (128)$$

This measure of strain is quite simple to use with the expermintal data obtained on uniaxial and biaxial tests since the principle directions are those of the experiment. Also the measure of strain is objective and provides a simple measure of actual volume change. This measure of strain has been used exclusively throughout this contract and has shown good results. In practice any measure of strain can be just as easily used as the Lagrangian measure, however, care should be taken to assure that an exact measure of dilatation is used. In future work the small strain theory will probably be used to preserve a one-to-one relationship with conventional methods of analyses and laboratory measurements. An exact measure of dilatation can be derived using small strain theory simply by retaining the higher order effects dropped from linear theory. The small strain exact measure of dilatation then becomes

$$I_d = \Delta V/V_o = I_1 + I_2 + I_3 \quad (129)$$

Where I_1, I_2, and I_3 are as defined above with the exception that the strains are the conventional small strain measure instead of the Lagrangian measure.

(b) Distortional Stress Strain Relationships

The stress-strain equations developed on this contract were developed in the usual manner of dividing the response into a distortional and a bulk contribution. In this sense the stress and strain states can be expressed as

$$\sigma_{ij} = \delta_{ij}\frac{\sigma_{kk}}{3} + \sigma'_{ij} \tag{130a}$$

$$E_{ij} = \delta_{ij}\frac{I_1}{3} + E'_{ij} \tag{130b}$$

The σ_{ij} and E_{ij} are the stress and strain tensors as related to the undeformed coordinates, $\sigma_{kk}/3$ is a mean pressure, $I_1/3$ is one third the first strain invariant, and σ_{ij}' and E_{ij}' are the distortional stress and strain tensors. In classical isotropic linear elasticity one has the simplifying relations

$$\sigma_{ij}' = 2GE_{ij}' \tag{131a}$$

$$\sigma_{kk} = (3\lambda + 2G)I_1 \tag{131b}$$

where

G = Shear modulus

λ = a bulk modulus

The same situation holds for isotropic linear viscoelasticity except that the moduli are time dependent and the stresses and strains are related by simple integral relations of the form

$$\sigma'_{ij}(t) = 2\int_0^t G(t-\xi)\dot{E}'_{ij}(\xi)\,d\xi \tag{132a}$$

$$\sigma_{kk}(t) = \int_0^t \left(3\lambda(t-\xi)+2G(t-\xi)\right)\dot{I}_1(\xi)\,d\xi \tag{132b}$$

Naturally in isotropic nonlinear viscoelastic relations the distortional and bulk contributions can be separated and the discussion below deals with just the distortional stress - distortional strain behavior.

(1) Prior Work

A great majority of the nonlinearites in the distortional stress-strain behavior of propellants has already been successfully modeled. Much of this work has already been presented in the first part of the technical discussion under the topic of Immediate Objectives. The earlier

work of Farris[7] on modeling the influence of dilatation, I_d, on the stress-strain behavior was quite successful. It produced a simple but quite effective unaxial stress-strain law of the form

$$\sigma = A_1\varepsilon - A_2 I_d \approx A_1\varepsilon \exp(-A_2 I_d / A_1\varepsilon) \tag{133}$$

This simple equation said nothing about the bulk behavior or time or history effects, nevertheless it did perform well for "Pressurized Uniaxial" experiments over a broad range of temperatures and strain rates over the entire range of strains to failure. This equation was derived from microstructural models relating instantaneous moduli to the vacuole dilatation state.

Farris later modeled the time and history dependent behavior of propellants in terms of a time dependent failing microstructure for constant volume conditions[1,9]. This later work yielded a simple stress-strain relation of the form

$$\sigma'_{ij}(t) = A_1 E'_{ij} + A_2 \left(\frac{I_\gamma}{||I_\gamma||_{P_1}}\right)^{M_1} E'_{ij} + \int_0^t A_3(t-\xi)\dot{E}'_{ij}(\xi)\,d\xi$$

$$+ \left(\frac{I_\gamma}{||I_\gamma||_{P_4}}\right)^{M_4} \int_0^t A_4(t-\xi)\,\dot{E}'_{ij}(\xi)\,d\xi \tag{134}$$

In the above equation I_γ is the octahedral shear strain, A_1 and A_2 are constant moduli while A_3 and A_4 are time dependent moduli. The first term in the equation represents linear elastic effects, the second represents irreversible time effects, the third represents reversible time effects, and the fourth is an interaction term. This equation has shown excellent results in predicting the distortional stress response to very complex deformation histories using uniaxial and biaxial data. Temperature effects were tested experimentally and it was found valid to include thermal effects by the standard method of a time-temperature equivalence. This modified equation predicted accurately over very broad ranges of temperatures including complex stress response to time varying temperature-deformation histories. This latter equation has been successfully programed assuming linear elastic bulk response to obtain a working two-dimensional nonlinear transient thermoviscoelastic finite element stress code.

In both of these approaches no apparent requirement for second order nonlinearities of any type were required such as reversible nonlinear effects. It should be pointed out that both equation 133 and equation 134 are of order one or better said, mathematically homogeneous to degree one in strain. This is a property shared by linear materials in that doubling the deformation tensor doubles the stresses. These equations are not linear and predict quite nonlinear stress-strain-time response. They are the simplest form of nonlinear behavior since at least one of the rules of linearity is satisfied by these equations. The concept of mathematically homogeneous constitutive equations has helped shed considerable light on propellant behavior and the types of mathematics required to describe the response

(2) A General Distortional Representation

Since the previous work had been successful in modeling and describing propellant response for specific restrictive deformation conditions, the first main emphasis on this contract was to develop mathematical representations that would include both of the previously cited effects, namely distortional softening and irreversible time effects. In terms of an isotropic distortional stress-strain law the simplest of all possible equations containing each of the previous models was found to be

$$\sigma'_{ij}(t) = f_1(I_i)\left\{A_1 E'_{ij}(t) + A_2\left(\frac{|f_2(I_i)|}{||f_2(I_i)||_{p_\gamma}}\right)^{M_1} E'_{ij}(t)\right.$$

$$\left. + \int_0^t A_3(t-\xi)\dot{E}'_{ij}(\xi)d\xi + \left(\frac{|f_2(I_i)|}{||f_2(I_i)||_{p_4}}\right)^{M_4} \int_0^t A_4(t-\xi)\dot{E}'_{ij}(\xi)d\xi\right\} \qquad (135)$$

In the above equation f_1 and f_2 are functions of the strain invariants I_1, I_2, and I_3.

This type of equation and many variations of it were examined theoretically and tested against very complex experiments. Most of the forms selected worked very well for states of zero superimposed pressure. At small strains, however, these equations did not handle were data taken under pressurized conditions, since pressure caused non-zero invariant values which accumulated in the Lp norm registers predicting hysteresis effects on the first pull stress-strain behavior. Furthermore this hysteresis was dependent upon how long the sample was under pressure prior to pulling. Experimentally hysteresis is not observable on first pull pressurized experiments, even for samples stored a fair time under pressure prior to pulling. Also no change in modulus with pressure is observable experimentally prior to vacuole dilatation. To eliminate the effects being observed in the mathematics meant simply that the function, f_2 (I_1, I_2, I_3), must vanish for pure hydrostatic conditions. Obviously the simplest of all possible functions is that f_2 must be a function of the octahedial shear strain,

I_γ, which vanishes when the principle strains are equal, which for isotropic materials is only possible with hydrostatic pressure or hydrostatic tension conditions. Careful analytical examination indicates any homogeneous function of I_γ would produce the same effect in the equation. This can be simply shown using the properties of L_p norms. Consider the function f_2 to be given by

$$f_2 = CI_\gamma^m \qquad C, m = \text{constants} \tag{136}$$

Then from the definition of an L_p norm we have

$$||CI_\gamma^m||_p = |C| \cdot ||I_\gamma^m||_p \tag{137}$$

and

$$||I_\gamma^m||_p = \left(||I_\gamma||_{mp} \right)^m$$

Since the terms containing the function f_2 in the constitutive equation have the form

$$\left(\frac{|f_2|}{||f_2||_p} \right) \tag{138}$$

where p and n are arbitrary constants, substituting equation (136) into this term and using the properties of L_p norms and the fact that I_γ is always positive yields

$$\left(\frac{|f_2|}{||f_2||_p} \right)^n = \left[\frac{|CI_\gamma^m|}{||CI_\gamma^m||_p} \right]^n = \left[\frac{|C| \cdot |I_\gamma|^m}{|C| \cdot (||I_\gamma||_{mp})^m} \right]^n = \left(\frac{|I_\gamma|}{||I_\gamma||_{mp}} \right)^{n \cdot m} \tag{139}$$

It is apparent from this simple proof that the constant C has no effect and the exponent m has no real effect since it simply changes the values of n and p which were already stated as being arbitrary. Any form different from the one given for f_2 will destroy the homogeneity of the equation in strain. Since it has been shown that all possible forms for f_2 preserving homogeneity are equivalent, the simplest form has been selected and that is

$$f_2 = I_\gamma \tag{140}$$

The only other factor that needed more work was the function f_1. Going back to earlier work described by Farris and reanalyzing the data in the form of a simplified three dimensional equation it became apparent that again any homogeneous function of degree zero would work as a modulus multiplier. In the simple one dimensional studies the term $\exp(-\beta I_d/\varepsilon)$ was used. Actually any exponentials involving the ratios of I_d to powers of any other invariant would function quite well on simple tests like uniaxial or biaxial. However the only invariant quantity that is non-zero (to eliminate division by zero) for distortion is again the octahedral shear strain. To assure ourselves then that the equation would be well behaved for all possible states of strain the following representation was selected.

$$\sigma'_{ij}(t) = e^{-BI_d/I_\gamma}\left\{A_1 E'_{ij}(t) + A_2\left(\frac{I_\gamma}{|I_\gamma|_{P_2}}\right)^{m_2} E'_{ij}(t) + \int_0^t A_3(t-\xi)\,\dot{E}'_{ij}(\xi)d\xi + \left(\frac{I_\gamma}{|I_\gamma|_{P_4}}\right)^{m_4} \int_0^t A_4(t-\xi)\,\dot{E}'_{ij}(\xi)d\xi\right\} \tag{141}$$

This type of equation was tested and studied. It does a good job of fitting the isothermal distortional stress-strain behavior for complex deformation histories using pressurized uniaxial and pressurized biaxial experiments. It was also found and experimentally verified that the concept of a time-temperature equivalence was applicable. The experimental verification was established by straining the material at high temperatures and holding it at constant strain while slowly cooling from high to very low temperatures. Analytically this is a means of freezing time and since the strain is constant no stress variation is permissible in a thermorheologically simple equation of state. These observations were born out experimentally in that only small stress variations were measured and those were attributed to straining caused by thermal contraction. Temperature effects could therefore be included using the time-temperature equivalence concept.

One other observation which appeared consistently throughout the experimentation is as follows. If two samples are deformed along identical strain-time paths and then the straining for one sample is interrupted, by holding the strain constant for a time t_o, and then continued, the stress-strain behavior after the interruption is identical to that of the sample which saw no interruption. Furthermore the time of the interruption t_o, appears to have no influence on the later behavior.

This ability to completely forget about the time interruption and rejoin the original curve takes a very special type of mathematical representation, namely L_p norm type representations and then only in the absence of hereditary integral terms such as those of linear viscoelasticity. These same arguments were presented by Farris in his earlier work and have been again substantiated on propellants on this contract. It means that for monotonic deformation conditions no fading memory viscoelasticity can be present. This is not to say that these terms are not present on unloading, in fact they are required on unloading since that is the only way possible to get compressive stresses with tensile strains on cyclic loading which is a readily observable fact with propellants. To not have these terms present on monotonic inputs, have them present on unloading, and have them disappear again whenever the strain magnitudes exceed the last highest value requires the same special mathematics, however, it is contained within the framework of equation (141). Note that setting $P_4 = \infty$ and the functions $A_3 = -A_4$ gives

$$\sigma'_{ij}(t) = e^{-BId/I_\gamma} \left\{ A_1 E'_{ij}(t) + A_2 \left(\frac{I_\gamma}{||I_\gamma||_{P_2}} \right)^{m_2} E'_{ij}(t) \right.$$

$$\left. + \left(1 - \left(\frac{I_\gamma}{||I_\gamma||_{\infty}} \right)^{m_4} \right) \int_0^t A_3(t-\xi) \dot{E}'_{ij}(\xi) d\xi \right\} \qquad (142)$$

The quantity $||I_\gamma||_{\infty}$ mathematically represents the super norm or infinite norm which is precisely the magnitude of the largest value the function has had in the time range zero to t.

$$||I_\gamma||_{\infty} = \text{Max} \left| I_\gamma(\xi) \right|_0^t \qquad (143)$$

Hence the multiplier to the hereditary integral term is identically zero whenever the current value of the argument is the largest value and is non-zero for all other values, which is what was desired from a mathematical interpretation of the physical phenomenon observed.

The ability for this simple equation to contain such complex behavior strongly suggests that L_p measures are a necessary part of propellant constitutive theory for they are the only functions that appear to have this property. Incorporating this effect and the temperature reduced time concept into the equations yields a simple equation which was slightly expanded upon to facilitate computer characterization. The final equation programed for distortional stress-distortional strain effects had the form

$$\sigma_{ij}'(t) = e^{-BI_d/I_\gamma}\left\{A_1 E_{ij}'(t) + \sum_{i=1}^{7} A_i \left(\frac{I_\gamma}{||I_\gamma||_{P_i}}\right)^{n_i} E_{ij}'(t) + \left(1 - \left(\frac{I_\gamma}{||I_\gamma||_\infty}\right)^{n_8}\right) \int_0^t A_8(t'-\xi')\dot{E}_{ij}'(\xi)d\xi\right\} \quad (144)$$

Where $t'-\xi' = \int_\xi^t d\xi/A_T(\xi)$

A_T = Time-temperature shift function

n_8, B, n_i, P_i, A_i = constants for i = 1,7

A_8 = function of reduced time

$$||I_\gamma||_p = \left\{\int_0^t I_\gamma(\xi)^p \, d\xi/A_T(\xi)\right\}^{1/p}$$

As will be shown in a later section this equation does a good job of fitting the response of composite propellants subjected to complex conditions of temperature, history, and degrees of multiaxiality.

To minimize the computer computational effort it is important to recognize that

$$\sigma_{11}' - \sigma_{22}' = \sigma_{11} - \sigma_{22} \quad \text{and}$$
$$E_{11}' - E_{22}' = E_{11} - E_{22} \quad (145)$$

and for pressurized uniaxial conditions $\sigma_{11}-\sigma_{22} = \sigma_{11}-\sigma_{33}$ and $\sigma_{22}-\sigma_{33} = 0$, while for biaxial conditions σ_{33} is unknown. The computer codes therefore operate on deviatoric stresses and strains reducing the computational effort by a factor of one third. This approach results in the same coefficients and other parameters appearing in equation (144). Note that by taking $\sigma_{11}'-\sigma_{22}'$ results in the equation

$$\sigma_{11}'(t)-\sigma_{22}'(t)=\sigma^{(D)}(t) = e^{-BI_d/I_\gamma}\left\{A_1 E^{(D)}(t) + \sum_{i=1}^{7} A_i \left(\frac{I_\gamma}{||I_\gamma||_{P_i}}\right)^{N_i} E^{(D)}(T) + \left(1 - \left(\frac{I_\gamma}{||I_\gamma||_\infty}\right)^{N_8}\right)\int_0^t A_8(t'-\xi')\dot{E}^{(D)}(\xi)d\xi\right\} \quad (146)$$

(c) Bulk Stress-Strain Behavior

(1) Discussion of Problem

The distortional stress-strain behavior discussed in the previous section was not very difficult to handle since considerable work had already been done and it was only necessary to piece the puzzle together filling in a few blank pieces. The bulk behavior, on the other hand, has never been seriously studied and any ease in working out the distortional problem was more than offset by the difficulties encountered with the bulk behavior. Unlike the distortional behavior the bulk behavior is not strongly time dependent and for the most part an elastic time independent approach would appear well justified. The difficulty lies in the fact that the distortional and bulk effects are coupled. Since the bulk dilatation influences the distortional dependence it is mandatory that the distortion influence the bulk response. Propellants subjected to pure hydrostatic compressive stresses change in volume only slightly, yielding bulk moduli in the range from 500,000 psi to 1,000,000 psi. For conditions of pressure and high distortion, however, propellants greatly increase in volume and can yield bulk moduli under 200 psi. This great change in bulk compliance is easily visualized when one understands that for pure hydrostatic compression the dilatation is the dilatation of the actual propellant ingredients whereas for large tensile or distortional stresses the dilatation observed is almost entirely caused by vacuole cavitation due to microstructural breakdown. This over 1000 fold decrease in bulk moduli due to distortion and/or hydrostatic tension is very difficult, if not impossible, to describe using simple representations.

The bulk response is further complicated by the fact that the total dilatation observed can be a relatively large positive quantity. A 10% increase is not uncommon in pressurized distortional experiments, even though the mean pressure, $\sigma_{kk}/3$, is negative. Normally one associates increases in volume with positive normal stresses and decreases in volume with compressive normal stresses. These normal dilatational effects are observed for pure hydrostatic conditions (i.e. no distortional stresses or strains) however when distortion is present it is not uncommon to observe that the so-called bulk modulus, $\sigma_{kk}/3I_d$, changes signs, since I_d starts being zero when σ_{kk} is zero, becomes slightly negative as hydrostatic pressure is applied and then increases to large positive values as the material is distorted in a constant superimposed pressure environment. In going from a negative to a positive value the dilatation must naturally pass through zero, and since the mean pressure, $\sigma_{kk}/3$, is not generally zero at this point, the bulk moduli must start at about 10^6 psi and increase to positive infinity with distortion, change signs, becoming negative infinity, and increase to roughly 200 psi at large distortions.

This type of behavior is observed with soils and other granular media, however little has been done in that field that is applicable to propellants. Various methods have been considered and tried, however considerable difficulty has been experienced. Much of the problem is that dilatation can usually only influence the distortional stiffness by a factor of two to ten. Although a fairly strong effect, small variations in dilatation measurements caused by experimental error or simply material variability do not destroy the ability to simultaneously fit dozens of experiments accurately to the distortional equation of state. On the other hand, the influence on the bulk stiffness is over a thousand fold, and worse yet, the bulk stiffness can change signs with distortion. Small variations in dilatation between samples appears to completely destroy any computer fits because of the errors introduced on such strong functions. Ways of circumventing these problems have been partially successful and the problem is near being solved. However at this point, improvements can be made in handling the completely general case of arbitrary loading conditions.

The problem is by no means as bad as spelled out above for special cases, namely near constant pressure. The mean pressures in rocket motors subjected to gravitational and thermal loads is generally quite small and surely no higher than $\pm$ 30 psi. This type of data can be handled with fairly good precision using the bulk equations developed in this section. For that matter it appears that for any near constant pressure condition, $P_0 \pm 30$ psi, the math works quite well. Only when one tries to fit several experiments having mean pressure data varying from + 100 psi to -500 psi do characterization difficulties arise. It appears the mathematical models do contain the essence of the behavior, but determining best fit relations to large masses of data is going to require further work. The discussion below describes the bulk relations being used on this contract and how they were derived.

(2) An Elastic Strain Energy Approach

Although propellants are not conservative elastic materials considerable information about their stress-strain behavior can be obtained using an energy approach. Defining the strain energy per unit volume for an isotropic material as the function E, it can simply be shown that

$$\sigma_{ij} = \frac{\partial E}{\partial \epsilon_{ij}} \tag{147}$$

For linear elastic solids the strain energy is defined in terms of small strain theory as

$$E = \frac{\lambda + 2G}{2} I_1^2 - 2GI_2, \tag{148}$$

from which one can obtain by differentiation

$$\sigma_{ij} = \frac{\partial E}{\partial \varepsilon_{ij}} = \delta_{ij}\lambda I_1 + 2G\varepsilon_{ij}, \tag{149}$$

which is the linear isotropic stress-strain law.

In a similar manner the strain energy can be written in terms of the distortional and dilatational strains simply as

$$E = \frac{1}{2}\left(\lambda + \frac{2}{3}G\right) I_1^2 - 2GI_2' \tag{150}$$

where $\sigma_{kk}/3 = \frac{\partial E}{\partial I_1} = \left(\lambda + \frac{2}{3}G\right) I_1$

and $$\sigma_{ij}' = \frac{\partial E}{\partial \varepsilon_{ij}'} = 2G\varepsilon_{ij}' = 2G\left(\varepsilon_{ij} - I_1/3\right) \tag{151}$$

where $\sigma_{ij} = \sigma_{ij}' + \sigma_{kk}/3$

Recall that earlier it was stated that the propellant distortional stress-strain relation depended upon dilatation and was homogeneous to degree one, yet it was nonlinear. To obtain a constitutive equation that is homogeneous to degree one simply means the energy equation must be of quadratic form. There are many combinations of the invariants that will yield energy equations that are second order equations. The simplest to consider is

$$E = A_1 I_1^2 + A_2 I_\gamma^2 - A_3 I_1 I_\gamma \tag{152}$$

where $A_i > 0$

Differentiating this equation to obtain the distortional stress yields

$$\sigma_{ij}' = \frac{\partial E}{\partial \varepsilon_{ij}'} = \frac{2}{3} A_2 \varepsilon_{ij}' - \frac{A_3 I_1 \varepsilon_{ij}'}{3 I_\gamma}, \text{ or}$$

$$\sigma_{ij}' = \frac{2A_2}{3} \varepsilon_{ij}' \left(1 - \frac{A_3}{2A_2} \frac{I_1}{I_\gamma}\right) \approx \frac{2A_2}{3} \varepsilon_{ij}' e^{-\frac{A_3}{2A_2} \frac{I_1}{I_\gamma}} \qquad (153)$$

Now this equation is very similar to that derived from microstructural models by Farris. Since the energy must be positive definite, a constraint on equation (152) is

$$A_3^2 < 4A_1A_2 \qquad (154)$$

The bulk stresses can be derived in a similar manner yielding

$$\sigma_{kk}/3 = 2A_1 I_1 - A_3 I_\gamma, \qquad (155)$$

which indicates distortion can produce pressure, or equivalently solving for the dilatation

$$I_1 = \frac{\sigma_{kk}/3}{2A_1} + \frac{A_3}{2A_1} I_\gamma \qquad (156)$$

This simple equation will produce negative dilatation with pure pressure and if the pressure is maintained and the material is distorted sufficiently the dilatation can go through zero and become positive, which is observed experimentally with propellants. It is this type of equation that is likely to be successful describing propellant bulk response since it contains key features of propellant behavior.

This type of equation has been expanded upon and it is the expanded equation that is programmed in the characterization code NL002. It is also important to note that propellants can and do have very nonlinear pressure-volume behavior in the absence of distortion when they are subjected to hydrostatic tension. This effect is caused by the negative pressure causing cavitation just as distortion can cause cavitation in the microstructure. Hence equations like (156) must also provide for nonlinear dependence on I_1 (assumed here to be the dilatation for small strain theory). The equation currently programmed in NL002 has the form

$$\sigma_{kk}/3 = \sum_{i,j=0}^{n} A_{ij} I_1^i I_Y^j, \quad A_{oo} = 0 \qquad (157)$$

As discussed earlier, and will be shown in the next section, this type of equation predicts the bulk stress with good precision so long as it does not vary greatly. However when tests are input using hydrostatic pressure conditions from zero to 1000 psi pressure, meaningless results are obtained, even when very high order expansions are used (20 terms). Although equation (153) is similar to that derived earlier by Farris, it should be pointed out that equation (153) is a three dimensional equation and is subject to constraints, whereas Farris' earlier equation was from a one-dimensional phenomenological model. Taking equations (153) and (155) and subjecting them to the constraints of a uniaxial test, with or without superimposed pressure, $\sigma_{22} = \sigma_{33}$ = constant pressure P_o, and determining the σ_{11} and diltational behaviors versus axial strain predicts nothing like that observed for propellant, no matter what value the constants. When additional nonlinear terms are added, such as in equation (157), it appears a better job is done, but it is far from satisfactory. In summary then, even though the distortional data can be accurately described for complex loading conditions, the bulk stress-strain data cannot be described even for a few simple conditions if the mean pressure varies greatly. In desperation high order expansions involving I_1, I_2 and I_3, from which any invariant measure can be calculated, were tried, again producing poor results. The conclusions from all this work attempting to express the bulk stress in terms of the strain invariants are as follows:

- The bulk stress is probably a non-analytic function of the strain invariants and cannot be represented by polynomial type expansions.
- Attempting to treat the compressibility of the added vacuole or gas phase by a continuum equation is a poor choice for bulk representations.
- The accuracy and reproducibility of the dilatational measurements overshadow the bulk equation in regression techniques since all errors are assumed to occur on the left side of the equation. This effect can be caused because the bulk stress is a very strong function having to undergo great changes with only small variations in distortional and dilatational strains. In this sense it would be much better to express the dilatation in terms of the bulk stress and octahedral shear strain, since the errors would appear in the dilatation and would be very small as is shown in the next section.

(3) The Addition of Gas Phase Compressibility

In an attempt to overcome the difficulties observed in predicting bulk stresses a new approach was needed. It was decided to attempt to model the compressibility of the gas voids caused by vacuole dilatation by treating them as spherical voids contained in an elastic media. Surland[136] and Herrmann[137] have both treated this problem to describe the compressibility of slightly voided materials when subjected to pure pressure. In their analysis it was assumed that the voids themselves offered no resistance and that all the void dilatation was caused by distortion of the surrounding elastic material. It was also assumed that there was no interaction between voids. The equation they obtained had the form

$$\left(\frac{\Delta V}{V_o}\right)^* = \left(\frac{\Delta V}{V_o}\right) + \delta(1-e^{-3P/4G}) \qquad (158)$$

where $\left(\frac{\Delta V}{V_o}\right)^*$ = Total volume change, void + matrix

$\left(\frac{\Delta V}{V_o}\right)$ = Matrix volume change

δ = Fractional void content at P = 0

P = Hydrostatic pressure (assumed positive)

G = Shear modulus of matrix

A very similar equation was obtained for cylindrical voids, the only difference being the exponent 3/4 changed to unity.

In the above work it was assumed the voids already existed and could be squeezed out by pressure. The resulting equation predicted quite accurately for void contents up to about 5%. Their equation definitions and the concepts used in this report are different, but only in a complimentary manner. They predict the amount a voided system will be compressed with the application of a pressure, P. The gas dilatometer, on the other hand, measures the void content remaining, assuming zero initial void content. Hence to convert their equations to reflect the void content remaining results in

$$\delta - \left(\frac{\Delta V}{V_o}\right) = \text{Vacuole dilatation} = I_d \qquad (159)$$

After adding back in the matrix dilatation their equation becomes

$$I_d = \left(\frac{\Delta V}{V_o}\right) + \delta e^{-3P/4G} \tag{160}$$

Recall that δ is the void content at P = 0. Now it is not too difficult to expand δ in terms of the octahedral shear strain indicating the formation and growth of voids with strain[7]. Existing dilatation data indicates a power-law equation is a good approximation

$$\delta = A_2 I_\gamma^n \tag{161}$$

Similarly assuming that the bulk behavior is linear yields

$$\left(\frac{\Delta V}{V_o}\right) = A_1 P \tag{162}$$

Substituting these equations into equation (160) produces

$$I_d = A_1 P + A_2 I_\gamma^n e^{-\frac{3P}{4G}} \tag{163}$$

It is interesting to note that this type of equation seems to overcome all of the earlier difficulties and sheds light on the types of problems that occurred earlier. First it should be said that a simple equation of this type does a fine job of predicting the dilatational behavior in terms of the mean pressure and the octahedral shear strain as will be shown in the next section. Also it should be pointed out that Farris' earlier work indicated an exponential dependence of the same form on the rate of dilatation with straining (see Figure 22).

In light of the earlier difficulties equation (163) can be interpreted as follows:

- The pressure p cannot be solved for explicitly and expressed in terms of the dilatation and the octahedral shear strain. This is precisely what was attempted earlier and only yielded poor results, even for very high order expansions. In fact careful examination of this equation indicates an inverse expansion would be exceedingly difficult for a large range of P, but quite simple for a small range of P.

- It places the dilatation on the left side of the equation, hence all errors in regression techniques are assumed in the dilatation.

Equation (163) can be improved upon since it does not, for example, include cavitation due to pure hydrostatic tension. That effect can be added in by adding nonlinear terms in p to the linear term describing the matrix compressibility in the absence of distortion. These features have been included and a slightly expanded version of equation (163) is what has been programmed in the characterization code NL003. Currently the equation format programmed in NL003 is as follows:

$$I_d = \sum_{i=1}^{4} A_i \, \sigma_{kk}{}^{i} + e^{A_5 \sigma_{kk}} (A_6 I_\gamma + A_7 I_\gamma{}^2 + A_8 I_\gamma{}^3)$$

$$+ e^{A_9 \sigma_{kk}} (A_{10} I_\gamma + A_{11} I_\gamma{}^2 + A_{12} I_\gamma{}^3) \qquad (164)$$

This equation is used in regression analyses and only those terms that are significant are retained.

(d) Equation Applications

The equations programmed in the characterization codes NL002 and NL003 have been fitted to the large masses of experimental data obtained on the contract. These codes are identical in their treatment of the distortional effects and are different in their treatment of the bulk effects. NL002 expresses the bulk stress in terms of the strain invariants while NL003 expresses the dilatation in terms of the bulk stress and the octahedral shear strain and as the earlier discussion has pointed out NL003 is far superior to NL002.

(1) Propellants Studied

Three propellants have been studied experimentally over the course of this contract, ANB-3066 which is an 88 weight percent solids polybutadiene propellant, ANB-3335-1, which is on 86% solids PBAN propellant, and a very highly filled nitroplasticized polyurethane propellant. All of these propellants are approximately 75 volume percent solids and their applications to this contract are discussed below

(a) ANB 3066

This propellant was specified in the original proposal request as the propellant to be used on this contract. One major concern in our experimental effort was the change in properties with age, since this was originally to be an 18 month contract. Repeat experiments were performed over the first few months and it was found that variations of over ± 30% in stiffness were observable. These were attributed to post cure, loss of volatiles, and oxidative attack on the small samples being tested. Considerable information regarding the stress-strain behavior and the types of equations necessary to describe this behavior was obtained from ANB-3066. However, it appeared hopeless to assume that an accurate representation of the data taken over this long contract could be made because of the variability problem. Aerojet recommended a change in propellants and the Air Force accepted this recommendation.

(b) ANB-3335-1

ANB-3335-1 propellant is an unplasticized-low aluminum propellant that has been stripped of volatiles prior to mixing. It is designed for space vacuum storage and was the best possible substitute for ANB-3066 on this contract. This propellant shows little aging effects, dilates considerably, is quite extensible, and undergoes a great change in modulus and strength over the temperature range -65°F to +150°F. Considerable test data was obtained over a nearly 18 month period with this propellant and all of the data is stored on magnetic tape. It is available to other researchers to test their theories regarding the response of composite propellants. Typical experiments on this propellant are repeatable within ± 10% when performed over a short period of time. It is estimated that a ± 15% variation could be expected over the 18 month period in which testing was performed. In an attempt to minimize the variability all the experiments at a single temperature were performed over as short a period of time as possible. However, due to having to construct the biaxial dilatometer system much of the biaxial data was obtained about 6 months after the uniaxial data. Data from this propellant are presented in this report using characterization codes NL002 and NL003.

(c) Nitroplasticized Polyurethane

This propellant was characterized for another program towards the end of this contract. This propellant data probably best represents the potential for these equations since the experiments were conducted over a two month period.

(2) Characterization Code NL002

The data in Figures 64 through 67 illustrate typical comparisons between theory and observed data for a few experiments at constant test pressure. This code does an excellent job of fitting the distortional behavior, but will only fit the bulk behavior at near constant pressure conditions. When tests covering a wide range of hydrostatic pressure conditions are used meaningless results are obtained. Since this code recombines the distortional and bulk stresses to yield σ_{11}, σ_{22}, and σ_{33}, these data are presented as the final output and are illustrated in the figures. NL002 might be useful in thermal stress analysis wherein the bulk stresses never vary greatly, however the emphasis of the present work has been on NL003 since describing the bulk stress in terms of the strain invariants seems a hopeless task for completely general conditions.

(3) Characterization Code NL003

Data are presented in this section on the polyurethane propellant and the PBAN propellant. Typical polyurethane propellant data is presented in Figures 68 through 75. This propellant was characterized using pressurized uniaxial and biaxial experiments at 0°F, 40°F, 77°F, and 110°F at pressures ranging from atmospheric to 1000 psi. The data used in the characterization process was the entire stress-strain response to failure. The characterization included 37 experiments involving 814 total data points. In this characterization the standard deviation of the fit was 16.2 percent of the observed values for the distortional stress. It is felt that this is an excellent fit since the experiments themselves are only reproducible to about $\pm$ 10% when material variability and other factors are included.

Typical data for the PBAN propellant are presented in Figures 75 through 96. The data presented include the entire stress strain response to failure. As mentioned earlier this experimental effort was carried out over an 18 month period to study propellant behavior and use the experimental observations to develop a constitutive theory. The data at any constant temperature was taken over a much shorter time period. In fitting this data to the theory each temperature was first studied separately and it was found that for an average of roughly 40 experiments at each temperature the data had a standard error of $\pm$ 12% of the observed distortional stress values. Hence 68% of the data would fall within $\pm$ 12% and 95% within $\pm$ 24%. At each temperature complex deformation histories were used involving different strain rates, strain reversals, multiple relaxations, etc. on both pressurized uniaxial and biaxial data. The dilatation was only predictable to approximately $\pm$ 21% on the average at each constant temperature condition. When all of these different temperatures were assembled together the problem becomes much more complex in that thermal effects must be included in the form of a reduced time. The code NL003 is currently limited to about 100 experiments due to storage problems. When these 100 experiments were assembled and the regression analysis performed the standard error was found to be $\pm$ 17.6% for the

distortional stresses and ± 35% for the dilatation. These values could no doubt be improved upon since the function A_T must be estimated by trial and error, and strongly influences the analysis. These 100 experiments consisted of over 2000 data point sets and required a run time of 3.5 minutes and provided over 500 pages of comparisons between predicted and observed behavior. The total computer costs are about $35.00 on prime time. The data presented in the figures are "typical" data and not selected to show how good the fits might be. Trying to display the data to demonstrate the quality of the mathematical representations by presenting a five hundred page appendix or 100 extra figures does not seem appropriate. The point is, NL003 has just recently been developed as have the new three dimensional equations for propellant. There is much room for improvement in these codes and in the representations. These codes do demonstrate, however, that the nonlinear behavior of propellants can be described and described quite accurately for general loading conditions.

FIGURE 64 - COMPARISON OF PREDICTED AND OBSERVED STRESS-STRAIN BEHAVIOR FOR THE PBAN PROPELLANT USING CHARACTERIZATION CODE NL002

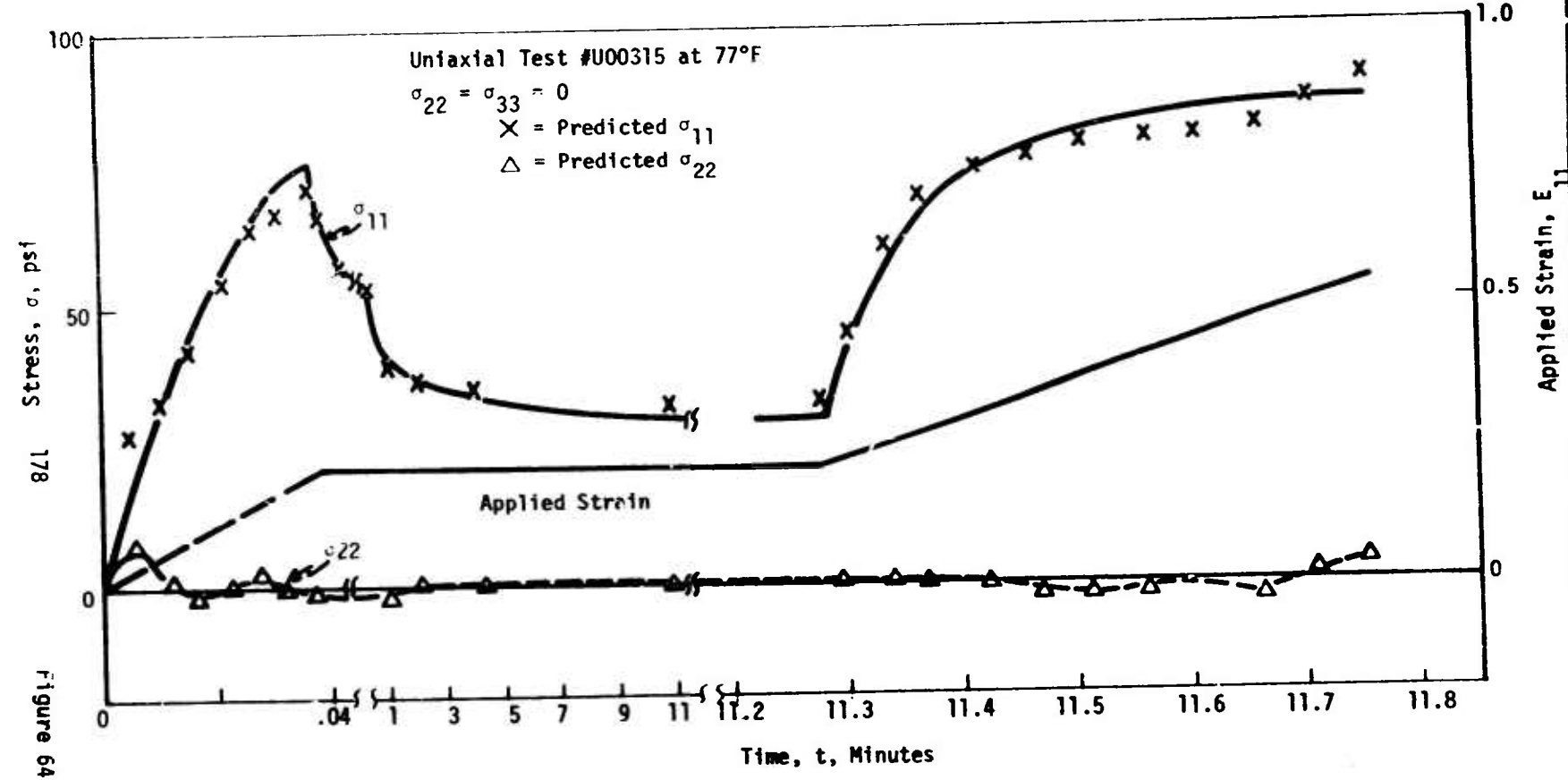

Figure 64

FIGURE 65 - COMPARISON OF PREDICTED AND OBSERVED STRESS-STRAIN BEHAVIOR FOR THE PBAN PROPELLANT USING CHARACTERIZATION CODE NL002

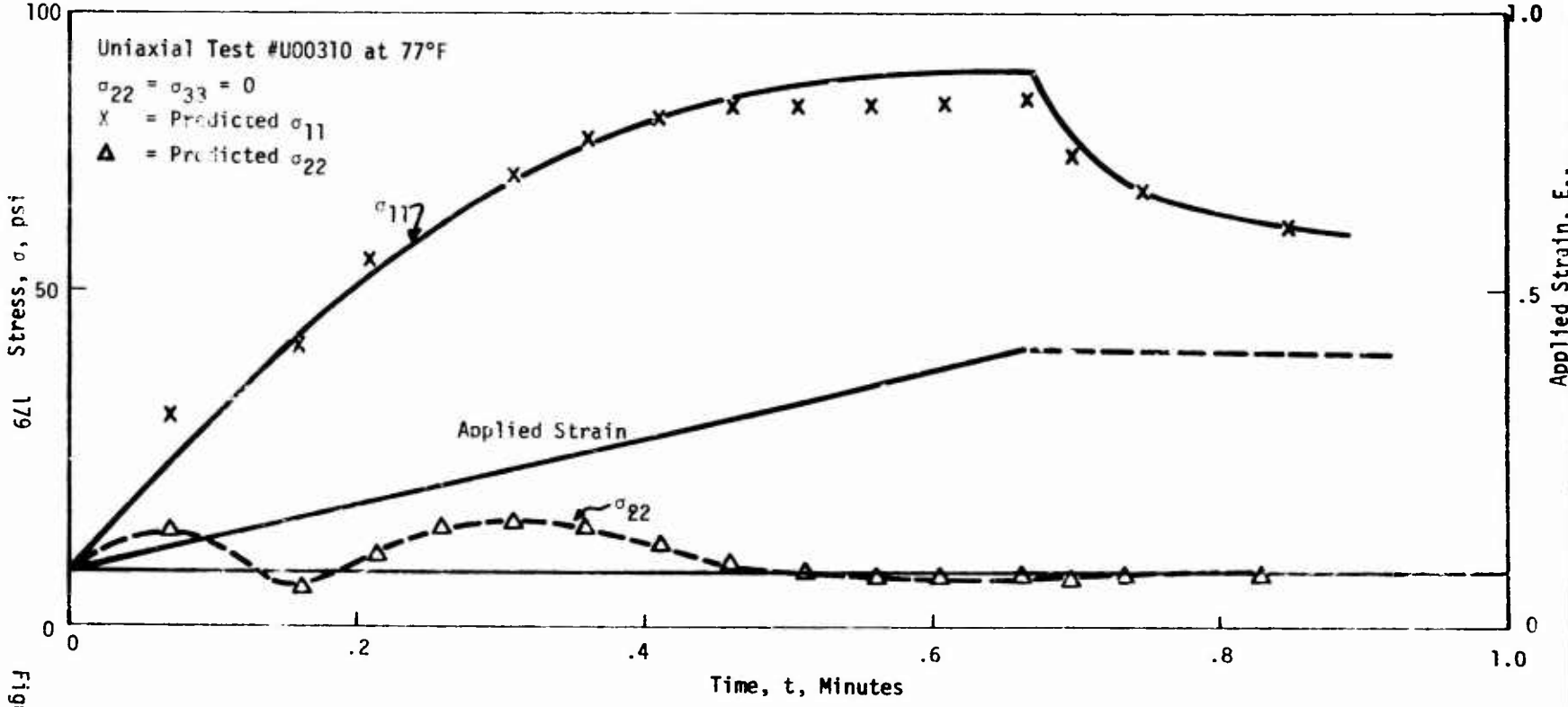

Figure 65

FIGURE 66 - COMPARISON OF PREDICTED AND OBSERVED STRESS-STRAIN BEHAVIOR FOR THE PBAN PROPELLANT USING CHARACTERIZATION CODE NL002

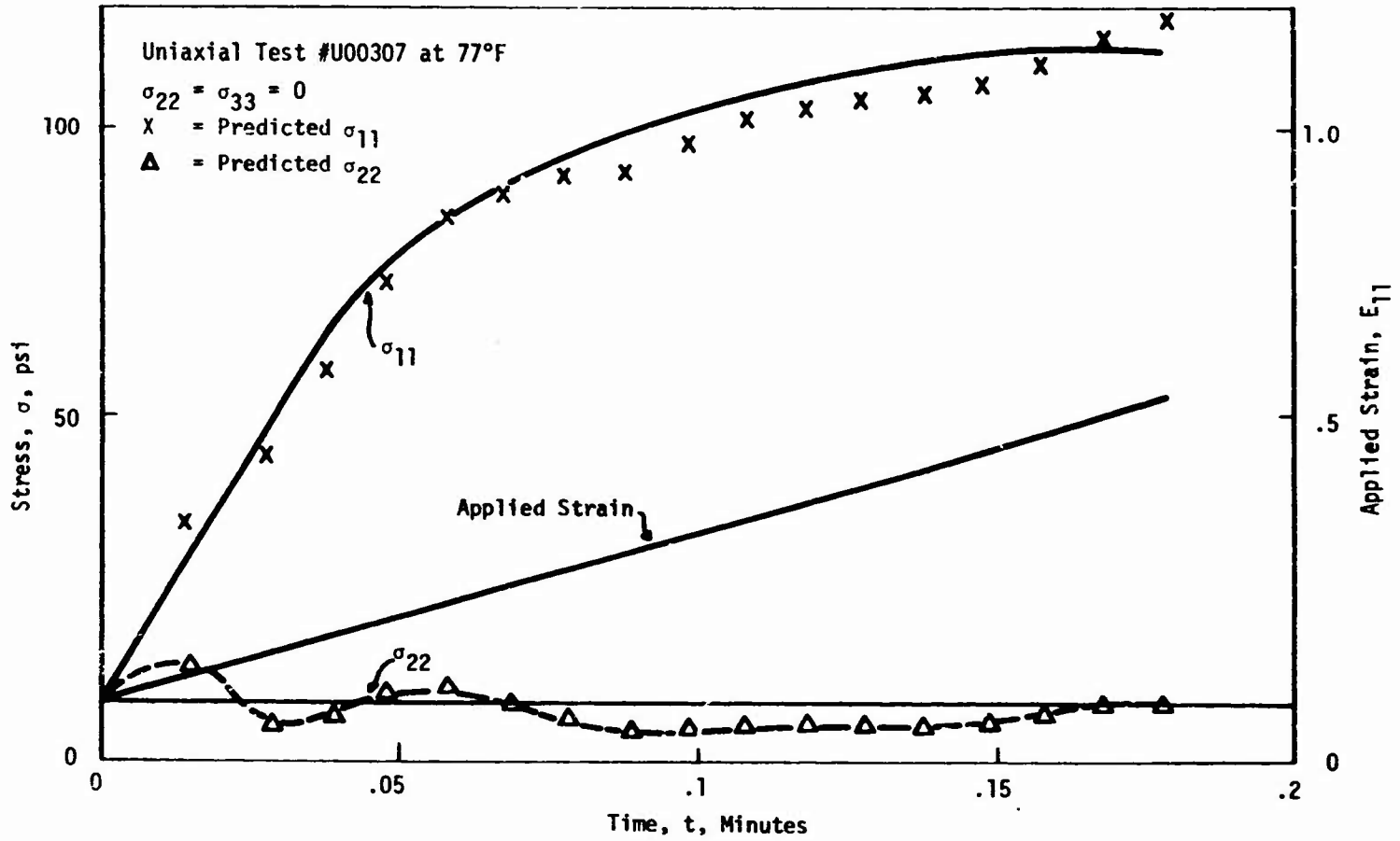

Figure 66

FIGURE 67 - COMPARISON OF PREDICTED AND OBSERVED STRESS-STRAIN BEHAVIOR FOR THE PBAN PROPELLANT USING CHARACTERIZATION CODE NL002

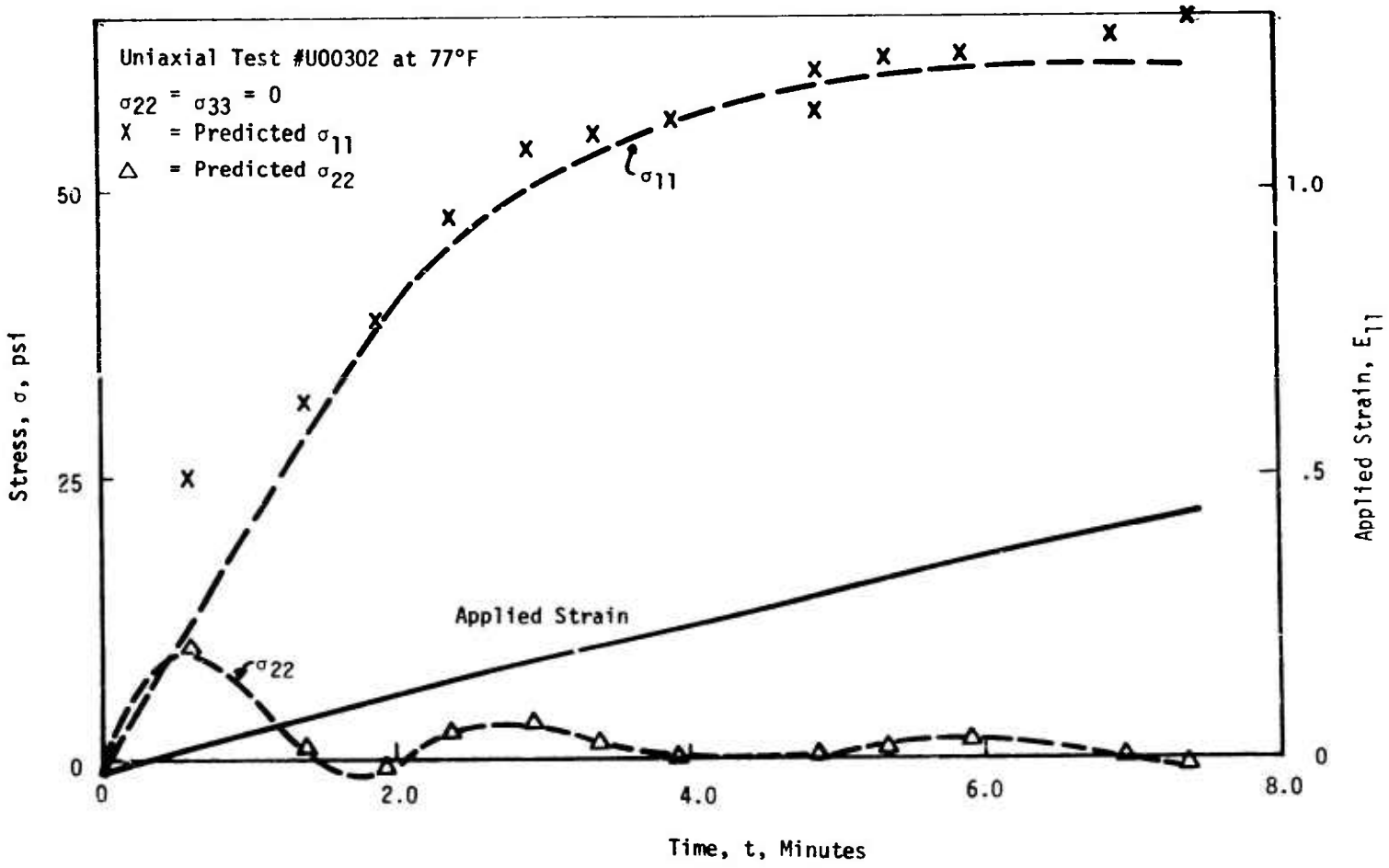

Figure 67

FIGURE 68 - COMPARISON OF PREDICTED AND OBSERVED STRESS-STRAIN BEHAVIOR FOR THE POLYURETHANE PROPELLANT USING CHARACTERIZATION CODE NL003

Figure 68

FIGURE 71 - COMPARISON OF PREDICTED AND OBSERVED STRESS-STRAIN BEHAVIOR FOR THE POLYURETHANE PROPELLANT USING CHARACTERIZATION CODE NL003

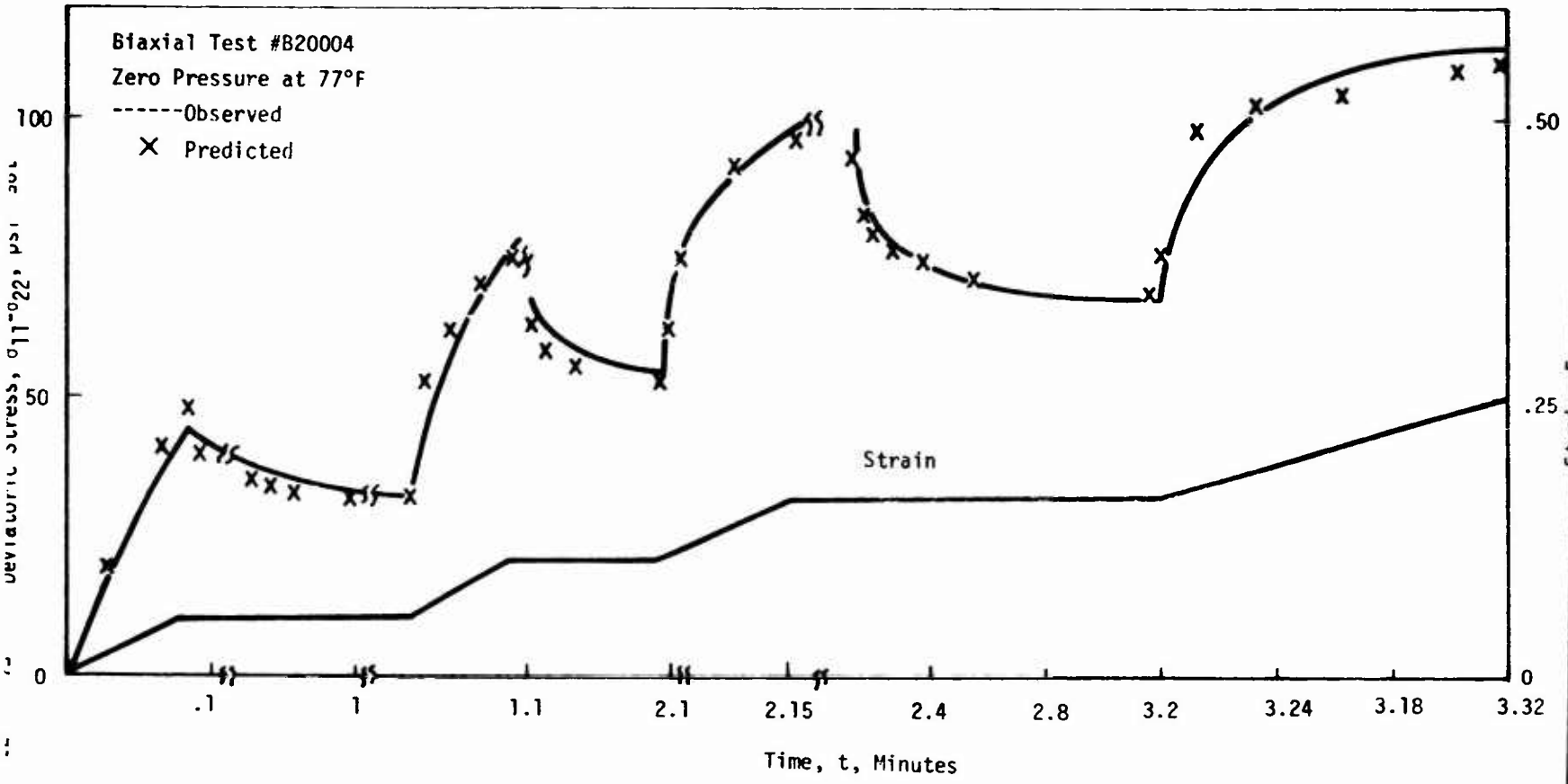

FIGURE 72 - COMPARISON OF PREDICTED AND OBSERVED STRESS-STRAIN
BEHAVIOR FOR THE POLYURETHANE PROPELLANT
USING CHARACTERIZATION CODE NL003

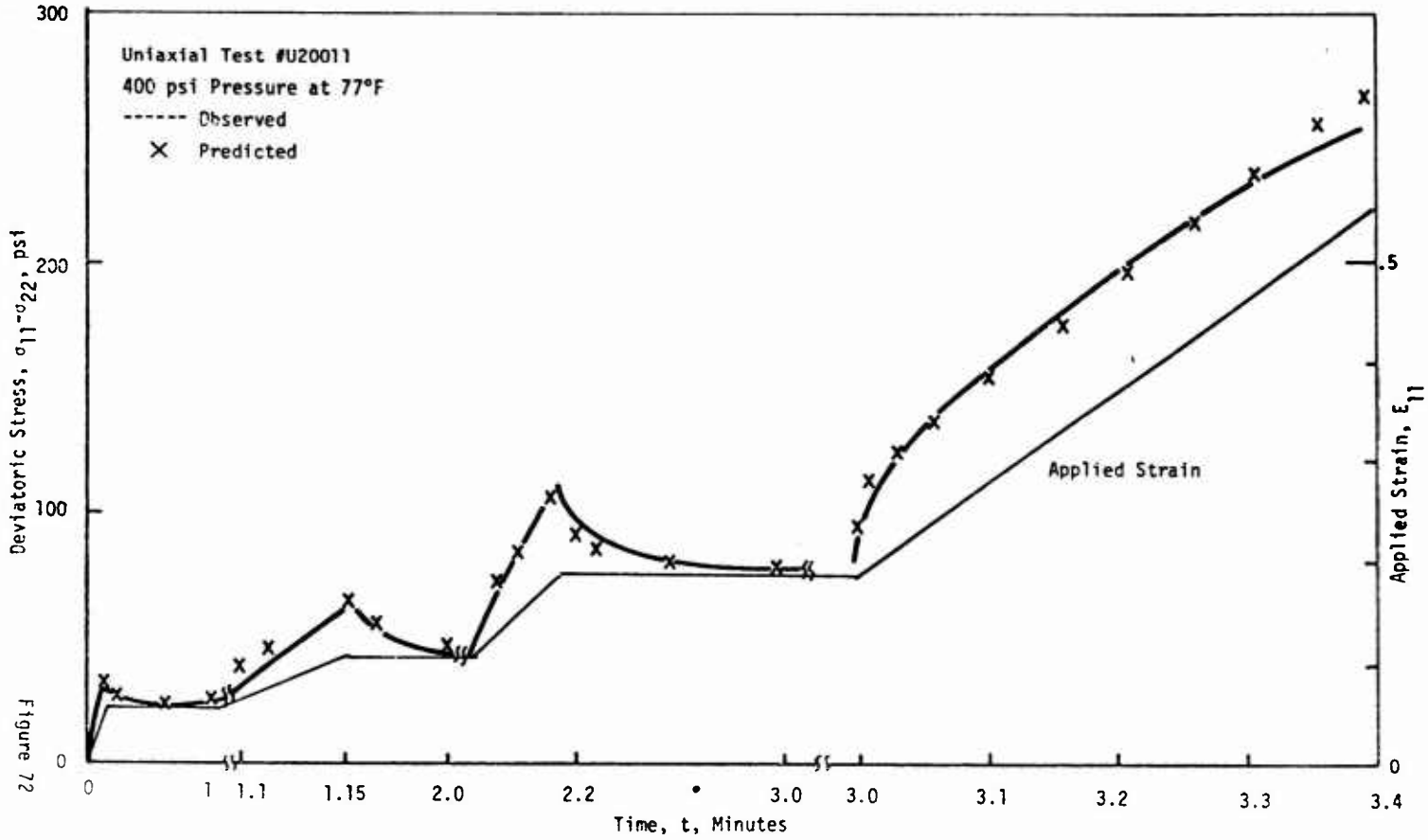

Figure 72

FIGURE 73 - COMPARISON OF PREDICTED AND OBSERVED STRESS-STRAIN BEHAVIOR FOR THE POLYURETHANE PROPELLANT USING CHARACTERIZATION CODE NL003

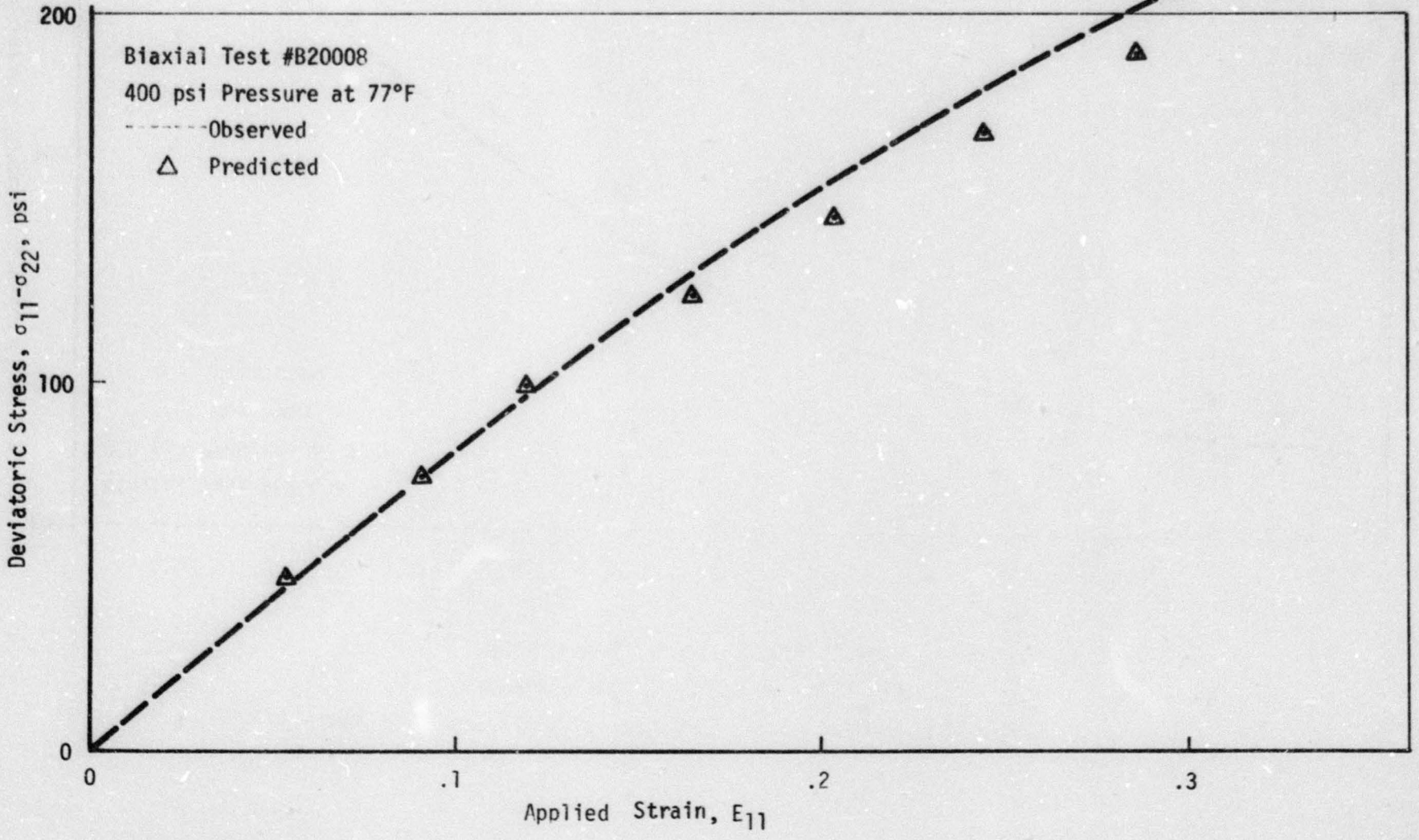

Figure 73

FIGURE 74 - COMPARISON OF PREDICTED AND OBSERVED STRESS-STRAIN BEHAVIOR FOR THE POLYURETHANE PROPELLANT USING CHARACTERIZATION CODE NL003

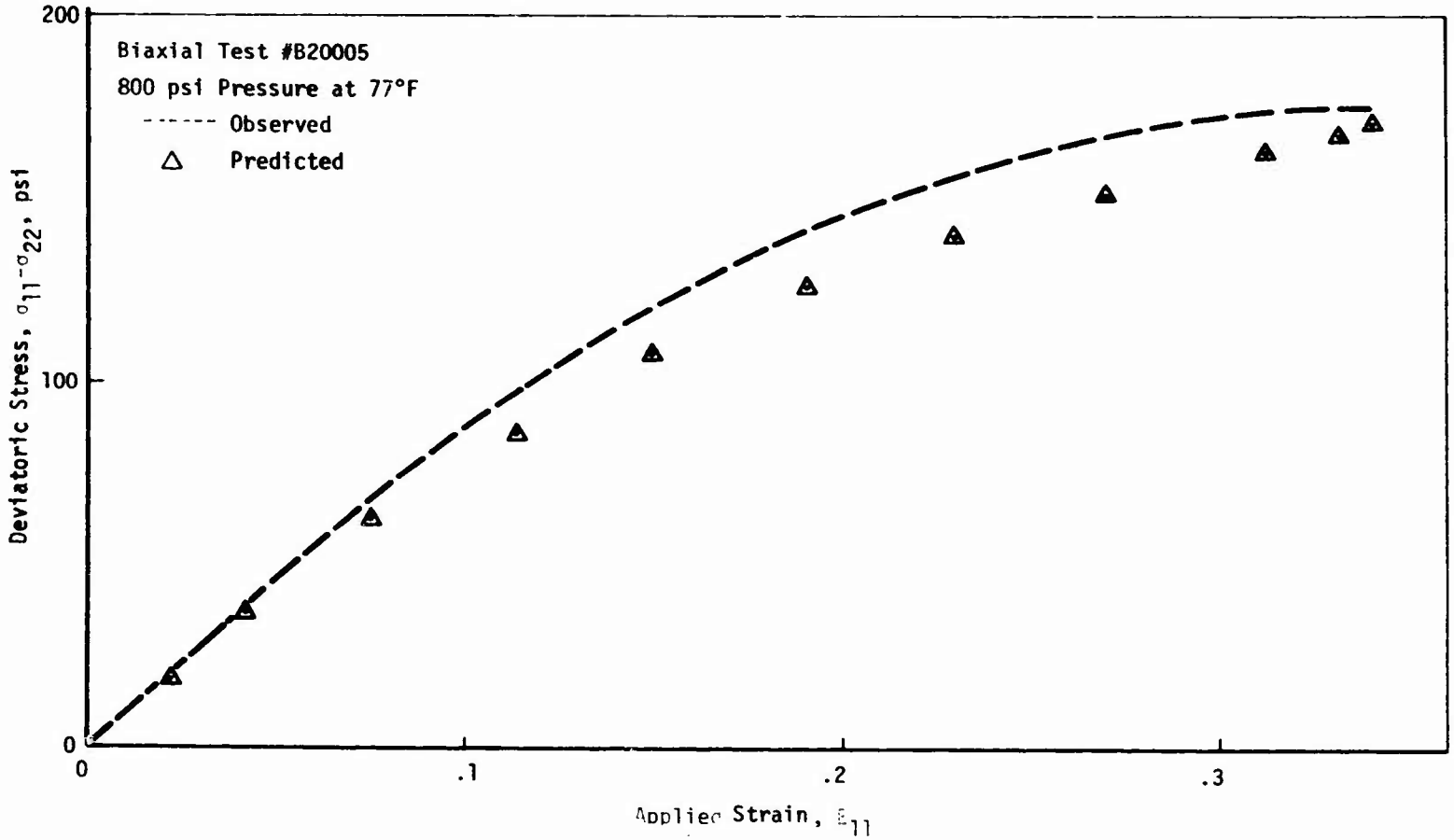

Figure 74

FIGURE 75 - COMPARISON OF PREDICTED AND OBSERVED STRESS-STRAIN BEHAVIOR FOR THE POLYURETHANE PROPELLANT USING CHARACTERIZATION CODE NL003

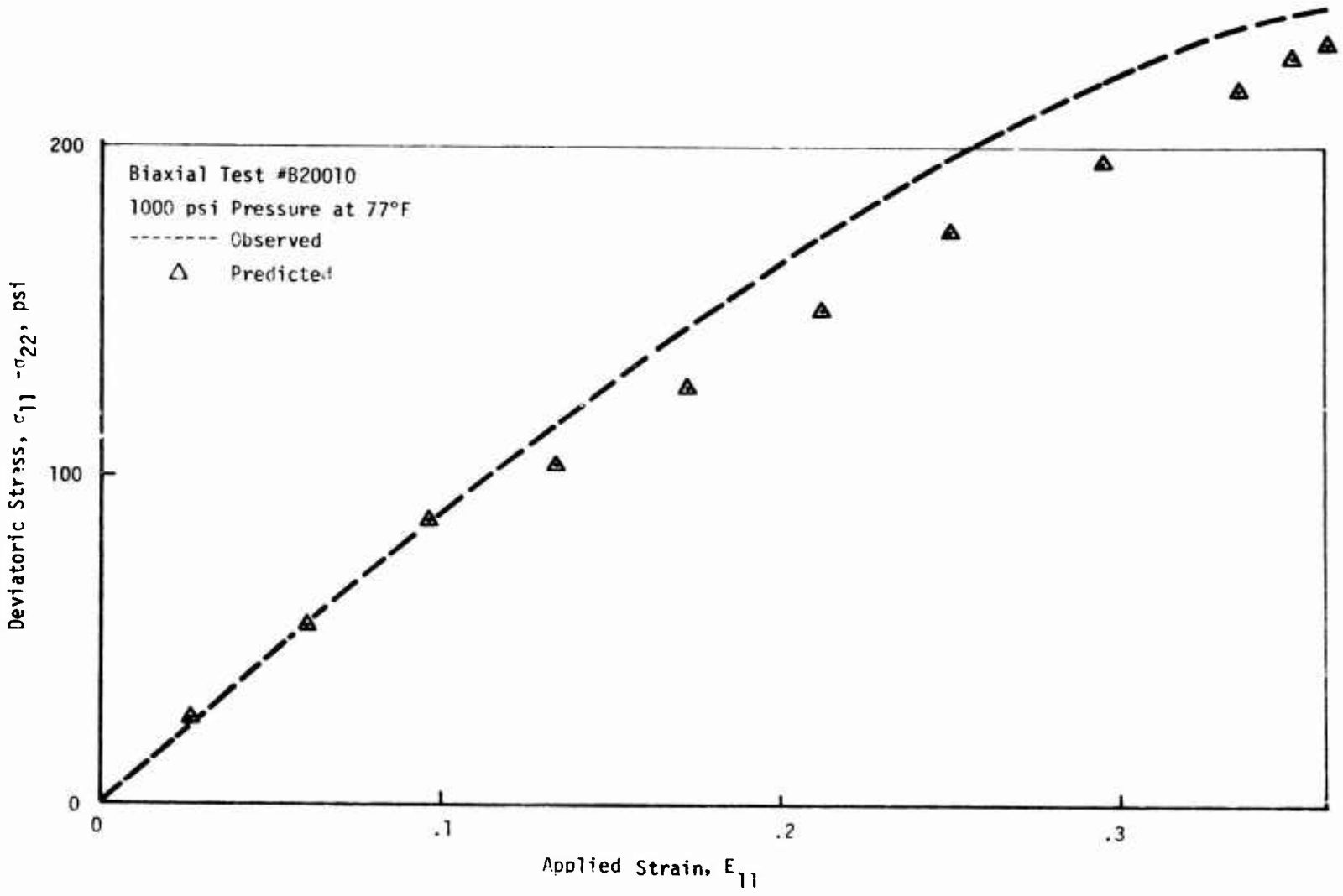

Figure 75

FIGURE 76 - COMPARISON OF PREDICTED AND OBSERVED STRESS-STRAIN-
DILATATIONAL RESPONSE FOR THE PBAN PROPELLANT AT 77°F
USING CHARACTERIZATION CODE NL003

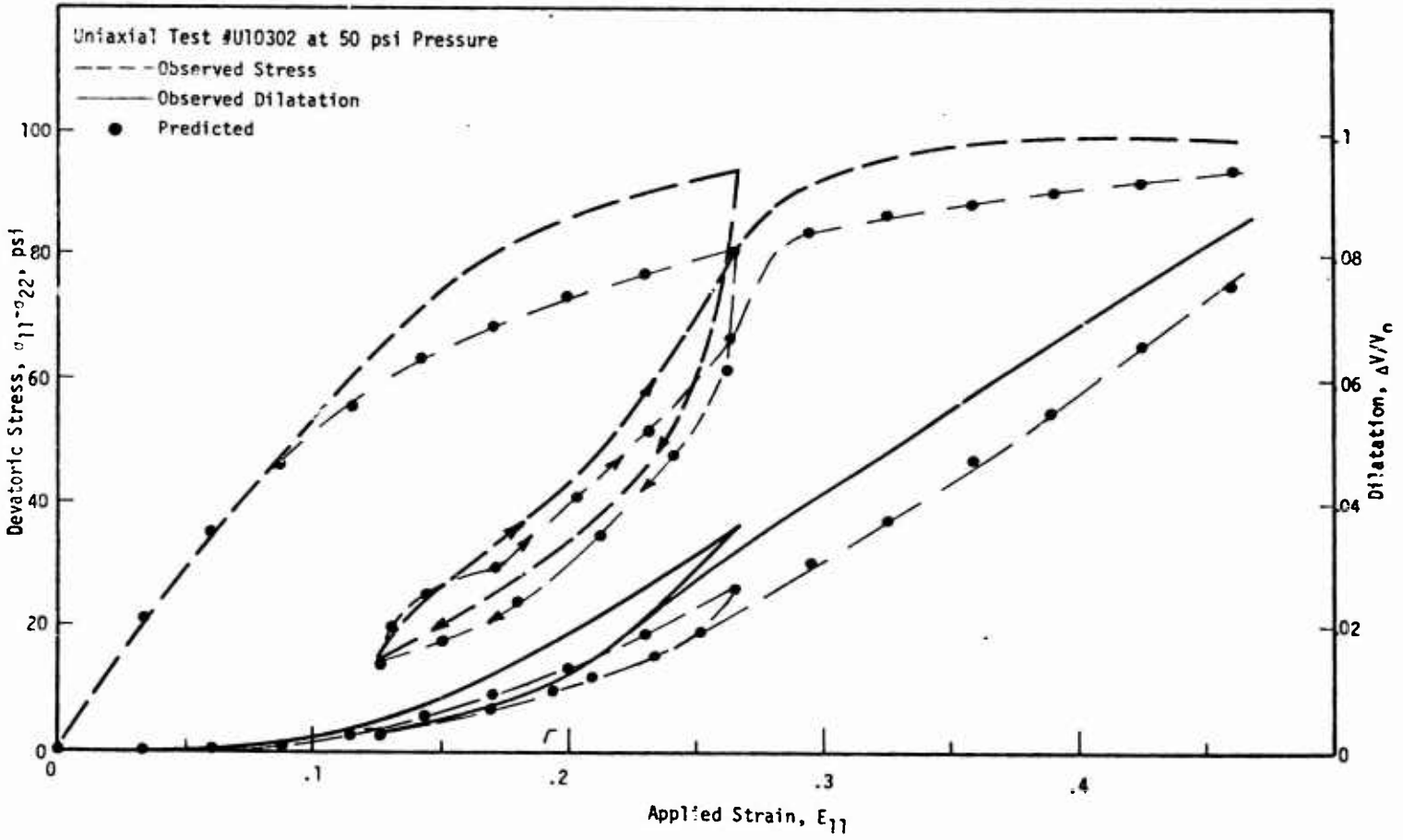

FIGURE 77 - COMPARISON OF PREDICTED AND OBSERVED STRESS-STRAIN-DILATATIONAL RESPONSE FOR THE PBAN PROPELLANT AT 77°F USING CHARACTERIZATION CODE NL003

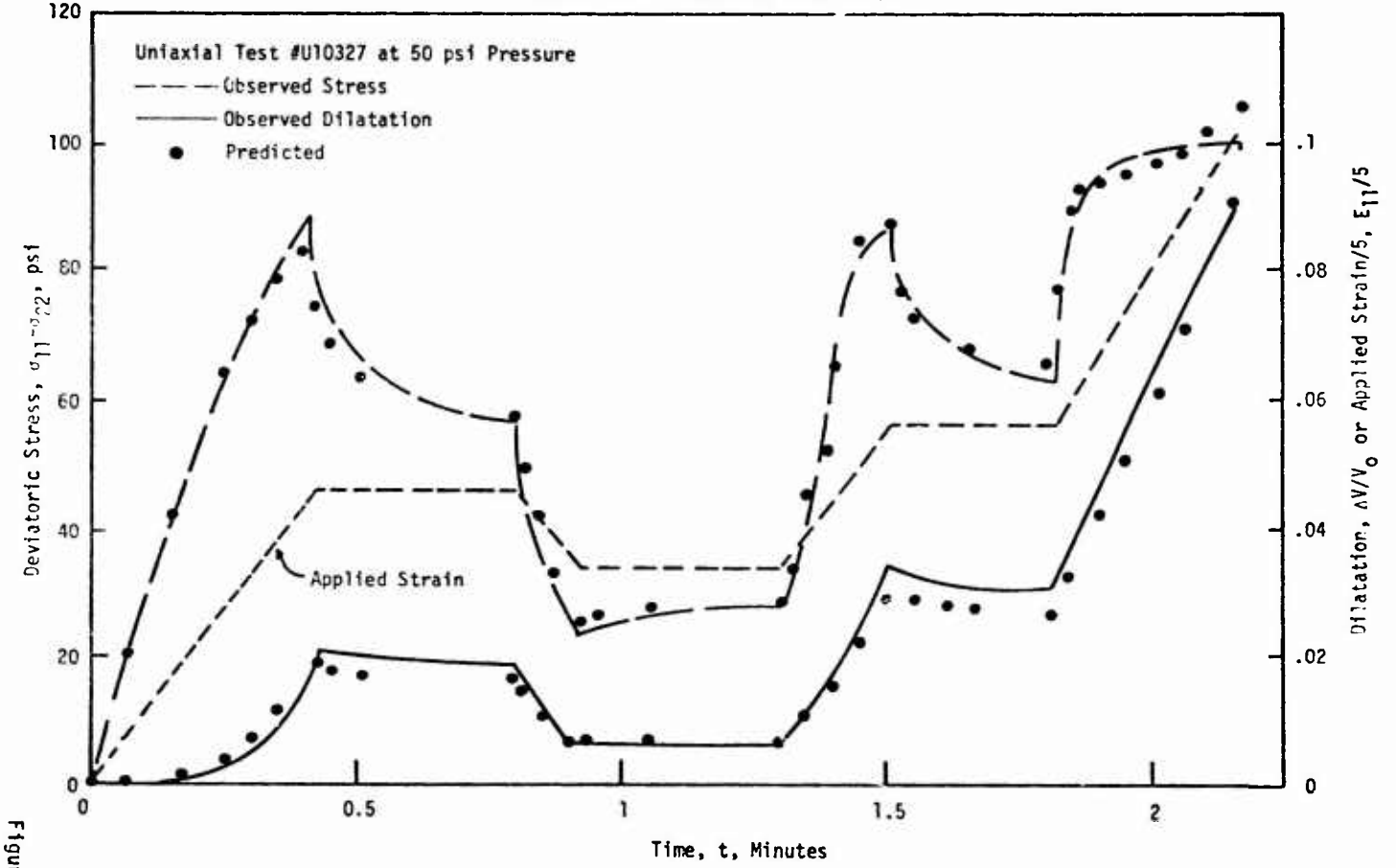

Figure 77

FIGURE 78 - COMPARISON OF PREDICTED AND OBSERVED STRESS-STRAIN-DILATATIONAL RESPONSE FOR THE PBAN PROPELLANT AT 77°F USING CHARACTERIZATION CODE NL003

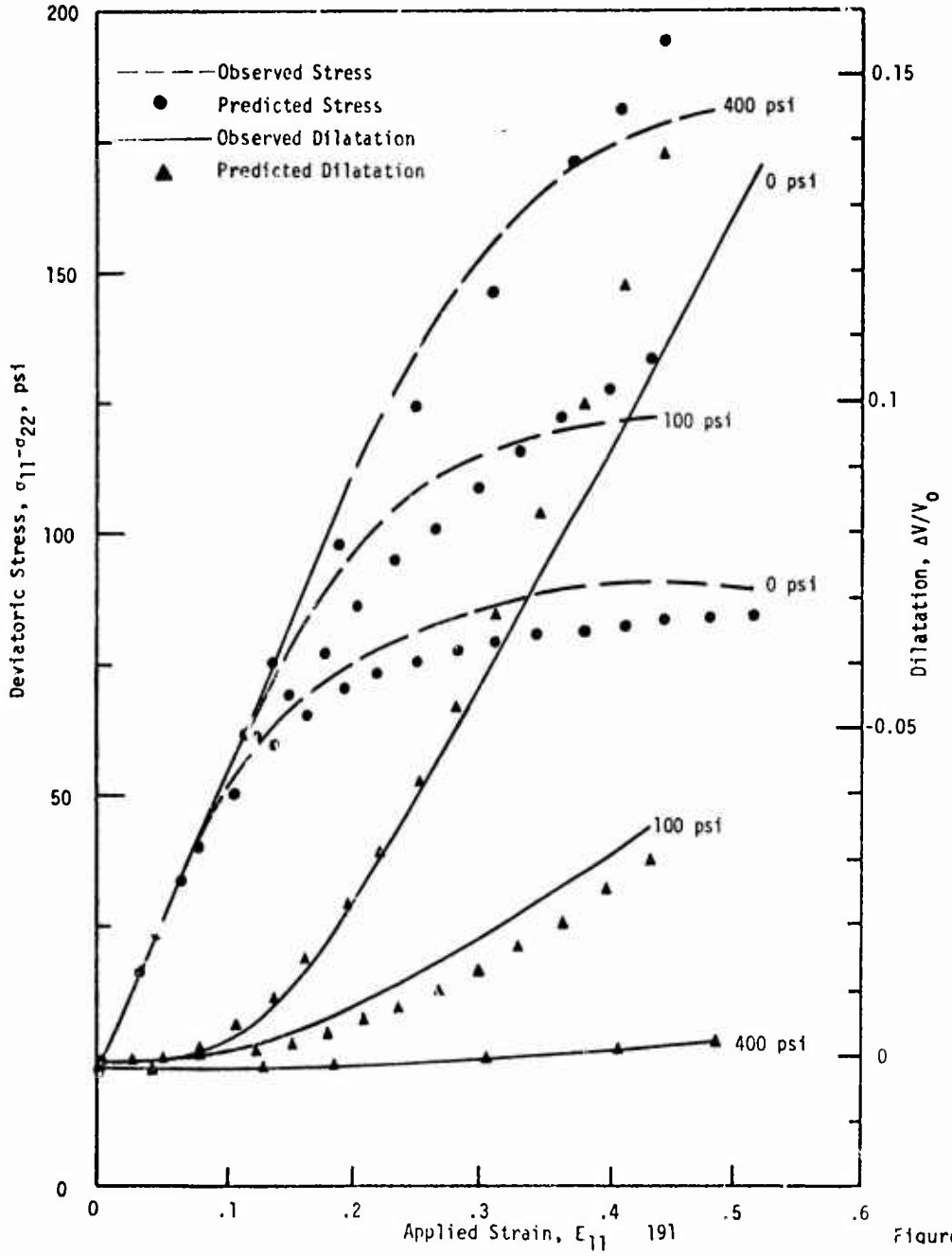

191

Figure 78

FIGURE 79 - COMPARISON OF PREDICTED AND OBSERVED STRESS-STRAIN-
DILATATIONAL RESPONSE FOR THE PBAN PROPELLANT
USING CHARACTERIZATION CODE NL003

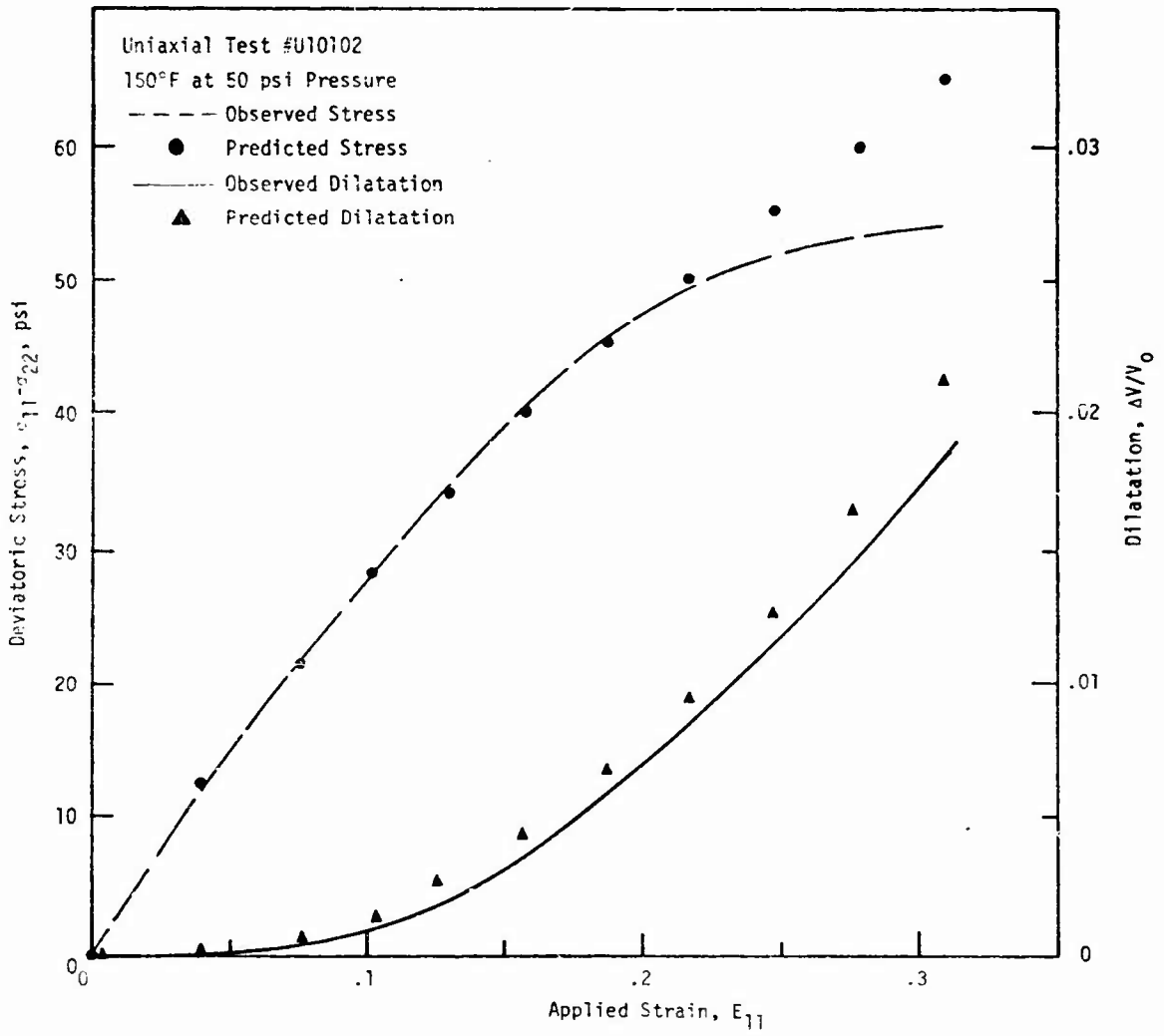

Figure 79

FIGURE 80 - COMPARISON OF PREDICTED AND OBSERVED STRESS-STRAIN-
DILATATIONAL RESPONSE FOR THE PBAN PROPELLANT
USING CHARACTERIZATION CODE NL003

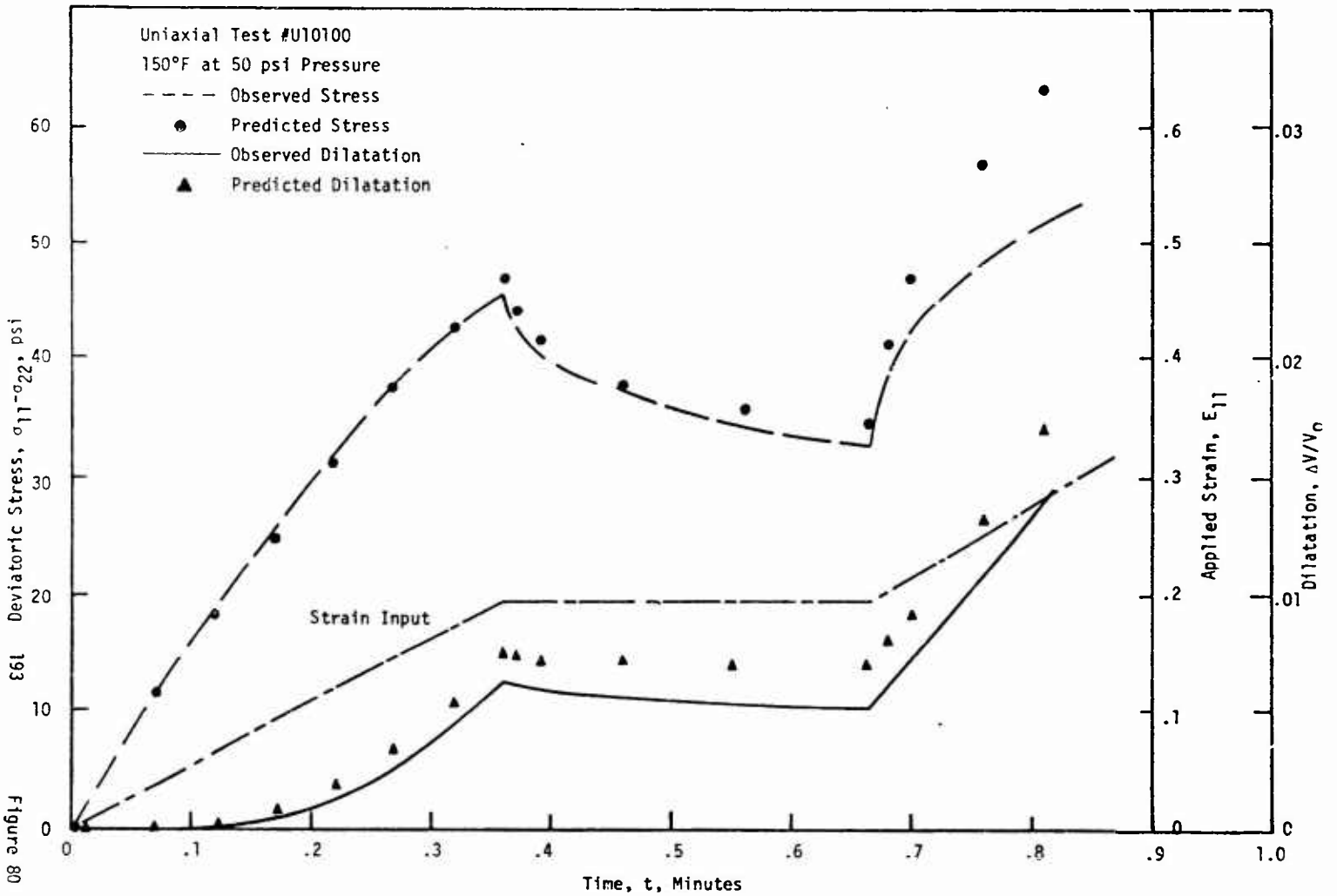

Figure 80

FIGURE 81 - COMPARISON OF PREDICTED AND OBSERVED STRESS-STRAIN-DILATATIONAL RESPONSE FOR THE PBAN PROPELLANT USING CHARACTERIZATION CODE NL003

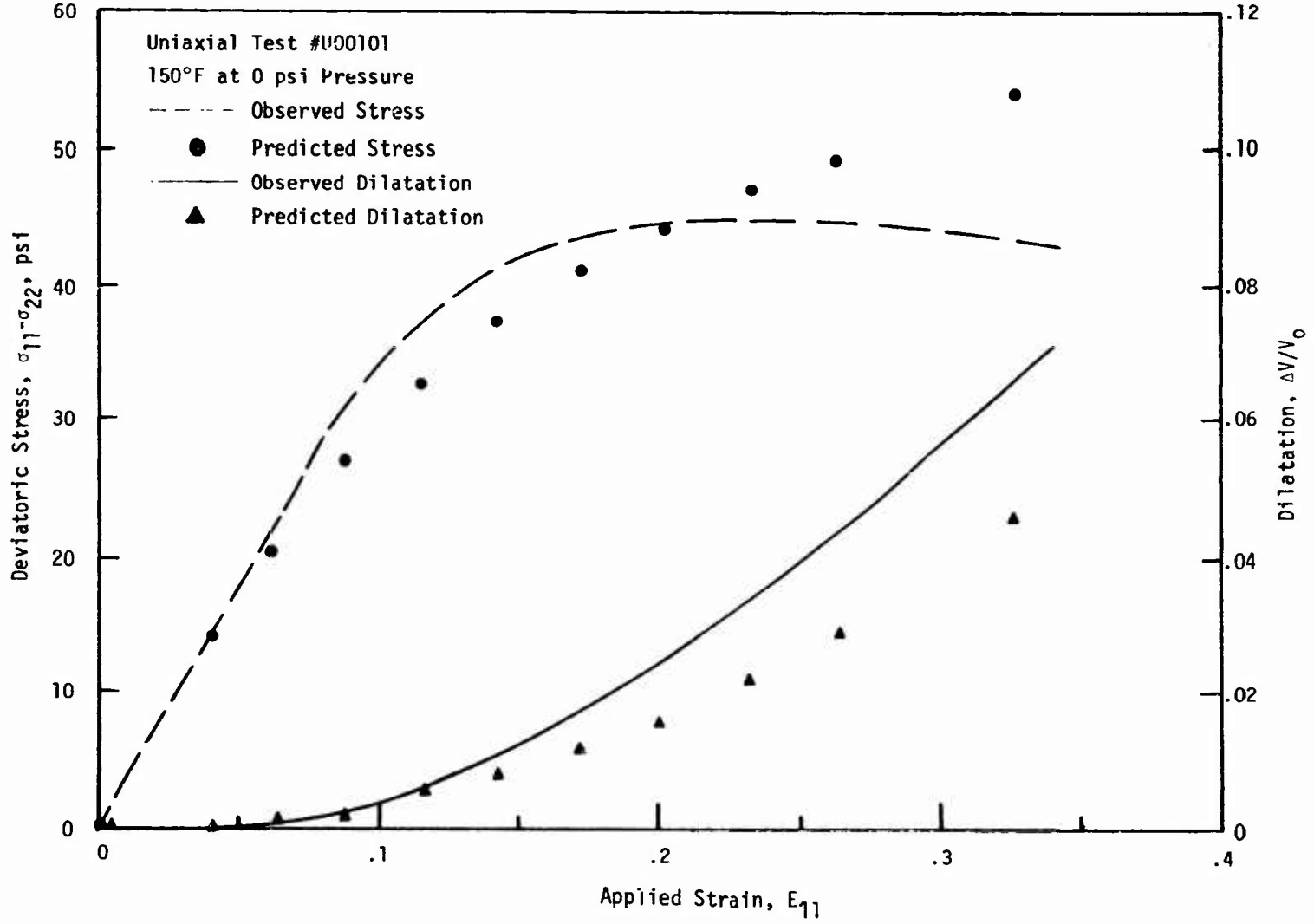

Figure 81

FIGURE 82 - COMPARISON OF PREDICTED AND OBSERVED STRESS-STRAIN-
DILATATIONAL RESPONSE FOR THE PBAN PROPELLANT
USING CHARACTERIZATION CODE NL003

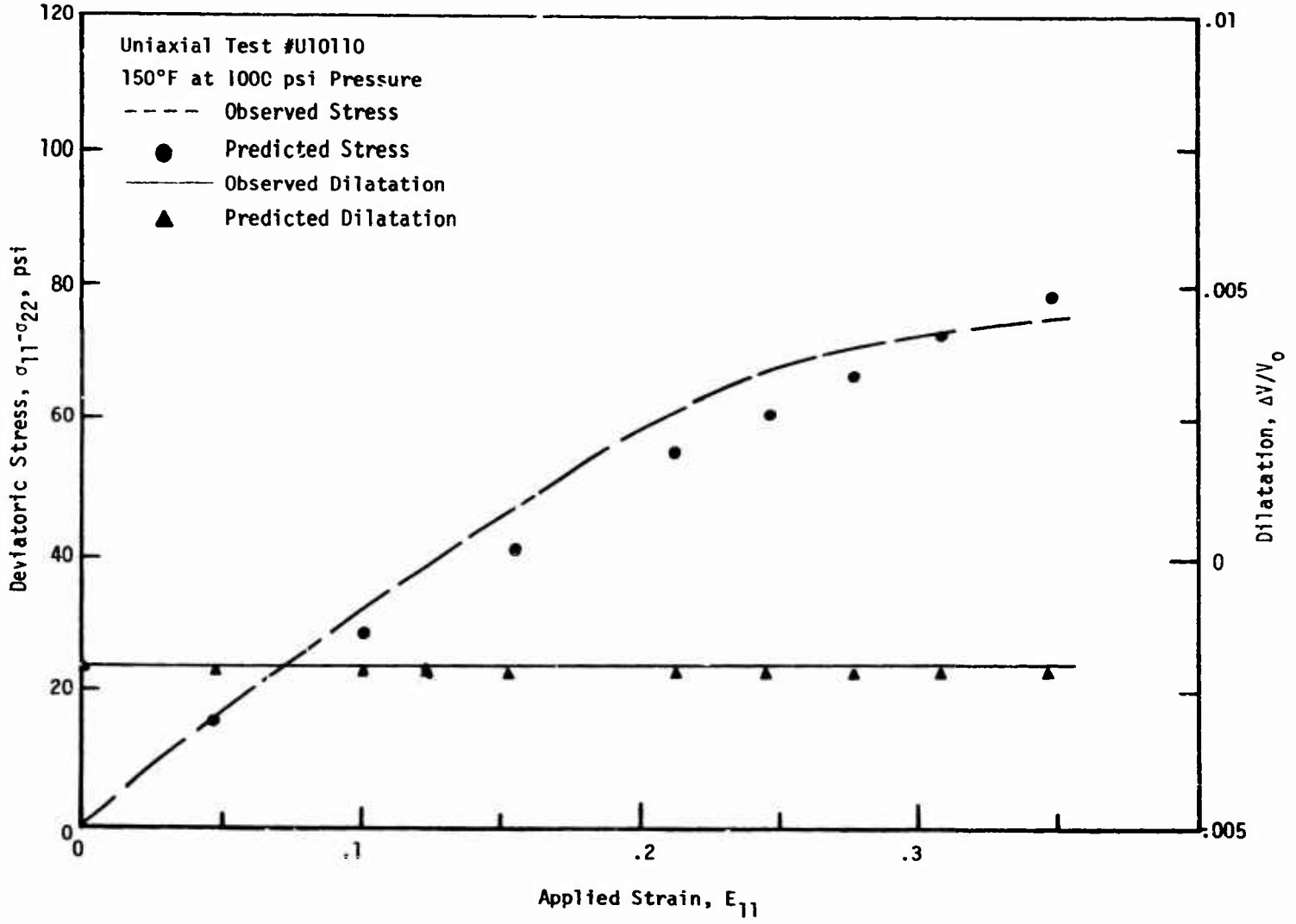

Figure 82

FIGURE 83 - COMPARISON OF PREDICTED AND OBSERVED STRESS-STRAIN-DILATATIONAL RESPONSE FOR THE PBAN PROPELLANT USING CHARACTERIZATION CODE NL003

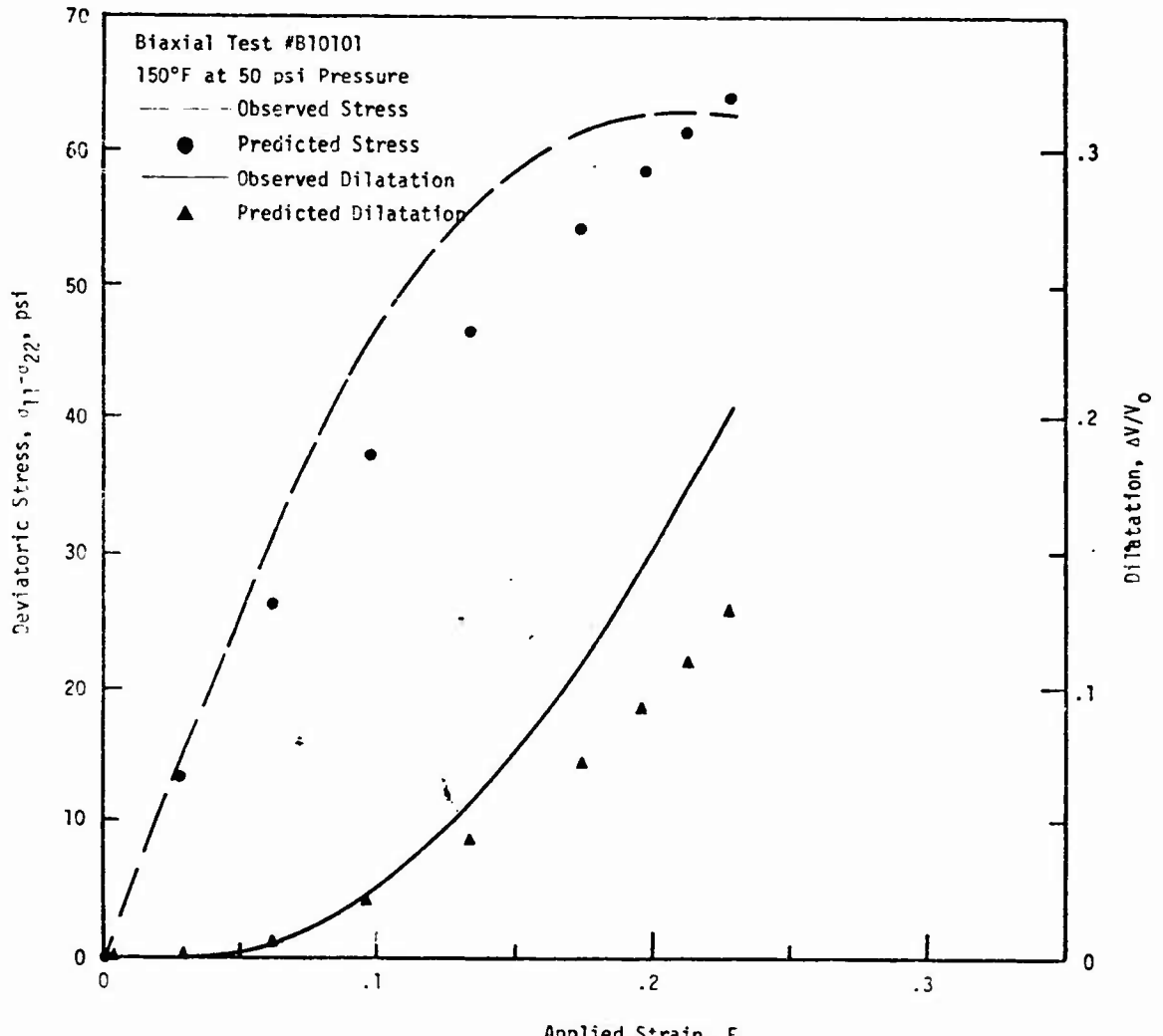

Figure 83

FIGURE 84 - COMPARISON OF PREDICTED AND OBSERVED STRESS-STRAIN-
DILATATIONAL RESPONSE FOR THE PBAN PROPELLANT
USING CHARACTERIZATION CODE NL003

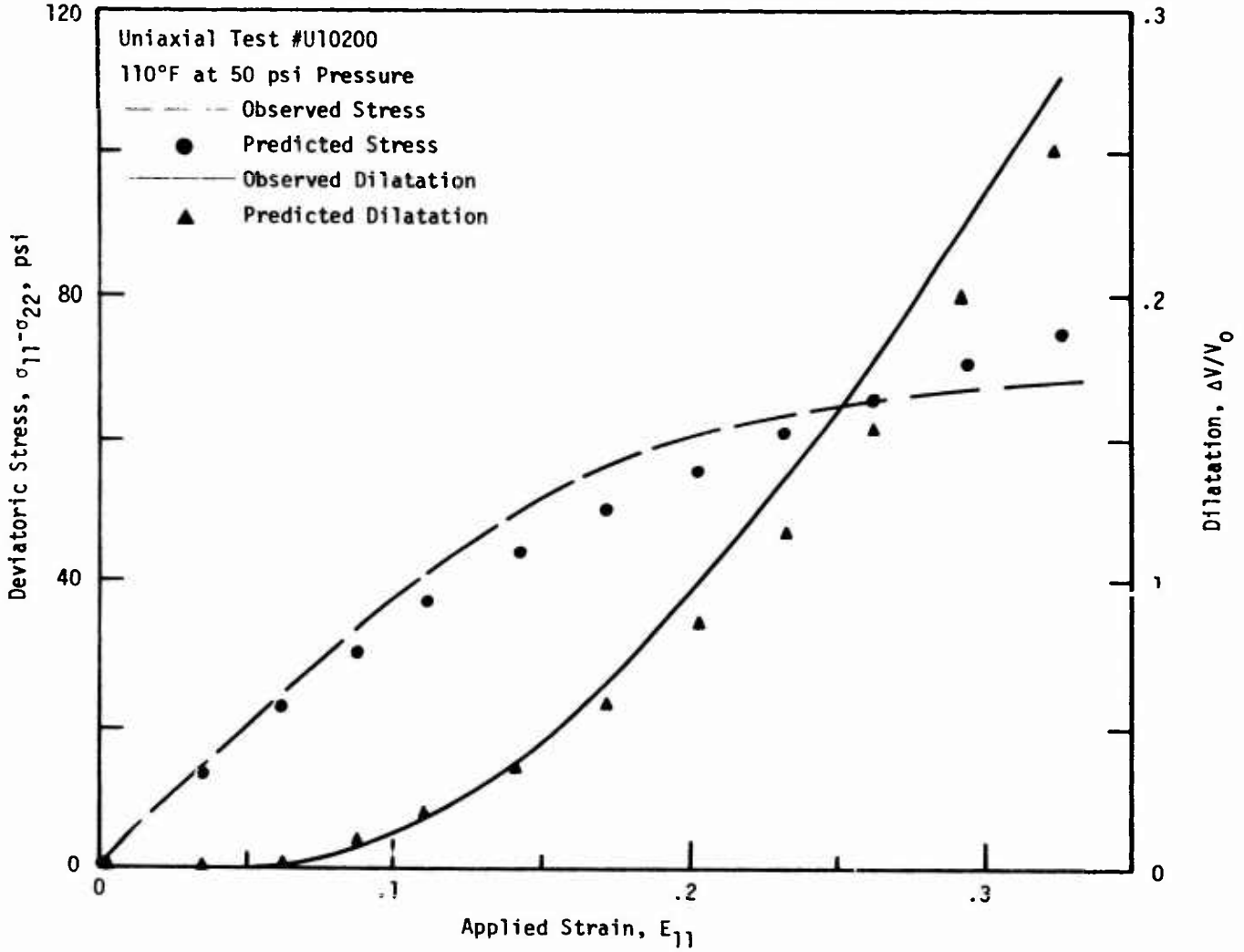

Figure 84

FIGURE 85 - COMPARISON OF PREDICTED AND OBSERVED STRESS-STRAIN-
DILATATIONAL RESPONSE FOR THE PBAN PROPELLANT
USING CHARACTERIZATION CODE NL003

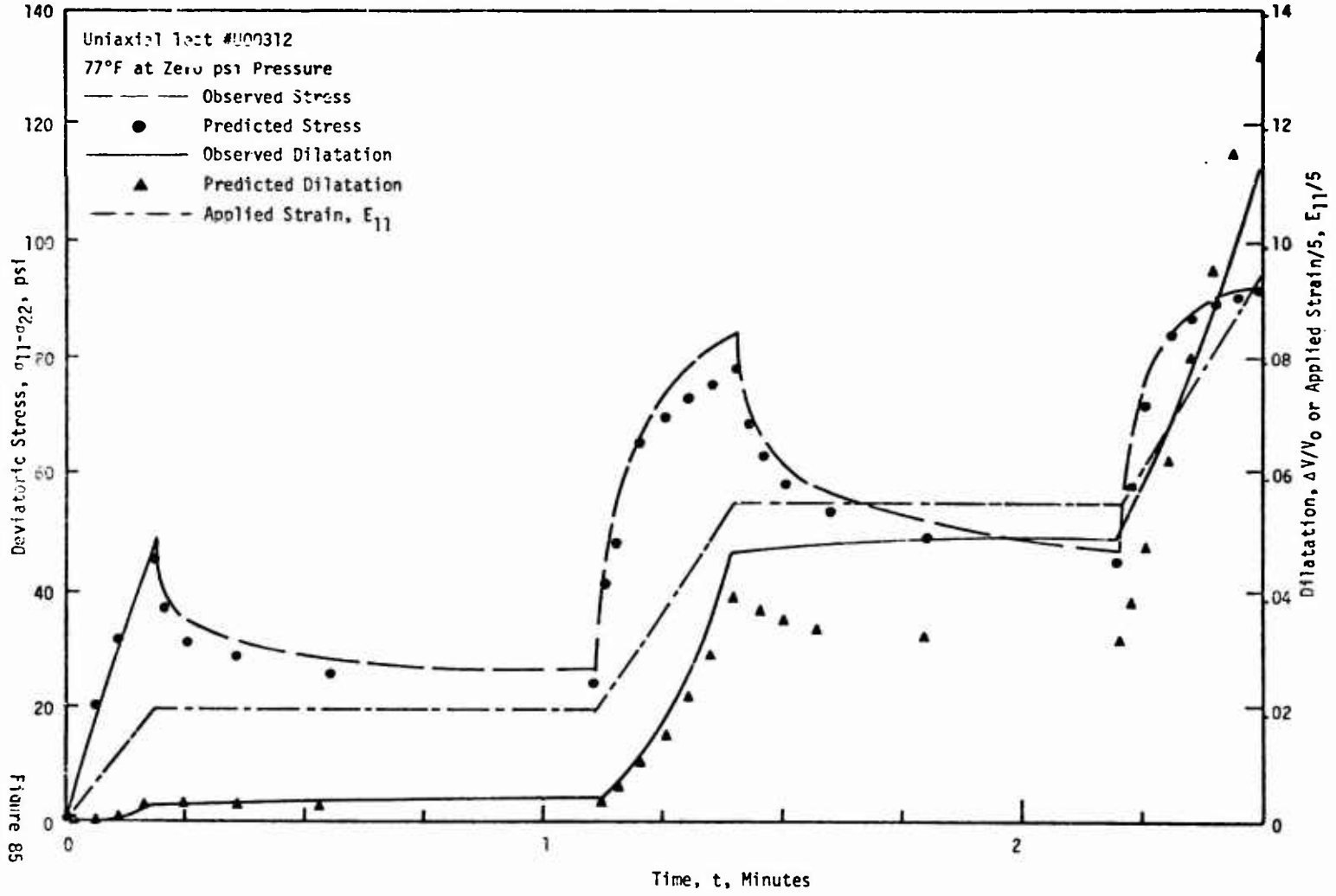

Figure 85

FIGURE 86 - COMPARISON OF PREDICTED AND OBSERVED STRESS-STRAIN-
DILATATIONAL RESPONSE FOR THE PBAN PROPELLANT
USING CHARACTERIZATION CODE NL003

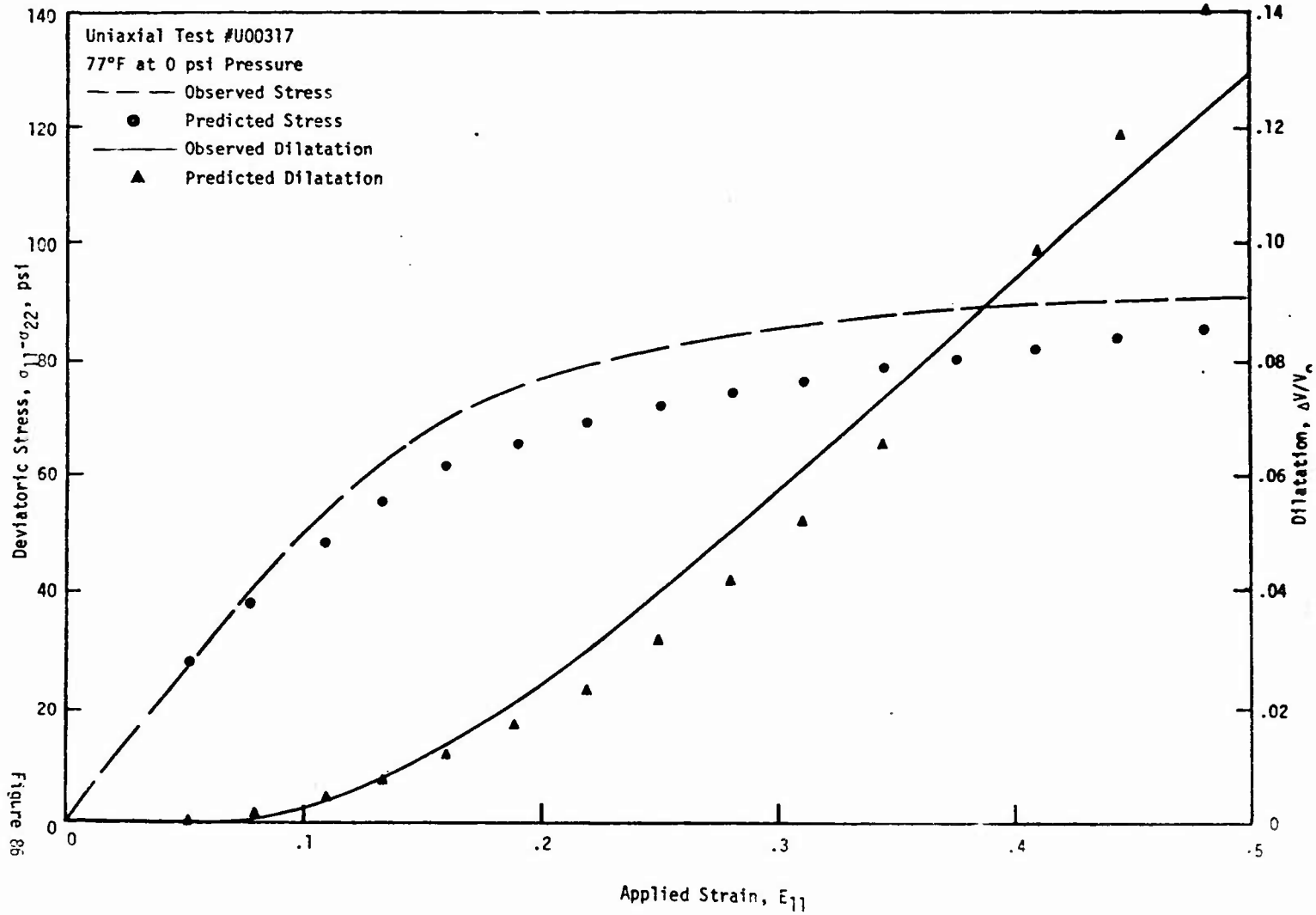

Figure 86

FIGURE 87 - COMPARISON OF PREDICTED AND OBSERVED STRESS-STRAIN-
DILATATIONAL RESPONSE FOR THE PBAN PROPELLANT
USING CHARACTERIZATION CODE NL003

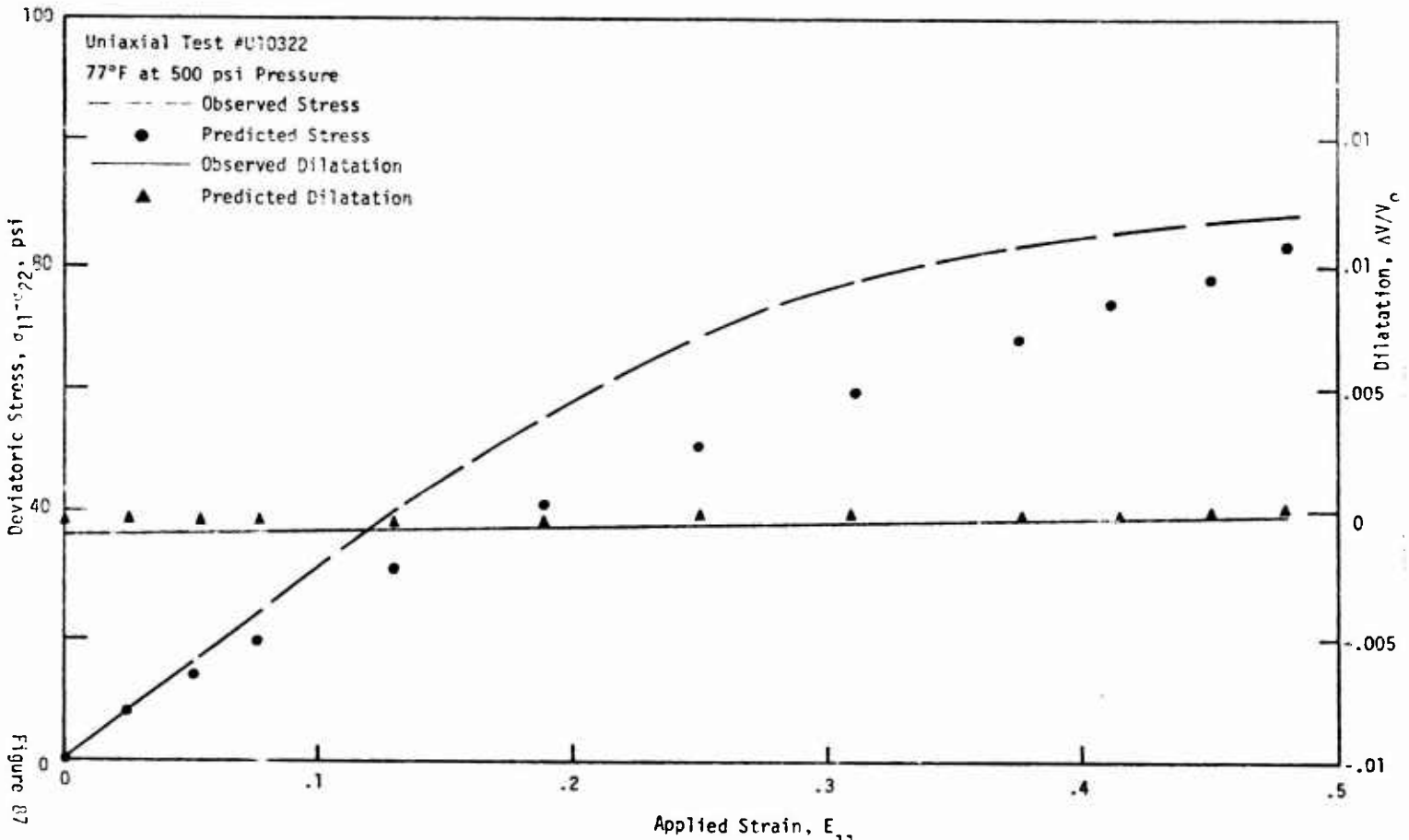

Figure 87

FIGURE 88a - COMPARISON OF PREDICTED AND OBSERVED STRESS-STRAIN-
DILATATIONAL RESPONSE FOR THE PBAN PROPELLANT
USING CHARACTERIZATION CODE NL003

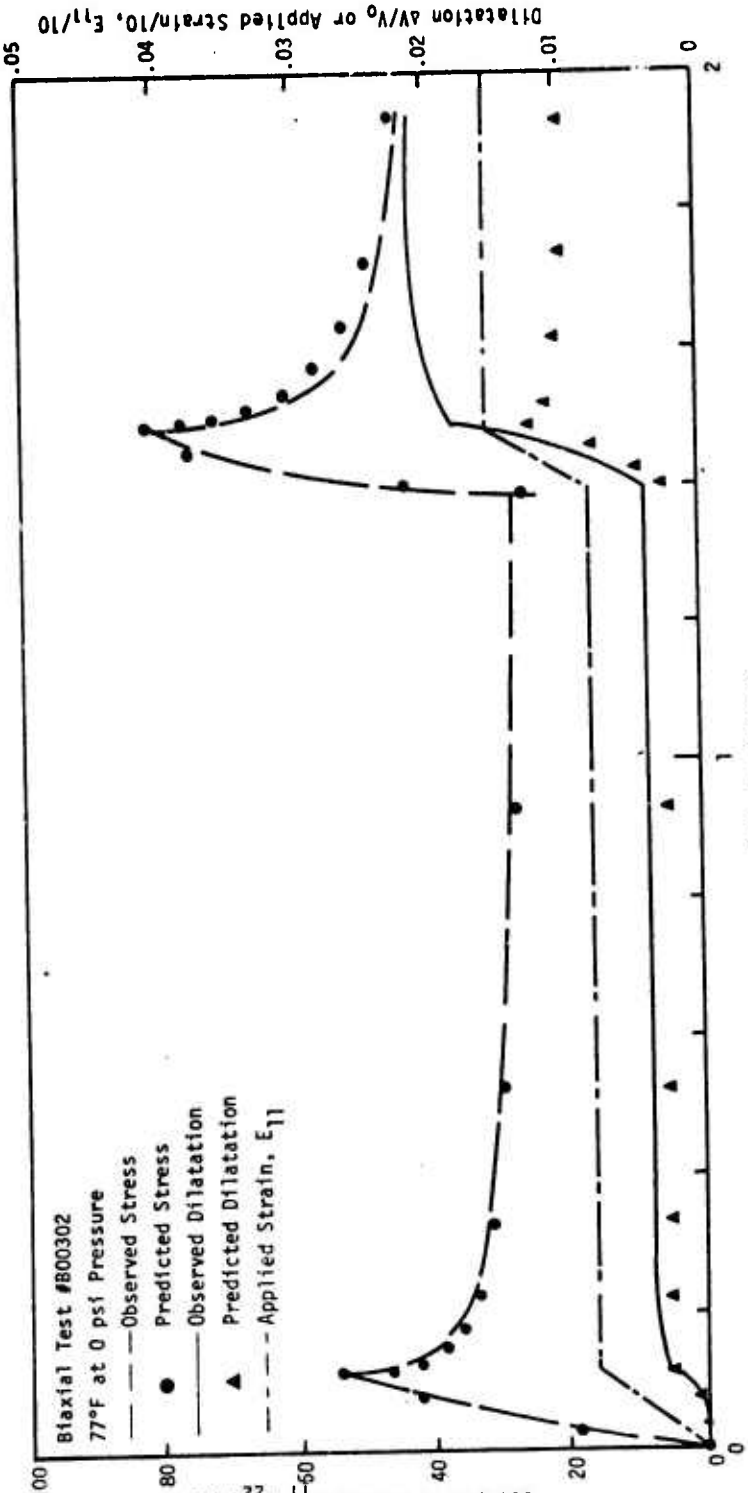

Figure 88a

FIGURE 88b - COMPARISON OF PREDICTED AND OBSERVED STRESS-STRAIN-DILATATIONAL RESPONSE FOR THE PBAN PROPELLANT USING CHARACTERIZATION CODE NL003

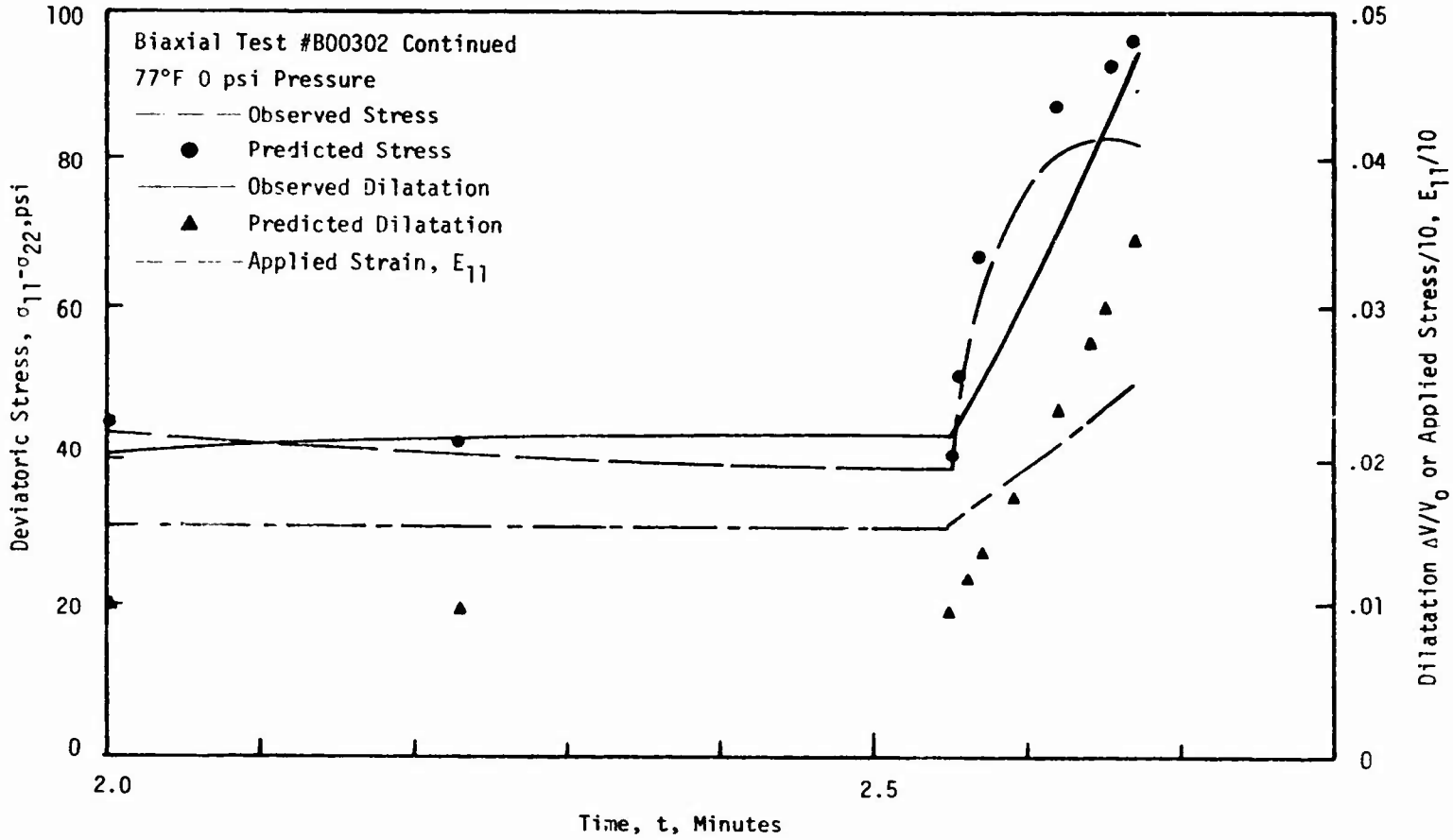

Figure 88b

FIGURE 89 - COMPARISON OF PREDICTED AND OBSERVED STRESS-STRAIN-DILATATIONAL RESPONSE FOR THE PBAN PROPELLANT USING CHARACTERIZATION CODE NL003

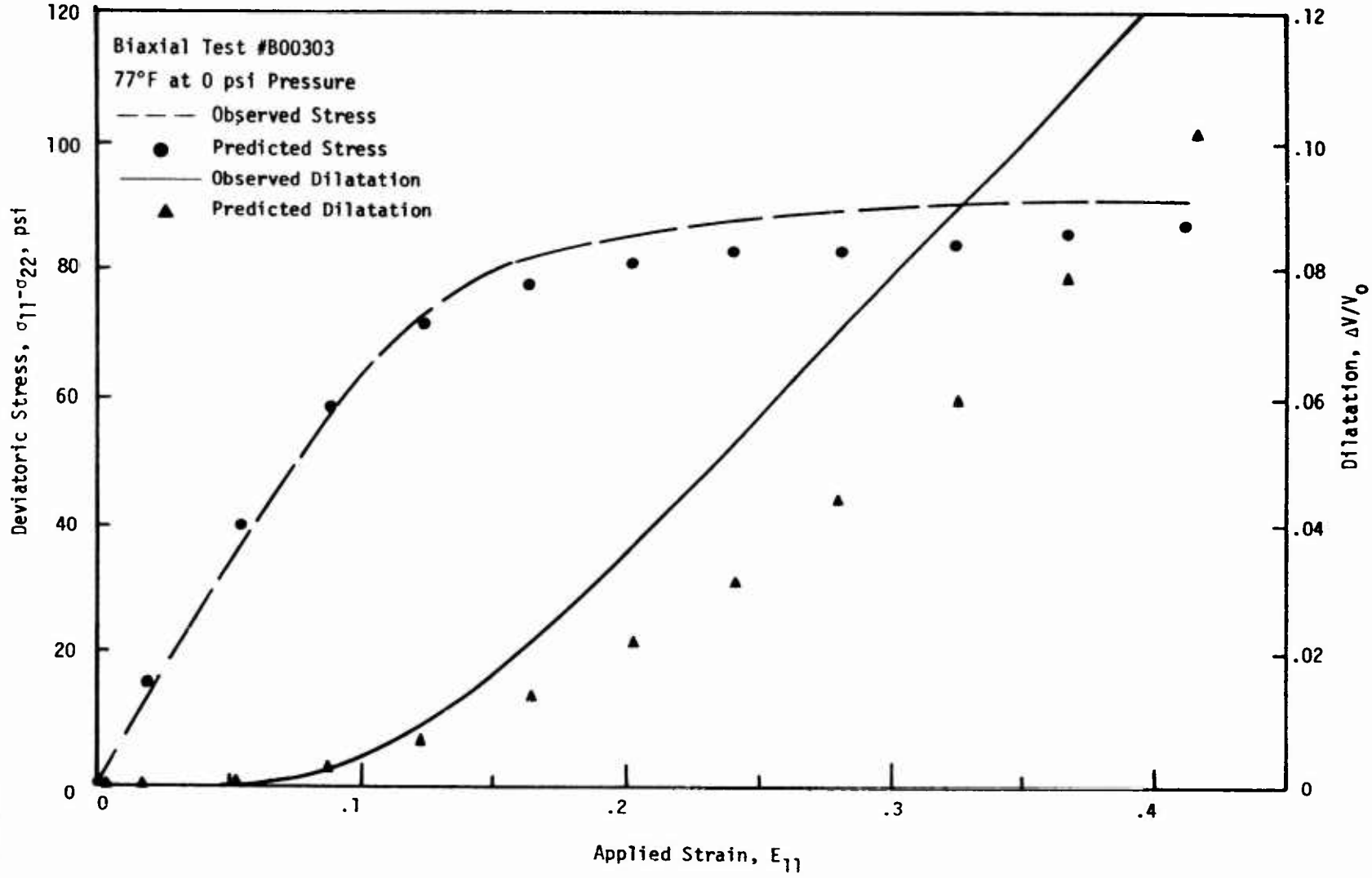

Figure 89

FIGURE 90a - COMPARISON OF PREDICTED AND OBSERVED STRESS-STRAIN-
DILATATIONAL RESPONSE FOR THE PBAN PROPELLANT
USING CHARACTERIZATION CODE NL003

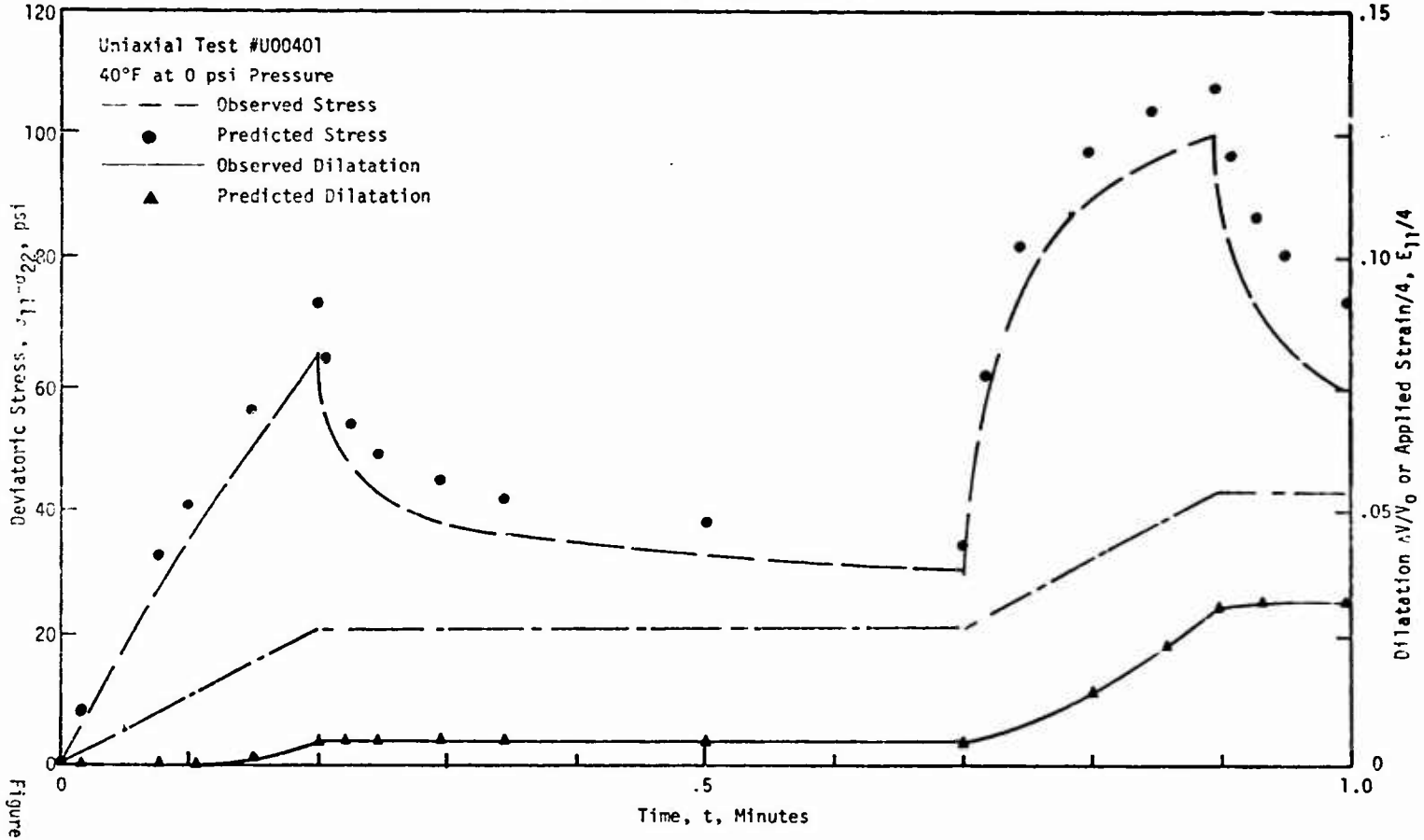

Figure 90a

FIGURE 90b - COMPARISON OF PREDICTED AND OBSERVED STRESS-STRAIN-
DILATATIONAL RESPONSE FOR THE PBAN PROPELLANT
USING CHARACTERIZATION CODE NL003

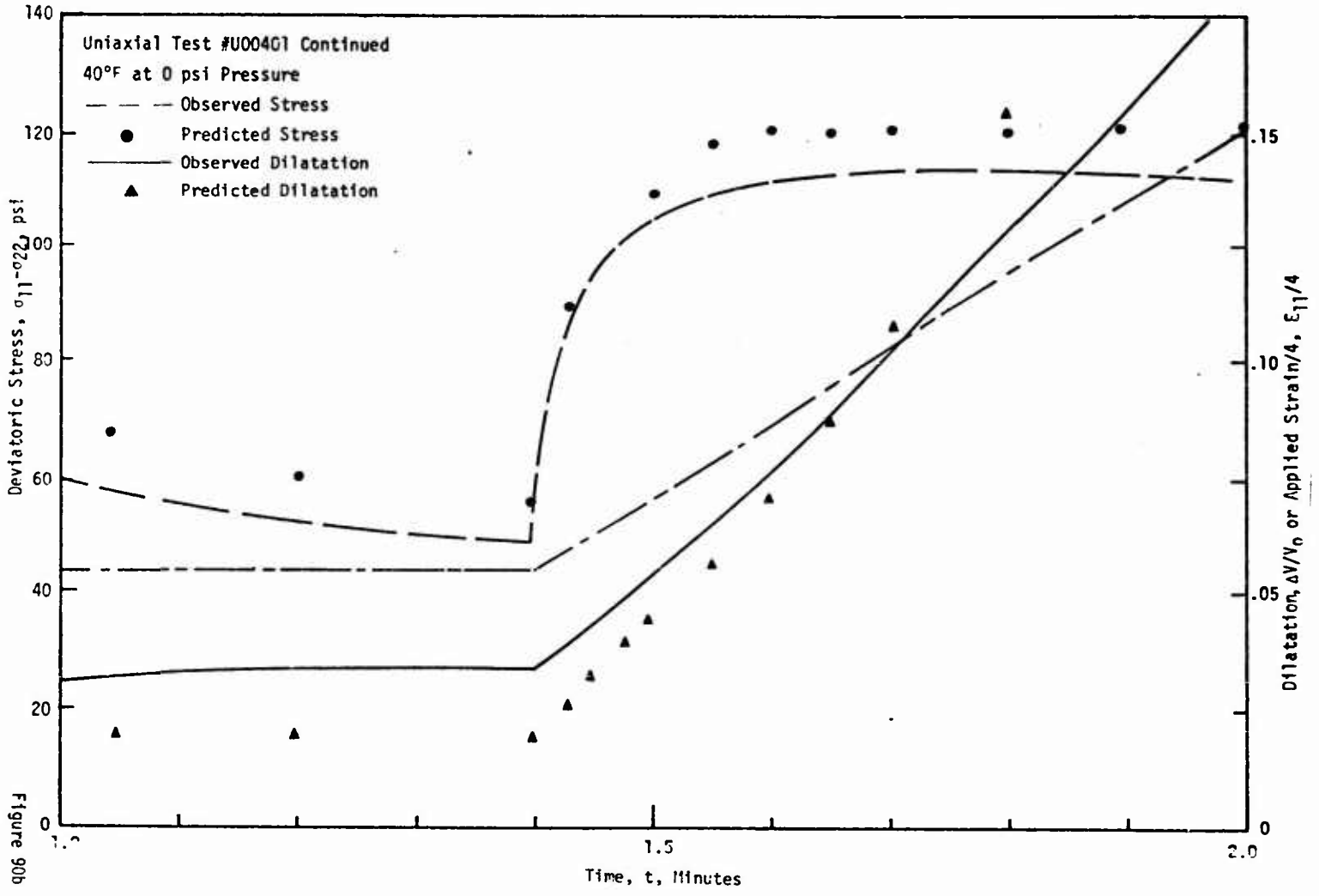

Figure 90b

FIGURE 91 - COMPARISON OF PREDICTED AND OBSERVED STRESS-STRAIN-
DILATATIONAL RESPONSE FOR THE PBAN PROPELLANT
USING CHARACTERIZATION CODE NL003

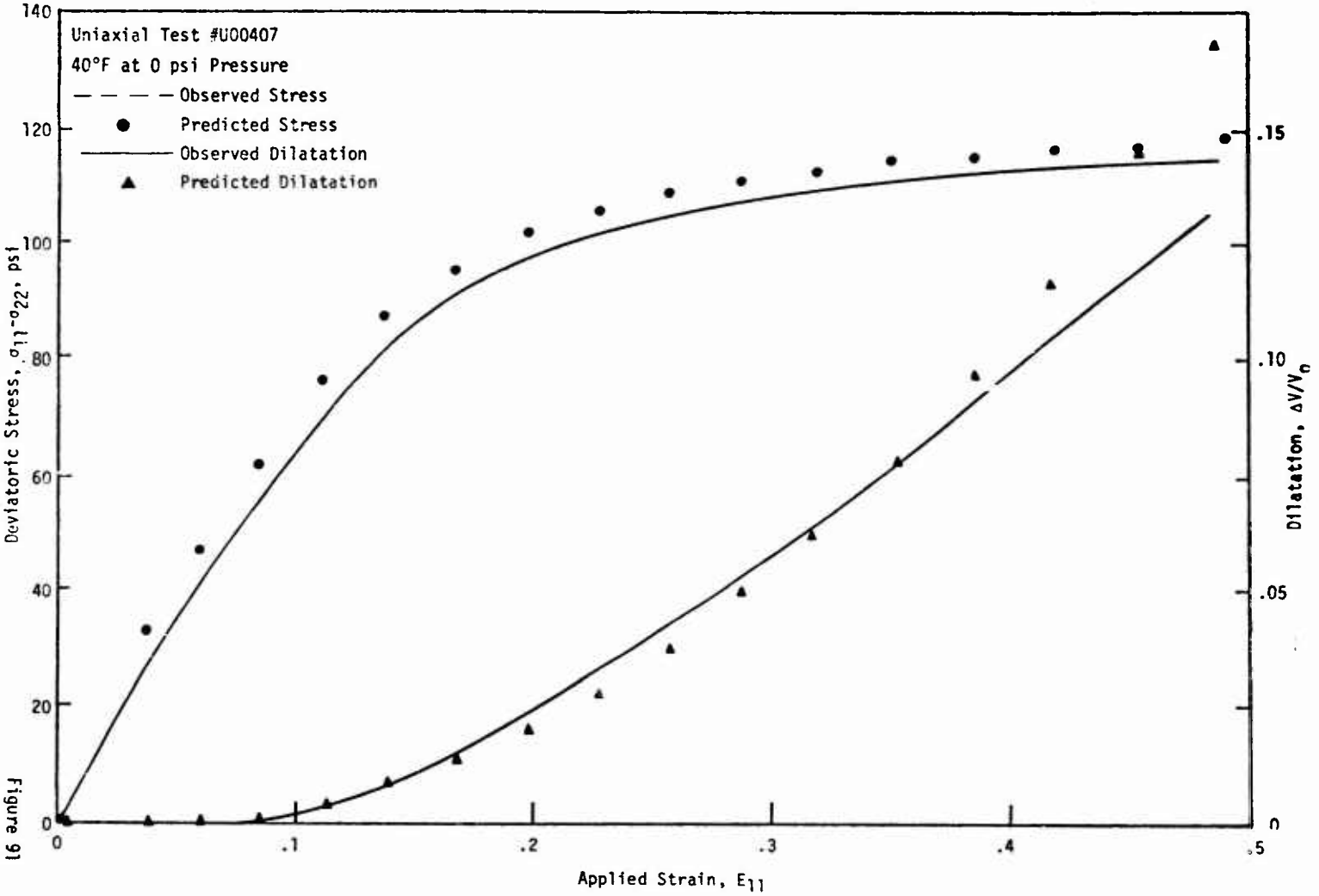

Figure 91

FIGURE 92 - COMPARISON OF PREDICTED AND OBSERVED STRESS-STRAIN-
DILATATIONAL RESPONSE FOR THE PBAN PROPELLANT
USING CHARACTERIZATION CODE NL003

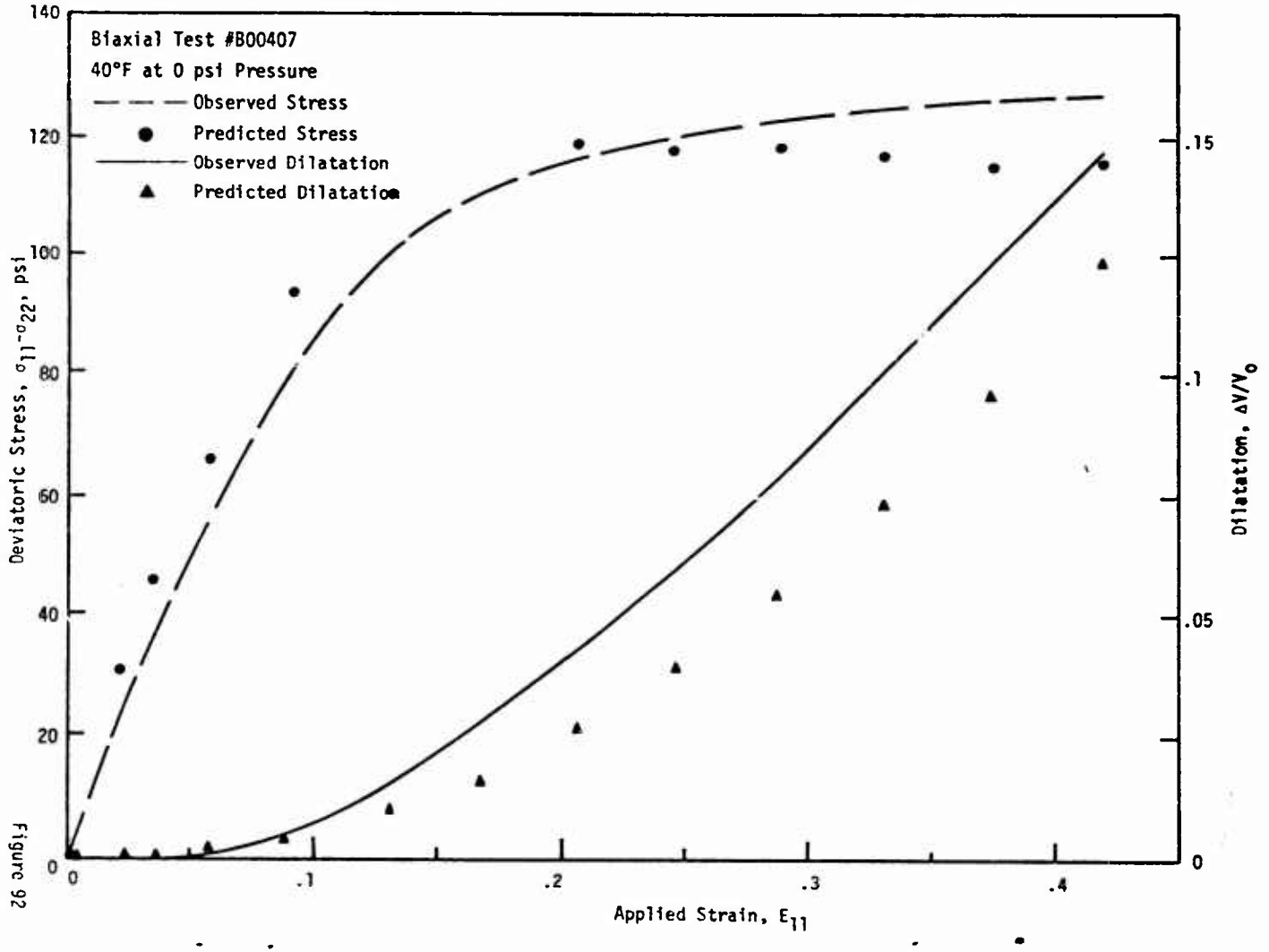

Figure 92

FIGURE 93 - COMPARISON OF PREDICTED AND OBSERVED STRESS-STRAIN-
DILATATIONAL RESPONSE FOR THE PBAN PROPELLANT
USING CHARACTERIZATION CODE NL003

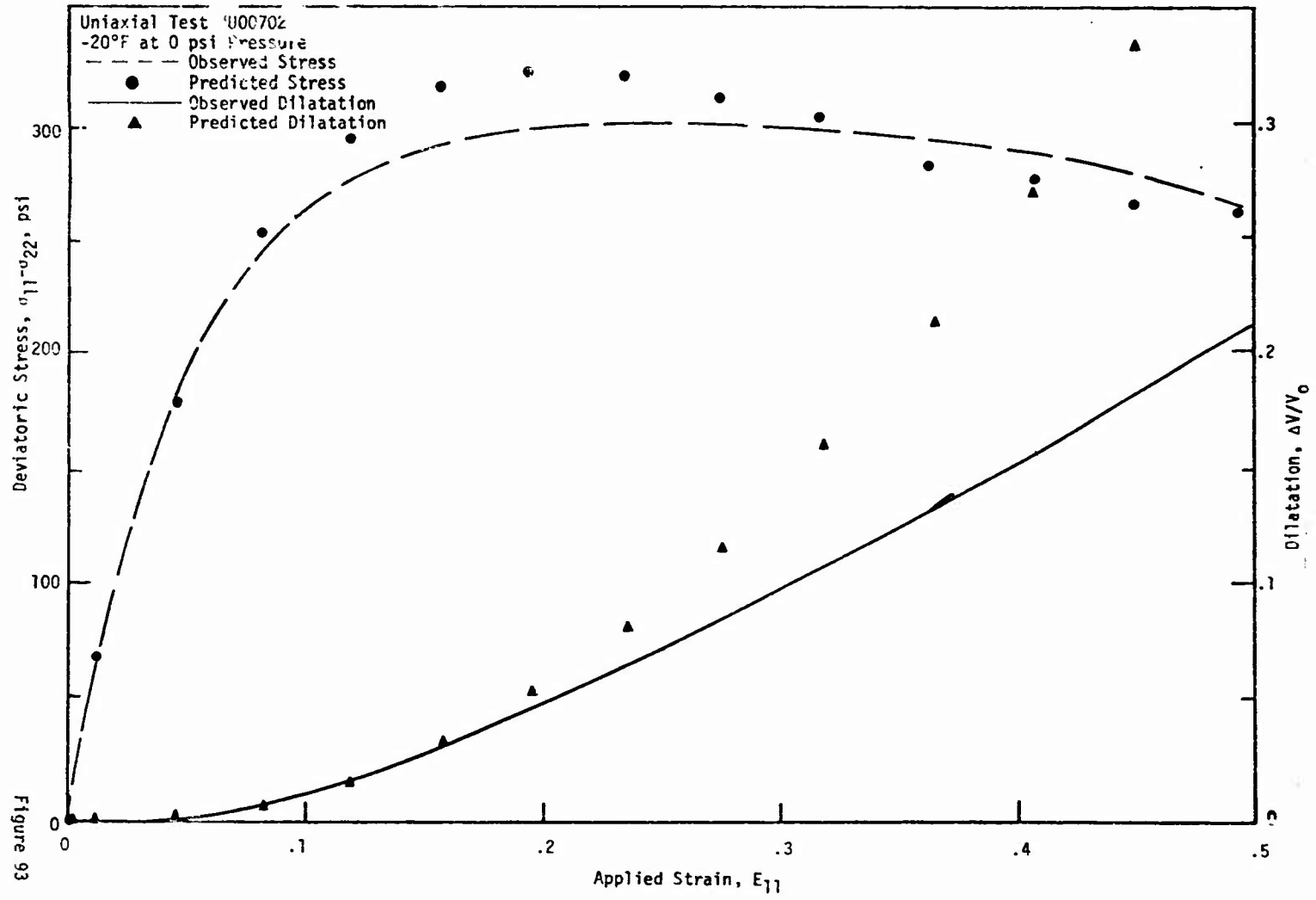

Figure 93

FIGURE 94 - COMPARISON OF PREDICTED AND OBSERVED STRESS-STRAIN-DILATATIONAL RESPONSE FOR THE PBAN PROPELLANT USING CHARACTERIZATION CODE NL003

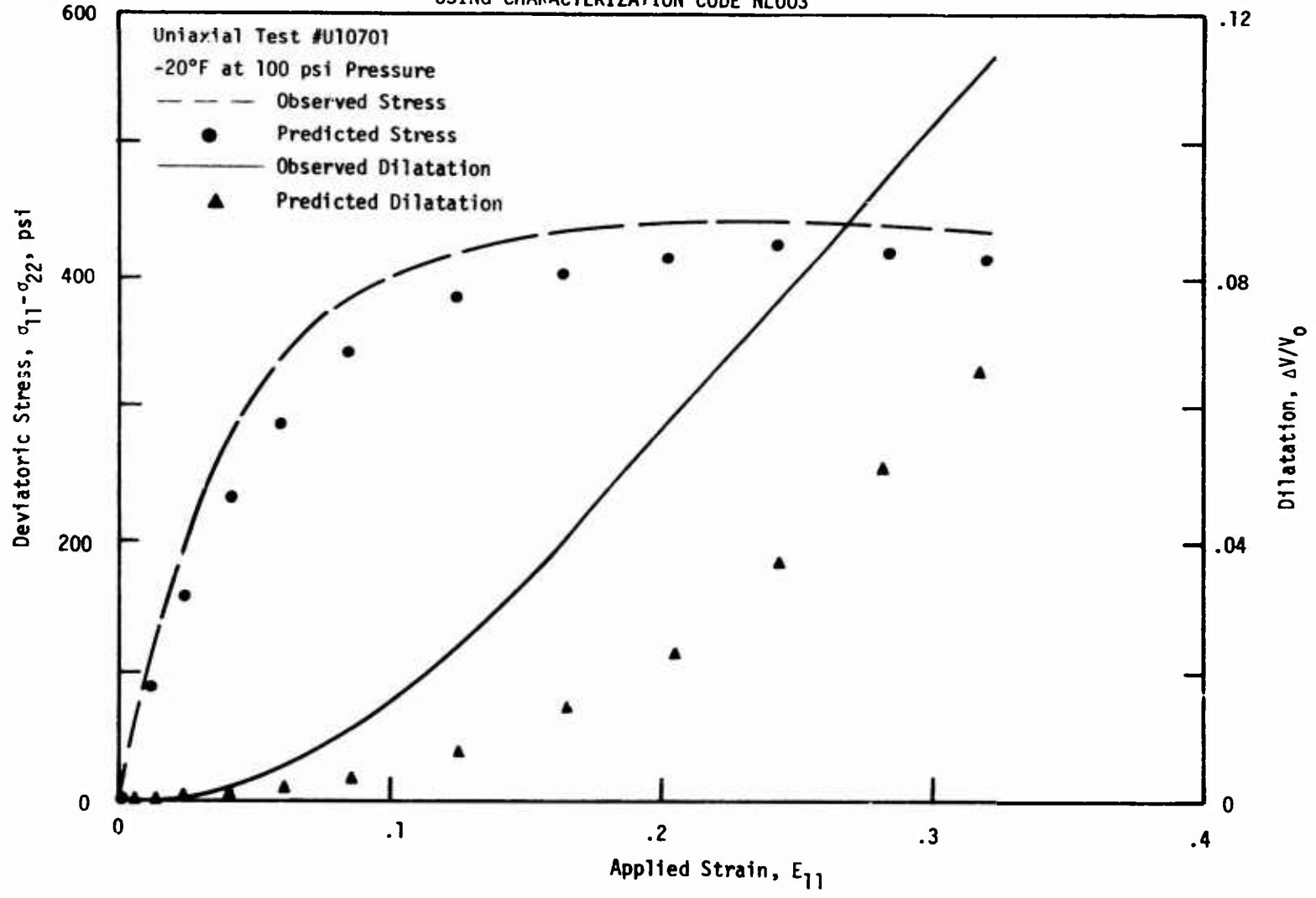

Figure 94

FIGURE 95 - COMPARISON OF PREDICTED AND OBSERVED STRESS-STRAIN-
DILATATIONAL RESPONSE FOR THE PBAN PROPELLANT
USING CHARACTERIZATION CODE NL003

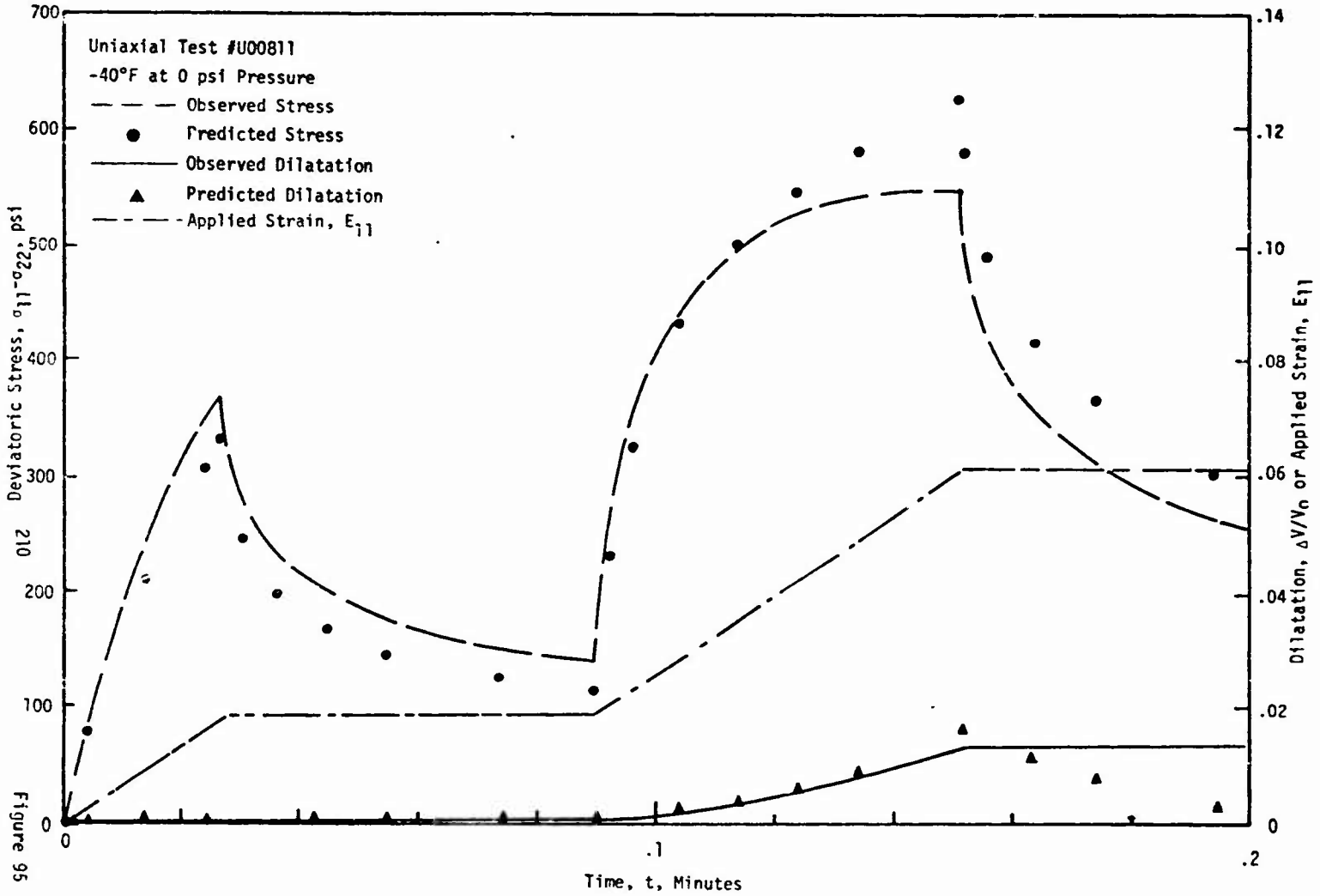

Figure 95

FIGURE 96 - COMPARISON OF PREDICTED AND OBSERVED STRESS-STRAIN-DILATATIONAL RESPONSE FOR THE PBAN PROPELLANT USING CHARACTERIZATION CODE NL003

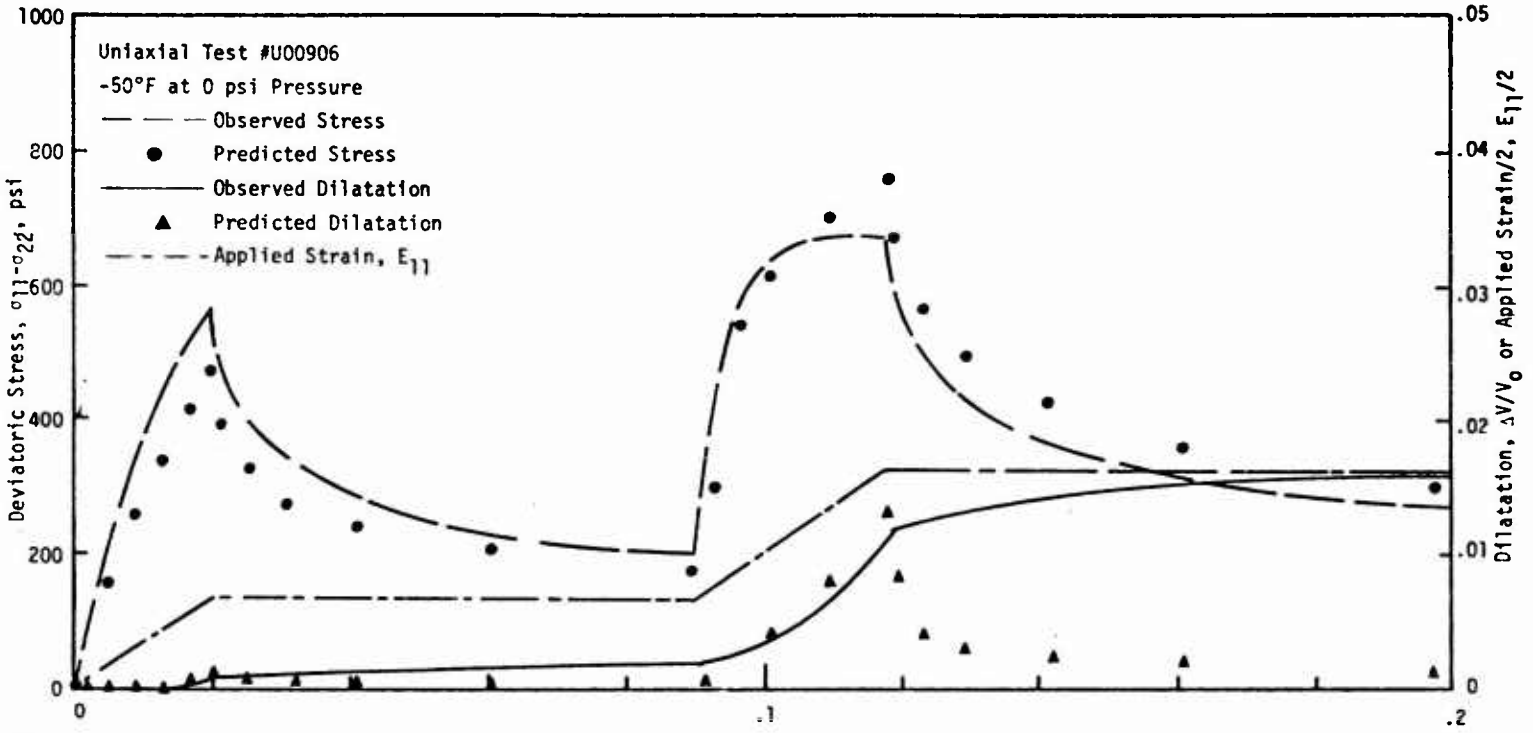

Figure 96

SECTION IV

RECOMMENDATIONS FOR FUTURE WORK

Although this contract was successful in meeting its objectives considerable work still must be accomplished before rocket grains can be analyzed using realistic constitutive modeling for general loading conditions. Many of these problems will be solved on Aerojet's follow-on contract, F04611-71-C-0046, which again is being sponsored by the Air Force Rocket Propulsion Laboratory, Edwards, California. However, even after successful completion of those goals many characteristics of propellant behavior important to a structural analysis will still not be included. The discussion below describes the objectives of the follow-on contract and identifies additional problems not contained in the follow-on effort.

1. Follow-on Effort

The follow-on effort is a twelve month contract which began on 15 May 1973. Technical support on this contract will come from Professor R. A. Schapery, Texas A&M University, and Professors L. R. Herrmann and J. R. Hutchinson, University of California, Davis. The program consists of four tasks which are discussed below.

(1) Task I - Automatic Constitutive Characterization Code

This effort will consist of developing a computerized multiaxial nonlinear viscoelastic characterization code applicable to propellant materials. It will contain a representation that is as simple as possible yet contains propellant behavior. The code will be capable of handling large masses of experimental data and will completely determine all unknown parameters in the constitutive representation, including the time-temperature shift function and nonlinear exponents. The linear coefficients are the only parameters obtained from the current analyses methods, all others must be estimated. In addition to the response characterization the code will also perform a failure characterization based on nonlinear cumulative damage theory. This code will be a user oriented tool and will include many numerical refinements to streamline its operation. The intent is to produce a response and failure characterization code for which the user need not be an expert in the theories being employed.

(2) Task II - Characterization Code Demonstration

In addition to the data obtained on the current contract, three additional propellants will be experimentally characterized. These data will be input to the characterization code to provide a test of both

the viscoelastic theory the failure theory, and the numerical methods being employed. The propellants are to include a Hercules double base propellant, a Thiokol 90% solids HTPB propellant and an Aerojet fast burning HTPB formulation.

(3) Task III - Finite Element Computer Code Development

This phase of the contract will be devoted to the goal of developing computerized nonlinear thermoviscoelastic structural analysis methods based on finite element procedures. The code will be designed to handle quasistatic one and two dimensional problems for multilayered materials in cylindrical geometries, including an elastic motor case. The loads considered will be time varying pressure, gravity, and transient thermal conditions. The constitutive theory utilized for the propellant will be the nonlinear viscoelastic equations developed on the current contract and will include strain dilatation. The finite element code will be designed to utilize as input all the information generated by the characterization code including the cumulative damage failure characterization. In this sense the finite element code will be capable of both stress and strain analyses, as well as failure predictions.

(4) Task IV - Finite Element Code Demonstration

The purpose of Task IV is to verify the validity of the finite element computer code developed in Task III by comparing analytical predictions with experimental observations on instrumented small propellant grains. Actually Task IV checks not only the finite element code but also the constitutive representation and the heat conduction equations as well. The experiments to be performed are (1) transient thermal bond stress and bore displacement measurements on small case bonded grains using through-the-case transducers, and (2) isothermal pressurization experiments in caseless grains where both inner and outer dimensional changes are monitored. These experiments will be conducted using the Aerojet propellant.

In addition nonlinear predictions will be compared to experimental observations using samples with complex geometries so as to produce spatial gradients of stress and strain. These experiments will be conducted on all three propellants.

2. Remaining Problems

(1) Aging Effects

Even after the problems of improved analysis methods and failure criteria are successfully handled for unaged propellants the accuracy of grain structural integrity evaluations will still be subjected to the limitations imposed by inadequate knowledge of propellant aging behavior.

If the propellant were aged while in the unstressed state, or if the propellant were truly elastic, the problem would be quite simple, since only a recharacterization of the properties would be required. However, when aging occurs under conditions of stress and strain, the problem is most complex, even if the aging process is not coupled by stress. The differences between aging then deforming, deforming then aging, or deforming and aging simultaneously can result in stress differences at the end points in time as large as those observed when specimens are cooled then stretched, stretched then cooled, or cooled and stretched simultaneously. Obviously, the aging stress-strain functional should be very path sensitive. Experimental observations indicate that during aging under deformed conditions such things as postcure, oxidative crosslinking, or any mechanism leading to chain scission and reformation can cause large changes in grain stress-free temperature, or stress-free configuration.

Today aged propellant structures are generally treated as though they were purely elastic, that is, their reference stress-free configurations never changes, and the aging process is not stress or strain-coupled. This is a gross oversimplification. It is interesting to note from the work of Tobolsky[37] that many crosslinked amorphous polymeric materials, which are normally thought of as elastic, can undergo large amounts of permanent set or changes in reference configuration during aging while exhibiting little or no change in response properties. Similar behavior has been observed with propellants but it usually receives little attention in normal aging evaluations, even though the shifting in the stress-free configuration for many systems is probably more important to consider in an analysis than changes in response properties.

The need for aging type constitutive equations will be very difficult to satisfy for many reasons. First, aging is a chemical phenomenon which in itself is not clearly understood. Secondly, aging-type constitutive equations are in principle easy to construct, but in practice interpreting the chemical or physical phenomenon in an abstract mathematical functional relationship will require a significant effort. Further, to make the mathematical development possible the proper types of experimental data must be obtained. Currently, all that is done is to age and then test. What is really required is to test and age simultaneously, something that is relatively difficult and rarely done except in real motors. Again, to make this informatin useful stress analysis programs would have to be rewritten to account for the aging phenonomenon.

Because of the many complexities involved characterization and stress analysis of aged grains will continue to be a major problem for some time unless an organized, systematic attack upon the areas of deficiency is mounted soon. Any insight gained into the chemical-mechanical response of aged grains is valuable and can be used qualitatively, if not quantitatively.

Conventionally, aging studies are conducted by chemists or statisticians with little training or experience in the area of applied mechanics. Aging tests historically have not been designed to characterize the material response, but as quality control tests which hopefully will show trends and give some estimate of useful life. Factors important to a stress analysis, such as changes in reference configuration, are rarely, if ever, considered.

With the recent advances made in materials characterization[1-3] the necessary tools are now available to approach this problem realistically with a reasonable chance of making significant progress. Therefore, it is recommended that this special study program be funded by the Air Force for the purpose of studying the theoretical and experimental aspects of aging from an applied mechanics point of view. Such a program, properly conceived and conducted, will go far toward accelerating the development of improved stress analysis methods for aged grains and increasing the reliability of techniques for service life prediction.

In summary, good constitutive theory and good analysis methods are needed for unaged propellant grains to initially design a good system. Aging constitutive equations are needed to predict what will happen to that system with time, and thereby allow determination of environmental restrictions and margins of safety required in the initial design to assure a successful storage and service life.

(2) Dynamic Response

The main effort to date has been associated with describing the mechanical response due to quasi-static conditions. Also of importance is the response of propellants to high frequency cyclic loading conditions. Because of the difficulties in measuring the total strain state under these conditions this type of data has not been used in the equation development. Considerable data however suggests that the vibration response should be highly strain sensitive and depend strongly upon constant superimposed deformation states. Currently dynamic linear viscoelastic analyses are used in the design of rocket grains however to handle nonlinearities of the type observed in the quasi-static analyses situation would be very difficult. The dynamic problem would be a natural extension of the current refinement work if these efforts are highly successful.

REFERENCES

1. Farris, R. J., "Homogeneous Constitutive Equations for Materials with Permanent Memory," Ph.D. Dissertation, College of Engineering, University of Utah (June 1970).

2. Farris, R. J., "Applications of Viscoelasticity to Filled Materials," Master's Thesis, University of Utah, Department of Civil Eng. (June 1969).

3. Leeming, H. et. al., "Final Report, Solid Propellant Structural Test Vehicle and Systems Analysis," Lockheed Propulsion Company Technical Report AFRPL-TR-70-10.

4. Bornstein, G. A., "Transient Thermoviscoelastic Analysis of a Uniaxial Bar," Bulletin of the 7th ICRPG Mechanical Behavior Working Group, Vol. 1, CPIA Pub. No. 177, page 23 (1968).

5. Farris, R. J., "Dilatation of Granular Filled Elastomers Under High Rates of Strain," J. Appl. Polymer Sci., 8, page 25 (1964).

6. Farris, R. J., "The Character of the Stress-Strain Function for Solid Propellants," Trans. Soc. Rheol., 12, 308-315 (1968).

7. Farris, R. J., "The Influence of Vacuole Formation on the Response and Failure of Highly Filled Polymers," Trans. Soc. Rheol., 12, 315-334 (1968).

8. Farris, R. J., "Prediction of the Viscosity of Multimodal Suspensions from Unimodal Viscosity Data," Trans. Soc. Rheol., 12, 281-302 (1968).

9. "Applications of Non-Linear Viscoelasticity and Cumulative Damage (A Realistic Evaluation of Real Propellant Behavior)" NOSC Contract No. N00017-70-C-4441, Aerojet Solid Propulsion Company, Final Report 1565-26F, May 1971.

10. Green, A. E., and Rivlin, R. S., "The Mechanics of Non-Linear Materials with Memory, Part One," Arch. Rat. Mech. Anal., 1, 1-21 (1959).

11. Green, A. E., Rivlin, R. S., and Spencer, A. J. M., "The Mechanics of Non-Linear Materials with Memory, Part Two," Arch. Rat. Mech. Anal., 3, 82-90 (1959).

12. Green, A. E., and Rivlin, R. S., "The Mechanics of Non-Linear Materials with Memory, Part Three," Arch. Rat. Mech. Anal., 4, 387-404 (1959).

13. Rivlin, R. S., "Non-Linear Viscoelastic Solids," SIAM Review, 7, 323-340 (1965).

REFERENCES (Cont.)

14. Coleman, B. D., "Thermodynamics of Materials with Memory," Arch. Rat. Mech. Anal., 17, 1-46 (1965).

15. Coleman, B. D. and Noll, W., "Foundations of Linear Viscoelasticity," Rev. Mod. Phys., 33, 239-249 (1961).

16. Coleman, B. D., and Noll, W., "An Approximation Theorem for Functionals with Applications in Continuum Mechanics," Arch. Rat. Mech. Anal., 6, 355-370 (1960).

17. Noll, W., "A Mathematical Theory of the Mechanical Behavior of Continuous Media," Arch. Rat. Mech. Anal., 2 (1958).

18. Noll, W., "On the Continuity of Solid and Fluid States," J. Rat. Mech. Anal., 4, 3-81 (1955).

19. Truesdell, C., The Elements of Continuum Mechanics, Springer-Verlag, Inc., New York (1966).

20. Truesdell, C., ed., Continuum Mechanics (Reprints), New York: Gordon and Breach, Vol. 1, 1966; Vols 2, 3, 4 (1965).

21. Wang, C. C., "Stress Relaxation and the Principle of Fading Memory," Arch. Rat. Mech. Anal., 18, 117-226 (1965).

22. Wang, C. C., "The Principle of Fading Memory," Arch. Rat. Mech. Anal., 18, 343-366 (1964).

23. Volterra, V., Theory of Functionals and of Integral and Integro-Differential Equations, Dover Publications, Inc., New York (1959).

24. Pipkin, A. C., "Small Finite Deformations of Viscoelastic Solids," Rev. Mod. Phys., 36, 1034-1041 (1965).

25. Pipkin, A. C., and Rogers, T. G., "A Non-Linear Integral Representation for Viscoelastic Behavior," J. Mech. Phys. Solids, 16, 59-72 (1968).

26. Herrmann, L. R., "On a General Theory of Viscoelasticity," J. Franklin Inst., 280, 244-255 (1965).

27. McGuirt, C. W., and Lianis, G., "Experimental Investigation of Non-Linear Non-Isothermal Viscoelasticity," Int. J. Eng. Sci., 7, 579-599 (1969).

28. Goldberg, W., and Lianis, G., "Stress Relaxation in Combined Torsion-Tension," Quarterly Transactions of ASME, Vol. 37, Series E, #1, J. Appl. Mech., 53-60, (March 1970).

REFERENCES (Cont.)

29. Lianis, G., "Integral Constitutive Equations on Non-Linear Thermo-Visco-Elasticity,) Purdue University Report, Astronautics and Engineering Sciences, 65-1 (1965).

30. Shapery, R. A., "A Theory of Non-Linear Thermoviscoelasticity Based on Irreversible Thermodynamics," Proc. Fifth U. S. Nat. Cong. of Appl. Mech., ASME, 511-530 (1966).

31. Shapery, R. A., "On the Characterization of Non-Linear Viscoelastic Materials," Polymer Eng. Sci., 9, 295-310 (1969.

32. Shapery, R. A., "On a Thermodynamic Constitutive Theory and its Application to Various Nonlinear Materials," Proc. IUTAM Symp. on Thermoelasticity, Springer-Verlag (1969).

33. Huang, N. C. and Lee, E. H., "Nonlinear Viscoelasticity for Short Time Ranges," J. Appl. Mech., Trans. ASME, 313 (June 1966).

34. Dong, R. G., "Constitutive Equations Involving Chronological Variables," University of California Radiation Laboratory Report 12228, Livermore, California (Dec. 1964).

35. Dong, R. G., "Studies in Mechanics of Non-Linear Solids," Ph.D. Dissertation, University of California, Livermore, Lawrence Radiation Lab. (1964).

36. Williams, M. L., "Structural Analysis of Viscoelastic Materials," AIAA J., 2, 785-808 (1964).

37. Tobolsky, A. V., Properties and Structure of Polymers, 160, John Wiley and Sons, Inc., New York (1960).

38. Tobolsky, A. V., "Stress Relaxation Studies on the Viscoelastic Properties of Polymers," in Rheology, ed. F. R. Erich, 2, 63-81, New York, Academic Press Inc. (1958).

39. Alfrey, T., Mechanical Behavior of High Polymers, New York; Interscience Publishers, Inc. (1948).

40. Ferry, J. D., Viscoelastic Properties of Polymers, New York: John Wiley and Sons, Inc. (1961).

41. Fréchet, M., "Sur Les Fonctionnelles Continues," Ann. de L'Ecole Normale Sup., 27, 3rd Series (1910).

42. Eringen, A. C., Mechanics of Continua, John Wiley and Sons, Inc., New York (1967).

43. Eringen, A. C., Non-Linear Theory of Continuous Media, McGraw-Hill Book Co., New York (1962).

44. Malvern, L. E., Introduction to the Mechanics of a Continuous Media, Prentice-Hall, Inc., New Jersey (1969).

45. Coleman, B. D. and Mizel, V. J., "On the General Theory of Fading Memory," Arch. Rat. Mech. Anal., 29, 19-31 (1968).

46. Coleman, B. D. and Mizel, V. J., "Norms and Semi-Groups in the Theory of Fading Memory," Arch. Rat. Mech. Anal., 23, 88-123 (1966).

47. Rivlin, R. J., "Red Herrings and Sunday Unidentified Fish in Nonlinear Continuum Mechanics," Tech. Report No. CAM-100-9 (Sept. 1969), Center for the Application of Mathematics, LeHigh University.

48. Eringen, N. C. and Grot, R. A., "Continuum Theory of Nonlinear Viscoelasticity," Mechanics and Chemistry of Solid Propellants, Proc. 4th Symp. on Naval Structural Mechanics, Pergammon Press (1965).

49. Oldroyd, J. G., "On the Formulation of Rheological Equations of State," Royal Society Proceedings, Series A., 200 (1949).

50. Hsiao, C. C., Moghe, S. R. and Von Schmelling, H. H. R., "Time-Dependent Mechanical Strength of Oriented Media," J. Appl. Phys., 39, 3857-3861 (1968).

51. Nakada, O., "Theory of Nonlinear Responses," J. Physical Soc. of Japan, 15, No. 12, 2280-2288 (1960).

52. Lai, J. S. Y. and Findley, W. N., "Prediction of Uniaxial Stress Relaxation from Creep of Nonlinear Viscoelastic Media," Trans. Soc. Rheol., 12, 243-258 (1968).

53. Lai, J. S. Y. and Findley, W. N., "Stress Relaxations of Nonlinear Viscoelastic Material Under Uniaxial Strain," Trans. Soc. Rheol., 12, 259-280 (1968).

54. Findley, W. N. and Onaran, K., "Product Form of Kernel Functions for Nonlinear Viscoelasticity of PVC Under Constant Stresses," Trans. Soc. Rheol., 12, 217-242 (1968).

55. Onaran, K. and Findley, W. N., "Combined Stress-Creep Experiments on a Non-Linear Viscoelastic Material to Determine the Kernel Functions for a Multiple Integral Representation of Creep," Trans. Soc. Rheol., 1, 299-327 (1965).

56. Findley, W. N. and Lai, J. S. Y., "A Modified Superposition Principle Applied to Creep of Nonlinear Viscoelastic Material Under Abrupt Changes in State of Combined Stress," Trans. Soc. Rheol., 11, 361-380 (1967).

57. Lai, J. S. Y. and Findley, W. N., "Behavior of Nonlinear Viscoelastic Material Under Simultaneous Stress Relaxation and Creep in Torsion," Tech. Report No. 3. (Jan. 1968) Eng. Matls. Res. Lab., Brown University, Providence, R. I.

58. Gottenberg, W. G., Bird, J. O., Agrawal, G. L., "An Experimental Study of a Nonlinear Viscoelastic Solid in Uniaxial Tension," J. Appl. Mech. Trans. ASME, 1 (1969).

59. Lockett, F. J., and Stafford, R. O., "On Special Constitutive Relations in Non-Linear Viscoelasticity," Intern. J. Eng. Sci., 7, 917-930 (1969).

60. Lockett, F. J., "Nonlinear Viscoelasticity of Almost-Elastic Materials," Tech. Report No. 195, Dept. of Applied Mechanics, Stanford University (1969).

61. Valanis, K. C. and Landel, R. F., "Large Multiaxial Deformation Behavior of a Filled Rubber," Trans. Soc. Rheol., 11, 243-256 (1967).

62. Nicholas, T. and Freudenthal, A. M., "The Mechanical Behavior of a Filled Elastomer at High Strain Rates," Trans. Soc. Rheol., 13, 323-334 (1969).

63. Ward, I. M. and Onat, E. T., "Nonlinear Mechanical Behavior of Oriented Polypropylene," J. Mech. Phys. Solids, 11, 217-229 (1963).

64. Ward, I. M. and Wolfe, J. M., "The Nonlinear Mechanical Behavior of Polypropylene Fibres Under Complex Loading Programs," J. Mech. Phys. Solids, 14, 131-140 (1966).

65. Hadley, D. W. and Ward, I. M., "Nonlinear Creep and Recovery Behavior of Polypropylene Fibres," J. Mech. Phys. Solids, 13, 397-411 (1965).

66. Berg, C. A., "A Unified Derivation of Constitutive Relations for Irrecoverable Deformations," Trans. Soc. Rheol., 9, 159-170 (1965).

67. Kelly, J. M., "Generalization of Some Elastic-Viscoplastic Stress-Strain Relations," Trans. Soc. Rheol., 11, 55-76 (1967).

68. Neis, V. V. and Sachman, J. L., "An Experimental Study of a Nonlinear Material with Memory," Trans. Soc. Rheol., 11, 307-337 (1967).

69. Tanner, R. I., "Comparative Studies of Some Simple Viscoelastic Theories," Trans. Soc. Rheol., 12, 155-182 (1968).

70. Bird, H. B. and Marsh, B. O., "Viscoelastic Hysteresis Part I, Model Prediction; Part II, Numerical and Experimental Examples," Trans. Soc. Rheol., 12, 479-488, 489-510 (1968).

71. Adeyeri, J. B. Krizek, R. J. and Achenbach, J. D., "Muliple Integral Description of the Nonlinear Viscoelastic Behavior of a Clay Soil," Trans. Soc. Rheol., 14, 375-392 (1970).

72. Schippel, H. F., Ind. Eng. Chem., 12, 33 (1920).

73. Payne, A. R., in Composite Materials, L. Holliday, ed., Elsevier Pub. Co., N. Y., 300 (1966).

74. Mullins, L. J., "Effect of Stretching on the Properties of Rubber," J. Rubber Res., 16, 275-289 (1947).

75. Mullins, L. J., "Permanent Set in Vulcanized Rubber," Ind. Rubber World, 63-69 (1949).

76. Mullins, L. J., "Studies in the Absorption of Energy by Rubber," J. Rubber Res., 16, (1947).

77. Mullins, L. J., Rubber Chem. Tech., 21, 281 (1948).

78. Bueche, F. "Molecular Basis for the Mullins Effect," J. Appl. Polymer Sci., 4, 107-114 (1960).

79. Bueche, F., "Mullins Effect and Rubber-Filler Interaction," J. Appl. Polymer Sci., 5, 271-281 (1961).

80. Smith, T. L., Trans. Soc. Rheol., 3, 113 (1959).

81. Oberth, A. E., "Principle of Strength Reinforcement in Filled Polymers," Rubber Chem. Tech., 40, 1337-1362 (1967).

82. Neilsen, L. E., "Creep and Dynamic Mechanical Properties of Filled Polyethylenes," Trans. Soc. Rheol., 13, 141-166 (1969).

83. Freudenthal, H. M., "Strain Sensitive Response of Filled Elastomers," Tech. Report No. 24, Dept. of Civil Eng. and Eng. Mech., Columbia University.

84. Kelley, F. N., "Properties of Highly Filled Elastomers," Interagency Chemical Rocket Propulsion Group, Solid Propellant Mechanical Behavior Manual, Chemical Propulsion Information Agency Publication No. 21, Section 2.5.1 (Sept. 1963).

85. Schwarzl, F. R., "On the Mechanical Properties of Unfilled and Filled Elastomers," Mech. and Chemistry of Solid Propellants, Proc. 4th Symposium on Naval Structural Mechanics, Pergamon Press (1965).

86. Hess, W. M. and Ford, F. P., Rubber Chem. Tech., 36, 1220 (1963).

87. Dannenberg, E. M., "Properties and Performance of Rubber Fillers," Rubber Age, 85 (1959).

88. Dannenberg, E. M., "Molecular Slippage Mechanism of Reinforcement," Trans. Institute Rubber Industry, 42, 26-42 (1966).

89. Einstein, A., Ann. Physik, 19, 286, 1906, 34, 591 (1911).

90. Brinkman, H. C., Appl. Sci. Research, London, A-2, 190 (1949).

91. Roscoe, R., Brit. J. Appl. Phys., 3, 267 (1952).

92. Sweeny, K. H. and Geckler, R. D., J. Appl. Phys., 25, 1135 (1954).

93. Robinson, J. V., Proc. Phys. Soc., 4, 338 (1949).

94. Fidleris, V. and Whitmore, R. L., Rheologica Acta, 1, No. 4-6 (1961).

95. Mooney, M., J. Colloid Sci., 6 (1951).

96. Vand, V., J. Phys. Colloid Chem., 52, 277 (1948).

97. Eilers, H., Kolloid Zeit, 102, 154 (1954).

98. Chung, J. S., "Rheology of Concentrated Suspensions," Ph.D. Thesis, University of Utah (1962).

99. Schwarzl, F. W., Bree, H. W. and Struik, L. C., ICRPG Bulletin, 5th Meeting, Working Group on Mech. Behavior, CPIA Pub. No. 119, 1, 133 (1966).

100. Blatz, P. J., McQuarrie, D. A. and Shen, M. C., "On the Simple Tensile Deformation of an Incompressible Rubber Matrix Filled with Non-Adherent Rigid Spheres of Uniform Size Distribution," ICRPG Mech. Beh. Working Group, CPIA Pub. 119, 1, 121-132 (1966).

REFERENCES (Cont.)

101. Rinde, J. A., "Application of Finite Viscoelastic Theory to Solid Propellants," Bulletin of 4th ICRPG Working Group on Mech. Behavior, CPIA Pub. 94U, 243-254 (1965).

102. Williams, M. L., Blatz, P. J. and Schapery, R. A., "Fundamental Studies Relations to Systems Analysis of Solid Propellants," GALCIT SM 61-S, California Institute of Technology, Pasadena, California, Feb. 1961. Also published in Interagency Chemical Rocket Propulsion Group, Solid Propellant Mechanical Behavior Manual, Chemical Propulsion Information Agency, Pub. No. 21, Section 2.3 (1963).

103. Farris, R. J., and Fitzgerald, J. E., "Deficiencies of Viscoelastic Theories as Applied to Solid Propellants," Presented at the First JANNAF Meeting, Working Group on Mechanical Behavior, U. S. Naval Weapons Center, China Lake, California (Nov. 1969).

104. Bills, K. W., Jr., Svob, G. J., Planck, R. W. and Erickson, T. L., "A Cumulative-Damage Concept for Propellant-Liner Bonds in Solid Rocket Motors," J. of Spacecraft, 3, 408-412 (1966).

105. Beyer, R. B., "Dependence of Solid Propellant Failure Properties on Binder Network Characteristics and Filler Content," ICRPG Mech. Behavior Working Group, CPIA Pub. 119, 1, 83-120 (Oct. 1966).

106. Ledbetter, W. B. and Elliott, P. M., "Microstructural Damage and Its Influence on the Dilational-Strain Properties of a Filled Elastomeric Material," Bulletin of 7th ICRPG Mech. Beh. Working Group (Nov. 1967).

107. Treloar, L. R. G., The Physics of Rubber Elasticity, Oxford, Clarendon Press (1949).

108. Miner, M. A., "Cumulative Damage in Fatigue," J. Appl. Mech., 12, 159-164 (1945).

109. Robinson, E. L., "Effect of Temperature Variation on the Long-Time Rupture Strength of Steels," Trans. ASME, 74, 777-780 (1952).

110. Tobolsky, A. and Eyrins, H., "Mechanical Properties of Polymeric Materials," J. Chem. Phys., 11, 125-134 (1943).

111. Eyring, H., "Viscosity, Plasticity, and Diffusion as Examples of Absolute Reaction Rates," J. Chem. Phys., 4, 283-291 (1936).

112. Andrews, E. H., Fracture in Polymers, American Elsevier, New York (1968).

113. Coleman, B. D., "Application of the Theory of Absolute Reaction Rates to the Creep Failure of Polymeric Filaments," J. Pol. Sci., 20, 447-455 (1956).

114. Zhurkov, S. N., "Kinetic Concept of the Strength of Solids," Int. J. Fract. Mech., 1, 311-323 (1965).

115. Henderson, C. B., Graham, P. H. and Robinson, C. N., "A Comparison of Reaction Rate Models for the Fracture of Solids," Int. J. Fract. Mech., 6, 33-40 (1970).

116. Iwan, W. D., "A Distributed-Element Model for Hysteresis and its Steady-State Dynamic Response," J. Appl. Mech., Trans. ASME, 893-900 (Dec. 1966).

117. Iwan, W. D., "On a Class of Models for the Yielding Behavior of Continuous and Composite Systems," J. Appl. Mech., Trans. ASME, 612-617 (Sept. 1967).

118. Grounes, M., "A Reaction-Rate Treatment of the Life Fraction Hypothesis in Creep Testing," ASME Paper 69-MET-A (1969).

119. Grounes, M., "A Reaction-Rate Treatment of the Extrapolation Methods in Creep Testing," ASME Paper No. 69-MET-B (1969).

120. Leeming, H., et. al., Solid Propellant Structural Test Vehicle, Cumulative Damage and Systems Analysis, Final Report No. AFRPL-TR-68-130, Lockheed Propulsion Company (October 1968).

121. Gent, A. N. and Lindley, P. B., Proc. Roy. Soc. London, A249, 195 (1959).

122. Lindsey, G. H. and Murch, S. A., "On the Mechanical Behavior of Dewettable Solids," JANNAF Mech. Behavior Working Group Bulletin, Vol. 1, CPIA Pub. 193, 139-152 (Mar. 1970).

123. Drucker, D. C., "A Definition of Stable Inelastic Material," J. Appl. Mech., 26, Trans. ASME, 81, Series E, 101-106 (1959).

124. Onat, E. T., "Description of Mechanical Behavior of Inelastic Solids," Proc. of 5th U. S. Nat. Congress of Appl. Mech. 421-434 (1966).

125. Surland, C. C., Boyden, J. R., and Givan, G. R., "The Effect of Hydrostatic Pressure on the Uniaxial Tensile Properties of Solid Propellants," 20th Meeting Bulletin, JANAF-ARPA-NASA Panel on Physical Properties of Solid Propellants, SPIA Pub. 140, 1, 341-356 (1967).

126. Lou, Y. C., and Schapery, R. A., "Viscoelastic Characterization of a Nonlinear Fiber-Reinforced Plastic," to be published in J. Composite Materials (April 1971).

127. Halpin, J. C., "Nonlinear Rubberlike Viscoelasticity-A Molecular Approach," J. Appl. Phys., 36, 2975-2982 (1965).

128. Schapery, R. A., "Application of Thermodynamics to Thermochemical Fracture and Birefringent Phenomena in Viscoelastic Media," J. Appl. Phys., 35, 1451-1465 (1964).

129. Fung, Y. C., Fundamentals of Solid Mechanics, Prentice Hall, Inc., New Jersey (1965).

130. Schapery, R. A., "Further Development of a Thermodynamic Constitutive Theory: Stress Formulation," Purdue University Report No. AA&ES 69-2 (1969).

131. Green, A. E, and Zerna, W., Theroetical Elasticity, Oxford Press (1963).

132. Cantey, D., "Solid Propellant Integrity Investigations: Dynamic Response and Failure Mechanisms," Lockheed Propulsion Co. Report No. 618-F (RPL-TDR 64-32, Vol I) (April 1964).

133. Schapery, R. A., and Cantey, D., "Thermomechanical Response Studies of Solid Propellant Subjected to Cyclic and Random Loading," AIAA J., 4, 255-264 (1966).

134. Morland, L. W., and Lee, E. H., "Stress Analysis for Linear Viscoelastic Systems with Temperature Variation," Trans. Soc. Rheol., 4, 233-263 (1960).

135. Knauss, W. G., and Dietmann, H., "Crack Propagation Under Variable Load Histories in Linearly Viscoelastic Solids," Int. J. Eng'g Sciences, 8, 643-657 (1970).

136. Surland, C. C., "Compressibility of Elastomers with Crystalline Fillers and Microvoid Inhomogeneities Related to Various Empirical Equations of State for Liquids and Solids," J. Appl. Pol. Sci. II, 1227-1249, (1967).

137. Herrmann, L. R., "Effect of Voids on the Dilative Behavior of Rubber-Like Materils," Bulletin of Second Meeting of ICRPG for Mech. Behavior I, CPIA 27, 97-108, November 1963.